Functional properties of 4-PIOL at synaptic and extrasynaptic GABA-A receptors

Bijal Patel

A thesis submitted to University College London for the Degree of Doctor of Philosophy

October 2014

Department of Neuroscience, Physiology and Pharmacology

University College London

Gower Street

WC1E 6BT

Declaration

I, Bijal Patel, confirm that the work presented in this thesis is my own. Where information has been derived from other sources, I can confirm that this has been indicated in the thesis.

Abstract

$GABA_A$ receptors are the major inhibitory ligand-gated ion channels in the mammalian CNS. They mediate their physiological effects via two temporally and spatially distinct forms of signalling, denoted as phasic and tonic inhibition. These two forms of inhibition are mediated by distinct $GABA_A$ receptor subtypes, with phasic inhibition relying on the activation of synaptically-located γ2 subunit-containing receptors, and tonic inhibition requiring the activation of extrasynaptic receptors, predominantly thought to contain δ-subunits.

The importance of tonic inhibition in regulating cell and network excitability has become increasingly apparent. Moreover, elevated tonic currents accompany neurological disorders such as stroke and absence epilepsy, suggesting that selectively reducing tonic inhibition might be therapeutically useful. Due to a lack of δ-selective antagonists, the theoretically predominant antagonist profile of the weak partial agonist, 4-PIOL, was studied as a potential mechanism for selectively reducing tonic inhibition.

The functional effects of 4-PIOL were investigated firstly on whole-cell GABA-activated currents of several recombinant γ2- and δ-containing receptors expressed in HEK293 cells. As expected for a partial agonist, 4-PIOL exhibited both agonist- (at γ2-subunit $GABA_A$ receptors) and antagonist-type (at δ-subunit receptors) behaviours, depending on the GABA concentration. 4-PIOL was then assessed on tonic and phasic currents of cerebellar granule cells (CGCs), hippocampal pyramidal neurons and thalamic relay-neurons. In CGCs, 4-PIOL inhibited tonic currents, without affecting spontaneous inhibitory postsynaptic currents (sIPSCs); whereas in hippocampal and thalamic relay neurons, 4-PIOL enhanced, or reduced, tonic currents depending on the extrasynaptic GABA concentration, consistent with an action at extrasynaptic γ2-containing receptors. Moreover, 4-PIOL antagonised sIPSCs in these two brain regions, in accord with targeting presynaptic and postsynaptic $GABA_A$ receptors.

In conclusion, the therapeutic potential of $GABA_A$ receptor partial agonists, such as 4-PIOL will be critically dependent on not only the ambient GABA concentration, but also on the relative expression of different $GABA_A$ receptor subtypes.

Acknowledgements

Firstly, my heartfelt thanks goes to my supervisor and mentor, Prof. Trevor Smart. I will be forever grateful for his unending support, guidance and enduring positivity, which have been invaluable on both an academic, and personal level. I would also like to thank the MRC, for providing the financial support to complete this project.

This project would not have been possible without the unwavering support, and invaluable feedback provided by Damian and Martin. Their excellent teaching and guidance have helped unravel, what was sometimes a very confusing project! I would also like to thank, both past and present members of the Smart lab (especially Phil and Megan), who have been a great source of support and entertainment over the past few years, and have made every day in the lab a fun and enjoyable experience.

I am grateful to my amazing friends and family, for all their love and support over the past few years. In particular, a special thanks goes to the Biomeds, the ‘Baywatch babes’, my Ricards ladies and the Lemmons, who have each been an excellent source of encouragement and entertainment. Finally, my biggest thanks goes to my family, especially my mum, dad and brother, whose love and ‘encouragement’ have given me the strength to complete this PhD.

Contents

List of figures

List of Tables

List of equations

List of Abbreviations

AA29504	N-[2-Amino-4-[[(2,4,6-trimethylphenyl)methyl]amino]phenyl]-carbamic acid-ethyl ester
Aβ	β-amyloid
aCSF	Artificial cerebrospinal fluid
AD	Alzheimer's disease
AED	Anti-epileptic drug
AP2	Clathrin-adaptor protein 2
α_m	$\alpha4^{L297S}$ mutant $GABA_A$ receptor subunit
α5IA	1,2,4-Triazolo[3,4-a]phthalazine, 3-(5-methyl-3-isoxazolyl)-6-[(1-methyl-1H-1,2,3-triazol-4-yl)methoxy]-,3-(5-Methylisoxazol-3-yl)-6-(1-methyl-1,2,3-triazol-4-yl)methoxy-1,2,4-triazolo[3,4-a]phthalazine
ANOVA	Analysis of Variance
AMPA	2-amino-3-(3-hydroxy-5-methyl-isoxazol-4-yl)propanoic acid
APP	Amyloid precursor protein
Baclofen	β-(4-chloro-phenyl)-γ-aminobutyric acid
BBB	Blood-brain barrier
BC	Basket cell
BDNF	Brain-derived neurotrophic factor
Best1	Bestrophin 1
BDZ	Benzodiazepine
BGT1	Betaine-GABA transporter 1
BIC	Bicuculline
β_m	$\beta3^{L284S}$ mutant $GABA_A$ receptor subunit
BME	Basal medium Eagle
CA1 – CA3	C*ornu ammonis* (CA) regions 1-3 of the hippocampus
CAE	Childhood absence epilepsy
CaMKII	Ca^{2+}/calmodulin-dependent kinase II
CCV	Clathrin-coated vesicles
cDNA	Complementary deoxy-ribonucleic acid
CGC	Cerebellar granule cell
CNS	Central nervous system
cRNA	Complementary ribonucleic acid
CT	Corticothalamic
CT1	Creatine transporter 1
Ctrl	Control
DS	Down's syndrome
DGGC	Dentate gyrus granule cell
DIC	Differential interference contrast
DIV	Days *in vitro*
dLGN	Dorsal lateral geniculate nucleus
δ_m	δ_{sep}^{L288S} mutant $GABA_A$ receptor subunit

DGGC	Dentate gyrus granule cell
DMEM	Dulbecco's modified Eagle's medium
DMSO	Dimethyl sulfoxide
DS2	4-Chloro-*N*-[2-(2-thienyl)imidazo[1,2-*a*]pyridin-3-yl]benzamide
DZP	Diazepam
EC_{15}	The concentration of substance eliciting 15% of the maximal response
EC_{50}	The concentration of substance eliciting 50% of the maximal response
EDTA	Ethylene-diamine-tetra-acetic acid
EEG	Electroencephalogram
eGFP	Enhanced green-fluorescent protein
EGTA	Ethylene glycol tetra-acetic acid
ELIC	Ligand-gated ion channel from *E. chrysanthemi*
ER	Endoplasmic reticulum
EM	Electron microscopy
FCS	Foetal calf serum
GABA	γ-aminobutyric acid
GAERS	Genetic Absence Epilepsy Rat from Strasbourg
GAT	GABA transporter
GLIC	Ligand-gated ion channel from *G. violaceus*
GluCl	Glutamate-gated chloride channel from *C. elegans*
GoC	Golgi cell
γ2S	Short splice variant of the γ2 subunit
γ2L	Long splice variant of the γ2 subunit
GABA	Gamma-aminobutyric acid
$GABA_A$	Gamma-aminobutyric acid type-A
$GABA_B$	Gamma-aminobutyric acid type-B
GABARAP	$GABA_A$ receptor associated protein
HAP1	Huntingtin-Associated Protein-1
HBS	HEPES buffered solution
HBSS	Hank's Balanced salt solution
HEK293	Human embryonic kidney 293
HEPES	4-(2-hydroxyethyl)piperazine-1-ethanesulfonic acid
HS	Horse serum
$5\text{-}HT_3$	$5\text{-hydroxytryptamine}_3$
IC_{50}	Concentration of antagonist producing a 50% maximal inhibition
IGE	Idiopathic generalized epilepsies
IPSCs	Inhibitory post-synaptic currents
JAE	Juvenile absence epilepsy
JME	Juvenile myoclonic epilepsy
KCC2	Potassium-chloride co-transporter 2
KIF5	Kinesin motor protein 5
LB	Luria broth

L-655,708	11,12,13,13a-Tetrahydro-7-methoxy-9-oxo-9*H*-imidazo[1,5-*a*]pyrrolo[2,1-c][1,4]benzodiazepine-1-carboxylic acid
LGIC	Ligand-gated ion channel
L9'S	9' leucine to serine
LTP	Long-term potentiation
M1- M4	Transmembrane helices 1 – 4
MEM	Minimum essential media
mIPSCs	Miniature inhibitory post-synaptic currents
nACh	Nicotinic acetylcholine
NEC	Non-epileptic
NKCC1	Sodium, potassium and chloride co-transporter 1
NMDA	*N*-Methyl-*D*-aspartate
NNC-711	1,2,5,6-Tetrahydro-1-[2-[[(diphenylmethylene)amino]oxy]ethyl]-3-pyridinecarboxylic acid hydrochloride
NREM	Non-rapid eye movement
NRT	Thalamic reticular nucleus
ns	Not statistically significant
P	Postnatal
PAM	Positive allosteric modulator
PBS	Phosphate buffered saline
PCR	Polymerase Chain Reaction
PFA	Paraformaldehyde
4-PIOL	5-(4-piperidyl)isoxazol-3-ol
pLGICs	Pentameric-ligand gated ion channels
PLIC-1	Protein that Links Integrin-associated Protein with the Cytoskeleton-1
PKA, PKB, PKC, PKG	Protein kinase A, B, C and G
PP1/PP2A	Protein phosphatases 1 and 2A
PS1	Presenilin-1
PRIP1/2	Phospholipase-C Related Inactive Protein 1 and 2
PTZ	Pentylenetetrazole
PC	Purkinje cell
PY	Pyramidal
R^2	Coefficient of determination
RMS	Root mean square
RO-493851	3-bromo-10-(difluoromethyl)-9H-benzo[f]imidazol[1,5-a][1,2,4]triazolo[1,5-d][1,4]diazepine
r.p.m	Revolutions per minute
Rs	Series resistance
RT	Room temperature
SA	Spontaneous activity
SC	Stellate cell
SEM	Standard error of the mean
sep	Super-ecliptic phluorin
sIPSC	Spontaneous inhibitory postsynaptic current

SLC6	Solute carrier 6
SWD	Spike-wave discharge
TauT	Taurine transporter
TC	Thalamocortical
THDOC	Tetrahydrodeoxycorticosterone
THIP	4,5,6,7-Tetrahydroisoxazolo[5,4-*c*]pyridin-3-ol
TTX	Tetrodotoxin
WT	Wild-type
VB	Ventrobasal
vLGN	Ventral lateral geniculate nucleus

Chapter 1: Introduction

1.1. $GABA_A$ receptors

Gamma-aminobutyric acid (GABA) is the major inhibitory neurotransmitter in the mammalian central nervous system (CNS). GABA mediates its actions through two distinct classes of receptor: ionotropic GABA type-A ($GABA_A$) and metabotropic GABA type-B ($GABA_B$) receptors. The main focus of this thesis will be the $GABA_A$ receptor family, which are the main class of inhibitory ligand-gated ion channels (LGIC) in the mammalian CNS. $GABA_A$ receptors are pentameric complexes comprised of five subunits arranged around a central Cl^- and HCO_3^- permeable pore (*Fig*. 1.1 A). $GABA_A$ receptors, along with glycine, nicotinic acetylcholine (nACh), 5-hydroxytryptamine$_3$ ($5\text{-}HT_3$; serotonin) and zinc-activated channels (ZAC), belong to the Cys-loop containing LGIC family, which together with their bacterial homologues from *G. violaceus* (GLIC) and *E. chrysanthemi* (ELIC), and eukaryotic glutamate-gated chloride channels from *C. elegans* (GluCl), form part of the pentameric LGIC (pLGIC) super family (Miller and Smart, 2010; Corringer *et al*., 2012). Structural information for Cys-loop-containing receptors comes from the electron microscope studies of nACh receptors (Unwin, 2005), and high-resolution X-ray structures of ELIC (Hilf and Dutzler, 2008), GLIC (Bocquet et al., 2009), GluCl (Hibbs and Gouaux, 2011; Althoff et al., 2014), mouse $5\text{-}HT_3$ receptors (Hassaine et al., 2014) and human homomeric β3 $GABA_A$ receptors (Miller and Aricescu, 2014).

1.1.1. $GABA_A$ receptor structure

To date, 8 classes of $GABA_A$ receptor subunits have been identified, half of which have multiple isoforms: α(1-6), β(1-3), γ(1-3), δ, ε, θ, π, ρ(1-3). Further subunit diversity can arise from alternative splicing of RNA (Farrant and Nusser, 2005; Möhler, 2006). For instance, the γ2 subunit can exist as a short (γ2S) or long (γ2L) splice variant, with the latter isoform containing an eight amino acid cassette in the M3 - M4 intracellular loop that is absent in the γ2S isoform (Whiting *et al*., 1990; Kofuji *et al*., 1991). Each receptor subunit comprises a large extracellular N-terminus, four transmembrane domains (M1 – M4), a short extracellular C-terminus, and a large intracellular M3 – M4 domain (*Fig*. 1.1 B). While the N-terminus contributes to the orthosteric binding site and contains a Cys-loop formed by a disulphide bond between two cysteine residues (a characteristic of all Cys-loop LGICs), the M2 region forms the channel pore. The large intracellular loop between M3 and M4 is important for protein-protein interactions and contains phosphorylation consensus sequences (discussed in *Section* 1.1.4).

In recombinant expression systems, functional $GABA_A$ receptors can sometimes be formed by expressing a single subunit (e.g. ρ or β3 subunits), or more typically, two (e.g. α and β subunits), or three subunit classes (e.g. α, β and γ subunits). Despite this potentially huge structural diversity, it appears that only a limited number of native subunit combinations exist within the CNS. The expression profile of each subunit varies between, and within, brain regions and also within single cells, and can vary during development (Laurie *et al*., 1992b; Pirker *et al*., 2000; Hörtnagl *et al*., 2013). Protein and mRNA co-distribution studies (assessed by immunostaining and *in situ* hybridisation respectively), combined with co-immunoprecipitation studies, indicate that the majority of native $GABA_A$ receptors are composed of α1β2γ2 subunits (~ 40 – 60 %), with the other, less common subunit combinations being α2β2γ2 (15 - 20 %), α4βδ/α4βγ2 (< 5 %) and α6βδ/α6βγ2 (< 5 %) subunits (McKernan and Whiting, 1996; Sieghart and Sperk, 2002; Möhler, 2006). There is also evidence from co-immunoprecipitation studies that different α isoforms may co-assemble within the same receptor complex (e.g. α1α6βγ2 receptors in the cerebellum; Pollard

et al., 1995). Subunit composition appears to be an important determinant of subcellular localisation in neurons. For instance, δ-containing receptors seem to be located exclusively at extrasynaptic sites in several brain regions (see *Section* 1.3.1), while γ2-containing receptors typically accumulate at inhibitory synapses (Sieghart and Sperk, 2002). However, these rules may vary, since typical synaptic subunits (e.g. α1 and γ2) have also been detected at extrasynaptic sites in several neuronal cell types (e.g. cerebellar granule cells, hippocampal pyramidal neurons and thalamic relay neurons; Soltesz *et al*., 1990; Nusser *et al*., 1998; Mangan *et al*., 2005; Thomas *et al*., 2005; Kasugai *et al*., 2010).

Although the precise subunit stoichiometry of native $GABA_A$ receptors is yet to be elucidated, recombinant αβγ $GABA_A$ receptors are widely believed to have a subunit stoichiometry of 2α: 2β: 1γ, with a likely βαβαγ anticlockwise subunit arrangement in the pentamer when viewed externally (*Fig*. 1.1 C; Backus *et al*., 1993; Chang *et al*., 1996; Tretter *et al*., 1997). For the other $GABA_A$ receptor isoforms, it is generally assumed that the δ, ε, or π subunits simply replace the γ2 subunit within the receptor complex (Sieghart and Sperk, 2002; Olsen and Sieghart, 2008). However, this may not be a firm assembly rule, since at least for δ-containing receptors, there is some debate regarding their precise subunit stoichiometry. While one study demonstrated a subunit stoichiometry of 2α: 2β: 1δ for recombinant α4β3δ receptors using atomic force microscopy (Barrera *et al*., 2008), another co-immunoprecipitation-based study revealed that the number of incorporated δ subunits could be varied by increasing the relative amount of δ-encoding cDNA during transfection (Wagoner and Czajkowski, 2010). Moreover, studies using concatamers indicate that the δ subunit can also assume multiple positions within the αβδ receptor pentamer, and may potentially also contribute to a novel GABA binding site (Baur *et al*., 2009; Kaur *et al*., 2009). Thus, subunit composition critically defines the functional and pharmacological properties of $GABA_A$ receptors, a feature that will be further discussed in *Section*s 1.1.5 and 1.2.3.

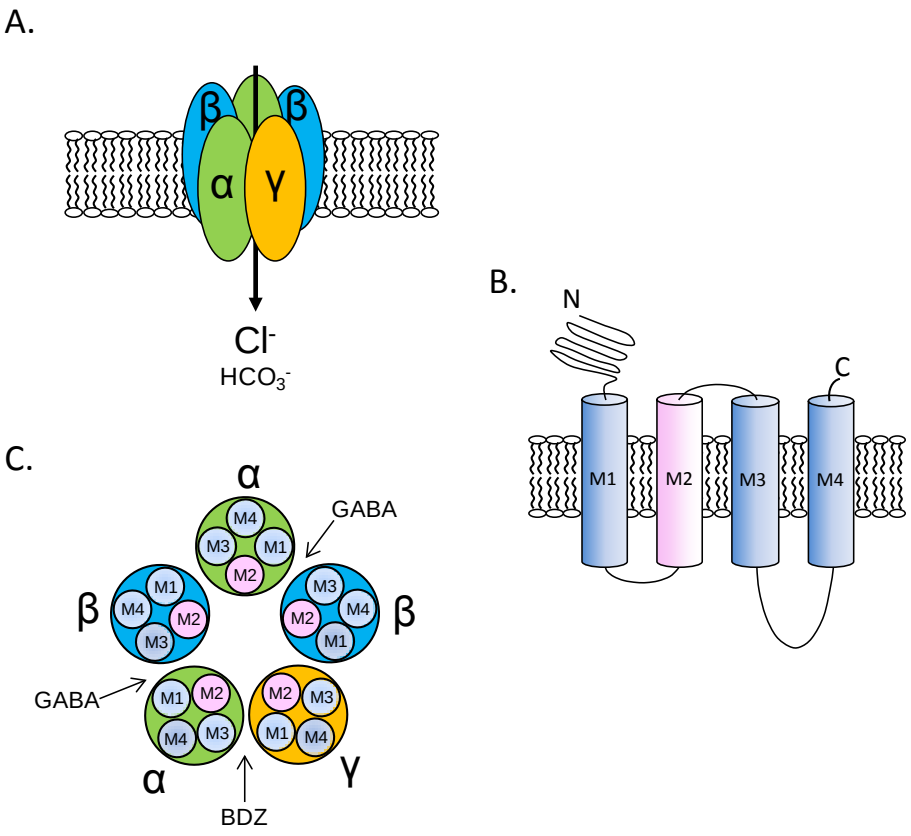

Figure 1.1 – Structure of $GABA_A$ receptors

A. $GABA_A$ receptors are pentameric assemblies of five subunits arranged around a central Cl^--(and HCO_3^--) permeable pore region. **B.** Each $GABA_A$ receptor subunit is composed of a large extracellular amino (-NH_2) terminus, four transmembrane helices (M1 – M4), a large intracellular loop between M3 and M4, and a short carboxy (-COOH) terminus. The M2 region forms the pore-lining domain, while the M3-M4 intracellular loop is a major site for protein-protein interactions and phosphorylation. **C.** The proposed subunit stoichiometry and subunit arrangement of αβγ receptors, as viewed from the extracellular space. Subunits show a subunit stoichiometry of 2α: 2β: 1γ, with an anticlockwise subunit arrangement of βαβαγ. The respective binding sites for GABA and benzodiazepine (BDZ) ligands are also indicated, at the β/α (the orthosteric binding site) and α/γ interfaces (an example of an allosteric binding site).

1.1.2. Assembly of $GABA_A$ receptors

$GABA_A$ receptor assembly occurs in the endoplasmic reticulum (ER), and the specificity of this process limits the diversity of $GABA_A$ receptors expressed at the cell surface. For α, β and γ subunits, sequences in the N-terminus have been identified as important determinants of subunit oligomerization (Lüscher *et al*., 2011), which appear to promote specific subunit partnerships. For instance, four amino acids (G171, K173, E179 and R180) in the N-terminus of β3 subunits are required for the formation of β3 homo-oligomers in recombinant expression systems, but not for the formation of α1 and β3 heteromers (Taylor *et al*., 1999). Moreover, an N-terminal residue (R66A) in the α1 subunit is important for the formation of binary α1β2 subunits, but not α1β1 or α1β3 receptors (Bollan *et al*., 2003). An insight into the preferred subunit partnerships of native $GABA_A$ receptors comes from gene knockout studies. For instance, in cerebellar granule cells (CGCs), genetic knockdown of the α6 subunit produces a concomitant loss of δ subunit protein levels (Jones *et al*., 1997), while in the forebrain, δ knockout (δ-/-) mice show a significantly reduced α4 immunoreactivity (Peng *et al*., 2002). Thus, δ appears to preferentially co-assemble with α4 and α6 subunits, although a compensatory association of α4 and γ2 subunits has also been detected in δ-/- knockout mice (Peng *et al*., 2002), indicating that other subunit combinations can occur in the absence of preferred oligomerization partners.

1.1.3. Trafficking of $GABA_A$ receptors

$GABA_A$ receptor trafficking is a dynamic and complex process that regulates the efficacy of GABAergic neurotransmission. Several receptor-associated proteins alter the number and distribution of $GABA_A$ receptors on the cell surface of neurons, by regulating the delivery, internalisation and lateral mobility of cell surface $GABA_A$ receptors (*Fig*. 1.2). Although an extensive discussion of these processes is beyond the scope of this thesis, some key components will be described below. Many of these proteins associate with the intracellular M3 –

M4 loop of $GABA_A$ receptor subunits (Lüscher and Keller, 2004; Lüscher *et al*., 2011; Vithlani *et al*., 2011).

PLIC-1 (Protein that Links Integrin-associated protein with the Cytoskeleton-1), a ubiquitin-like protein, appears to be critical for forward trafficking of receptors, since it appears to increase the stability of $GABA_A$ receptors in the secretory pathway and prevents their degradation, probably by inhibiting ubiquitin-dependent degradation (Lüscher *et al*., 2011; Vithlani *et al*., 2011). In accord with this, blocking the interaction of PLIC-1 with the intracellular domains of α and β subunits reduces cell surface receptor expression levels of $GABA_A$ receptors (Bedford *et al*., 2001). Other proteins that facilitate the delivery of $GABA_A$ receptors to the cell surface include the HAP1/KIF5 (Huntingtin-Associated Protein-1/kinesin motor protein 5) complex, GABARAP ($GABA_A$ receptor associated protein) and PRIP1/2 (Phospholipase-C Related Inactive Protein 1 and 2). The KIF5/HAP1 complex is important for the fast delivery of $GABA_A$ receptors to synapses (Kittler *et al*., 2004; Twelvetrees *et al*., 2010), since disrupting this complex causes a rapid (within minutes) reduction in synaptic cluster size, and synaptic current amplitude (Twelvetrees *et al*., 2010). GABARAP also appears to promote the cell surface expression of $GABA_A$ receptors, since its overexpression in hippocampal neurons also enhances surface expression of the γ2 subunit (Leil *et al*., 2004). Originally, GABARAP was implicated in synaptic clustering, due to its ability to directly interact with the γ2 subunit, tubulin, and gephyrin (a synaptic scaffolding protein) *in vitro* (Wang *et al*., 1999; Kneussel *et al*., 2000). However, due to its absence from synaptic sites, and predominant intracellular location in neurons (Kneussel *et al*., 2000; Kittler *et al*., 2001), GABARAP is now thought to be involved in the intracellular trafficking of $GABA_A$ receptors. Consistent with this role, genetic knockdown of PRIP1/2, proteins which seem to facilitate the interaction of GABARAP with γ2 subunits, produces a reduction in cell surface expression of γ2-containing receptors (Mizokami *et al*., 2007), although it is important to note that PRIP1/2 may also alter receptor trafficking through other mechanisms (see *Section* 1.1.4).

The number of $GABA_A$ receptors on the cell surface is also critically dependent on the dynamics of receptor internalization and membrane insertion. In both

recombinant expression systems, and neuronal preparations, $GABA_A$ receptors undergo constitutive endocytosis via a clathrin-dependent mechanism (Kittler *et al*., 2000). This process requires the direct interaction of β and γ subunits with clathrin-adaptor protein 2 (AP2; Kittler *et al*., 2000; Smith *et al*., 2008), and is regulated by the phosphorylation state of these subunits (see *Section* 1.2.1; Lüscher *et al*., 2011).

In addition, $GABA_A$ receptors also show lateral mobility within the plasma membrane, allowing them to move into and out of synapses (Thomas *et al*., 2005; Bogdanov *et al*., 2006). The synaptic and extrasynaptic distribution of $GABA_A$ receptors is critically dependent on both subunit composition (discussed in *Section* 1.2.1), and specific interactions with post-synaptic scaffolding proteins. One scaffolding protein that appears to be important for the synaptic clustering of $GABA_A$ (and glycine) receptors, is gephyrin. Clustering of gephyrin itself is also critically dependent on the γ2 subunit, since γ2 knockout mice show a concomitant loss of gephyrin clustering (Essrich *et al*., 1998). However, since no direct interaction between gephyrin and γ2 subunits has yet been identified, the mechanisms that underlie this interdependence are unknown. In fact, the only $GABA_A$ receptor subunits known to directly interact with gephyrin *in vitro*, are α(1 – 3) subunits (Tyagarajan and Fritschy, 2014). Intriguingly, gephyrin knockout mice show a subtype selective loss of α2βγ2 and α3βγ2 $GABA_A$ receptors from GABAergic synapses (Kneussel *et al*., 1999; Lévi *et al*., 2004), which might in part, be explained by the specific interactions of gephyrin with different α subunits (Tyagarajan and Fritschy, 2014). The existence of gephyrin-independent clustering mechanisms have also been proposed, since $GABA_A$ receptor synaptic clustering, and miniature inhibitory post-synaptic currents (IPSCs) are still detected in gephyrin knockout mice (Kneussel *et al*., 1999; Lévi *et al*., 2004). Intriguingly, the actin binding protein, radixin was shown to promote clustering of α5 subunit-containing receptors in hippocampal neurons (Loebrich *et al*., 2006). However, unlike gephyrin-dependent clustering, radixin-dependent clustering occurs only at extrasynaptic sites (Loebrich *et al*., 2006), indicating that $GABA_A$ receptors may also be specifically anchored to extrasynaptic sites to support tonic inhibition.

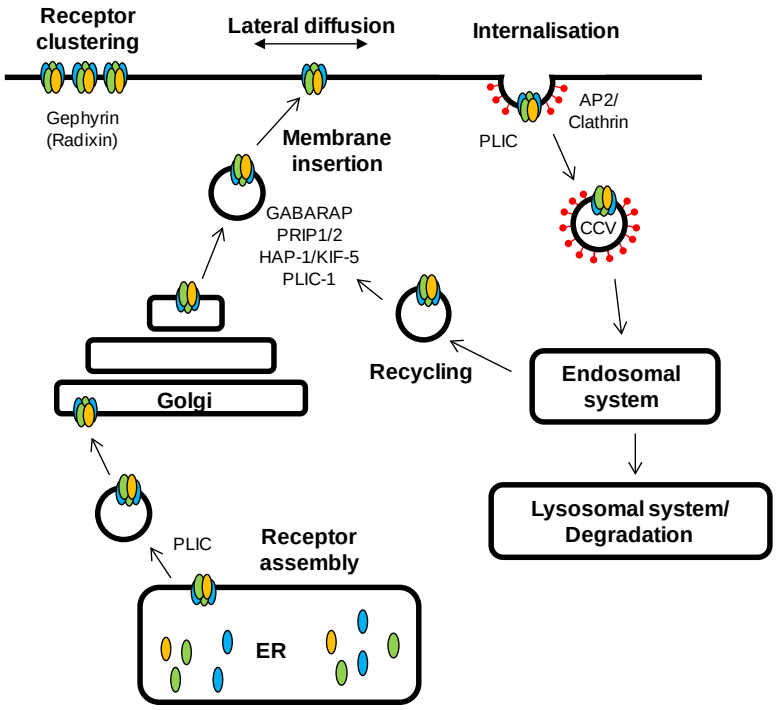

Figure 1.2 – Schematic of the major $GABA_A$ receptor trafficking processes

$GABA_A$ receptors are assembled as pentameric complexes in the endoplasmic reticulum (ER). The forward trafficking of correctly assembled $GABA_A$ receptors is facilitated by PLIC-1, which prevents $GABA_A$ receptor degradation, and promotes receptor stability through the secretory pathway. Other key proteins that are implicated in the trafficking of $GABA_A$ receptors to the cell surface are GABARAP and PRIP1/2 and the HAP1/KIF5 complex. $GABA_A$ receptors at the cell surface are subject to lateral diffusion, and can interact with scaffolding proteins such as gephyrin (α1 -3 subunits) and radixin (α5 subunits), which promote receptor clustering at synaptic and extrasynaptic sites respectively. Receptor internalisation largely occurs via a direct interaction of β and γ subunits with the clathrin-adaptor protein 2 (AP2), an interaction that is regulated by phosphorylation. Following clathrin-mediated endocytosis into clathrin-coated vesicles (CCV), receptors are recycled back to the cell surface or targeted for lysosomal degradation. Figure was compiled using reviews by (Lüscher and Keller, 2004; Lüscher *et al*., 2011; Vithlani *et al*., 2011).

1.1.4. $GABA_A$ receptor modulation: Phosphorylation

Several phosphorylation consensus sequences have been identified in the M3 – M4 intracellular loops of α4, β(1-3) and γ2 subunits, which act as substrates for several different serine-threonine and tyrosine kinases (*Fig.* 1.3). Phosphorylation at these sites can differentially regulate the biophysical properties, pharmacology and trafficking of $GABA_A$ receptors (Lüscher *et al*., 2011; Vithlani *et al*., 2011). However, the functional outcome of phosphorylation will depend on which $GABA_A$ receptor subunits are modified, the identity of the kinase, the experimental conditions used (e.g. the expression system used), and the compartment in which phosphorylation occurs. For instance, Ca^{2+}/calmodulin-dependent kinase II (CaMKII)-mediated potentiation of α1β3- or α1β3γ2-GABA currents was only supported in a neuroblastoma (NG108-15) cell line, but not in a human embryonic kidney 293 (HEK293) expression system (Houston and Smart, 2006). Moreover, this modulation was dependent on the β3 subunit since no effect of CaMKII activation was observed on α1β2- or α1β2γ2-GABA currents (Houston and Smart, 2006), even though a CaMKII phosphorylation site has been identified on the β2 subunit (S410; *Fig*. 1.3; Lüscher *et al*., 2011; Vithlani *et al*., 2011). However, it must be noted that a lack of effect in recombinant expression systems does not exclude the possibility that β2-containing receptors may undergo CaMKII-mediated modulation in neurons.

Protein kinase C (PKC) phosphorylation of β and γ2 subunits disrupts their interaction with AP2, leading to reduced clathrin-mediated endocytosis, and consequently, increased GABA currents in recombinant expression systems, and cortical neurons (Kittler *et al*., 2005; Vithlani *et al*., 2011). More recently, it was demonstrated that phosphorylation of S443 on α4 subunits prevents run down of GABA currents by promoting plasma membrane insertion rates of recombinant α4β3 receptors in HEK293 cells (Abramian *et al*., 2010). However, PKC activation has also been shown to decrease cell surface expression levels of recombinant α4β2δ receptors via the S410 residue on the β2 subunit (Bright and Smart, 2013). Given that the δ subunit does not appear to be phosphorylated by PKC in recombinant expression systems (Abramian *et al*.,

2010), the discrepancy between these studies might arise from the use of different β isoforms, which may be differentially regulated by PKC in α4-containing receptors. Moreover, the subcellular compartment in which phosphorylation occurs may also be important, since phosphorylation at the same site on the β subunit can have opposing effects on $GABA_A$ receptor trafficking in different subcellular compartments (Lüscher *et al*., 2011). Indeed, it is unclear whether the reduced cell surface expression of α4β2δ receptors following PKC phosphorylation is attributable to reduced cell surface delivery, or increased endocytosis of $GABA_A$ receptors (Bright and Smart, 2013).

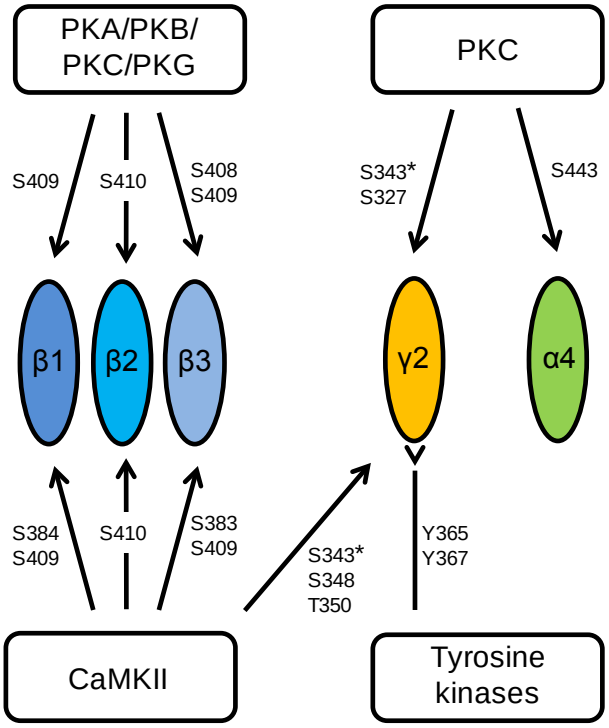

Figure 1.3 – Phosphorylation sites on $GABA_A$ receptors

A diagram showing the phosphorylation sites (serine (S), threonine (T) or tyrosine (Y) residues) identified on $GABA_A$ receptor subunits, along with the kinases capable of phosphorylating them. The M3 - M4 intracellular loop of all three β subunits contain phosphorylation consensus sequences for Ca^{2+}/calmodulin-dependent kinase II and Protein kinases A, B, C and G (PKA, PKB, PKC, PKG), whereas the γ2 subunit contains consensus sequences for PKC, CaMKII and tyrosine kinase-mediated phosphorylation. *Note that S343 is present in the γ2L isoform, but not the γ2S isoform. For α subunits, only one serine residue has been identified to date on the α4 subunit that can act as a substrate for PKC-mediated phosphorylation. This figure was constructed using reviews by (Houston *et al*., 2009; Abramian *et al*., 2010; Lüscher *et al*., 2011; Vithlani *et al*., 2011).

The phosphorylation of $GABA_A$ receptors *in vivo* may be dynamically regulated by endogenous factors. For instance, acute treatment of cultured cortical and hippocampal neurons with brain-derived neurotrophic factor (BDNF) induces a transient increase, followed by a prolonged depression of mIPSC amplitudes (Jovanovic *et al*., 2004). Moreover, this effect is achieved by indirectly influencing the phosphorylation state of recombinant and native $GABA_A$ receptors (Lüscher *et al*., 2011; Vithlani *et al*., 2011). The enhancement of mIPSC amplitude coincides with increased β3 subunit expression at the cell surface, and is temporally associated with an increase and subsequent decrease in PKC-mediated phosphorylation of β3 subunits (Jovanovic *et al*., 2004; Kanematsu *et al*., 2006). The latter reduction in mIPSC amplitude is thought to involve the recruitment of protein phosphatases 1 and 2A (PP1/PP2A) by the phosphatase adaptor protein, PRIP, and a subsequent dephosphorylation of β3 subunits. However, it is uncertain whether this prolonged depression of mIPSCs arises from reduced cell surface expression of β3-containing receptors (Kanematsu *et al*., 2006), or reduced currents without altered cell surface expression (Jovanovic *et al*., 2004).

1.1.5. $GABA_A$ receptor modulation: Pharmacology

As discussed in *Section* 1.1, GABA mediates its actions via two distinct classes of receptor: ionotropic $GABA_A$ and metabotropic $GABA_B$ receptors. These two receptor classes display distinct functional properties; $GABA_A$ receptors are Cl^- permeable ion channels, whereas $GABA_B$ receptors couple to Ca^{2+} and K^+ channels via G-proteins and second messenger systems (Bowery et al., 2002; Bettler et al., 2004; Olsen and Sieghart, 2008). In addition, these two receptor isoforms show distinct pharmacological profiles. $GABA_A$ receptors, but not $GABA_B$ receptors are sensitive to the inhibitory actions of the $GABA_A$ receptor antagonists, bicuculline, gabazine and picrotoxin, although $GABA_A$ receptors containing the ρ subunit (previously termed $GABA_C$ receptors), are insensitive to bicuculline and gabazine (Chebib and Johnston, 1999; Olsen and Sieghart, 2008). Conversely, the GABA analogue, β-(4-chloro-phenyl)-γ-aminobutyric

acid (baclofen) is a potent agonist at $GABA_B$ but not $GABA_A$ receptors (Bowery et al., 2002; Olsen and Sieghart, 2008).

$GABA_A$ receptors are modulated by a wide range of endogenous and synthetic compounds, including Zn^{2+}, barbiturates, benzodiazepines, neurosteroids and general anaesthetics (e.g. propofol). The best characterised of these, are benzodiazepine agonists, which represent the most widely prescribed drugs for the treatment of anxiety and insomnia disorders (Rudolph and Knoflach, 2011). Benzodiazepine agonists (e.g. diazepam) act as positive allosteric modulators of the $GABA_A$ receptor, by increasing the apparent affinity of receptors to GABA (Rogers *et al*., 1994), and promoting the creation of a pre-activation state prior to receptor gating (Gielen *et al*., 2012). Classical benzodiazepines require the presence of an α/γ interface, and absence of the benzodiazepine-insensitive α subunit variants (α4 and α6). Therefore, only α(1, 2, 3 or 5)-containing receptors can be modulated by classical benzodiazepines, since they contain the N-terminal histidine residue ($\alpha1^{H101}$, $\alpha2^{H101}$, $\alpha3^{H126}$ or $\alpha5^{H105}$) that is crucial for benzodiazepine binding (Wieland *et al*., 1992) and potentiation (Benson *et al*., 1998). By generating benzodiazepine-insensitive knock-in mice, which carry a histidine to arginine (H to R) mutation in selected α subunits, the behavioural effects of benzodiazepines have been attributed to individual α isoforms. For instance, the α1 subunit largely mediates the sedative and muscle relaxant properties of benzodiazepine agonists, while the α2 subunit significantly contributes to their anxiolytic actions (Rudolph and Knoflach, 2011). Thus generating α-selective benzodiazepine agonists may provide more condition-specific treatments, with fewer unwanted side effects. Indeed, there has been a recent drive to develop α5-selective benzodiazepine-site inverse agonists, since they may promote recovery following stroke (Clarkson *et al*., 2010), and improve learning and memory deficits in Down's syndrome (DS) and Alzheimer's disease (AD; discussed in detail in *Section* 1.3.1; Brickley and Mody, 2012).

Neurosteroids (e.g. allopregnanolone and tetrahydrodeoxycorticosterone (THDOC)) represent an important class of endogenous compounds that can biphasically modulate $GABA_A$ receptor function. At low (nM) concentrations, neurosteroids have been demonstrated to potentiate GABA currents via a

conserved glutamine residue in the α subunit (e.g. $\alpha1^{Q241}$; Hosie *et al*., 2006, 2009), while higher (μM) concentrations are capable of directly activating $GABA_A$ receptors via a distinct site at the α/β interface (Belelli and Lambert, 2005). The potentiating profile of neurosteroids is only minimally affected by which α or β isoform is incorporated into the receptor complex (Lambert *et al*., 2003). By comparison, neurosteroids produce a greater enhancement in efficacy at δ-containing receptors compared to their γ2-containing counterparts (Belelli *et al*., 2002; Brown *et al*., 2002; Wohlfarth *et al*., 2002), thus conferring some degree of selectivity between these two receptor isoforms, at least when studied in recombinant expression systems. However, since the potentiating neurosteroid binding site is entirely confined to the α subunit (Hosie *et al*., 2009), this selectivity profile is unlikely to reflect a direct interaction of neurosteroids with the δ subunit. Instead, it is thought to reflect the relative ability of neurosteroids to increase the efficacy of a full agonist verses a partial agonist (Bianchi and Macdonald, 2003), since GABA is considered a partial agonist at δ-containing receptors, but a full agonist at γ2-containg receptors (Ebert *et al*., 1994; Mortensen *et al*., 2004). However, factors independent of subunit composition may also influence the modulatory actions of neurosteroids, as will be discussed in *Section* 1.2.3.

1.2. Tonic and Phasic currents in the CNS

$GABA_A$ receptors play a crucial role in controlling neuronal excitability. The functional outcome of $GABA_A$ receptor activation largely depends on the transmembrane electrochemical gradient of Cl^-, since $GABA_A$ receptors are significantly more permeable to Cl^- than HCO_3^- (by ~ 5 – fold; Bormann et al., 1987). In most mature neurons, the potassium-chloride co-transporter 2, KCC2, extrudes Cl^- to produce a chloride equilibrium potential (E_{Cl}) that is usually more negative than the resting membrane potential. Consequently, the activation of $GABA_A$ receptors produces a net influx of Cl^- ions, leading to membrane hyperpolarisation away from action potential threshold. However, in most immature (Ben-Ari *et al*., 2012), and some mature neurons (e.g. in hippocampal interneurons; Michelson and Wong, 1991; Banke and McBain, 2006; Song *et al*., 2011), the activation of $GABA_A$ receptors can lead to membrane depolarisation, due to the presence of a depolarising Cl^- electrochemical gradient set by the sodium, potassium and chloride co-transporter 1 (NKCC1; Ben-Ari *et al*., 2012). In both cases (whether Cl^- is depolarising or hyperpolarising), the activation of $GABA_A$ receptors can cause an increase in membrane conductance giving rise to a shunting of excitatory potentials, depending on their incoming temporal profile (Mitchell and Silver, 2003). Thus, $GABA_A$ receptors can reduce neuronal excitability via two main mechanisms: either by membrane hyperpolarisation and/or shunting inhibition (Farrant and Nusser, 2005).

$GABA_A$ receptor mediated signalling can occur via two main, spatially and temporally distinct forms of receptor activation: phasic and tonic. Phasic inhibition, involves the activation of synaptically located $GABA_A$ receptors by transiently high concentrations of GABA (in the mM range; Maconochie *et al*., 1994; Jones and Westbrook, 1995), released from presynaptic nerve terminals. This gives rise to inhibitory post-synaptic currents (IPSCs; see *Fig*. 1.4). In contrast, tonic inhibition involves the continuous activation of $GABA_A$ receptors residing outside inhibitory synapses (extrasynaptic), by low ambient GABA concentrations (ranging from nanomolar to low micromolar; Farrant and Nusser, 2005). Thus, whilst phasic currents provide a brief but intense inhibition of cell

excitation, tonic currents provide a low intensity, persistent inhibition, important for fine-tuning the ability of neurons to generate action potentials, but also for altering the input-output relationship, and gain (slope) of neuronal firing rates (Mitchell and Silver, 2003; Farrant and Nusser, 2005; Lee and Maguire, 2014).

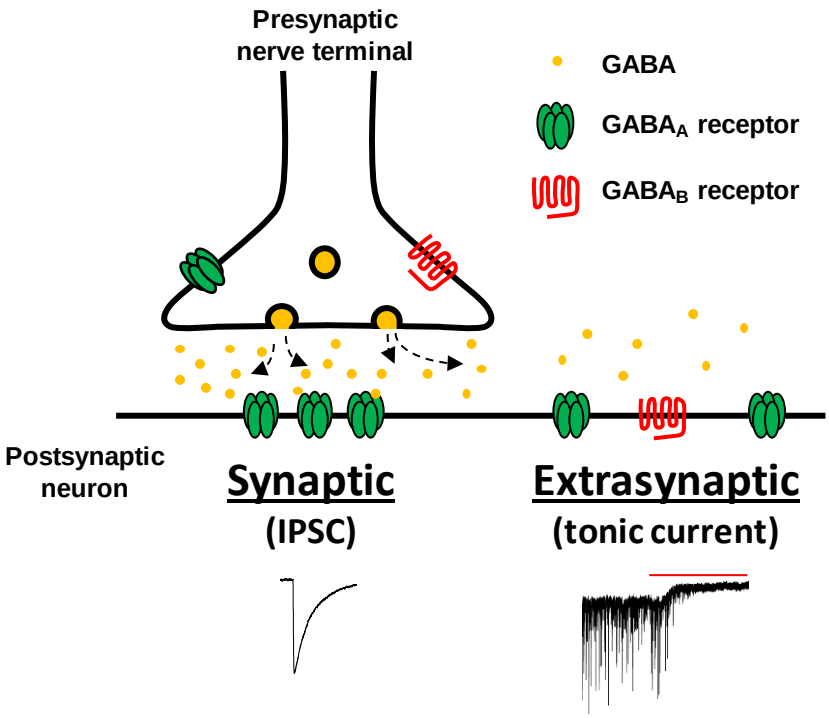

Figure 1.4 – A schematic of GABAergic transmission in the CNS

GABA is released from presynaptic nerve terminals, where it can activate ionotropic $GABA_A$ or metabotropic $GABA_B$ receptors. Activation of postsynaptic $GABA_A$ receptors residing in the synapse, gives rise to inhibitory post-synaptic currents (IPSCs), whereas a continuous activation of extrasynaptically located $GABA_A$ receptors by ambient GABA, can give rise to tonic currents. Note that the magnitude of a $GABA_A$-receptor mediated tonic current can be revealed by measuring the change in holding current induced by applying a $GABA_A$ receptor antagonist (e.g. for the duration indicated by the red horizontal line).

1.2.1. Subunit composition of synaptic and extrasynaptic $GABA_A$ receptors

Evidence indicates that distinct $GABA_A$ receptor isoforms mediate tonic and phasic currents in the CNS, and the identity of these receptors varies between different brain regions. Although tonic currents have been detected in several neuronal cell types (see Lee and Maguire, 2014; depicted in *Fig*. 1.5), the ensuing section will discuss the identities of tonic and phasic mediating $GABA_A$ receptors expressed in hippocampal pyramidal neurons, thalamocortical (TC) relay neurons and CGCs. These specific cell types were chosen since they demonstrate well-characterised tonic and phasic $GABA_A$ receptor conductances, which will be the main focus of this thesis (see *Section* 1.4).

CGCs were the first cell-type in which a $GABA_A$ receptor mediated tonic current was demonstrated (Kaneda *et al*., 1995). Protein and mRNA co-distribution studies indicated that mature CGCs showed a strong expression pattern for α1, α6, β2/3, γ2 and δ subunits (Laurie *et al*., 1992a; Wisden *et al*., 1992; Pirker *et al*., 2000; Hörtnagl *et al*., 2013). By analysing the subcellular distribution of these subunits using electron microscopy (EM) and immunofluorescence techniques, the δ subunit was demonstrated to reside exclusively at extrasynaptic sites, while the α1, α6, β2/3 and γ2 subunits were found to be concentrated at synaptic sites, but could also be detected at extrasynaptic sites (Fritschy *et al*., 1992; Somogyi *et al*., 1996; Nusser *et al*., 1998). These data, combined with co-immunoprecipitation studies (Khan *et al*., 1994; Pollard *et al*., 1995), indicated that CGCs most likely express α1βγ2, α6βγ2, α6βδ, and α1α6βγ2 receptors (Sieghart and Sperk, 2002). The synaptic location of α1βγ2, α6βγ2, and α1α6βγ2 receptors indicates that these receptor isoforms are likely to mediate phasic currents in CGCs, while tonic currents are likely to be mediated by α6βδ receptors, since this receptor isoform is found exclusively at extrasynaptic sites, and exhibits a high sensitivity to GABA (Saxena and Macdonald, 1996). In accord with this, CGCs from α6 knockout (α6-/-) mice, which also lack the δ subunit (Jones *et al*., 1997), show a complete ablation of the $GABA_A$ receptor mediated tonic currents (Brickley *et al*., 2001).

In pyramidal neurons of the *Cornu ammonis* (CA) regions 1 and 3 of the hippocampus, α5-containing receptors may contribute to both tonic and phasic currents. In CA1/CA3 pyramidal neurons, immunostaining and *in situ* hybridisation studies suggest that α5 subunits localise to both synaptic (Serwanski *et al*., 2006), and extrasynaptic sites (Fritschy *et al*., 1998; Brünig *et al*., 2002; Crestani *et al*., 2002), thus making them ideally situated to mediate both types of inhibitory neurotransmission. However, knocking out the α5 subunit has little effect on either miniature, or spontaneous IPSCs, suggesting that α5-containing receptors do not significantly contribute to phasic inhibitory currents (Caraiscos *et al*., 2004; Glykys *et al*., 2008). However, this lack of effect on IPSCs might also arise from compensatory changes in receptor expression, which is a major caveat of gene knockout studies. Indeed, Prenosil *et al*. (2006) demonstrated that slow IPSCs (but not fast IPSCs) from wild-type (WT) mice were partially inhibited by 11,12,13,13a-Tetrahydro-7-methoxy-9-oxo-9*H*-imidazo[1,5-*a*]pyrrolo[2,1-c][1,4]benzodiazepine-1-carboxylic acid (L-655,708; an α5-selective benzodiazepine inverse agonist), while another study demonstrated that the diazepam sensitivity of slow IPSCs was ablated in mice expressing a diazepam-insensitive α5 subunit (Zarnowska *et al*., 2009). Thus, α5-containing receptors appear to mediate slow, but not fast IPSCs.

CA1 pyramidal neurons from α5 knockout (α5-/-) mice exhibit reduced tonic currents (Caraiscos *et al*., 2004; Glykys *et al*., 2008), indicating that α5-containing receptors contribute to tonic currents. However, by using a pharmacological approach, CA1 tonic currents were demonstrated to be either inhibited (Caraiscos *et al*., 2004), or unaffected (Prenosil *et al*., 2006) by L-655,708, indicating that although they are present at extrasynaptic sites, α5-containing receptors may not contribute to CA1 tonic currents. However, some of these conflicting observations may be explained by differing ambient GABA levels between different slice preparations, which may influence the $GABA_A$ receptor isoforms that contribute to tonic currents, and the inhibitory profile of L-655,708 (Scimemi *et al*., 2005). Moreover, other $GABA_A$ receptor subtype(s) may also contribute to CA1/CA3 tonic currents, especially since α5-/- mice display a residual tonic current (Caraiscos *et al*., 2004; Glykys *et al*., 2008). Given the extrasynaptic distribution of δ subunits on hippocampal pyramidal

neurons (Mangan *et al*., 2005), and that double α5-/-, δ-/- knockout mice show a complete loss of the residual tonic currents present in α5-/- single mutant mice (Glykys *et al*., 2008), it is likely that δ-containing receptors also contribute to CA1/CA3 tonic currents. However, there is also evidence that αβ receptors may partly mediate CA1/CA3 tonic currents (Mortensen and Smart, 2006), and so contributions by other $GABA_A$ receptor subtypes cannot be discounted.

In mature thalamic relay neurons, phasic currents are largely thought to be mediated by α1βγ2 receptors since these subunits have been detected at synaptic (and extrasynaptic) sites by EM (Soltesz *et al*., 1990). In accord, the IPSCs recorded from adult mice expressing a diazepam-insensitive α1 subunit mice appear to be largely insensitive to diazepam (Peden *et al*., 2008). However, α2βγ2 receptors may also contribute to phasic currents within the first month of postnatal development (Okada *et al*., 2000; Peden *et al*., 2008). Tonic currents have only been reported in a few thalamic nuclei, including the ventrobasal nucleus (VB; the somatosensory thalamus; Belelli *et al*., 2005; Jia *et al*., 2005; Herd *et al*., 2009), the medial geniculate body (the auditory thalamus; Richardson *et al*., 2011)) and the dorsal lateral geniculate nucleus (dLGN; the visual thalamus; Cope *et al*., 2005; Bright *et al*., 2007; Nani *et al*., 2013; Ye *et al*., 2013). Several studies indicate that tonic currents in the thalamus are restricted to thalamic relay neurons, and are predominantly mediated by α4βδ receptors. This $GABA_A$ receptor isoform appears to be ideally suited to mediating tonic currents, owing to its high GABA sensitivity (Brown *et al*., 2002; Stórustovu and Ebert, 2006; Mortensen *et al*., 2010), and slower desensitisation profile, relative to synaptic γ2-containing receptors (Brown *et al*., 2002; Feng *et al*., 2009; Mortensen *et al*., 2010; Bright *et al*., 2011). Indeed, high expression levels of α4 and δ subunits have been detected in the thalamus (Wisden *et al*., 1992; Pirker *et al*., 2000; Hörtnagl *et al*., 2013), and co-immunoprecipitation studies indicate that δ subunits only co-assemble with α4 subunits in this brain region (Sur *et al*., 1999). Moreover, thalamic relay neurons from α4 knockout mice show a complete loss of $GABA_A$ receptor mediated tonic currents (Chandra *et al*., 2006), and δ knockout mice show considerably diminished responses to the δ subunit-selective agents, 4,5,6,7-

tetrahydroisoxazolo[5,4-c]pyridin-3-ol (THIP; Herd *et al*., 2009) and 4-Chloro-*N*-[2-(2-thienyl)imidazo[1,2-a]pyridin-3-yl]benzamide (DS2; Jensen *et al*., 2013).

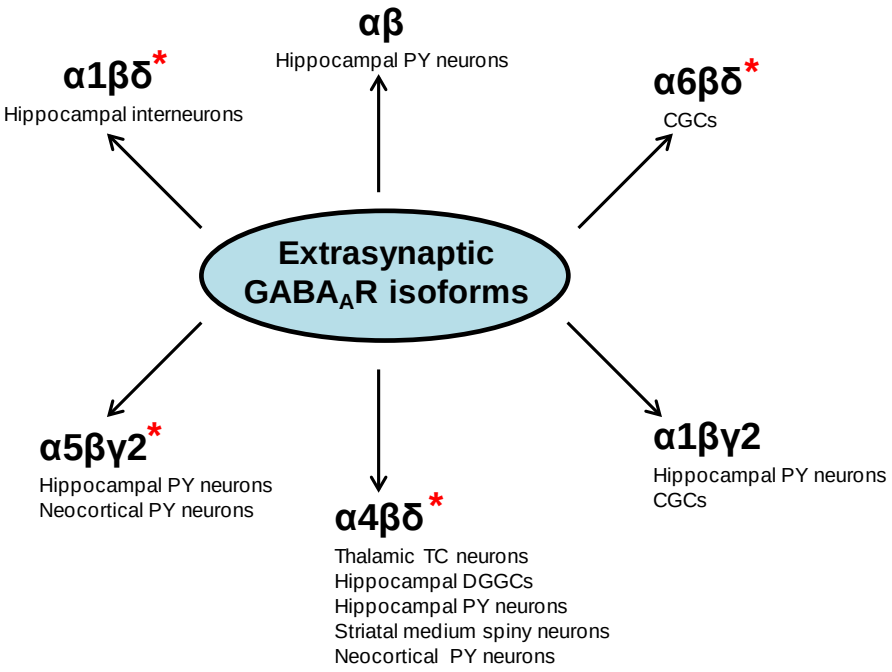

Figure 1.5 – Extrasynaptic GABA$_A$ receptor isoforms

Schematic showing the major GABA$_A$ receptor isoforms found at extrasynaptic sites in the CNS, along with their cellular distributions. Isoforms highlighted with a red astrix (*) represent high affinity extrasynaptic GABA$_A$ receptors that are proposed to mediate tonic currents in the CNS. Tonic currents have been identified in several cell types, including hippocampal pyramidal (PY) neurons, cerebellar granule cells (CGCs), dentate gyrus granule cells (DGGCs), thalamocortical (TC) relay neurons, neocortical PY neurons and striatal medium spiny neurons (Farrant and Nusser, 2005; Brickley and Mody, 2012; Lee and Maguire, 2014).

1.2.2. Sources and estimates of ambient GABA levels

The magnitude of tonic currents is critically defined by the extracellular concentration of GABA. On the basis of microdialysis studies, *in vivo* estimates of ambient GABA range from 30 nM to 2.9 μM (Glaeser and Hare, 1975; Lerma *et al*., 1986; de Groote and Linthorst, 2007; Wlodarczyk *et al*., 2013). However, these estimates may reflect conditions under pathological rather than physiological states, since microdialysis probes can induce extensive tissue damage and inflammation, which may alter local neurotransmitter levels (van der Zeyden *et al*., 2008). Moreover, the chromatographic method that is commonly used to quantify dialysate GABA levels is sensitive to changes in pH, which may influence the levels of GABA detected (van der Zeyden *et al*., 2008). In addition, GABA levels may vary between tissue compartments, and indeed during different behavioural states. For instance, in the cat thalamus, GABA levels are higher during non-rapid eye movement (NREM) sleep relative to waking states (Kékesi *et al*., 1997), while GABA levels in the rat hippocampus are elevated during stressful situations (e.g. exposure to an unfamiliar cage; de Groote and Linthorst, 2007).

There is debate regarding the source of ambient GABA responsible for the activation of extrasynaptic $GABA_A$ receptors. Although a neuronal origin is likely, agents that affect neurotransmitter release (e.g. tetrodotoxin (TTX), or low Ca^{2+}) have yielded inconsistent results in microdialysis studies, making it difficult to confirm, or rule out, other sources (Timmerman and Westerink, 1997; van der Zeyden *et al*., 2008). *In vitro*, ambient GABA appears to be predominantly derived from synaptic spillover, since reducing neurotransmitter release with TTX or low Ca^{2+}, also reduces $GABA_A$ receptor mediated tonic currents in CA1 pyramidal neurons, CGCs and TC relay neurons (Kaneda *et al*., 1995; Brickley *et al*., 1996; Rossi *et al*., 2003; Bright *et al*., 2007, 2011; Glykys and Mody, 2007). However, some studies have also demonstrated TTX-insensitive tonic currents in adult CGCs and CA1 interneurons (Kaneda *et al*., 1995; Wall and Usowicz, 1997; Hamann *et al*., 2002; Song *et al*., 2013), leading to suggestions that non-vesicular derived GABA may also contribute to tonic currents (Rossi *et al*., 2003). In accord, it was recently suggested that GABA

release through bestrophin 1 (Best1) anion channels (Lee *et al*., 2010), or the reversal of GABA transporters (see below; Wu *et al*., 2007; Héja *et al*., 2012) may also contribute to ambient GABA levels, although it is unclear whether this occurs under physiological conditions (see Diaz *et al*., 2011; Kersanté *et al*., 2013), or just during pathological disease states (see *Section* 1.3.1).

Under physiological conditions, GABA transporters (GATs) can tightly regulate ambient GABA levels, by bidirectionally transporting GABA into or out of the extracellular space. The direction of transport is dependent on the electrochemical gradients of co-transported solutes (GABA, Na^+ and Cl^-; Scimemi, 2014), which can be transported with a stoichiometry of $2Na^+$: $1Cl^-$: 1GABA. Based on this stoichiometry, GATs are predicted to reach equilibrium when extracellular GABA levels are 0.1 to 0.4 µM (Attwell *et al*., 1993; Richerson and Wu, 2003), indicating that ambient GABA levels will be maintained within this small range.

To date, six GABA transporters, which are members of the solute carrier 6 (SLC6) family, have been identified, which in humans and rats, are defined as GAT1, GAT2, GAT3, betaine-GABA transporter 1 (BGT1), taurine transporter (TauT) and creatine transporter 1 (CT1; Scimemi, 2014). In mice, the nomenclature for BGT1, GAT2 and GAT3 is different, and are assigned as GAT2, GAT3 and GAT4, respectively. The best characterised of these are GAT1, GAT2 and GAT3, although GAT1 and GAT3 represent the major isoforms expressed in the brain (GAT2 is found almost exclusively in the leptomeninges; Scimemi, 2014). Immunohistochemical and *in situ* hybridisation studies indicate that GAT1 and GAT3 are widely distributed throughout the brain (Borden, 1996; Minelli *et al*., 1996), although they show distinct cellular and subcellular distributions. While GAT1 is mainly confined to axonal terminals in the neocortex (Minelli *et al*., 1995; Ribak *et al*., 1996; Yan *et al*., 1997), GAT3 is predominantly localised to astrocytes (Minelli *et al*., 1996; Ribak *et al*., 1996). However, these distributions may vary between brain regions, since GAT1 is exclusively localised to astrocytes in the thalamus (De Biasi *et al*., 1998; Vitellaro-Zuccarello *et al*., 2003), and is additionally found on both astrocytic cell membranes in the cortex and hippocampus (Minelli *et al*., 1995; Ribak *et al*., 1996; Vitellaro-Zuccarello *et al*., 2003).

GAT1 and GAT3 appear to play distinct roles in regulating tonic and phasic currents. The largely synaptic location of GAT1 indicates that it may be involved in regulating the time course of GABAergic synaptic transmission and/or limiting the spatial and temporal extent of GABA spillover from the synaptic cleft (Scimemi, 2014). Indeed, evidence suggests that GAT1 inhibitors (e.g. 1,2,5,6-Tetrahydro-1-[2-[[(diphenylmethylene)amino]oxy]ethyl]-3-pyridinecarboxylic acid hydrochloride (NNC-711) and tiagabine) can alter the time course of GABAergic synaptic currents, although this modulation is heavily dependent on a number of factors, including the density of transporters, the magnitude and duration of the synaptic GABA transient, and the number of simultaneously active synapses (Dalby, 2003; Overstreet and Westbrook, 2003; Scimemi, 2014). Recent evidence indicates that GAT1 also plays a critical role in regulating ambient GABA levels derived from vesicular sources (Kersanté *et al*., 2013; Song *et al*., 2013). By contrast, GAT3 appears to be more important for regulating ambient GABA derived from non-vesicular sources (Kersanté *et al*., 2013; Song *et al*., 2013), although it may also regulate GABA levels derived from vesicular sources when GAT1 function is compromised, or during sustained neuronal activity (Keros and Hablitz, 2005; Kersanté *et al*., 2013). Thus, GAT1 and GAT3 appear to act synergistically to control ambient GABA derived from vesicular and non-vesicular sources (Keros and Hablitz, 2005; Kersanté *et al*., 2013; Song *et al*., 2013).

1.2.3. Pharmacology of tonic and phasic currents

Given that extrasynaptic $GABA_A$ receptors are the main mediators of tonic inhibition in the CNS, and may contribute to the pathology of several neurological disorders (Brickley and Mody, 2012; Egawa and Fukuda, 2013; Rudolph and Möhler, 2014; Whissell *et al*., 2014), there has been a huge drive in recent years to identify compounds that can preferentially modulate their activities. Several synthetic and endogenously expressed compounds have been identified as functional modulators of either α5 or δ subunit-containing receptors, some of which are described below, and also listed in *Table* 1.1.

Several α5-selective benzodiazepine site inverse agonists have been developed in recent years, including 1,2,4-Triazolo[3,4-a]phthalazine, 3-(5-methyl-3-isoxazolyl)-6-[(1-methyl-1H-1,2,3-triazol-4-yl)methoxy]-,3-(5-Methylisoxazol-3-yl)-6-(1-methyl-1,2,3-triazol-4-yl)methoxy-1,2,4-triazolo[3,4-a]phthalazine (α5IA), L-655,708, and 3-bromo-10-(difluoromethyl)-9*H*-benzo[f]imidazo[1,5-a][1,2,4]triazolo[1,5-d][1,4]diazepine (RO-493851; Atack *et al*., 2006; Ballard *et al*., 2009; Atack, 2010). The α5-selective profile of these compounds is largely based on their relatively low affinities and/or efficacies for other α(1 - 3)βγ2 isoforms. For instance, α5IA binds to recombinant α(1,2,3 or 5)βγ2 receptors with similar affinities, but modulates α5-containing receptors to a greater extent (~ 40 % inhibition; Atack, 2010). By comparison, L-655,708 modulates α2βγ2 and α5βγ2 receptors to a similar extent (~ 20% inhibition), but at a maximally effective concentration, is classed as an α5-selective agent based on its higher affinity for α5βγ2 receptors (K_i values: α5βγ2 ~ 1 nM and α2βγ2 ~ 50 nM; Atack *et al*., 2006). Varying effects of these compounds have been observed in hippocampal neurons in slice preparations (Caraiscos *et al*., 2004; Prenosil *et al*., 2006), possibly due to low ambient GABA concentrations *in vitro*. Nonetheless, α5-selective negative allosteric modulators may be therapeutically useful as cognitive enhancers, or improving functional recovery after stroke (see *Section* 1.3).

The orthosteric agonist, THIP, is often described as a ‘super-agonist’ at recombinant αβδ and αβ receptors (Brown *et al*., 2002; Stórustovu and Ebert, 2006; Mortensen *et al*., 2010), due to its higher macroscopic efficacy at these two receptor isoforms, relative to GABA. By comparison, THIP only acts as a partial agonist at γ2-containing receptors (Brown *et al*., 2002; Mortensen *et al*., 2010), and also appears to act as a partial agonist at αβδ receptors under steady-state conditions (Houston *et al*., 2012). The δ-selective profile of THIP arises from its low apparent affinity for γ2-containing receptors (EC_{50} ~ 100 μM) relative to δ-containing receptors (EC_{50} ~ 10 μM), leading to low concentrations of THIP (500 nM – 1 μM) being selective for δ-containing receptors (Brown *et al*., 2002; Stórustovu and Ebert, 2006; Mortensen *et al*., 2010). In accord, low δ-selective concentrations of THIP enhance tonic currents, but not phasic currents, in WT, but not δ-/- mice (Cope *et al*., 2005; Herd *et al*., 2009),

indicating that THIP can selectively activate δ-containing receptors in neurons, as well as in heterologous expression systems. Of therapeutic interest, THIP was demonstrated to act as a hypnotic in humans (Faulhaber *et al*., 1997), which was attributable to its selective actions on δ-containing receptors (Winsky-Sommerer *et al*., 2007). Unfortunately, THIP failed Phase III clinical trials as a hypnotic, due to adverse effects (*Table* 1.1.1; Brickley and Mody, 2012), but remains a widely used tool for the identification and characterisation of δ-mediated tonic currents (e.g. Cope *et al*., 2005; Drasbek and Jensen, 2006).

As discussed in *Section* 1.1.5 potentiating neurosteroids exert their effects on all major $GABA_A$ receptor isoforms, but can enhance the efficacy of δ-containing receptors to a far greater extent than γ2-containing receptors (Belelli *et al*., 2002; Brown *et al*., 2002; Wohlfarth *et al*., 2002). In neurons, neurosteroids can enhance both phasic and tonic GABA-evoked currents, by respectively prolonging IPSC decay times (Belelli and Herd, 2003), and/or increasing the magnitude of tonic currents (Stell *et al*., 2003). However, the relative neurosteroid sensitivities of tonic and phasic currents appears to vary between different cell types, with some cells displaying tonic currents that are more sensitive than synaptic currents (e.g. DGGCs and CGCs; Stell *et al*., 2003; Bright and Smart, 2013), whereas other cells display synaptic currents more, or equally as sensitive, to neurosteroid modulation (e.g. VB and dLGN relay neurons; Porcello *et al*., 2003; Cope *et al*., 2005). These discrepancies do not necessarily correlate with differences in subunit composition. For instance, TC neurons and DGGCs show different neurosteroid sensitivities but are both proposed to express α4βδ-mediated tonic currents. Instead, neurosteroid sensitivity may be additionally influenced by a wide range of factors including the cell type studied, ambient GABA levels, the recording temperature and phosphorylation status (extensively reviewed by Herd *et al*., 2007). Nonetheless, neurosteroids are important endogenous modulators of $GABA_A$ receptor function, and the variability in neurosteroid sensitivity might mean that some cells are modulated under basal conditions, whereas others cell types might only be modulated when neurosteroid levels are increased (Harney *et al*., 2003).

Only a couple of synthetic compounds have been identified as positive allosteric modulators of δ-containing $GABA_A$ receptors. Recently, N-[2-Amino-4-[[(2,4,6-trimethylphenyl)methyl]amino]phenyl]-carbamic acid-ethyl ester (AA29504), an analogue of the anti-epileptic drug (AED) retigabine was shown to preferentially increase the macroscopic efficacy of αβδ receptors but not αβγ receptors, consistent with a δ-selective profile (Hoestgaard-Jensen *et al*., 2010). However, AA29504 also increased the GABA potency of both αβγ and αβδ receptors, and enhanced the activity of voltage gated K^+ channels, indicating that its selectivity profile may be limited (Hoestgaard-Jensen *et al*., 2010). In neurons, a δ-selective concentration of AA29504 (1 μM) showed no effect on tonic, or phasic, currents under control conditions, but could increase the magnitude of THIP-induced currents (Hoestgaard-Jensen *et al*., 2010; Vardya *et al*., 2012). Thus, AA29504 can potentiate δ-mediated currents in neurons, but its modulatory actions may be dependent on ambient GABA levels, which may have been too low under control conditions (Hoestgaard-Jensen *et al*., 2010; Vardya *et al*., 2012).

Another recently identified δ-selective positive allosteric modulator is DS2 (Wafford *et al*., 2009; Jensen *et al*., 2013). This compound was demonstrated to significantly increase the efficacy of GABA at α4/6βδ receptors (% control EC_{20} GABA response ~ 1600 %), whilst only having modest effects on α1βγ2 receptors (% EC_{20} GABA response: ~ 140 %). Since DS2 does not appear to act via the same site as muscimol (an orthosteric agonist), flumazenil (a benzodiazepine antagonist), etomidate, neurosteroids, or barbiturates (Jensen *et al*., 2013), its actions are likely to be mediated via a novel site, which has yet to be identified. Consistent with its δ-selective profile, DS2 has been demonstrated to enhance tonic but not phasic currents in TC neurons and CGCs (Wafford *et al*., 2009; Ye *et al*., 2013), and its actions are considerably diminished in TC neurons from δ-/- mice (Jensen *et al*., 2013).

Thus, several δ-selective compounds exist that can enhance the activities of αβδ receptors. However, there is a significant lack of synthetic compounds that can selectively reduce δ-mediated tonic currents, without affecting γ2-mediated phasic currents. In fact, some groups have demonstrated that low concentrations of gabazine (SR-95531), a $GABA_A$ receptor competitive

antagonist, can paradoxically inhibit phasic currents over tonic currents (Bai *et al*., 2001; Yeung *et al*., 2003; McCartney *et al*., 2007; Park *et al*., 2007; Yamada *et al*., 2007; Bieda *et al*., 2009), although other groups have been unable to replicate these findings (e.g. Cope *et al*., 2005). Similarly, the open channel blocker, penicillin, has also been demonstrated to preferentially inhibit phasic currents (Yeung *et al*., 2003; Feng *et al*., 2009), indicating that both gabazine and penicillin are unsuitable for selectively inhibiting δ-mediated tonic currents.

By contrast, the endogenously expressed cations, Zn^{2+} and Cu^{2+} have been shown to preferentially inhibit δ-containing receptors over γ2-containing receptors in recombinant expression systems and/or neurons (Saxena and Macdonald, 1994; Stórustovu and Ebert, 2006; McGee *et al*., 2013). Recombinant $GABA_A$ receptors containing the γ2 subunit show a low sensitivity to the inhibitory actions of Zn^{2+}, as demonstrated by the relatively high concentration of Zn^{2+} required to produce half-maximal inhibition of GABA responses at αβγ receptors (IC_{50}: 300 μM; Krishek *et al*., 1998; Hosie *et al*., 2003). By contrast, αβ and αβδ receptors show a higher sensitivity to Zn^{2+} inhibition, displaying IC_{50}s of ~ 100 nM and ~ 10 μM respectively (Krishek *et al*., 1998; Hosie *et al*., 2003; Stórustovu and Ebert, 2006). Similarly, Cu^{2+} was also demonstrated to preferentially inhibit αβδ receptors (IC_{50} ~ 65 nM) over αβγ receptors (IC_{50} ~ 85 μM; McGee *et al*., 2013). However, it is important to note that the actions of Zn^{2+} and Cu^{2+} are not restricted to $GABA_A$ receptors, since they can also modulate the activities of other ion channels within the CNS (e.g. K^+ channels; Mathie *et al*., 2006). Thus, their use as δ-selective $GABA_A$ receptor-inhibitors is limited.

Table 1.1 – The isoform selectivity of pharmacological agents

Compound	Mechanism of action	Therapeutic implications/ References
αβγ-selective		
Classical BDZ agonists e.g. diazepam	PAM (α1, 2, 3 and 5)	BDZs are widely (but with restrictions) prescribed for insomnia and anxiety disorders (Rudolph and Knoflach, 2011).
δ-selective		
THIP (0.5 - 1 μM)	Orthosteric agonist	Hypnotic, failed Phase III clinical trials due to adverse effects e.g. hallucinations and disorientation (Brickley and Mody, 2012).
AA29504	PAM	Yet to be characterised (Hoestgaard-Jensen *et al*., 2010; Vardya *et al*., 2012).
DS2	PAM	Poor BBB penetrability (Wafford *et al*., 2009; Jensen *et al*., 2013).
α5-selective NAMs		
α5IA	BDZ inverse agonist (max. efficacy ~ 40 %)	Increases learning and memory, but also induced renal toxicity in pre-clinical screens (Dawson *et al*., 2006; Atack, 2010)
L-655,708	BDZ inverse agonist (max. efficacy ~ 20 %)	Cognitive enhancer but also anxiogenic (Navarro *et al*., 2002; Atack *et al*., 2006).
RO-493851	BDZ inverse agonist (max. efficacy ~ 40 %)	Enhances cognitive function in Wistar rats (Ballard *et al*., 2009) and Ts65Dn mice (Braudeau *et al*., 2011; Martínez-Cué *et al*., 2013). Currently in Phase I clinical trial for DS (Rudolph and Möhler, 2014).

A list of subtype-selective compounds for the different $GABA_A$ receptor isoforms. Abbreviations: BDZ (benzodiazepine); PAM (positive allosteric modulator); BBB (blood-brain barrier); NAM (negative allosteric modulator); DS (Down's syndrome).

1.3. Pathophysiological conditions associated with elevated $GABA_A$ receptor tonic conductances

Impaired GABAergic neurotransmission has been implicated in a wide range of neurological disorders, including epilepsy, affective and stress disorders, autism spectrum disorders (e.g. Fragile X syndrome) and cognitive disorders. Although many of these conditions are associated with alterations in phasic transmission, and/or reduced tonic currents (extensively reviewed by Brickley and Mody, 2012; Egawa and Fukuda, 2013; Whissell *et al*., 2014), elevated tonic currents have also been implicated in the pathogenesis of several of these conditions. The following section will focus on neurological disorders in which elevated tonic currents have been implicated, since the aim of this thesis is to investigate a way of pharmacologically reducing tonic currents for such conditions (see *Section* 1.4).

1.3.1. Learning and memory/Cognitive impairments

Cognitive behaviours such as attention, learning, memory, and sensory encoding are thought to involve rhythmic γ-oscillations (30 – 120 Hz) in the activity of cortical networks (Mann and Mody, 2010; Rudolph and Möhler, 2014). The generation of these γ-oscillations is widely believed to depend on the rhythmic output of local GABAergic interneurons in the hippocampus, which modulate $GABA_A$ receptor-mediated phasic inhibition (Mann and Mody, 2010; Rudolph and Möhler, 2014). However, γ-oscillations are also modulated by extrasynaptic $GABA_A$ receptors, since δ-/- and α5-/- mice show altered γ-oscillation profiles (Towers *et al*., 2004; Mann and Mody, 2010). In particular, the α5 subunit appears to be critical for regulating learning and memory, since α5-/- mice show an enhanced spatial learning profile (Collinson *et al*., 2002), while benzodiazepine insensitive $\alpha5^{H105R}$ mice, which also show a partial reduction in α5 subunit expression, also show enhanced associative learning (Crestani *et al*., 2002; Yee *et al*., 2004). Similarly, pharmacological agents that

enhance, or inhibit, α5-mediated tonic currents also modulate learning and memory. The general anaesthetic etomidate, which acts as a positive allosteric modulator of $GABA_A$ receptors, was shown to impair hippocampal-dependent learning, and long-term potentiation (the main form of synaptic plasticity thought to underlie learning and memory; Bliss and Collingridge, 1993; Malenka and Bear, 2004) in WT mice, but not α5-/- mice, indicating that its amnesic actions occur via an α5-dependent mechanism (Cheng *et al*., 2006; Martin *et al*., 2009). Conversely, α5-selective benzodiazepine-site inverse agonists, such as α5IA, L-655,708 and RO-493851 (listed in *Table* 1.1) have been demonstrated to improve learning and cognitive behaviours in rodents (Navarro *et al*., 2002; Atack *et al*., 2006; Ballard *et al*., 2009; Atack, 2010), indicating that α5-containing receptors impair such processes. In addition, the selective activation of δ-containing receptors has also been demonstrated to impair cognitive functions, since THIP was found to impair LTP and memory behaviours in WT mice but not δ-/- mice (Whissell *et al*., 2014).

It has been proposed that enhanced hippocampal tonic currents may contribute to cognitive deficits in Down's syndrome (DS; Lott and Dierssen, 2010), although decreased tonic currents have also been reported in CGCs from Ts65Dn mice (Szemes et al., 2013). DS is the most common chromosomal disorder in humans, which gives rise to a broad range of physical and mental disabilities, caused by a third copy (trisomy) of chromosome 21 (Lott and Dierssen, 2010). The cellular and molecular mechanisms that underlie cognitive deficits have largely been studied using Ts65Dn mice, which possess an extra copy of chromosome 16, the murine ortholog of human chromosome 21 (Davisson *et al*., 1990). Ts65Dn mice exhibit many of the features observed in DS, including deficits in LTP, and impaired spatial learning and object recognition (Kleschevnikov *et al*., 2004; Fernandez *et al*., 2007). It has been suggested that enhanced $GABA_A$ receptor-mediated inhibition may contribute to the cognitive deficits observed in these mice, since not only do they show an enhanced mIPSC frequency in dentate gyrus granule cells (DGGCs), but also, low (non-convulsive) concentrations of picrotoxin (a non-competitive $GABA_A$ receptor antagonist) restores LTP and improves object recognition in Ts65Dn mice (Kleschevnikov *et al*., 2004; Fernandez *et al*., 2007). Moreover, another

non-selective $GABA_A$ receptor antagonist, pentylenetetrazole (PTZ) was also shown to restore LTP and improve cognitive function in Ts65Dn mice, and promisingly, these effects persisted for up to two months after cessation of PTZ treatment (Fernandez *et al*., 2007; Colas *et al*., 2013). More specifically, α5-containing receptors appear to be particularly important for regulating learning and memory processes in Ts65Dn mice, since α5-selective inverse agonists, such as α5IA or RO4838581 have been demonstrated to improve learning capabilities in this DS mouse model (Navarro *et al*., 2002; Atack *et al*., 2006; Ballard *et al*., 2009; Atack, 2010; Braudeau *et al*., 2011; Martínez-Cué *et al*., 2013). Thus, selectively inhibiting α5-containing receptors may prove therapeutically useful for treating DS.

Alzheimer's disease (AD) represents another condition in which memory and cognitive function is greatly compromised. While β-amyloid (Aβ) and tau deposits represent the major pathological hallmarks of AD, the cellular mechanisms that underlie cognitive decline in AD patients have not yet been ascertained (although glutamate excitoxicity, Aβ-induced cell death, oxidative stress and lysosomal dysfunction have all been implicated; reviewed by Mattson, 2004). Intriguingly, recent studies have implicated excessive $GABA_A$ receptor activity as a contributory factor, since low (non-convulsive) concentrations of picrotoxin improve spatial learning and object recognition in the amyloid precursor protein/presenilin-1 (APP/PS1) mouse model of AD (Yoshiike *et al*., 2008). In particular, enhanced tonic currents may contribute to the cognitive deficits displayed by these mice, since enhanced $GABA_A$ receptor-mediated tonic currents were observed in two AD mouse models (APP/PS1 and 5xFAD mice; Jo *et al*., 2014; Wu *et al*., 2014), and L-655,708 not only reduced DGGC tonic currents, but also restored LTP and working memory in 5xFAD mice (Wu *et al*., 2014). The elevated tonic currents observed in APP/PS1 and 5xFAD mice correlated with a specific dysfunction of bestrophin 1 channels (Jo *et al*., 2014) or GAT3 (Wu *et al*., 2014), contributing to elevated ambient GABA levels (*Fig*. 1.6). Indeed, a similar mechanism may exist in humans, since post-mortem analysis of hippocampal tissue derived from AD patients showed elevated GABA expression levels (Jo *et al*., 2014; Wu *et al*., 2014). Thus, raised ambient GABA levels have been implicated in the pathology of AD, and

reducing tonic currents in the hippocampus may provide a useful way of improving cognitive function in AD patients.

1.3.2. Motor recovery after stroke

Recently, elevated tonic currents were also reported in a mouse model of cortical stroke, which could be attributed to impaired GABA uptake via GAT3 (Clarkson *et al*., 2010; *Fig*. 1.6). The increased tonic current was located in the peri-infarct zone, a region adjacent to the site of stroke damage, which allows for re-mapping of sensory processes from damaged areas. Thus, these elevated tonic currents may inhibit recovery by impairing neuronal development (Clarkson *et al*., 2010; Clarkson, 2012). The motor deficits displayed by mice following stroke induction, could be partially reduced by the α5-selective inverse agonist, L655,708, or by genetic knockout of the δ or α5 subunits, indicating that extrasynaptic $GABA_A$ receptors may impede functional recovery following stroke. Thus, reducing the activity of extrasynaptic $GABA_A$ receptors may provide a way of alleviating motor deficits following stroke (Clarkson *et al*., 2010).

1.3.3. Absence epilepsy

Absence seizures are non-convulsive epileptic seizures that are a defining feature of most idiopathic generalized epilepsies (IGE), including childhood absence epilepsy (CAE), juvenile myoclonic epilepsy (JME) and juvenile absence epilepsy (JAE; Crunelli and Leresche, 2002). The behavioural arrest and loss of consciousness exhibited during such seizures is accompanied by a characteristic 3Hz spike-wave discharge (SWD) in the electroencephalogram (EEG), which is thought to represent abnormal neuronal activity between the reciprocally connected thalamus and cortex (Crunelli and Leresche, 2002). The main cellular components implicated in the pathogenesis of absence seizures

are, pyramidal neurons in the cortex, TC relay neurons of the VB, and GABAergic interneurons of the thalamic reticular nucleus (NRT).

Although the precise cellular mechanisms underlying absence seizures are not fully understood, impaired GABA function has been implicated in the aetiology of this disorder. Several $GABA_A$ receptor subunit mutations have been identified in IGE patients suffering from typical absence seizures (e.g. $\alpha1^{A322D}$ and $\gamma2^{R43Q}$), that when expressed in heterologous expression systems seem to mostly reduce the activity of $GABA_A$ receptors by impairing subunit oligomerization, receptor trafficking and/or receptor function (Macdonald *et al*., 2010). Mice harbouring the best characterised $\gamma2^{R43Q}$ familial mutation exhibit absence seizures, and also demonstrate a region specific reduction of $GABA_A$ receptor mediated phasic currents in layer 2/3 cortical neurons (Tan *et al*., 2007). Moreover, reduced GABAergic transmission in the cortex has been suggested to specifically contribute to seizure generation, since local cortical applications of bicuculline (a $GABA_A$ receptor antagonist) can induce SWDs in cats (Steriade and Contreras, 1998).

In the thalamus, phasic currents show cell-type specific changes, which vary in different genetic models of absence seizures. For instance, the amplitudes of IPSCs recorded from NRT interneurons were either increased (Bessaïh *et al*., 2006), or unchanged (Cope *et al*., 2009), in the Genetic Absence Epilepsy Rat from Strasbourg (GAERS), whereas they appeared reduced in β3 knockout (β3-/-) mice (Huntsman *et al*., 1999). Moreover, $\gamma2^{R43Q}$ mice showed no change in NRT phasic currents (Tan *et al*., 2007). By contrast, TC neurons from rodent models of absence epilepsy show a more consistent lack of change in phasic currents (e.g. in GAERS, lethargic, tottering, $\gamma2^{R43Q}$ and β3-/- mice; Caddick *et al*., 1999; Huntsman *et al*., 1999; Bessaïh *et al*., 2006; Tan *et al*., 2007; Cope *et al*., 2009). Thus changes in thalamic phasic currents may not be necessary for the expression of seizures, since seizures can occur even in rodent models which exhibit normal phasic currents in NRT and TC neurons (e.g. $\gamma2^{R43Q}$).

By contrast, a robust enhancement of $GABA_A$-receptor mediated tonic currents has been observed in the TC neurons of several genetic and pharmacological models of absence epilepsy (Cope *et al*., 2009). These elevated tonic currents

were attributed to elevated ambient GABA levels, arising from reduced GABA uptake, or non-vesicular release of GABA by GAT1 (*Fig*. 1.6). Importantly, genetic, or pharmacological, disruption of GAT1 using GAT1 knockout (GAT1-/-) mice or, intrathalamically administered NNC-711, was sufficient for the expression of SWDs. Moreover, the expression of SWDs appeared to be dependent on thalamic δ-containing $GABA_A$ receptors since δ-/- mice were unaffected by pharmacological agents that typically induce seizures (e.g. γ-butyrolactone) in WT mice. Notably, the intrathalamic administration of THIP was sufficient to induce absence seizures in WT rats (Cope *et al*., 2009); and intrathalamic knockdown of the δ subunit in GAERS significantly reduced the frequency and duration of absence seizures (Cope *et al*., 2009). These findings are consistent with previous reports showing that systemic, or intrathalamic, administration of $GABA_A$ receptor agonists, such as muscimol and THIP, can induce SWDs in rats (Fariello and Golden, 1987; Danober *et al*., 1998). Moreover, these observations might also explain why some typical AEDs which promote GABAergic neurotransmission, such as vigabatrin (a GABA transaminase inhibitor) and tiagabine (a GABA uptake blocker), actually exacerbate absence seizures in both humans (Perucca *et al*., 1998) and several rodent models of absence epilepsy (Marescaux *et al*., 1992; Hosford and Wang, 1997).

Overall, these findings indicate that enhanced tonic inhibition, but not phasic currents, in TC neurons is a pre-requisite for seizure genesis in both genetic and pharmacological models of absence epilepsy. Specifically reducing δ-mediated tonic currents in TC neurons may provide a novel way of treating such absence seizures.

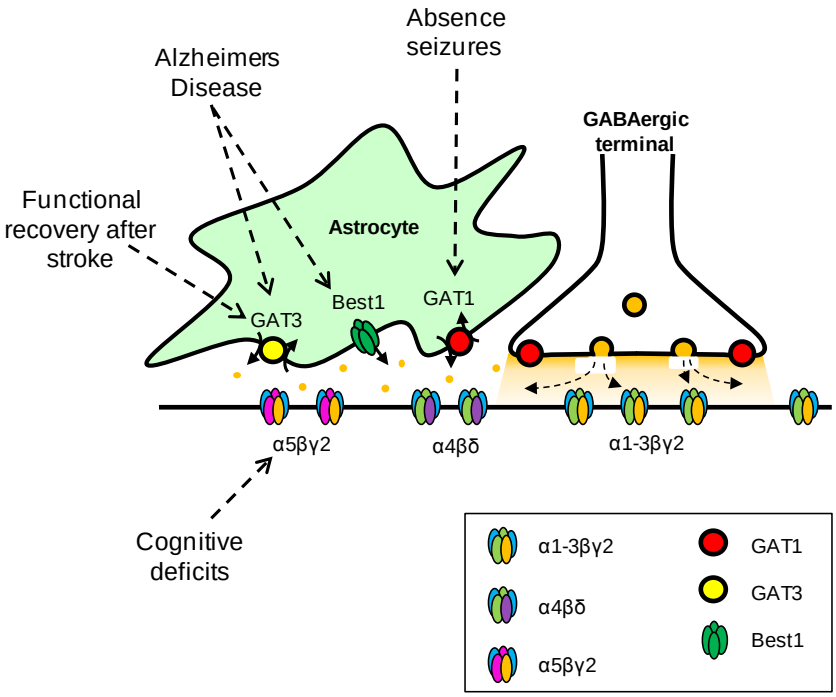

Figure 1.6 – Regulation of ambient GABA levels and CNS disorders

Ambient GABA levels are defined by the level of vesicular release, and the activities of GABA transporters present on astrocytic (e.g. GAT1 and GAT3) or axonal membranes (e.g. GAT1). In addition, non-vesicular release of GABA, for instance via bestrophin 1 (Best1) anion channels, may also contribute to ambient GABA levels. Enhanced tonic currents have been reported in the pathology of several neurological disorders (indicated by the dashed arrows), which can be attributed to a specific dysfunction in GAT1, GAT3 and/or Best1. Thus, selectively inhibiting α5- or δ-mediated tonic currents may provide a novel way of treating such disorders.

1.4. Thesis Aims:

As discussed in *Section* 1.3, selectively reducing tonic inhibition mediated by α5 or δ subunit-containing receptors may provide a novel way of improving cognitive function in DS and AD, improving motor function following stroke, or treating absence seizures (Brickley and Mody, 2012; Egawa and Fukuda, 2013; Rudolph and Möhler, 2014). In addition, this strategy might also prove useful for treating alcohol- or general anaesthetic-induced amnesia, since α5-selective inverse agonists have been demonstrated to improve learning and memory deficits in these conditions (Nutt *et al*., 2007; Saab *et al*., 2010; Zurek *et al*., 2012). Although one α5-selective inverse agonist, RO4938581, is currently in Phase I clinical trials for DS, clinical trials involving the other α5-selective inverse agonists (e.g. α5IA and L-655,708) have proved to be unsuccessful due to adverse effects (see *Table* 1.1; Rudolph and Möhler, 2014). Moreover, as discussed in *Section* 1.2.3, there is a significant lack of synthetic compounds that can selectively inhibit δ-containing $GABA_A$ receptors.

As an alternative to using $GABA_A$ receptor antagonists, it occurred to us that low efficacy partial agonists may be used as functional competitive antagonists, given their ability to compete with GABA for the orthosteric binding site, and their reduced ability to activate $GABA_A$ receptors (Krogsgaard-Larsen *et al*., 2002). Moreover, low efficacy partial agonists may be therapeutically useful, since they may show a reduced propensity to induce convulsions, or unwanted effects.

Inspired by this prospect, we chose to explore the functionally competitive antagonist profile of the weak partial agonist, 5-(4-piperidyl)isoxazol-3-ol (4-PIOL). This compound was initially identified as a weak partial agonist at $GABA_A$ receptors on cat spinal neurons (Byberg *et al*., 1987). Subsequently, it was demonstrated that 4-PIOL acted as a weak $GABA_A$ receptor agonist on cultured hippocampal neurons, cerebral cortical neurons, CGCs and on recombinant α1β2γ2 receptors (Falch *et al*., 1990; Kristiansen *et al*., 1991; Frølund *et al*., 1995; Hansen *et al*., 2001; Mortensen *et al*., 2002, 2004). However, given its low agonist efficacy (~ 1 – 2 % of the maximum GABA

response) and low agonist potency (EC_{50}: ~ 100 – 300 μM) at recombinant and native $GABA_A$ receptors, 4-PIOL was shown to display a dominant antagonist profile (Kristiansen *et al*., 1991; Frølund *et al*., 1995; Hansen *et al*., 2001; Ebert *et al*., 2002; Mortensen *et al*., 2002, 2004).

Given these observations and background, we chose to explore the functional profile of 4-PIOL on synaptic-type and extrasynaptic-type $GABA_A$ receptors expressed in a HEK293 recombinant expression system (*Chapter* 4), in addition to assessing the effects of 4-PIOL on tonic and phasic currents in hippocampal neurons (*Chapter* 5), CGCs (*Chapter* 5) and TC relay neurons (*Chapter* 6).

Before assessing the effects of 4-PIOL on recombinant $GABA_A$ receptors, the functional expression of each receptor was validated using subtype-selective pharmacological tools (*Chapter* 3). Moreover, since some functional discrepancies have been observed for δ-containing receptors expressed in recombinant expression systems (e.g. variable GABA sensitivities; Wallner *et al*., 2003), which in part, have been proposed to arise from variable subunit stoichiometries (discussed in *Section* 1.1.1; Barrera *et al*., 2008; Baur *et al*., 2009; Kaur *et al*., 2009; Wagoner and Czajkowski, 2010), we additionally probed the subunit stoichiometry of α4β3δ receptors (*Chapter* 3).

1.4.1. Summary of thesis aims

1. To validate the functional expression of recombinant αβγ and αβδ receptors in a HEK293 expression system (*Chapter* 3).

2. To determine the subunit stoichiometry of recombinant α4β3δ receptors (*Chapter* 3).

3. To evaluate the functional profile of 4-PIOL at typical synaptic and extrasynaptic receptor isoforms expressed in HEK293 cells (*Chapter* 4).

4. To characterise the effects of 4-PIOL on phasic and tonic currents in cultured hippocampal neurons (*Chapter* 5).

5. To determine the effects of 4-PIOL on phasic and tonic currents in CGCs (*Chapter* 5).

6. To characterise the effects of 4-PIOL on phasic and tonic inhibition in TC neurons (*Chapter* 6).

Chapter 2: Materials and Methods

2.1. Site directed mutagenesis

Site directed mutagenesis was performed to generate mutant cDNAs encoding $\alpha4^{L297S}$, $\beta3^{L284S}$ and δ_{sep}^{L288S} (*Fig*. 2.1). The δ subunit was tagged at the N-terminus (between residues 13 and 14 of the mature protein) with a super-ecliptic phluorin (sep; Ashby *et al*., 2004). Mutagenic oligonucleotides were designed (*Table* 2.1) and obtained from Sigma-Aldrich (Steinheim, Germany).

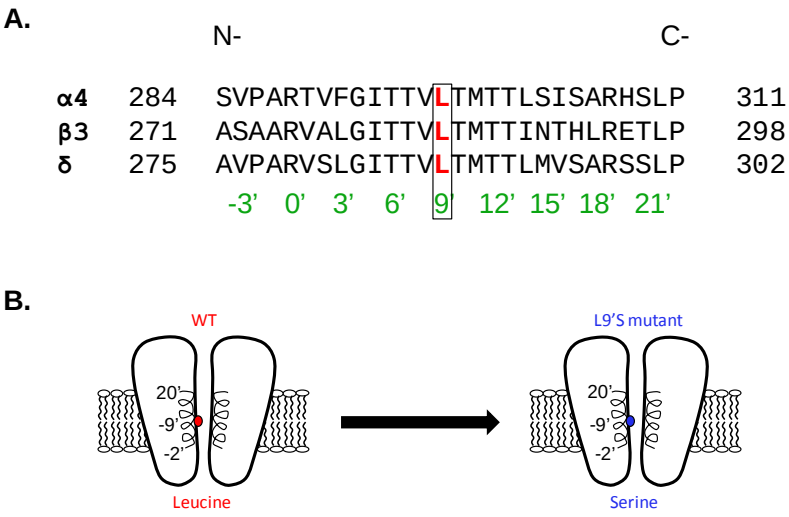

Figure 2.1 - Primary amino acid sequence alignment for the second transmembrane region (M2) of α4, β3 and δ subunits.

A. Prime notation (green) denotes the amino acids comprising the ion channel pore and is numbered from a conserved arginine residue at the base of M2, which is defined as 0' (Miller and Smart, 2010). The conserved hydrophobic 9' leucine residues (red) are boxed for α4, β3 and δ subunits, with their numbering appropriate to the mature subunit proteins. **B.** Diagram showing the approximate location of the 9' leucine residue (red) in the TM2 of a wild-type (WT) subunit. This residue was mutated to a hydrophobic serine residue (blue) in L9'S mutant subunits.

Construct	Forward primer sequence (5' – 3')	Reverse primer sequence (5' – 3')
$\alpha4^{L297S}$	CACGATGACCACCCTAAGCATC	GAGACTGTGGTTATTCCAAATACAG
$\beta3^{L284S}$	CCACCATGACAACCATCAACACTC	ACACGGTGGTAATCCCAAGGGCAA
$\delta_{sep}{}^{L288S}$	CGACAATGACCACACTCATGGTTA	ACACAGTGGTGATGCCTAGAGAT

Table 2.1 – PCR primers used to generate L9'S mutants.

Polymerase Chain Reactions (PCR) were assembled using a Phusion Hot Start High-Fidelity DNA Polymerase kit (Thermo Fischer Scientific, Rockford, Illinois, USA). The PCR was performed using a Px2 Thermal Cycler (Thermo Fischer Scientific Inc) programmed with the following protocol:

1. Activation: 98 °C for 30 s
2. DNA denaturation: 98 °C for 10 s,
3. Annealing: 65 °C for 30 s
4. Extension: 72°C for 5 min
5. Return to step 2, 40x
6. Final extension: 72°C for 10 min.

PCR products were run on a 1 % agarose gel, and successful PCR products were confirmed by the presence of a single band approximately 7 kb in size. The band for each construct was excised from the gel, and DNA purified using a QIAquick Gel Extraction Kit (Qiagen). The purified product was phosphorylated using T4 Polynucleotide Kinase (New England Biolabs, UK), and ligated overnight at 16 C, using T4 DNA Ligase (New England Biolabs).

The ligation products were transformed into competent 5-alpha *E.coli* cells (New England Biolabs), plated onto Luria broth (LB) agar plates containing 50 µg/mL ampicillin and incubated overnight at 37 C. Selected bacterial colonies were subsequently grown up overnight (as mini bacterial cultures) in LB culture medium, supplemented with 50 µg/mL ampicillin. The mutant cDNAs were purified using a QIAprep Spin Miniprep Kit (Qiagen), and successful mutations

were verified by DNA sequencing (DNA sequencing service, WIBR, UCL). Bacterial stocks expressing the desired mutant constructs were amplified further, by means of a maxi bacterial culture, and purified using a HiSpeed Plasmid Maxi Kit (Qiagen). The concentration of each cDNA was measured using a spectrophotometer (BioPhotometer; Eppendorf, Hamburg, Germany), prior to transfection in HEK293 cells. A summary of the cloning protocols used to generate L9'S mutants is shown in *Fig.* 2.2.

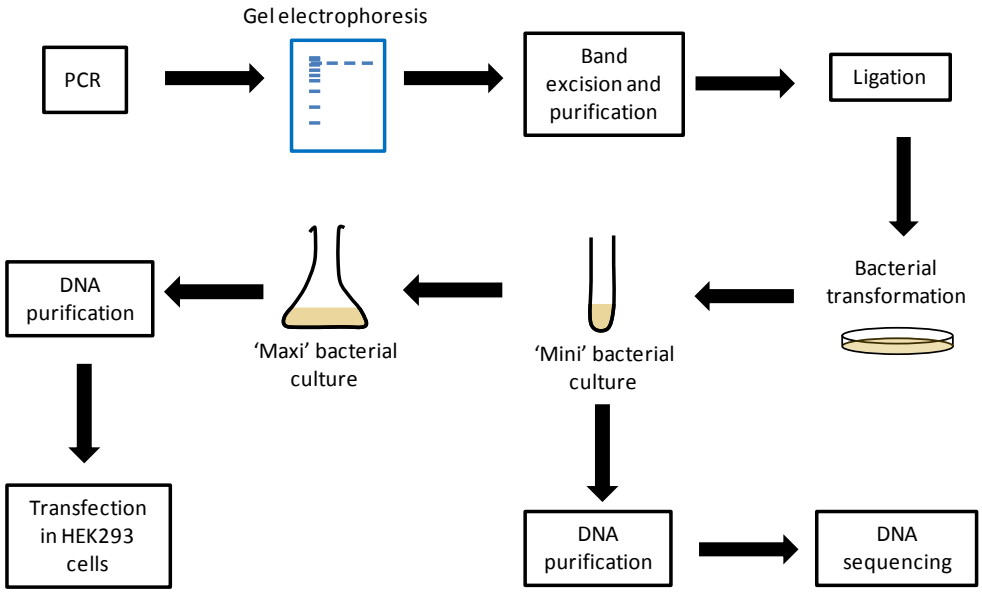

Figure 2.2 - A summary of the main cloning protocols used to generate L9'S mutants.

2.2. Reagents

Drugs solutions used for electrophysiological recordings were prepared, as described in *Table* 2.2.

Compound	Source	[Stock]	Stock solvent	[Final]
(+)-Bicuculline-methiodide	Sigma[1]	50 mM	Water	20 µM
CNQX	Abcam[2]	10 mM	Water	10 µM
D-AP5	Tocris[3]	20 mM	Water	20 µM
Diazepam	Roche[4]	10 mM	DMSO	< 0.5 µM
DS2	Tocris	10 mM	DMSO	10 µM
GABA	Sigma	1 M	Water	< 10 mM
Kynurenic acid	Sigma	-	aCSF	2 mM
NNC-711	Abcam	10 mM	Water	10 µM
Picrotoxin	Sigma	-	DMSO/Krebs	1 mM
4-PIOL	Gift from Dr Bente Frølund[5]	10 mM	Water or Krebs*	<1 mM
(S)-SNAP-5114	Tocris	20 mM	DMSO	20 µM
THIP	Tocris	1 mM	Water	1 µM
TTX	Abcam	0.5 mM	Water	0.5 µM
Zinc chloride	VWR[6]	1 M	Water	1 µM

Table 2.2 - List of compounds used during electrophysiological recordings.

List of compounds used during electrophysiological recordings, their sources, and details regarding stock, and final concentrations. Where drugs were dissolved in dimethyl sulfoxide (DMSO), the final concentration of DMSO was always < 0.05 % (v/v). *4-PIOL was either dissolved directly into Krebs solution or artificial cerebrospinal fluid (aCSF), or prepared from a 10 mM stock (in water). Concentrations of 4-PIOL > 100 µM reduced the pH of the Krebs solution, which was adjusted accordingly to pH 7.4 using 1 M NaOH. Manufacturer details: [1]Sigma-Aldrich Steinheim, Germany; [2]Abcam Biochemicals, Cambridge, UK; [3]Tocris Biosciences, Bristol, UK; [4]Roche, Basel, Switzerland; [5]University of Copenhagen, Copenhagen, Denmark; [6]VWR International, Leuven, Belgium.

2.3. HEK293 cell culture and Electrophysiology

2.3.1. HEK293 cell culture

HEK293 cells were cultured on 10 cm dishes (Greiner-Bio-One GmbH, Frickenhausen, Germany) in Dulbecco's modified Eagle's medium (DMEM) supplemented with 10 % v/v foetal calf serum (FCS), 100 U/mL penicillin-G, 100 µg/mL streptomycin and 2 mM glutamine (all from Gibco, Invitrogen Ltd.). Cells were incubated at 37°C in humidified 95 % air and 5 % CO_2 (BOC Healthcare, Manchester, UK). Upon reaching approximately 70 % confluency, cells were passaged at an appropriate dilution onto either 10 cm plates for maintenance, or onto 18 mm glass coverslips (VWR international) coated with 100 µg/mL poly-L-lysine (Sigma) for electrophysiology.

For passaging, cells were washed with 5 mL Hank's Balanced salt solution (HBSS; Gibco), and detached using 2 mL 0.05 % w/v trypsin-EDTA (Gibco). Cells were resuspended in 10 mL culture medium to quench the trypsin, and then pelleted at 1000 r.p.m for 2 min, using a MSE Mistral 2000 centrifuge (MSE, UK). The supernatant was aspirated, and the cell pellet was resuspended in 5 mL culture medium. Before plating, a single-cell suspension was achieved by tituration with a fire-polished glass Pasteur pipettes (VWR international).

2.3.2. HEK293 cell transfection

HEK293 cells were transfected approximately 4 hrs after plating, using a calcium phosphate protocol. A mixture of cDNAs encoding the required $GABA_A$ receptor subunits (α, β, γ or δ cDNA contained within a PRK5 plasmid vector) was mixed with cDNA encoding enhanced green-fluorescent protein (eGFP), 20 µl 340 mM $CaCl_2$ and 24 µl 2 x HBSS (50 mM HEPES, 280 mM NaCl and 2.8 mM Na_2HPO_4, pH 7.2). 1 µg of each cDNA was used, and a total of 4 µg cDNA

was used for each transfection. The cDNA-calcium phosphate suspension was applied to cells, and these were used for electrophysiology 18 - 48 hrs after transfection.

For transfections encoding WT α4, β3 and δ_{sep} subunits, and/or their L9'S mutants, cDNA transfection ratios of - 1:1:1, 1:1:10 or 10:1:10 were used. Since the δ subunit was tagged at the N-terminus (between residues 13 and 14 of the mature protein) with a super-ecliptic phluorin, eGFP was omitted from these transfections. Where WT and their respective L9'S cDNA's were co-expressed in the same cells, these were transfected in equal amounts, and the overall transfection ratio remained at 10α: 1β: 10δ. The total amount of cDNA was a constant 4 µg.

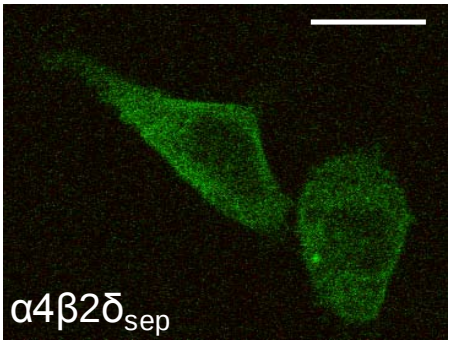

Figure 2.3 – A confocal image of δ_{sep}-positive HEK293 cells

A confocal image of HEK293 cells transfected with the super-ecliptic phluorin-tagged δ-subunit (δ_{sep}). Confocal images were acquired, as detailed in *Section* 2.7.2. Scale bar: 10 µm

2.3.3. HEK293 whole-cell electrophysiology

Transfected HEK293 cells were placed in a recording chamber and viewed with a Nikon Diaphot microscope and phase-contrast optics. Cells were continuously perfused at room temperature (RT) with Krebs solution containing (mM): 140 NaCl, 4.7 KCl, 1.2 $MgCl_2$, 2.52 $CaCl_2$, 11 glucose and 5 HEPES, adjusted to pH 7.4 with 1M NaOH. Transfected (eGFP- or sep-positive) cells were visualised using epifluorescence optics (Nikon Eclipse TE300, Nikon Instruments Europe B.V. Surrey, UK). Whole-cell currents were recorded from transfected cells voltage-clamped between -20 and -60 mV, depending on peak current size. Whole-cell currents were filtered at 5 kHz (-36dB, 6-pole Bessel filter), digitized at 50 kHz via a Digidata 1332A (Molecular Devices), and recorded to disk (Dell Pentium Dual Core-Optiplex 960). Patch pipettes (thin-walled borosilicate glass; Harvard Apparatus, UK) were fire polished to 2 - 4 MΩ and filled with an intracellular solution containing (mM): 120 KCl, 1 $MgCl_2$, 11 EGTA, 10 HEPES, 1 $CaCl_2$ and 2 adenosine triphosphate, adjusted to pH 7.2 with 1 M NaOH. The osmolarity of the internal solution was measured using a vapour pressure osmometer (Wescor Inc, Utah, USA), and was routinely 300 ± 20 milliOsmoles/litre (mOsm/l).

All drugs were applied locally via a Y-tube application system (*Fig*. 2.4; Mortensen and Smart, 2007), for both peak and steady-state recordings.

For peak recordings, GABA was applied alone, or in combination with other (pre-applied) drugs for a brief 2 - 4 s period. For steady-state recordings, prolonged GABA applications were applied either via the Y-, or auxiliary-tube for 1 - 2 min. A wash off period of 1, or 3 min was allowed between peak or steady-state GABA applications respectively, to allow the receptors to recover from desensitisation.

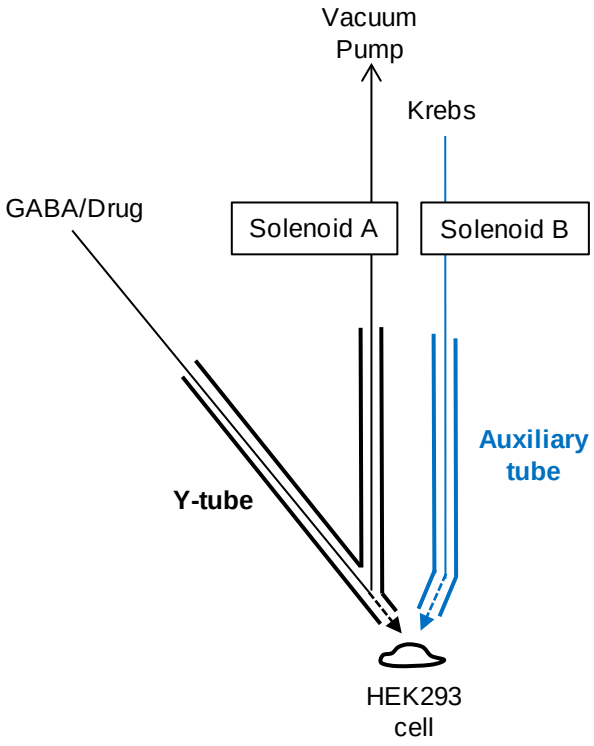

Figure 2.4 - Schematic diagram of the Y-tube.

Drugs were applied locally via a Y-tube (black), and washed off with an auxiliary tube (blue). During drug application, solenoids A and B remained closed, allowing drug to flow over the cell, in the absence of washing Krebs. Between drug applications, both solenoids remain open, allowing Krebs to perfuse the cell while the drug solution flows to waste under vacuum pressure. The fluid exchange time for solutions applied via the Y-tube, was approximately 100 ms.

To assess for current run-up, or run-down, a normalising concentration of GABA (routinely at a concentration of 1 mM) was applied to the same cell at regular intervals. Cell capacitance, series resistance and input resistance were measured from transient current changes induced by 10 mV hyperpolarising voltage steps. Series resistances (R_s) were monitored throughout each experiment and deviations >20 % resulted in the data being excluded from further analysis.

2.3.4. Analysis of GABA concentration-response curves

The amplitudes of peak and steady-state currents were measured in relation to the baseline holding current, using Clampfit software (version 9.2; Molecular Devices, USA). To generate peak GABA concentration-response curves, the peak response to a given concentration of GABA was normalised to the peak response achieved by a saturating concentration of GABA. For steady-state concentration-response curves, the steady-state current elicited by a given concentration of GABA was normalised to steady-state response achieved by a saturating concentration of GABA. The GABA concentration-response curves were fitted with a (single- or multi-component) Hill equation (*Equation* 2.1), or modified Hill equation (*Equation* 2.2; for curves generated in the presence of 4-PIOL), using a least-squares method. For the multi-component fits, some parameters were pre-fixed whilst others were allowed to free-run during the fitting process. This enabled better starting estimates of the parameters to be determined. When this was achieved, the final fit enabled most parameters to free run.

Equation 2.1: Hill equation

$$\frac{I_{GABA}}{I_{Max,GABA}} = \sum_{i=1}^{i=j} \frac{1}{1+(EC_{50}/[A])^{n_H}}$$

Where $I_{Max,GABA}$ is the maximum response to a saturating concentration of GABA, EC_{50} is the concentration of GABA ([A]) inducing a half-maximal current, n_H is the Hill coefficient and i is the number of components where j = 1 – 3.

Equation 2.2: Modified Hill equation

$$\frac{I_{GABA}}{I_{Max,GABA}} = I_{Min} + \left[\left(I_{Max,GABA} - I_{Min,GABA} \right) \frac{[A]^{n_H}}{[A]^{n_H} + EC_{50}} \right]$$

Where $I_{Min,GABA}$ is the minimum 'plateau' response induced by 4-PIOL (this is zero for GABA in the absence of 4-PIOL).

2.3.5. Calculating Spontaneous Channel Activity

The level of spontaneous receptor/channel activity (SA) was quantified according to *Equation* 2.3. The outward current induced by the GABA Cl^- channel blocker, picrotoxin ($I_{PTX;}$ 1 mM) was expressed as a percentage of the maximum current, defined as the sum of the current induced by a saturating (maximal) concentration of GABA ($I_{Max,GABA}$) and I_{PTX}. No spontaneous activity was observed for WT α4β3δ receptors.

Equation 2.3: Calculating spontaneous channel activity

$$SA(\%) = \frac{I_{PTX}}{I_{PTX} + I_{Max,GABA}}$$

2.4. Cerebellar granule cell cultures

Cerebellar cultures were prepared as described previously (Houston and Smart, 2006). Briefly, postnatal day 4 (P4) were Sprague-Dawley rats decapitated using a licensed procedure, in accordance with the *Animals (Scientific Procedures) Act, 1986* (ASPA). The cerebella were removed, and dissociated into single cells using 0.1 % w/v trypsin (Sigma) and triturated with fire-polished glass Pasteur pipettes. Cells were plated onto 22 mm glass coverslips coated with 500 µg/mL poly-D-ornithine (Sigma), in Basal medium Eagle (BME; Invitrogen) supplemented with 10 % v/v heat-inactivated FCS. After 1 hr, the medium was replaced with BME containing 5 % v/v heat-inactivated horse serum (HS; Invitrogen), 20 U/mL penicillin G, 20 µg/mL streptomycin, 2 mM L-glutamine, 0.5 % v/v glucose and a growth cocktail (5 mg/L insulin, 5 mgl/L transferrin, 5 mg/L selenium; Sigma). Electrophysiological recordings were performed from cultured CGCs, between 7 – 19 days *in vitro* (DIV).

2.5. Hippocampal cultures

Hippocampal cultures were prepared by Dr Philip Thomas. Briefly, cultured hippocampal neurons were prepared from E18 Sprague-Dawley rat embryos (a Schedule 1 procedure), as previously described (Thomas *et al*., 2005). The dissected hippocampi were dissociated into single cells using 0.1 % w/v trypsin and serially triturated with fire-polished glass Pasteur pipettes. Cells were plated onto 22 mm glass coverslips coated with 100 µg/mg poly-D-lysine (Sigma) in Minimum essential media (MEM; Invitrogen) supplemented with 5 % v/v FCS, 5 % v/v HS, 10 U/mL penicillin-G, 10 µg/mL streptomycin, 2 mM L-glutamine and 20 mM glucose. 2 hrs after plating, the media was replaced with Neurobasal-A (Invitrogen) media supplemented with 1 % v/v B-27 (Gibco), 50 U/mL penicillin-G, 50 µg/mL streptomycin, 0.5 % v/v Glutamax (Invitrogen) and 35 mM glucose. Electrophysiological recordings were performed from cultured hippocampal neurons, between 11 – 21 DIV.

2.6. Brain Slice electrophysiology

2.6.1. Animals

Young rats (P14) were decapitated under terminal isoflurane anaesthesia, in accordance with the *Animals (Scientific Procedures) Act, 1986* (ASPA). Given that $GABA_A$ receptors are a major molecular target of neurosteroids (Paul and Purdy, 1992), and neurosteroid levels are strongly influenced by the oestrus cycle in female mice (Corpéchot *et al*., 1997), only male mice were used for these experiments.

2.6.2. Preparation of brain slices

Following decapitation, the brain was rapidly removed and immersed in ice-cold slicing solution composed of (mM): 130 K-gluconate, 15 KCl, 0.05 EGTA, 20 HEPES, 4 Na-pyruvate, 25 glucose and 2 kynurenic acid (pH 7.4). Coronal thalamic slices (250 µm) were obtained using a Leica VT 1200s vibroslicer (Leica Microsystems GmBH, Wetzlar, Germany), and subsequently transferred to a holding chamber incubated at 37 ºC. The solution was slowly exchanged to aCSF containing (mM): 125 NaCl, 2.5 KCl, 1.25 NaH_2PO_4, 26 $NaHCO_3$, 2 $CaCl_2$, 1 $MgCl_2$, 25 glucose and 2 kynurenic acid (pH 7.4 when bubbled with 95 % O_2 and 5 % CO_2; BOC Healthcare). Slices were maintained in the holding chamber at RT until they were used for electrophysiology.

2.6.3. Whole-cell electrophysiology in slices and neuronal cultures

Neurons were visualised using a Slicescope Pro 6000 (Scientifica, UK) equipped with differential interference contrast (DIC) optics (Olympus, Tokyo, Japan) and a Basler scA750-60fm camera (Basler Vision Technologies, Ahrensburg, Germany).

Whole-cell currents were recorded at RT, as detailed for HEK293 cells (*Section* 2.3.3). Recordings were made using fire polished patch pipettes (2 - 4 MΩ) filled with an intracellular solution containing (mM): 140 CsCl, 2 NaCl, 10 HEPES, 5 EGTA, 2 $MgCl_2$, 0.5 $CaCl_2$, 2 Na-ATP and 2 QX-314 bromide (Abcam Biochemicals). The pH of the intracellular solution was adjusted using 1 M CsOH.

During recordings, slices, and neuronal cultures were perfused with recording solution at a flow rate of 4-6 mL/min. For slice recordings, the recording aCSF was supplemented with the glutamate receptor antagonist, kynurenic acid (2 mM), to isolate GABA-mediated responses. When recording from neuronal cultures, the NMDA (*N*-Methyl-*D*-aspartate) and AMPA (2-amino-3-(3-hydroxy-5-methyl-isoxazol-4-yl)propanoic acid)/ kainate receptor antagonists, D-AP5 (20 µM) and CNQX (10 µM) were used to block excitatory responses. A saturating concentration of (-)-bicuculline (20 µM; Ueno *et al*., 1997) was bath-applied at the end of all electrophysiological recordings, to confirm that all synaptic events were GABAergic, and to unveil any $GABA_A$-mediated tonic current. Some recordings were performed in the presence of 0.5 µM tetrodotoxin (TTX), to block spontaneous action potentials.

In a subset of thalamic recordings, the slices were pre-incubated for at least 30 min in aCSF containing the GAT uptake inhibitors NNC-711 (10 µM) and SNAP-5114 (20 µM). Both compounds were subsequently present throughout electrophysiological recordings. NNC-711 is a potent and selective antagonist of GAT1 transporters (IC_{50}: 0.38 µM at GAT1; 117 µM at GAT2; and 1700 µM at GAT3; Borden *et al*., 1994). By comparison, SNAP-5114 potently inhibits GABA

uptake by GAT2 and GAT3, with an IC_{50} of 21 µM and 5 µM respectively for each transporter (388 µM at GAT1; Borden, 1996).

2.6.4. IPSC analysis

The frequency (Hz) of sIPSCs was determined by detecting and manually selecting all events within 3 min epochs, using MiniAnalysis software (Synaptosoft Inc., Fort Lee, New Jersey, USA), and dividing this value by 180 s. During 4-PIOL application, a significant increase in root mean square (RMS) current noise was observed in hippocampal pyramidal and TC relay neurons, which might mask smaller sIPSCs, and introduce a bias towards larger events during 4-PIOL application compared to control. To limit this bias, only the largest hundred amplitude events from each condition were compared.

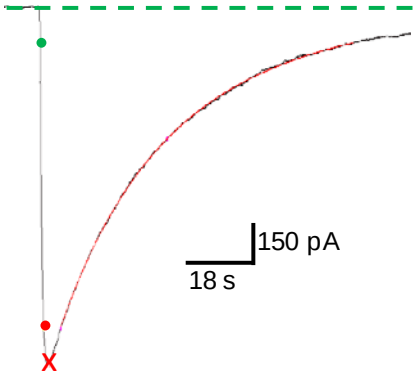

Figure 2.5 – sIPSC fitted with a bi-exponential decay function

The rise time was defined as the time taken for the synaptic event to rise from 10 (green dot) to 90 % (red) of the maximum current response (red cross). The decay phase (90 - 10 %) of each IPSC was fitted with a bi-exponential decay function (see *Equation* 2.4; red curve). The green dashed line indicates the baseline current.

The average decay kinetics for sIPSCs for each cell was determined by fitting the cleanest, uncontaminated events (> 50 events for each condition) with either a mono- or bi-exponential decay function (e.g. *Fig*. 2.5). The accuracy of each fit was determined visually, but also by increasing the coefficient of determination (R^2). To combine data obtained for mono- or bi-exponentially fitted events, decay times were transformed to a weighted decay time, τ_w, according to *Equation* 2.4:

Equation 2.4: Calculating Weighted tau

$$\tau_w = (A_1.\tau_1 + A_2.\tau_2) / (A_1 + A_2);$$

Where τ_1 and τ_2 represent the time constants for a bi-exponential decay, and A_1 and A_2 are the relative amplitude contributions of τ_1 and τ_2. For monoexponential decaying events, A_2 and τ_2 are zero.

The average sIPSC frequency, amplitude, 10 – 90 % rise time and τ_w were calculated for each cell, and the mean data for each parameter is expressed as a percentage, relative to the control condition.

An all-points histogram was generated for sIPSC amplitudes, before and after drug application. Each histogram was fitted with a Gaussian distribution function, according to *Equation* 2.5. Note that for each condition, equal numbers of sIPSCs were sampled, from the start of each recording, to limit sample number bias.

Equation 2.5: Gaussian distribution function

$$f(x) = A\frac{e^{-(x-\mu)^2/2\sigma^2}}{\sigma\sqrt{2\pi}} + C$$

Where A is the amplitude of the histogram, *C* is a constant representing the pedestal of the histogram, μ is the Gaussian mean, and σ is the standard deviation.

2.6.5. Analysis of tonic GABA currents

Two main methods were used to quantify the changes in tonic currents. The average holding current for a 30 s epoch, in each drug condition, was measured using WinEDR software (version 3.1; John Dempster, University of Strathclyde, Glasgow, UK). Changes in holding current were calculated by subtracting the average holding current after drug application, from the average holding current before the drug application. In addition, the RMS baseline noise was measured over a 30 s epoch, sampled every 100 ms. Since sIPSCs increase RMS baseline noise, Microsoft Excel was used to calculate a threshold for eliminating contaminated 100 ms epochs. A running threshold (routinely the median) was calculated at 5 s time intervals, over a 30 s recording period, and any RMS value greater than the calculated threshold, was automatically excluded from further analysis. Effective thresholding was validated by manually analysing a small section of each recording (~ 10 s), and manually eliminating 100 ms epochs contaminated by synaptic currents.

2.7. Fluorescent Imaging of brain slices

2.7.1. Preparation of brain slices for confocal imaging

In some thalamic recordings, Lucifer yellow (1 mg/mL; Sigma) was included in the internal medium to allow for confocal imaging of neuronal morphology. In these instances, slices were fixed for 16 - 24 hrs in 4 % w/v paraformaldehyde (PFA) diluted in phosphate buffered saline (PBS). Fixed slices were washed three times in PBS, and mounted on microscope slides using Vectashield mounting medium (Vector Laboratories, Burlingame, CA). Imaging of slices was performed within a week.

2.7.2. Image acquisition and analysis

Images were acquired using a Zeiss Axioskope LSM510 confocal microscope (Carl Zeiss Ltd., Welwyn, Garden City, Hertfordshire, UK), equipped with a 488 nM argon laser line, and a Plan Neofluor 40x oil-immersion DIC objective (numerical aperture (NA) 1.3; Carl Zeiss). Neurons were imaged as z-stacks, comprising of 2 µm optical sections. Each z-section was acquired as a mean of four scans in eight bits, and stored for analysis. Z-stack projections were constructed at a later date, using ImageJ (Version 1.42q).

2.8. Statistics

All data are expressed as mean ± SEM. Graphical representations of data were plotted using Microcal OriginPro (version 6; OriginLab Corporation, Northampton, MA, USA), or Microsoft Excel.

Where appropriate, statistical analyses were performed using a paired- or unpaired student t-test, or a one-way analysis of variance (ANOVA; InStat 3; GraphPad Software, La Jolla, California, USA). These statistical tests assume that the data is normally distributed, and that the variances of the compared groups do not vary significantly. The normality of each data set was assessed using a Kruskal-Wallis test, and where data did not meet the criteria for parametric analysis, a non-parametric t-test, or ANOVA, was performed. P-values < 0.05 were considered statistically significant.

Chapter 3: Functional characterisation of recombinant γ2- and δ subunit-containing receptors expressed in HEK293 cells

3.1. Introduction

In *Chapter* 4, the functional profile of 4-PIOL will be assessed on recombinant $GABA_A$ receptors expressed in HEK293 cells. HEK293 cells are a common expression system, used to study the pharmacology and biophysical properties of recombinant $GABA_A$ receptors. Due to their non-neuronal lineage, these cells are largely thought not to express endogenous $GABA_A$ receptors, although there is some evidence that β3, ε and γ3 subunits are expressed in low levels (Thomas and Smart, 2005). Nonetheless, despite frequent testing, we have consistently failed to detect the functional expression of these subunits in non-transfected HEK293 cells, allowing us to control the expression of different $GABA_A$-receptor subunits using the cDNA transfection protocol described in *Section* 2.3.2.

Although several $GABA_A$ receptor subtypes have been described at synaptic, and extrasynaptic sites in native neurons (see *Section* 1.2.1), here, the study is focused on recombinant α1βγ2, α5βγ2, α4βδ and α6βδ receptors, since these are the major subtypes thought to exist in hippocampal pyramidal neurons, CGCs (both investigated in *Chapter* 5) and TC relay neurons (studied in *Chapter* 6).

Before examining the functional profile of 4-PIOL on recombinant α1β3γ2, α5β3γ2, α6β2δ and α4β2δ receptors expressed in HEK293 cells, it was important to first validate the expression of these recombinant $GABA_A$ receptor subtypes in the HEK293-expression system. Evidence suggests that binary αβ subunits can efficiently co-assemble to form functional receptors in recombinant expression systems (Mortensen *et al*., 2011; Karim *et al*., 2013). To ensure that γ2 and δ were efficiently incorporated into functional heteropentamers, whole-

cell electrophysiological recordings were performed on HEK293 cells expressing various αβ, αβγ and αβδ subunit combinations. The GABA sensitivity of each receptor subtype was determined, and their relative sensitivities to subtype selective modulators such as diazepam (a γ subunit-selective potentiator (Pritchett *et al*., 1989) and zinc (αβ-selective inhibitor; Draguhn *et al*., 1990; Smart *et al*., 1991; Hosie *et al*., 2003) were assessed.

In addition to verifying efficient δ-expression, we also examined the subunit stoichiometry of functional recombinant α4β3δ receptors. Although the stoichiometry of major synaptic αβγ $GABA_A$ receptor isoforms has broad consensus support for 2α: 2β: 1γ (Backus *et al*., 1993; Chang *et al*., 1996; Tretter *et al*., 1997), a definitive view of the stoichiometry for extrasynaptic δ containing receptors remains elusive. Previous reports note that some functional discrepancies have been observed for αβδ receptors (e.g. variable GABA EC_{50} and ethanol sensitivity; Wallner *et al*., 2003), which have been postulated to arise, in part, from differences in subunit stoichiometry (Borghese *et al*., 2006; Wagoner and Czajkowski, 2010). While the stoichiometry of recombinant αβδ receptors has been investigated using atomic force microscopy (Barrera *et al*., 2008), biochemical analysis of recombinant receptors (Wagoner and Czajkowski, 2010) and concatamers (Baur *et al*., 2009; Kaur *et al*., 2009), there appears to be some discrepancy regarding the number of δ subunits incorporated into functional channels.

Using a similar approach to that adopted for nACh receptors (Filatov and White, 1995; Labarca *et al*., 1995), 5-HT_3 receptors (Yakel *et al*., 1993) and α1β2γ2 $GABA_A$ receptors (Chang *et al*., 1996; Chang and Weiss, 1999), we introduced polar substitutions for the highly conserved 9’ leucine residue in the M2 region (see *Fig*. 2.1) of the α4, β3 and δ $GABA_A$ receptor subunits. These 9’ leucine to serine (L9’S) substitutions were used as reporter mutations, since they produce a profound increase in agonist potency and consequently induce a leftward shift in the GABA concentration-response curve. The extent of the curve shift is correlated with the number of polar substitutions per ion channel complex and is used here to demonstrate a subunit stoichiometry of 2α: 2β: 1δ for functional α4β3δ receptors. Much of the work presented in this chapter, has been published (Patel *et al*., 2014).

3.2. Results

Using the cDNA transfection protocol described in *Section* 2.3.2, HEK293 cells were transfected with cDNAs encoding the specified subunit combinations (αβδ or αβγ), in combination with an expression plasmid encoding enhanced green fluorescent protein (eGFP). Note that the δ subunit was tagged at the N-terminus (between residues 13 and 14 of the mature protein) with a super-ecliptic phluorin, so eGFP was omitted from transfections including δ_{sep}. Transfected cells were identified by their green fluorescence, and whole-cell currents were recorded from these cells expressing recombinant $GABA_A$ receptors, in response to brief (2 - 4 s) drug applications (applied via a Y-tube application system; see *Fig.* 2.4).

3.2.1. Functional verification of γ2 subunit expression in HEK293 cells

The major $GABA_A$ receptor subtype(s) thought to exist at synaptic sites in the CNS are αβγ2 receptors (Farrant and Nusser, 2005). Although αβγ subunits have previously been shown to form functional receptors when expressed in heterologous expression systems (Sigel *et al*., 1990; Verdoorn *et al*., 1990; Angelotti and Macdonald, 1993), it was important to verify whether the γ2 subunit was efficiently incorporated into functional receptors in HEK293 cells used in this study.

Since αβ receptors have previously been shown to exhibit a higher sensitivity to GABA compared to αβγ receptors (Sigel *et al*., 1990; Mortensen *et al*., 2011), whole-cell currents were recorded from α1β3- or α1β3γ2L-expressing cells, in response to increasing concentrations of GABA (0.01 – 1000 μM; *Fig.* 3.1 A). The GABA concentration-response data generated for each cell was fitted using the Hill equation (*Equation* 2.1), and averaged to produce mean estimates of GABA potency (EC_{50}) and the Hill coefficient (n_H) for each receptor subtype (*Table* 3.1). Although the mean GABA EC_{50} for α1β3γ2L-expressing cells had a

tendency to be higher than that for α1β3 receptors (8.7 ± 2.3 μM and 3.3 ± 0.8 μM respectively; *Table* 3.1), this difference was not statistically significant (p = 0.06), possibly indicating that the γ2L subunit was not being efficiently incorporated into functional α1β3γ2L receptors.

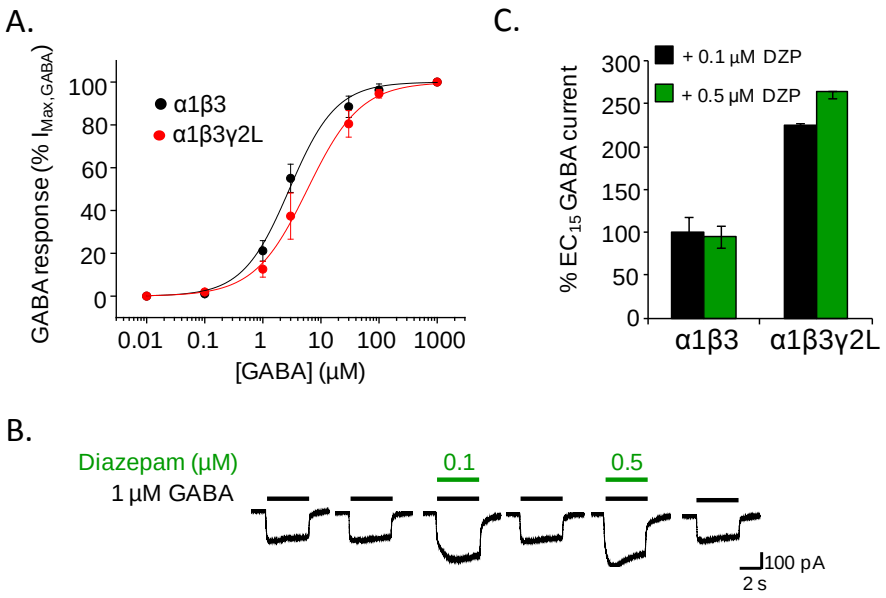

Figure 3.1 – Functional analysis of α1β3 and α1β3γ2L receptors expressed in HEK293 cells

A. Average GABA concentration-response curves for cells expressing α1β3 (black) and α1β3γ2L (red) receptors (mean ± SEM; n = 4 – 5 cells). The data from each cell was fitted with a Hill equation (continuous curves), using a least-squares method, and the average parameters for each construct are listed in Table 3.1. **B.** Representative traces of whole cell currents elicited by an EC_{15} GABA concentration (1 μM) for α1β3γ2L receptors, in the absence, and presence of 0.1 μM and 0.5 μM diazepam (DZP). The black and green horizontal bars respectively indicate the duration of GABA and diazepam applications. **C.** Bar graph showing the effect of 0.1 μM (black) and 0.5 μM (green) diazepam on GABA EC_{15} responses of α1β3- and α1β3γ2L-expressing cells. For each cell, the GABA response in the presence of pre-applied (and co-applied) diazepam was normalized to the GABA EC_{15} response measured in the absence of diazepam.

To check, an alternative pharmacological tool was adopted to assess whether the γ2L was being efficiently expressed. It is long established that α(1,2,3 and 5)βγ receptors, but not αβ receptors, undergo positive allosteric modulation by benzodiazepines, such as diazepam (Pritchett *et al*., 1989; Rudolph and Möhler, 2004). Therefore, we assessed the modulation of α1β3 and α1β3γ2L receptor mediated GABA-activated currents by diazepam. Whole-cell currents elicited by EC_{15} concentrations of GABA (the concentration of GABA eliciting 15 % of the maximal GABA response) were recorded from cells expressing α1β3 and α1β3γ2L receptors, in the absence, and presence of 0.1 μM and 0.5 μM diazepam (*Fig.* 3.1 B). These concentrations of diazepam have previously been shown to potently potentiate αβγ receptors (Baur and Sigel, 2005). While the responses of α1β3γ2L receptors were significantly potentiated by diazepam (% control (= 100 %) GABA EC_{15} current: 225 ± 1.3 and 263 ± 6.6 for 0.1 μM and 0.5 μM diazepam respectively; *Fig.* 3.1 C), α1β3 receptors showed no discernible potentiation by diazepam (% control GABA EC_{15} current: 100.3 ± 12.5 and 94.7 ± 12.2 for 0.1 μM and 0.5 μM diazepam respectively; *Fig.* 3.1 C). Thus, although we cannot exclude the possibility that some α1β3-heteromers were also present in α1β3γ2L-expressing cells, these data indicate that γ2L was efficiently incorporated into functional receptors.

Table 3.1 – Peak GABA concentration response parameters for synaptic and extrasynaptic $GABA_A$ receptors

Subunit combination	GABA EC_{50} (μM)	n_H
α1β3	3.3 ± 0.8	1.3 ± 0.1
α5β3	2.7 ± 0.5	1.0 ± 0.03
α4β2	1.1 ± 0.02	0.9 ± 0.04
α4β3	1.0 ± 0.1	1.5 ± 0.2
α6β2	0.6 ± 0.04	1.0 ± 0.1
α1β3γ2L	8.7 ± 2.3	1.3 ± 0.1
α5β3γ2L	11.9 ± 3.6	1.1 ± 0.1
α4β2δ	0.7 ± 0.1	1.3 ± 0.1
α4β3δ	1.9 ± 0.5	1.1 ± 0.1
α6β2δ	0.3 ± 0.03	1.1 ± 0.04

The normalised GABA concentration-response curves for each subunit combination was fitted using a single component Hill equation (*Equation* 2.1) using a least-squares method. Listed are the mean values for GABA potency (EC_{50}) and the Hill slope (n_H) obtained, which are expressed as mean ± SEM (n = 4 – 7).

As for α1β3 and α1β3γ2L receptors, the GABA and diazepam sensitivities of recombinant α5β3 and α5β3γ2L receptors were also investigated. GABA concentration-response curves generated for each subunit combination (*Fig*. 3.2 A) revealed that recombinant α5β3γ2L receptors were apparently less sensitive to GABA than α5β3 receptors (EC_{50}s: 11.9 ± 3.6 μM and 2.7 ± 0.5 μM respectively), although this difference was not statistically significant (p = 0.10). Moreover, the EC_{15} GABA responses of α5β3γ2L receptors showed appreciable potentiation by both 0.1 μM and 0.5 μM diazepam (% control GABA EC_{15} current: 189 ± 2.9 and 225.7 ± 4.0 respectively; *Fig.* 3.2 B), unlike α5β3 receptors, which showed no significant potentiation by diazepam (% control GABA EC_{15} current: 96.5 ± 17.3 and 97.3 ± 20.5 for 0.1 μM and 0.5 μM diazepam respectively; *Fig.* 3.2 B). Therefore, it appears that the γ2L subunit was also efficiently incorporated into functional α5β3γ2L heteropentamers.

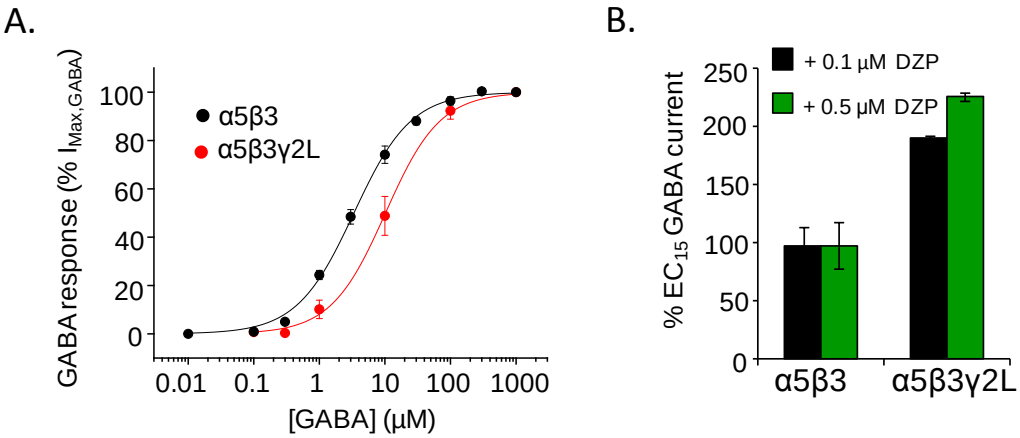

Figure 3.2 – Functional analysis of α5β3 and α5β3γ2L receptors expressed in HEK293 cells

A. Average GABA concentration-response curves for cells expressing α5β3 (black) and α5β3γ2L (red) receptors (mean ± SEM; n = 4 – 5 cells). The data from each cell was fitted with a Hill equation (continuous curves), using a least-squares method, and the average parameters for each construct are listed in *Table* 3.1. **B.** Bar graph showing the effect of 0.1 μM (black) and 0.5 μM (green) diazepam on GABA EC_{15} responses of α5β3- and α5β3γ2L-expressing cells. For each cell, the GABA response in the presence of pre-applied (and co-applied) diazepam was normalized to the GABA EC_{15} current measured in the absence of diazepam.

3.2.2. Functional verification of δ subunit expression in HEK293 cells

Whilst the γ2 subunit readily forms functional heteropentamers with αβ subunits, greater difficulty has been observed with the recombinant expression of the δ subunit. Therefore, to promote the expression of α6β2δ and α4β2δ receptors, a transfection ratio of 10α: 1β: 10δ was used, on the assumption that αδ pairs would form early in the assembly pathway, as is the case for α6δ pairs in the cerebellum (Jones *et al*., 1997). Cell surface expression of the δ subunit was initially confirmed by the presence of green fluorescence, arising from a super-ecliptic phluorin (sep) tag on the N-terminus of the δ subunit (see *Fig*. 2.3).

To assess whether the δ subunit was successfully incorporated into functional α6β2δ receptors, the GABA sensitivities of α6β2- and α6β2δ-expressing cells were first compared. The average GABA concentration-response curve for each receptor subtype (*Fig.* 3.3 A) revealed that α6β2δ receptors exhibited a significantly higher sensitivity to GABA compared to α6β2 receptors (0.3 ± 0.03 μM and 0.6 ± 0.04 μM respectively; *Table* 3.1; $p = 0.0012$). Curiously, α6β2 receptors displayed significantly smaller maximum currents compared to α6β2δ receptors (56.6 ± 9.5 pA and 589.7 ± 62.4 pA respectively; $p = 0.0008$). This difference was not attributable to any differences in cell size, since α6β2 receptors also exhibited a smaller maximum current density (calculated by normalising a response to 1 mM GABA to the whole-cell capacitance) than α6β2δ-expressing cells (*Fig.* 3.3 B; $p = 0.008$). Although not specifically probed here, these differences could arise if α6β2 receptors possess a lower open state probability, or single channel conductance than α6β2δ receptors (as has been demonstrated for α1β receptors; Moss *et al*., 1990; Verdoorn *et al*., 1990; Angelotti and Macdonald, 1993; Mortensen and Smart, 2006), or if α6β2 receptors are less efficiently assembled and/or trafficked to the cell surface. Nonetheless, the increased GABA sensitivity, and maximum current density of α6βδ-expressing cells (relative to α6β-expressing cells), is consistent with efficient δ-expression. Moreover, consistent with previous reports, α6β2δ receptors exhibit the highest sensitivity to GABA compared to all the other $GABA_A$ receptors listed in *Table* 3.1 (Mortensen *et al*., 2011).

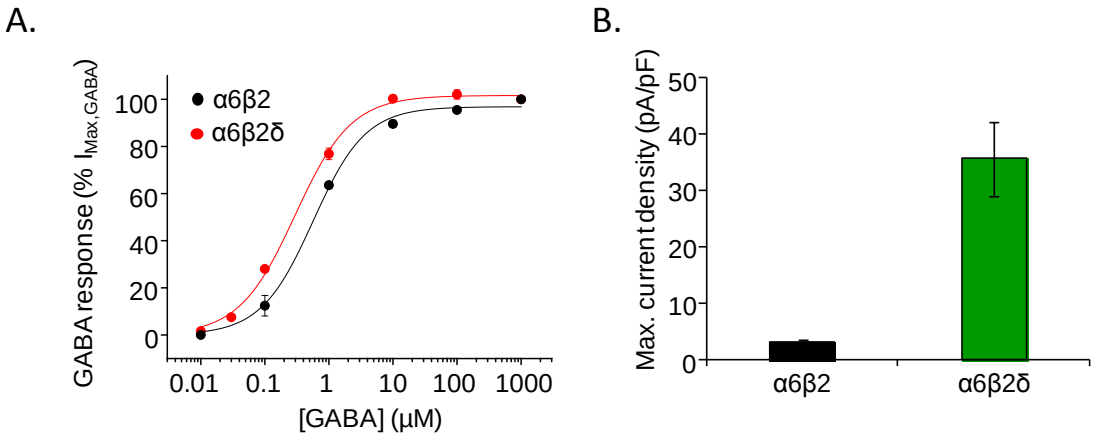

Figure 3.3 - Functional analysis of α6β2 and α6β2δ receptors expressed in HEK293 cells

A. Average (mean ± SEM) GABA concentration-response curves for cells expressing α6β2 (black) and α6β2δ (red) receptors. The data from each cell was fitted with a Hill equation (continuous curves), using a least-squares method, and the average parameters for each construct are listed in *Table* 3.1. Each curve was generated by averaging data from 4 - 5 cells. **B.** Bar graph showing the maximum GABA current density (pA/pF) for α6β2- and α6β2δ-expressing cells. For each cell, the peak response (pA) to a saturating concentration of GABA (1 mM) was normalized to the whole cell capacitance (pF).

Similarly, the GABA sensitivities of α4β2 and α4β2δ receptors were also investigated. The average GABA concentration-response curves for α4β2- and α4β2δ-expressing cells (*Fig.* 3.4 A) revealed that α4β2δ receptors (GABA EC_{50}: 0.7 ± 0.1 μM) were significantly more sensitive to GABA than α4β2 receptors (GABA EC_{50}: 1.1 ± 0.02 μM; p = 0.006; *Table* 3.1). This difference in GABA sensitivity suggests that the δ subunit is expressed, and can form functional heteropentamers when co-expressed with α4 and β2 subunits.

To verify that α4β2δ-expressing cells did not contain a large population of binary αβ constructs, an alternative pharmacological approach was adopted. The subtype selective inhibitor, Zn^{2+} (Smart *et al*., 1991; Nagaya and Macdonald, 2001; Hosie *et al*., 2003) was used, since 1 μM Zn^{2+} has been shown to inhibit αβ receptors to a far greater extent than αβδ receptors (Krishek *et al*., 1998; Hosie *et al*., 2003; Stórustovu and Ebert, 2006). The EC_{50} current

responses for α4β2 and α4β2δ receptors were recorded in the absence, or presence of pre-applied (and co-applied) 1 μM Zn^{2+}. As expected, this concentration of Zn^{2+} significantly inhibited EC_{50} GABA responses of α4β2 receptors, by 80.0 ± 2.63 % (*Fig.* 3.4 B). By contrast, Zn^{2+} only produced a modest inhibition (11.2 ± 1.13 %) of the EC_{50} GABA responses of α4β2δ receptors (*Fig*. 3.4 B). These data strongly indicate that a significant proportion of functional receptors present in α4β2δ-expressing cells contain the δ subunit, although we cannot exclude the expression of some α4β2 receptors.

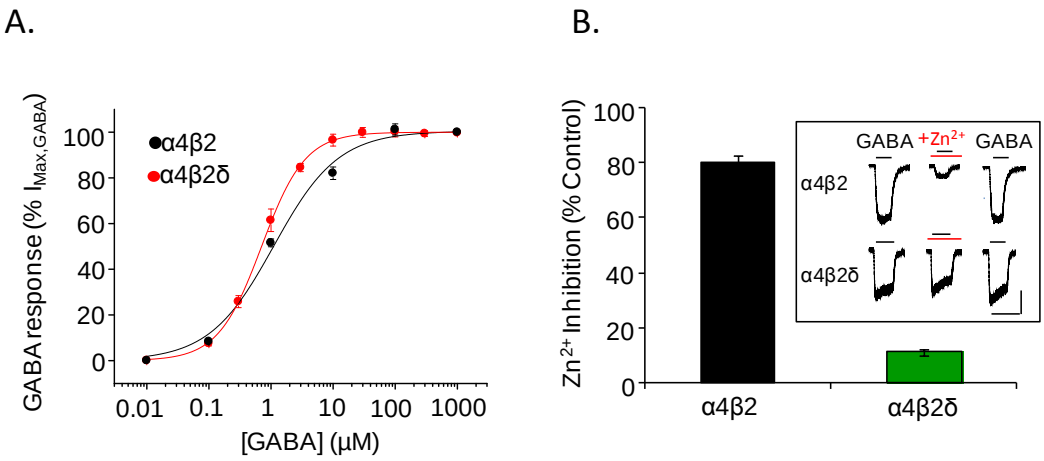

Figure 3.4 - Functional analysis of α4β2 and α4β2δ receptors expressed in HEK293 cells

A. Average (mean ± SEM) GABA concentration-response curves for cells expressing α4β2 (black) and α4β2δ (red) receptors. The data from each cell (n = 4 - 6) was fitted with a Hill equation (continuous curves), using a least-squares method, and the average parameters for each receptor type is listed in *Table* 3.1. **B.** Bar graph showing the inhibitory effects of 1 μM Zn^{2+} on the GABA EC_{50} responses of α4β2- and α4β2δ-expressing cells. For each cell, the peak response to 1 μM GABA (an approximate EC_{50} concentration for both α4β2 and α4β2δ receptors) was measured in the absence, or presence of pre-applied (and co-applied) Zn^{2+}, and each response was normalized to that elicited by GABA alone. The inset shows example traces of whole-cell currents, elicited by GABA (1 μM), in the absence or presence of pre-applied Zn^{2+} (1 μM), for α4β2- and α4β2δ-expressing cells. Calibration bars: 2 s (horizontal) and 100 pA (vertical).

3.2.3. Functional expression of WT and L9'S mutant α4, β3 and δ subunits

To examine the stoichiometry of α4β3δ receptors, we mutated the highly conserved 9' leucine residues in α4, β3 and δ subunits (see *Fig.* 2.1) to serine residues, as described in *Section* 2.1. The resultant $\alpha4^{L297S}$, $\beta3^{L284S}$ and $\delta_{sep}{}^{L288S}$ will be referred to as: α_m, β_m and δ_m, for the remainder of this chapter, while their WT counterparts are designated as α, β and δ.

Previous studies have demonstrated that L9'S mutations confer a profound increase in agonist sensitivity, manifested by a leftward shift in the agonist concentration-response curve. To verify the functional expression of L9'S mutants, GABA activated currents were recorded from HEK293 cells expressing WT, αβδ, and mutant, $\alpha\beta\delta_m$, $\alpha_m\beta\delta$ and $\alpha\beta_m\delta$, receptors (*Fig.* 3.5 A). Both WT and mutant expressing cells exhibited a concentration-dependent sensitivity to GABA, and notably, the currents recorded from mutant receptor expressing cells demonstrated prolonged deactivation phase compared to those for WT αβδ receptors (*Fig.* 3.5 A).

$\alpha\beta\delta_m$, $\alpha_m\beta\delta$ and $\alpha\beta_m\delta$, transfected with a 10α:1β:10δ transfection ratio but not αβδ receptors, exhibited spontaneous activity in the absence of exogenously-applied GABA, which was blocked by the Cl^- channel blocker, picrotoxin (1 mM; *Fig.* 3.5 B). Expressed as a proportion of the total GABA-activated plus spontaneous current ($I_{PTX}/(I_{PTX} + I_{Max,GABA}$; *Fig.* 3.5 B inset)), the levels of spontaneous receptor activity for $\alpha_m\beta\delta$ and $\alpha\beta\delta_m$ receptors were 21.9 ± 5.3 % and 16 ± 1 %, respectively. Notably, $\alpha\beta_m\delta$-expressing cells exhibited the highest level of spontaneous receptor activation (76.6 ± 6.5 %), relative to $\alpha\beta\delta_m$ ($p < 0.001$) and $\alpha_m\beta\delta$ ($p < 0.05$) receptors (non-parametric ANOVA – Kruskal Wallis test). The increased degree of spontaneous activation observed for the β mutant, likely reflects the predominant role this subunit plays in stabilising the open-shut GABA channel conformation(s). It is also noteworthy that β homomers can form spontaneously-opening ion channels (Krishek *et al*., 1996; Davies *et al*., 1997; Wooltorton *et al*., 1997; Cestari *et al*., 2000) unlike their α, γ or δ subunit counterparts.

Slower deactivation kinetics, and spontaneous channel openings are characteristic of LGICs containing 9' polar mutations (Revah *et al*., 1991; Filatov and White, 1995; Bianchi and Macdonald, 2001), and likely arise from receptor stabilisation in one or more open states (Filatov and White, 1995; Bianchi and Macdonald, 2001). Taken together, the distinctive current profiles of L9'S expressing cells, suggests that each mutant is efficiently co-assembled into functional αβδ receptors.

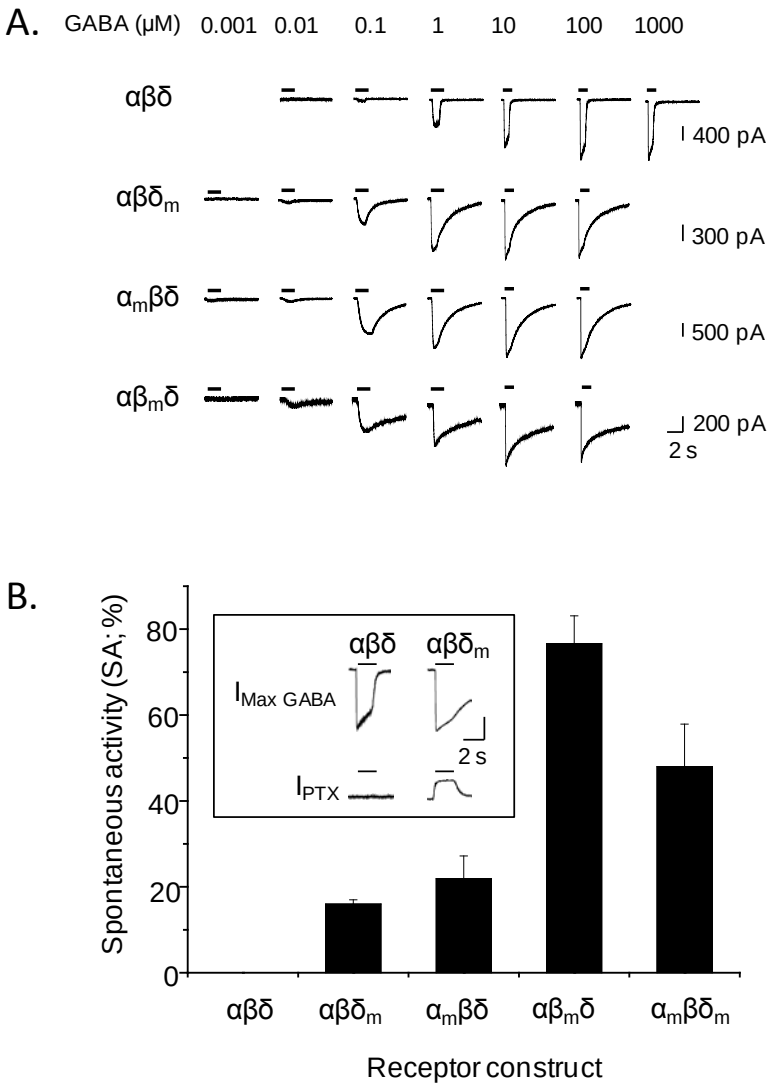

Figure 3.5 - Functional expression of WT and L9'S mutant α4, β3 and δ subunits.

A. Examples of whole cell currents recorded from HEK cells expressing recombinant αβδ, $\alpha\beta\delta_m$, $\alpha_m\beta\delta$ and $\alpha\beta_m\delta$ receptors, in response to increasing concentrations of GABA (0.001 - 1000 μM). The black horizontal bars indicate the duration of GABA application. Note the increased GABA sensitivity, and prolonged deactivation kinetics demonstrated by mutant expressing cells. A transfection ratio of 10α: 1β: 10δ was used. **B.** Bar graph showing the spontaneous activity for αβδ, $\alpha\beta\delta_m$, $\alpha_m\beta\delta$, $\alpha\beta_m\delta$ and $\alpha_m\beta\delta_m$ receptors. Values were calculated by expressing the outward current induced by picrotoxin ($I_{PTX;}$ 1 mM) as a percentage of the maximum current, defined as the sum of $I_{Max,GABA}$ and I_{PTX} (n = 4 - 11; mean ± SEM). No spontaneous activity (= 0 %) was observed for WT α4β3δ receptors. The inset shows example GABA-activated and picrotoxin-sensitive currents ($I_{Max,GABA}$ and I_{PTX}) for αβδ and $\alpha\beta\delta_m$ receptors. Current calibration bars: 300 pA (αβδ); 400 pA ($\alpha\beta\delta_m$).

3.2.4. L9'S mutations in α4, β3 and δ subunits increase GABA sensitivity

GABA concentration-response curves were generated for cells expressing the subunit combinations, αβδ, αβδ_m, α_mβδ, αβ$_m$δ, and α_mβδ$_m$. The GABA concentration-response curve for αβ$_m$δ receptors was generated by Dr Martin Mortensen. Cells expressing δ_m, α_m or β_m subunits demonstrated an increased GABA sensitivity compared to WT αβδ receptors, manifest by leftward shifts in the GABA concentration-response curves for mutant receptor expressing cells (*Fig.* 3.6 A). Whereas WT αβδ receptors had a GABA EC_{50} of 1.91 ± 0.47 μM, single mutant subunit-containing receptors possessed lower EC_{50} values of: 0.46 ± 0.11 μM (αβδ_m), 0.12 ± 0.03 μM (α_mβδ) and 0.11 ± 0.04 μM (αβ$_m$δ; *Table* 3.2). Notably, the GABA concentration-response curve for αβ$_m$δ receptors exhibited a significantly lower n_H (0.6 ± 0.1; *Table* 3.2) than those obtained for αβδ_m (1.4 ± 0.1) and α_mβδ (1.2 ± 0.2) receptors (p = 0.02 and p = 0.03 respectively). Although we cannot simply transpose the change in n_H to any physical attribute, it is possible that the L9'S mutations altered the gating kinetics of the receptor, which may account for the changes in n_H. Moreover, the effects on gating kinetics may be highly dependent on the subunit in which the mutation is inserted.

The αβδ_m receptors exhibited an ~ 4 - fold (4.2) increase in GABA sensitivity, relative to αβδ receptors. The increased GABA sensitivity of αβδ_m was not attributable to a large population of αβ receptors being present, since the EC_{50} for αβδ_m receptors (0.46 ± 0.11 μM) is significantly lower than that obtained for αβ receptors (1.0 ± 0.1 μM; *Table* 3.2; p = 0.01). By comparison the GABA sensitivities of α_mβδ and αβ$_m$δ receptors were even higher compared to δ_m-containing receptors, causing shifts of 16- (15.9) and 17- (17.4) fold respectively in the GABA EC_{50}.

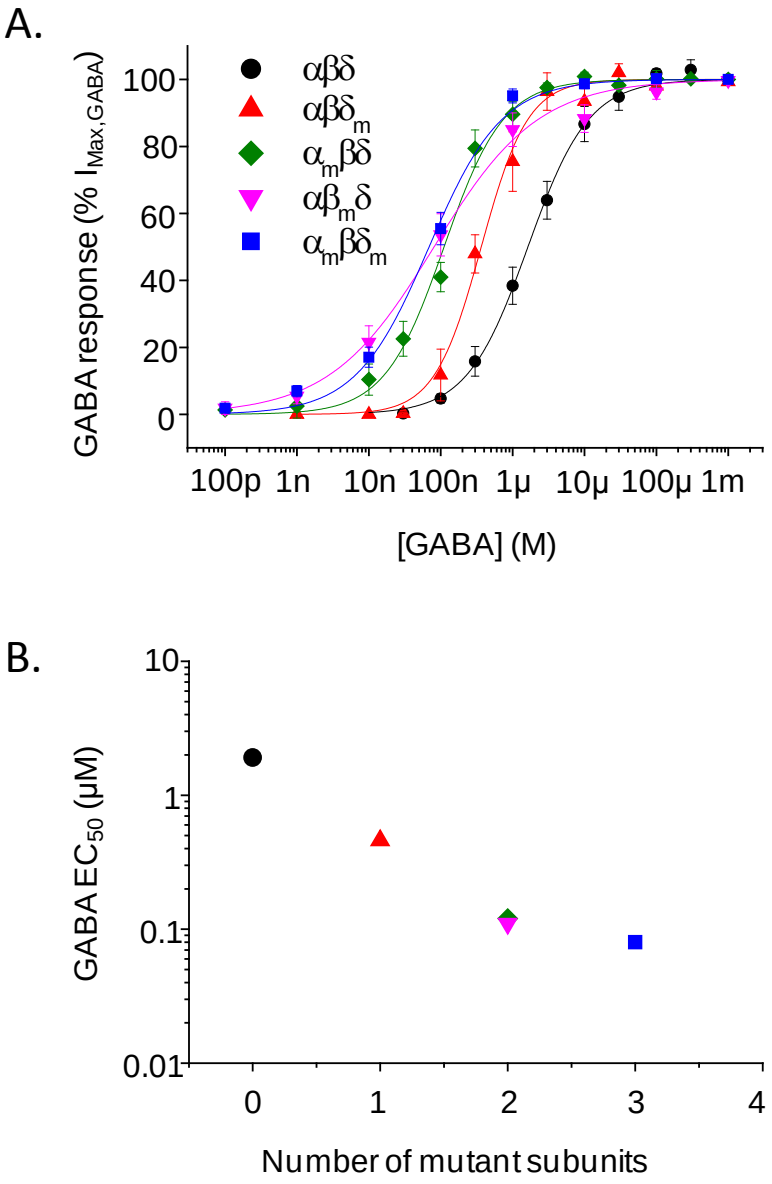

Figure 3.6 - L9'S mutations in α4, β3 and δ subunits increase GABA sensitivity.

A. GABA concentration-response curves for αβδ, αβδ_m, α$_m$βδ, αβ$_m$δ and α$_m$βδ$_m$ receptors. Data represent the mean ± SEM from n = 5 - 9. The data from each cell was fitted with a Hill equation (continuous curves), using a least-squares method, and the average parameters for each construct are listed in *Table* 3.2. **B.** Relationship between the average GABA EC_{50} values and number of mutant receptors incorporated into the receptor pentamer (assuming a stoichiometry of 2α: 2β: 1δ).

Table 3.2 – Peak GABA concentration response curve parameters for WT, and L9'S containing α4β3δ receptors.

Subunit combination	GABA EC_{50} (μM)	n_H	No. of mutants*
αβδ	1.91 ± 0.47	1.1 ± 0.04	0
$αβδ_m$	0.46 ± 0.11	1.4 ± 0.1	1
$αβ_mδ$	0.11 ± 0.04	0.6 ± 0.1	2
$α_mβδ$	0.12 ± 0.03	1.2 ± 0.2	2
$α_mβδ_m$	0.08 ± 0.02	1.0 ± 0.1	3

*Number of mutants within the pentamer assuming a 2α: 2β: 1δ stoichiometry. GABA concentration-response curves were obtained from 5 - 9 HEK293 cells expressing αβδ, $αβδ_m$, $αβ_mδ$, $α_mβδ$, or $α_mβδ_m$ receptors. The Hill equation was fitted to each data set, and the mean values for GABA potency (EC_{50}) and the Hill slope (n_H) are shown in the table as mean ± SEM.

To estimate the number of subunits likely to exist within each αβδ heteropentamer, we must make some assumptions. First, we assume that each subunit mutation has an equivalent effect on GABA potency and that this effect is independent of the subunit class (α, β, or δ) in which the L9'S mutation is inserted. Secondly, it is assumed that each additional L9'S substitution within the receptor complex acts independently. For $α_mβδ$ receptors, if we further assume that the receptor contains two α subunits, then we would expect the shift in GABA EC_{50} induced by the $α_m$ to be approximately the square of the change produced by a single α subunit. Thus, the EC_{50} shift of 15.9 observed for $α_mβδ$ receptors suggests that each $α_m$ subunit induced a 4 - fold change in GABA EC_{50}. Similarly for $αβ_mδ$ receptors, a 17.4 - fold shift indicates that each $β_m$ subunit (if two copies are present in the receptor) caused a 4.2 – fold change in GABA sensitivity. Since these changes are equivalent to that caused by the δ subunit (4.2), the findings therefore suggest that relative to the δ subunit, twice the number of α4 and β3 subunits are likely to exist in each receptor complex. Thus, since $GABA_A$ receptors are assumed to form pentameric complexes, $α_mβδ$, $αβ_mδ$ and $αβδ_m$ receptors most likely contained $2α_m$, $2β_m$ and $1δ_m$ subunits, respectively.

3.2.5. Increasing GABA sensitivity with the number of co-assembled L9'S mutant subunits

For muscle, heteromeric nACh receptors, each 9' polar substitution within the ion channel confers an additional ~ 10 – fold increase in agonist sensitivity (Filatov and White, 1995; Labarca *et al*., 1995). However, such a linear relationship has not been observed for recombinant α1β2γ2S $GABA_A$ receptors (Chang and Weiss, 1999), where mutations in α, β and γ subunits contribute unequally to the increased GABA sensitivity, thus precluding an estimate of αβγ stoichiometry (Chang and Weiss, 1999). For our α, β and δ subunit receptors, the EC_{50} shifts induced by each L9'S mutation appeared more consistent, with each mutation contributing an ~ 4 - fold increase in GABA sensitivity. We therefore investigated the relationship between GABA potency and the number of mutant substitutions within δ-containing receptors, by recording from $\alpha_m\beta\delta_m$ receptors.

Based on our predictions, $\alpha_m\beta\delta_m$ receptors would be expected to contain three mutant subunits (i.e. two α_m and one δ_m), and thus display an even greater sensitivity to GABA than $\alpha_m\beta\delta$ (double mutant) or $\alpha\beta\delta_m$ (single mutant) receptors.

The average GABA concentration-response curve for $\alpha_m\beta\delta_m$ receptors (*Fig.* 3.6 A) was used to determine a GABA EC_{50} of 0.08 ± 0.02 μM (*Table* 3.2) for this receptor type. This equates to a 23.9 - fold increase in GABA sensitivity, relative to WT αβδ receptors. We would expect the shift in GABA EC_{50} produced by the triple mutant ($\alpha_m\beta\delta_m$) to be approximately the cube of the change produced by a single mutant subunit. Thus for $\alpha_m\beta\delta_m$ receptors, the observed shift of 23.9 - fold approximates to a 3 - fold shift (2.9) per mutant subunit.

However, based on the double mutant receptors, we predicted a ~ 4 - fold shift per subunit and thus for three mutant subunits, we might have expected a 64 - fold increase in GABA sensitivity. The discrepancy between the predicted and actual shift observed for $\alpha_m\beta\delta_m$ could arise from the δ_m subunit being absent from $\alpha_m\beta\delta_m$ receptor expressing cells, leaving cell surface receptors mainly

composed of αβ receptors containing just two mutant α_m subunits. However, this seemed unlikely given that for $\alpha_m\beta\delta_m$ expressing cells, there was clear evidence of cell surface δ_m-GFP fluorescence. Furthermore, $\alpha_m\beta\delta_m$ expressing cells exhibited a level of spontaneous activity (49.4 ± 8.4 %) that was comparable to the combined spontaneous activities of $\alpha_m\beta\delta$ (21.9 ± 5.3 %) and $\alpha\beta\delta_m$ receptors (15.7 ± 1.3 %; *Fig.* 3.5 B). Taken together, these data suggest that both α_m and δ_m subunits were efficiently incorporated into functional $\alpha_m\beta\delta_m$ receptors.

Indeed, our predicted shift of 64 - fold for $\alpha_m\beta\delta_m$ receptors was based on the assumption that each additional mutant subunit within the receptor complex acts independently. The lower, experimentally derived, GABA EC_{50} shift observed for $\alpha_m\beta\delta_m$ receptors (23.9) suggests that although this assumption might hold for receptors with two mutant subunits, three mutant substitutions within a receptor complex might result in some degree of interaction between adjacent mutant subunits, and possibly give rise to deviations between the predicted and observed curve shifts.

3.2.6. cDNA transfection ratio has no effect on α4β3δ receptor stoichiometry

Recently, it was demonstrated that the number of δ subunits incorporated into recombinant α4β2δ receptors could vary with the cDNA transfection ratio (Wagoner and Czajkowski, 2010). This was achieved by inserting α-bungarotoxin binding sites into individual $GABA_A$ receptor subunits, and subsequently quantifying the bungarotoxin fluorescence of tagged cell surface receptors immunopurified from transfected HEK293 cells. The functional consequences of these stoichiometric changes were not directly analysed by Wagoner and Czajkowski (2010). Moreover, the functional significance of altering α:β:δ cDNA transfection ratio has, to date, been largely been assessed on recombinant α4β3δ receptors expressed in *Xenopus laevis* oocytes (another commonly used expression system used to study the function and pharmacology of recombinant receptors), yielding conflicting results. For

instance, while one group reported significantly higher GABA EC_{50} values from *Xenopus* oocytes injected with higher levels of δ cRNA (You and Dunn, 2007), another found no significant effect of altering transfection ratio on GABA, or Zn^{2+} sensitivity (Borghese and Harris, 2007).

Therefore, we studied the effect of altering the cDNA transfection ratio on the function, and stoichiometry of α4β3δ receptors expressed in a HEK293 expression system. Cells were transfected with one of the following three, commonly used, α:β:δ cDNA ratios - 1:1:1, 1:1:10 or 10:1:10 (Borghese *et al*., 2006; Stórustovu and Ebert, 2006; Barrera *et al*., 2008; Hoestgaard-Jensen *et al*., 2010).

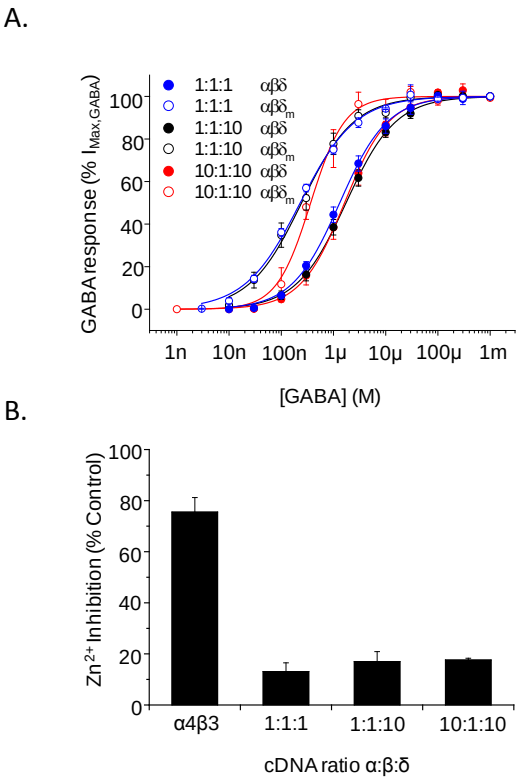

Figure 3.7 - cDNA transfection ratio has no effect on α4β3δ receptor stoichiometry.

A. GABA concentration-response curves for αβδ (filled circles) or $αβδ_m$ (open circles) expressing cells, transfected with the α:β:δ cDNA ratios: 1:1:1, 1:1:10 and 10:1:10. The Hill equation was fitted to each data set using a least-squares method (continuous curves). **B.** Inhibition by 1 μM Zn^{2+} of GABA EC_{50} currents for αβ, or αβδ receptors expressed following transfection with one of three α:β:δ cDNA ratios: 1:1:1 (blue), 1:1:10 (black) and 10:1:10 (red; n = 4 - 5; mean ± SEM). The total amount of cDNA used for each transfection was 4 μg.

First, the effect of varying the transfection ratio was studied on the GABA sensitivities of αβδ and $\alpha\beta\delta_m$ receptors. For WT αβδ receptors, altering the transfection ratio had no effect on GABA sensitivity (1.4 ± 0.2, 1.9 ± 0.3 and 1.9 ± 0.5 μM for α:β:δ ratios of 1:1:1, 1:1:10 and 10:1:10 respectively; one way ANOVA – Bonferroni: $p = 0.56$). Similarly, the GABA concentration-response curves for $\alpha\beta\delta_m$ expressing cells transfected with different ratios were also indistinguishable (*Fig.* 3.7 A), and their GABA EC_{50} values (0.2 ± 0.01, 0.3 ± 0.1 and 0.5 ± 0.1 μM for $\alpha:\beta:\delta_m$ ratios of 1:1:1, 1:1:10 and 10:1:10 respectively) did not vary significantly (one way ANOVA – Bonferroni: $p = 0.20$). Although there appears to be a trend for $\alpha\beta\delta_m$ expressing cells transfected with a 10:1:10 ratio to have higher n_H (1.4 ± 0.2; *Fig.* 3.7 A) than those transfected with either a 1:1:1 (0.8 ± 0.03) or 1:1:10 (0.9 ± 0.2) transfection ratio, this trend was not significant ($p = 0.09$ and $p = 0.17$ respectively).

Next, we determined the sensitivity of α4β3δ expressing cells to the subtype selective blocker, Zn^{2+} (Smart *et al*., 1991; Nagaya and Macdonald, 2001; Hosie *et al*., 2003). GABA EC_{50} current responses for α4β3 and α4β3δ receptors were recorded in the absence, or presence of (pre-applied and) co-applied 1 μM Zn^{2+}. Note that cells expressing α4β3 receptors were transfected with a cDNA transfection ratio of 1α: 1β. As with WT α4β2 receptors (see *Fig.* 3.4), 1 μM Zn^{2+} significantly inhibited the GABA EC_{50} response of α4β3 receptors by 75.5 ± 5.7 % (*Fig.* 3.7 B). By contrast, the Zn^{2+} sensitivity of α4β3δ expressing cells did not vary significantly with the αβδ transfection ratio (13.1 ± 3.4, 17.0 ± 3.9 and 17.6 ± 0.7 %; One way ANOVA – Bonferroni: $p = 0.5$), but all were significantly reduced compared to Zn^{2+} inhibition of αβ receptors (*Fig.* 3.7 B; One way ANOVA – Dunnetts: $p < 0.0001$).

Overall, these data indicate that altering cDNA transfection ratio has no significant effect on the GABA, or Zn^{2+}, sensitivities of WT α4β3δ receptors. Moreover, since the relative GABA EC_{50} shifts between δ and δ_m expressing cells (*Fig.* 3.7 *A*) remain unchanged with different cDNA transfection ratios, it appears that, at least for the three transfection ratios investigated, the number of δ subunits incorporated into functional α4β3δ receptors remains relatively constant in this expression system.

3.2.7. Co-expressing WT and mutant subunits confirms α4β3δ receptor stoichiometry

Our deductions so far, are based on the assumption that each subunit mutation has an equivalent effect on GABA potency, irrespective of the subunit in which the L9'S mutation is inserted. Although this holds for α4β3δ receptors, where mutations in α, β, or δ give rise to an ~ 4 - fold increase in GABA sensitivity, some deviation may occur when the number of mutant substitutions is increased above 1 - 2 per receptor pentamer, as noted for α1β2γ2S $GABA_A$ receptors (Chang *et al*., 1996), and heteromeric nACh receptors (Labarca *et al*., 1995). To overcome this methodological limitation, Chang *et al*. (1996) proposed an alternative approach for deducing subunit stoichiometry that does not rely on the relative EC_{50} shifts induced by different classes of mutant subunits, but instead upon co-expressing L9'S mutants with their WT counterparts in the same cells, to generate multiple populations of receptors (Chang *et al*., 1996).

In principle, the co-expression of WT subunits with their respective L9'S mutants (e.g. α and α_m) should introduce discrete and discernible components into the GABA concentration-response curve of expressing cells. For example, assuming there are two α subunits per receptor pentamer, these components would represent distinct $GABA_A$ receptors of: ααβδ, $\alpha_m\alpha_m$βδ and αα_mβδ and its equivalent, α_mαβδ. Thus, the GABA sensitivity exhibited by each individual receptor population would give rise to an inflection in the concentration-response curve, and the number of components displayed could be used to infer the subunit stoichiometry, as has been accomplished for α1β2γ2S $GABA_A$ receptors (Chang *et al*., 1996).

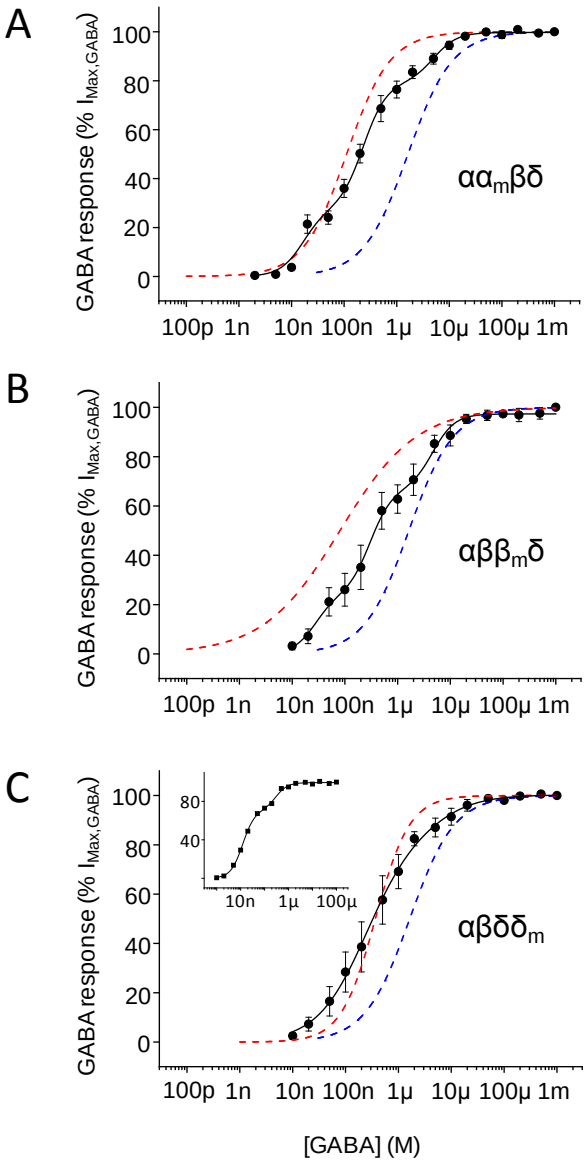

Figure 3.8 - Co-expression of WT and mutant L9'S α4, β3 and δ subunits.

Co-expression of WT and mutant L9'S α4, β3 and δ subunits. GABA concentration-response curves (black continuous curves) for (**A**) α,α_m,β,δ (n = 6); (**B**) α,β,β_m,δ (n = 6); and (**C**) α,β,δ,δ_m. (n = 10), fitted using a two or three-component Hill equation (using *Equation* 2.1). Also shown for each receptor class, are the Hill equation fits for the GABA concentration-response curves of WT αβδ receptors (blue dashed lines), and their respective L9'S mutants (red dashed lines): α_mβδ (**A**), αβ$_m$δ (**B**) and αβδ$_m$ (**C**). For α,β,δ,δ_m, the GABA concentration-response curves of 7/10 cells exhibited two discernible components. The inset is an example GABA concentration-response curve from a cell exhibiting two such components. The total amount of cDNA used for each transfection was 4 µg, and equal amounts of WT, and their respective L9'S mutant cDNA were used. Data points are shown as mean ± SEM.

Table 3.3 –Peak GABA concentration response curve parameters for $\alpha_m\alpha\beta\delta$, $\alpha\beta\beta_m\delta$ and $\alpha\beta\delta\delta_m$-expressing cells

	First component		Second component		Third component		
Receptor subunits	**EC_{50} (μM)**	**Proportion (%)**	**EC_{50} (μM)**	**Proportion (%)**	**EC_{50} (μM)**	**Proportion (%)**	**n_H**
$\alpha,\alpha_m,\beta,\delta$	0.02 ± 0.005	34.0 ± 3.3	0.3 ± 0.03	48.7 ± 5.6	5.7 ± 0.9	17.5 ± 2.7	1.6 ± 0.4
$\alpha,\beta,\beta_m,\delta$	0.03 ± 0.01	24.7 ± 3.5	0.3 ± 0.1	43.9 ± 3.5	4.7 ± 0.7	31.5 ± 2.6	2.1 ± 0.3
$\alpha,\beta,\delta,\delta_m$	0.21 ± 0.01	75.8 ± 3.0	-	-	2.1 ± 0.5	24.2 ± 2.8	0.9 ± 0.1

GABA concentration response curve Hill equation best-fit parameters derived from curve fitting data from 6 - 10 HEK293 cells expressing $\alpha,\alpha_m,\beta,\delta$, $\alpha,\beta,\beta_m,\delta$ or $\alpha,\beta,\delta,\delta_m$. Individual cells expressing, $\alpha,\alpha_m,\beta,\delta$; $\alpha,\beta,\beta_m,\delta$; or $\alpha,\beta,\delta,\delta_m$ were fit using a two- or three-component Hill equation. The relative component proportions (%), and GABA EC_{50} values are expressed as mean ± SEM. Cells were transfected with a cDNA transfection ratio of 10:1:10.

Taking a similar approach for α4β3δ receptors, we generated GABA concentration-response curves for cells co-transfected with β, δ and equal amounts of α and α_m cDNAs. Note that the overall αβδ cDNA transfection ratio was 10:1:10. The GABA concentration-response curves for α,α_m,β,δ-expressing cells exhibited three discernible components, which were described by the sum of three Hill equations (*Fig.* 3.8 A). The first and third components, accounted for 34.0 ± 3.3 % and 17.5 ± 2.7 % of the total receptor population, with GABA EC_{50} values of 0.02 ± 0.005 μM and 5.7 ± 0.9 μM, respectively (*Table* 3.3). These EC_{50} values are similar to those obtained for α_mβδ (0.46 ± 0.11 μM) and αβδ (1.91 ± 0.47 μM) receptors, suggesting these two components in the α,α_m,β,δ concentration-response curve (*Fig.* 3.8 A) are attributable to α_mβδ and αβδ receptors. Moreover, the presence of an intermediary component with an EC_{50} of 0.3 ± 0.03 μM (48.7 ± 5.6 %) suggested the expression of a third receptor population, containing one WT and one mutant subunit (i.e. αα_mβδ or α_mαβδ). Similar to α,α_m,β,δ expressing cells, the GABA concentration-response curves of α,β,β_m,δ expressing cells revealed three discernible components (*Fig.* 3.8 *B*). The first component (24.7 ± 3.5 %) had an EC_{50} of 0.03 ± 0.01 μM (*Table* 3.3), probably corresponding to the αβ_mδ receptor population. Approximately 31.5 ± 2.6 % of receptors exhibited an EC_{50} of 4.7 ± 0.7 μM, attributable to αβδ receptors. Again, the appearance of an intermediary component with an EC_{50} of 0.3 ± 0.1 μM (43.9 ± 3.5 %) was indicative of a third receptor population containing both β subtypes (i.e. β and β_m).

By contrast, the mean GABA concentration-response curve for α,β,δ,δ_m receptors did not exhibit obvious multiple components (*Fig.* 3.8 *C*). However, detailed analysis of individual concentration-response curves revealed that for most cells sampled (7/10), two components were discerned (*Fig.* 3.8 *C* inset). For those cells exhibiting two components, the majority of receptors (75.8 ± 3.0 %) exhibited a GABA EC_{50} of 0.21 ± 0.01 μM, while 24.2 ± 2.8 % of receptors exhibited an EC_{50} of 2.1 ± 0.5 μM. The GABA sensitivities of these two components are similar to those observed for αβδ_m (0.46 ± 0.11 μM; *Table* 3.2) and αβδ receptors (1.91 ± 0.47 μM; *Table* 3.2) respectively. Although the remaining cells (3/10) did not overtly display multiple components, their GABA sensitivities were intermediary to those of αβδ and αβδ_m expressing cells. The

absence of a third component suggested that α,β,δ,δ_m expressing cells exhibit only two receptor populations, likely αβδ and αβδ_m. This suggests that each αβδ receptor complex likely contains only one δ subunit.

Collectively, these data demonstrate that α4β3δ receptors most likely possess a stoichiometry of two α, two β and one δ subunit.

3.3. Discussion

Previous studies have demonstrated that binary αβ subunits can efficiently co-assemble to form functional receptors in recombinant expression systems (Mortensen *et al*., 2011; Karim *et al*., 2013). Therefore, in this body of work, we compared the functional and pharmacological profiles of α1βγ2L, α5βγ2L, α4βδ and α6βδ receptors, with their respective αβ counterparts, to verify that γ2 and δ subunits were efficiently incorporated into functional heteropentamers in the HEK293 expression system.

Additionally, whilst the stoichiometry of synaptic α1β2γ2 subunit-containing $GABA_A$ receptors has consensus support for 2α: 2β: 1γ (Backus *et al*., 1993; Chang *et al*., 1996; Tretter *et al*., 1997), the stoichiometry of extrasynaptic δ-containing receptors remains unclear, and potentially variable depending on the experimental conditions (Baur *et al*., 2009; Kaur *et al*., 2009; Wagoner and Czajkowski, 2010). We therefore probed the stoichiometry of recombinant α4β3δ receptors by analysing the electrophysiological and pharmacological consequences of inserting a well characterised L9'S reporter mutation into the M2 regions of α4, β3, and δ subunits.

3.3.1. γ2 subunits are efficiently incorporated into recombinant $GABA_A$ receptors

The positive allosteric modulator, diazepam was used to pharmacologically confirm γ2 expression, since receptors lacking the γ2 subunit (i.e. binary αβ constructs) are insensitive to the potentiating actions of diazepam (Pritchett *et al*., 1989). Indeed, diazepam significantly potentiated (by approximately 2.5 -fold) the EC_{15} GABA responses of α1βγ2L and α5βγ2L receptors, but not α1β3 or α5β3 receptors. Although we cannot exclude the possibility that some αβ-heteromers were also present in α1β3γ2L- and α1β3γ2L-expressing cells, these

data indicate that in our recombinant expression system, γ2L was efficiently expressed and co-assembled into functional receptors.

3.3.2. The δ subunit is efficiently incorporated into recombinant $GABA_A$ receptors

To promote δ-expression in our HEK293 cells, we initially used a cDNA transfection ratio of 10α: 1β: 10δ, since this transfection ratio has previously conferred efficient δ-expression in oocytes (Stórustovu and Ebert, 2006; Hoestgaard-Jensen *et al*., 2010). However, at least for α4β3δ receptors, varying the cDNA transfection ratio by 10 - fold (i.e. 1:1:1, 1:1:10 or 10:1:10) had no significant effect on receptor function, or subunit stoichiometry, suggesting that this was not crucial to ensuring efficient δ-expression.

Very few groups have compared the pharmacological differences between α6β and α6βδ receptors, largely due to the poor functional expression of α6β receptors in recombinant systems (Saxena and Macdonald, 1994; Stórustovu and Ebert, 2006). In our HEK293 expression system, both α6β2δ- and α6β2-expressing cells displayed GABA activated currents, although the latter displayed significantly smaller maximal GABA currents. The reduced maximal GABA current observed for recombinant α6β2 receptors suggests that either binary α6β2 constructs co-assemble fairly inefficiently in recombinant expression systems (as reported by Saxena and Macdonald, 1994; Stórustovu and Ebert, 2006), or that they display a lower single channel conductance, as has been demonstrated for α1β receptors (Verdoorn *et al*., 1990; Mortensen and Smart, 2006). Nonetheless, by generating GABA-concentration-response curves for α6β2- and α6β2δ-expressing cells, we found that the GABA sensitivity for α6β2δ receptors (EC_{50}: 0.3 ± 0.03) was significantly higher than that observed for α6β2 receptors (EC_{50}: 0.6 ± 0.04). This increased GABA sensitivity, coupled with the higher maximum GABA current observed for α6β2δ receptors indicates that δ is expressed, and co-assembled into functional α6β2δ receptors.

Notably, α6β2δ receptors exhibited the highest GABA potency compared to the other synaptic- and extrasynaptic-$GABA_A$ subtypes investigated in this chapter (see *Table* 3.1). This intrinsic property makes them ideally suited to mediate tonic currents, as they can respond to low ambient GABA levels.

Similarly both α4β2δ and α4β3δ receptors demonstrated high GABA potencies (0.7 ± 0.1 μM and 1.9 ± 0.5 μM respectively; *Table* 3.1). We confirmed that α4βδ-expressing cells did not contain a large population of αβ receptors, by using the subtype selective inhibitor, Zn^{2+} (Smart *et al*., 1991; Nagaya and Macdonald, 2001; Hosie *et al*., 2003). In our study, a subtype selective concentration of Zn^{2+} (1 μM; Krishek *et al*., 1998; Hosie *et al*., 2003; Stórustovu and Ebert, 2006) significantly inhibited the GABA EC_{50} responses of α4β receptors (by approximately 80 %), but produced relatively smaller inhibitions of the EC_{50} GABA responses for α4β3δ receptors, indicating again, that the δ subunit was efficiently incorporated into functional α4βδ heteropentamers.

For α4β3δ receptors, we found that altering the cDNA transfection ratio had no significant effect on GABA sensitivity, or the level of inhibition produced by 1 μM Zn^{2+}. The functional consequences of altering α:β:δ transfection ratios has previously been assessed on recombinant α4β3δ receptors expressed in oocytes, with conflicting outcomes. While one study demonstrated that increasing relative amounts of δ cRNA increased the GABA EC_{50} and decreased the Hill slopes for α4β3δ GABA concentration-response curves (You and Dunn, 2007), another study reported no significant effect of altering cRNA transfection ratio GABA, or Zn^{2+} sensitivity (Borghese and Harris, 2007). Since both studies were performed using the same oocyte expression system, the reasons for these discrepancies remain unclear. Nonetheless, by using a HEK293 expression system, no significant effect of altering cDNA transfection ratio was apparent on α4β3δ receptor function.

3.3.3. α4β3δ receptors display a subunit stoichiometry of 2α: 2β: 1δ

The subunit composition of $GABA_A$ receptors is an important determinant of their functional properties, as demonstrated by the distinct Zn^{2+} sensitivities of αβ and αβδ receptors. Given that many orthosteric, and allosteric, binding sites on $GABA_A$ receptors are interfacial (Sieghart *et al*., 2012), it is important to understand the preferred subunit stoichiometries of such receptors, since this will critically define the nature of these interfaces, and thus the GABA receptor's response to ligand binding.

We probed α4β3δ stoichiometry, by introducing a well-characterized 9' leucine-to-serine substitution into the M2 domains of α4, β3 and δ subunits. Each polar substitution increased the GABA sensitivity of mutant subunit-containing receptors (by approximately 4 - fold), in relative proportion with the number of mutant subunits assembled in the receptor. This, in conjunction with data derived from cells co-expressing mutant and respective WT subunits, revealed a relatively consistent subunit stoichiometry by these methods, of 2α, 2β and 1δ. Moreover, our data indicate that, at least for three commonly used α:β:δ transfection ratios 1:1:1, 1:1:10 or 10:1:10 (Borghese *et al*., 2006; Stórustovu and Ebert, 2006; Barrera *et al*., 2008; Hoestgaard-Jensen *et al*., 2010), the number of incorporated δ subunits seemingly remains fixed at one.

Our deductions regarding the stoichiometry of recombinant α4β3δ receptors are predicated on the assumption that the L9'S mutations do not perturb the 'normal' subunit stoichiometry of these receptors. Since N-terminal motifs are key determinants of $GABA_A$ receptor subunit assembly (Connolly *et al*., 1996; Taylor *et al*., 1999; Klausberger *et al*., 2001), it seems unlikely that a point mutation within the ion channel-lining, M2 region would alter receptor subunit stoichiometry. However, it is intriguing that for most α,β,δ,δ_m expressing cells, the component attributable to αβδ_m receptors was larger than that for αβδ receptors (~ 75 and 24 %, respectively; see *Table* 3.3), suggesting that δ_m might be more efficiently incorporated into functional receptors than δ.

Given the M2 location of the point mutation, a more likely explanation for the disproportionate percentage components is that the L9'S mutations may affect the gating kinetics of the receptor. Indeed, for nACh receptors (Filatov and White, 1995) and α1β3γ2L $GABA_A$ receptors (Bianchi and Macdonald, 2001), it has been demonstrated that 9' mutant containing receptors can exhibit altered single channel conductances and/or open probabilities. This could cause the relative proportions attributable to αβδ and $\alpha\beta\delta_m$ to vary (Chang *et al*., 1996). Nevertheless, since our conclusions rely on the number of observable components in the concentration-response curves and not on the relative contribution of each individual component, our conclusion that α4β3δ receptors contain only one δ subunit still remains valid.

To date, only two studies have investigated the subunit stoichiometry of unconstrained recombinant α4β2/3δ receptors. While a stoichiometry of 2α: 2β: 1δ has been demonstrated for recombinant α4β3δ receptors expressed in tsA cells, using atomic force microscopy (Barrera *et al*., 2008), the immunopurification of cell surface α4β2δ receptors from HEK293 cells has indicated that more than one δ can exist within the receptor complex (Wagoner and Czajkowski, 2010). Moreover, in the latter study, this increased δ incorporation coincided with a concomitant decrease in β2 incorporation, and was dependent on increasing the relative abundance of δ during transfection.

Although the reasons for the discrepancies between our observations, and those reported by Wagoner and Czajkowski (2010) remain unclear, one explanation might be the use of different β isoforms, since β2 and β3 subunits have been demonstrated to have distinctive assembly properties (Taylor *et al*., 1999). This might have important implications for their oligomerization with δ subunits.

3.3.4. The importance of subunit positioning

Whilst we demonstrate a stoichiometry of 2α: 2β: 1δ for α4β3δ receptors, our data gives little indication of subunit arrangement within the pentamer, which could be an important determinant of αβδ receptor function (Baur *et al*., 2009; Kaur *et al*., 2009). The subunit positional arrangement of α1βγ2 receptors is widely accepted to be βαβαγ (anticlockwise; Baumann *et al*., 2001; Baur *et al*., 2006; Smart and Paoletti, 2012). Given the conflicting evidence regarding the number of incorporated δ subunits, it is unsurprising that the subunit arrangement of recombinant αβδ also remains undefined. For α4β3δ receptors with a stoichiometry of 2α: 2β: 1δ, structural microscopic analysis has revealed a predominant βαβαδ anticlockwise arrangement (Barrera *et al*., 2008), suggesting δ can assume the position of the γ2 subunit in an αβγ receptor. However, in the same study, a minority of receptors (~ 21 %) were found to have an alternative βαβδα subunit arrangement, indicating more than one arrangement may be possible (Barrera *et al*., 2008). Indeed it has been recently demonstrated that δ can assume multiple positions when constrained within αβδ concatamers (Baur *et al*., 2009; Kaur *et al*., 2009). Intriguingly, concatameric α4β2δ receptors with the βαβαδ anticlockwise conformation (Shu *et al*., 2012) form functional receptors with similar pharmacological profiles to unconstrained recombinant α4β2δ receptors (Stórustovu and Ebert, 2006), whereas α1β3δ receptors formed from the alternative βαβδα anticlockwise arrangement, exhibit similar GABA and Zn^{2+} sensitivities to non-concatenated receptors (Kaur *et al*., 2009). Moreover, concatameric α1β3δ receptors with an βαβαδ (anticlockwise) subunit arrangement appear to be ~ 26 - fold less sensitive to GABA than receptors with the βαβδα (anticlockwise) subunit arrangement (Kaur *et al*., 2009), demonstrating the functional importance of subunit location within a receptor pentamer.

The potentially variable subunit arrangements indicated for recombinant α4β2δ (Shu *et al*., 2012), α4β3δ (Barrera *et al*., 2008) and α1β3δ (Kaur *et al*., 2009) receptors may reflect different co-assembly properties of δ, with different α and β subunits, or differences in the type of expression system used (mammalian cell lines versus oocytes). Overall, these findings indicate that the subunit

arrangement of recombinant, and indeed native δ containing receptors, is still open to question.

3.4. Conclusion

1. Diazepam selectively potentiates the GABA responses of α1β3γ2L and α5β3γ2L receptors, indicating that the γ2L subunit is efficiently co-assembled into functional receptors overexpressed in HEK293 cells.

2. The δ subunit is efficiently incorporated into functional α4β2/3δ and α6β2δ receptors overexpressed in HEK293 cells, assessed by receptor sensitivities to GABA and Zn^{2+}.

3. The subunit stoichiometry of heterologously-expressed α4β3δ receptors is 2α: 2β: 1δ.

4. Varying the cDNA transfection ratio by 10 - fold has no significant effect on the function (GABA and Zn^{2+} sensitivity) or stoichiometry of α4β3δ receptors.

Chapter 4: Functional effects of 4-PIOL on synaptic- and extrasynaptic-type, recombinant $GABA_A$ receptors

4.1. Introduction

As discussed in *Section* 1.3, elevated $GABA_A$-receptor mediated tonic currents are observed in several neurological disorders, including absence epilepsy, stroke, cognitive disorders and Alzheimer's disease (Brickley and Mody, 2012). Therefore, pharmacologically reducing tonic inhibition may offer a therapeutically useful approach for treating such disorders (Dawson *et al*., 2006; Clarkson *et al*., 2010; Errington *et al*., 2011; Martínez-Cué *et al*., 2013).

Unfortunately, as discussed in *Section* 1.2.3, there is a significant lack of $GABA_A$ receptor antagonists that can selectively reduce δ-mediated tonic currents, without affecting other γ2-mediated phasic currents. As an alternative to using $GABA_A$ receptor antagonists, it has previously been suggested that low efficacy partial agonists may be therapeutically useful, largely due to their functionally competitive antagonist profile when compared to full agonists, and reduced propensity to induce convulsions, or unwanted side effects (Krogsgaard-Larsen *et al*., 2002). In this chapter, the $GABA_A$ receptor subtype selectivity of the weak partial agonist, 4-PIOL, was studied. 4-PIOL was initially developed as a non-ring fused THIP analogue (*Fig*. 4.1), which acted as a weak $GABA_A$ receptor agonist on cat spinal neurons, as assessed using extracellular electrophysiological recordings (Byberg *et al*., 1987). Subsequently, whole-cell patch clamp electrophysiology demonstrated that 4-PIOL acted as a weak $GABA_A$ receptor agonist on cultured hippocampal neurons, cerebral cortical neurons, cerebellar granule cells and on recombinant α1β2γ2 receptors (Falch *et al*., 1990; Kristiansen *et al*., 1991; Frølund *et al*., 1995; Hansen *et al*., 2001; Mortensen *et al*., 2002, 2004). However, the low agonist efficacy (~ 1 – 2 % of the maximum GABA response) and low agonist potency (EC_{50}: ~ 100 – 300 μM) of 4-PIOL at recombinant and native $GABA_A$ receptors, resulted in 4-PIOL

exhibiting a dominant antagonist profile (Kristiansen *et al*., 1991; Frølund *et al*., 1995; Hansen *et al*., 2001; Ebert *et al*., 2002; Mortensen *et al*., 2002, 2004). Therefore, we decided to explore this antagonist profile further, and assess whether 4-PIOL might be capable of selectively antagonising tonic currents without affecting phasic currents.

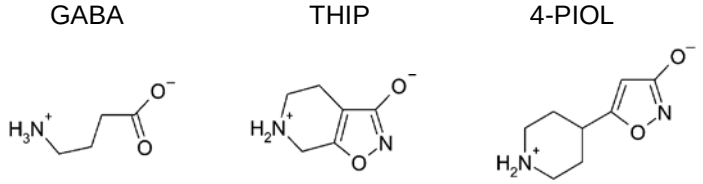

Figure 4.1 – Molecular structures of GABA, THIP and 4-PIOL

4-PIOL was chosen, based on a kinetic model that was devised using our knowledge about the biophysical parameters of $GABA_A$ receptors (Mortensen *et al*., 2002, 2010). Unfortunately, no kinetic data were available for the interaction of 4-PIOL with extrasynaptic-type δ-containing receptors. Therefore, we simulated how α1β3γ2 receptors would behave when activated by GABA alone, and when GABA was co-applied with 10, 100 or 1000 µM 4-PIOL (*Fig.* 4.2). As expected, 4-PIOL was predicted to displace the GABA concentration-response curve to the right in a concentration-dependent manner. Importantly for this synaptic $GABA_A$ receptor subtype, although 4-PIOL (1000 µM) was predicted to significantly inhibit the GABA responses to extrasynaptic concentrations of GABA (100 nM - 1 µM), we further predicted that there would be no significant inhibition of GABA responses to synaptic concentrations of GABA (> 1 mM; *Fig*. 4.2).

To validate this model experimentally, the functional effects of 4-PIOL were studied on recombinant α1β3γ2 receptors expressed in HEK293 cells. In addition, the agonist and antagonist profile of 4-PIOL was also studied on recombinant α5β3γ2, α4β2δ and α6β2δ receptors, since these represent the major extrasynaptic $GABA_A$ receptor isoforms expressed in hippocampal

neurons, thalamic relay neurons and cerebellar granule cells (Laurie *et al*., 1992a; Wisden *et al*., 1992; Pirker *et al*., 2000; Caraiscos *et al*., 2004; Cope *et al*., 2005; Glykys *et al*., 2008; Hörtnagl *et al*., 2013).

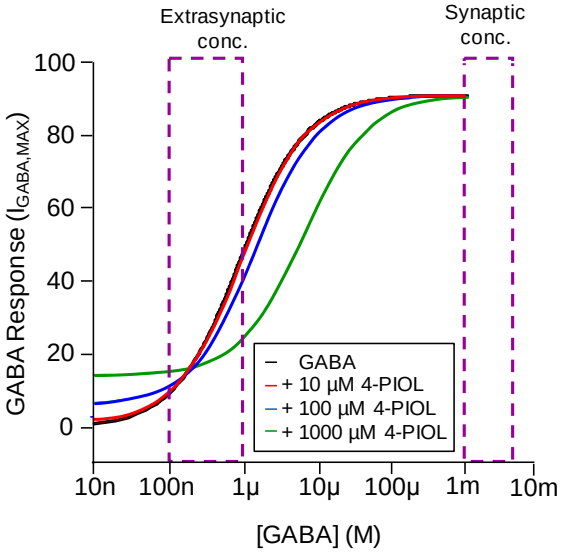

Figure 4.2 – Theoretical agonist and antagonist profiles of 4-PIOL at α1β3γ2 receptors.

The theoretical GABA concentration-response curves, in the absence (black), or presence, of 10 (red), 100 (blue), or 1000 µM (green) 4-PIOL were generated using a receptor model, and the biophysical parameters previously obtained for α1β3γ2 receptors (Mortensen *et al*., 2004, 2010). The purple boxes (dashed lines) represent GABA concentrations proposed to exist at extrasynaptic (100 nM – 1 µM) and synaptic sites (> 1 mM).

4.2. Results

4.2.1. 4-PIOL is a weak partial agonist at recombinant γ2-containing receptors

Given the previously described weak partial agonist profile of 4-PIOL (Kristiansen *et al*., 1991; Rabe *et al*., 2000; Hansen *et al*., 2001; Ebert *et al*., 2002; Mortensen *et al*., 2002, 2004), its agonist activity was further investigated using recombinant α1β3γ2L, α5β3γ2L, α4β2δ and α6β2δ receptors expressed in HEK293 cells.

Note that for some experiments, the short splice variant of the γ2 subunit (γ2S) was used, which differs from the γ2L variant (used in *Chapter* 3), by lacking an eight amino acid cassette in the M3 - M4 intracellular loop. Although the functional differences between γ2S and γ2L were not specifically probed here, previous data from our lab indicates both isoforms exhibit similar diazepam and GABA sensitivities, when expressed in recombinant expression systems (Mortensen *et al*., 2011; Gielen *et al*., 2012).

For α1β3γ2L-expressing cells, whole-cell currents were measured in response to increasing concentrations of 4-PIOL (0.1 – 3000 µM; *Fig.* 4.3 A). Since GABA is considered a full agonist (i.e. has a near maximum efficacy) at γ2-containing receptors (Ebert *et al*., 1994; Mortensen *et al*., 2004), a saturating concentration of GABA (1 mM) was applied to each cell, to assess the macroscopic efficacy of 4-PIOL, relative to GABA. Notably, 4-PIOL elicited significantly smaller whole-cell currents in α1β3γ2L-expressing cells (*Fig.* 4.3 B inset) than GABA. By normalising the peak current elicited by 3 mM 4-PIOL (i.e. a saturating 4-PIOL concentration) to the peak current produced by 1 mM GABA, the macroscopic efficacy of 4-PIOL relative to GABA was estimated to be 2.2 ± 0.2 % for α1β3γ2L receptors (*Fig.* 4.3 B; Fig. 4.3 C; *Table* 4.1).

The normalised concentration-response data for each cell was fitted using the Hill equation (*Equation* 2.1) to determine mean values for 4-PIOL potency (EC_{50}: the 4-PIOL concentration producing 50 % of the maximal 4-PIOL

response) and the Hill coefficient (n_H; *Table* 4.2). The mean 4-PIOL EC_{50} determined for α1β3γ2L receptors was 185.9 ± 60.5 μM, the large error occurring because of the small nature of 4-PIOL currents (*Fig.* 4.3 C).

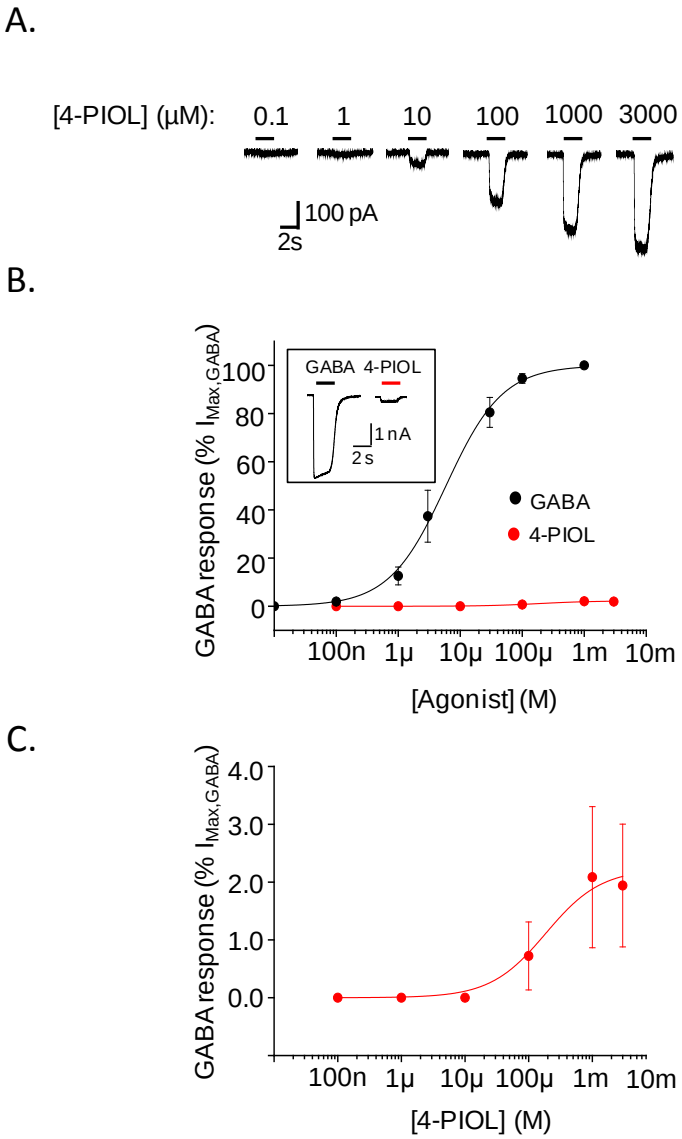

Figure 4.3 – Peak 4-PIOL and GABA concentration-response curves for recombinant α1β3γ2L receptors.

A. Examples of 4-PIOL-gated whole-cell currents generated for α1β3γ2L receptors. Traces represent the peak currents elicited by increasing concentrations of 4-PIOL (0.1 - 3000 μM). **B.** Average peak GABA (black) and 4-PIOL (red) concentration-response curves constructed for α1β3γ2L receptors (n = 5; mean ± SEM). The normalised data from each cell was fitted with a Hill equation (continuous lines), using a least-squares method, and the mean EC_{50}s calculated from these fits were 8.7 ± 2.3 μM and 185.9 ± 60.5 μM for GABA and 4-PIOL respectively. The continuous red and black lines represent Hill fits to the mean concentration-response data. Note that currents generated by 4-PIOL were normalised to the peak current elicited by a saturating concentration of GABA (1 mM) for each cell. The inset shows example traces of whole-cell currents elicited by 1 mM GABA and 3 mM 4-PIOL, both recorded from the same α1β3γ2L-expressing cell. **C.** An expanded version of the 4-PIOL concentration-response curve from panel B.

Similarly, 4-PIOL elicited agonist-induced currents at α5β3γ2L-expressing cells. Concentration-response curves were generated, as before, by applying increasing concentrations of 4-PIOL (0.1 – 3000 μM; *Fig.* 4.4) to α5β3γ2L-expressing cells. By fitting the 4-PIOL concentration-response data for each cell with the Hill equation (*Equation* 2.1), and averaging the resulting parameters (EC_{50} and n_H), the mean 4-PIOL potency for α5β3γ2L receptors was determined to be 90.2 ± 16.8 μM (*Fig.* 4.4; *Table* 4.1). The peak current produced by 3 mM 4-PIOL (a saturating concentration of 4-PIOL; *Fig.* 4.4) was normalised to the peak current elicited by a saturating 1 mM GABA concentration, revealing that the maximum 4-PIOL current for α5β3γ2L receptors was 8.3 % ± 2.2 % of the maximal GABA current (*Table* 4.1).

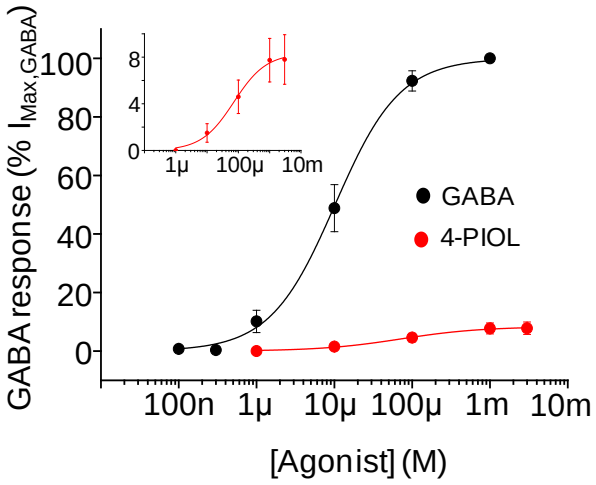

Figure 4.4 – Peak 4-PIOL and GABA concentration-response curves for recombinant α5β3γ2L receptors.

Average peak GABA (black) and 4-PIOL (red) concentration-response curves constructed for α5β3γ2L receptors. The normalised data from each cell (n = 4 - 5) were fitted with a Hill equation, using a least-squares method, and the mean EC_{50}s calculated from these fits was 11.9 ± 3.6 μM and 90.2 ± 16.8 μM for GABA and 4-PIOL, respectively. The continuous red and black curves represent Hill fits to the mean concentration-response data. Note that currents generated by 4-PIOL were normalised to the peak current elicited by a saturating concentration of GABA (1 mM) for each cell, revealing that the maximum 4-PIOL response was 8.3 ± 2.2 % of the maximum GABA response. Data are expressed as mean ± SEM. The inset is an expanded version of the 4-PIOL concentration-response curve.

Table 4.1 – 4-PIOL concentration-response curve parameters for recombinant α1β3γ2L and α5β3γ2L receptors.

Subunit combination	4-PIOL EC_{50} (μM)	n_H	4-PIOL efficacy (% $I_{Max,GABA}$)
α1β3γ2L	185.9 ± 60.5	1.4 ± 0.3	2.2 ± 0.2
α5β3γ2L	90.2 ± 16.8	1.0 ± 0.2	8.3 ± 2.2

4-PIOL concentration-response data from 4 – 5 cells expressing α1β3γ2L and α5β3γ2L receptors were normalised to the current elicited by 1 mM GABA ($I_{Max,GABA}$), and fitted using the Hill equation (*Equation* 2.1). Mean (± sem) values for 4-PIOL potency (4-PIOL EC_{50}), n_H, and macroscopic efficacy of 4-PIOL (expressed as a percentage of $I_{Max,GABA}$) are shown.

Intriguingly, 4-PIOL exhibited no discernible agonist activity at δ-containing receptors, when applied alone. For α4β2δ receptors, brief (~ 4 s) applications of 4-PIOL, at concentrations up to 1 mM, revealed no significant change in holding current (*Fig*. 4.5). In addition, using low to high 4-PIOL concentrations (10 or 100 μM) on recombinant α6β2δ receptors failed to produce any discernible agonist activity at this receptor isoform. These findings concur with a previous study showing that 4-PIOL exhibited no resolvable agonist activity at recombinant α4β3δ receptors expressed in *Xenopus* oocytes (Stórustovu and Ebert, 2006). However, in *Chapter* 6 (*Fig.* 6.6), we will demonstrate that at least for α4β2δ receptors expressed in HEK293 cells, co-application of 10 μM 4-PIOL with the δ-selective positive allosteric modulator, DS2 (Wafford *et al*., 2009; Jensen *et al*., 2013), unveils a 4-PIOL-gated agonist current, indicating that at least for α4β2δ receptors, 4-PIOL is capable of activating the receptor.

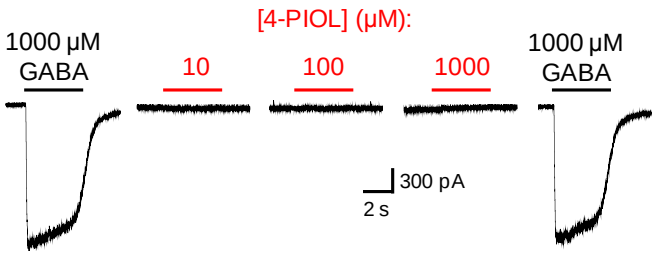

Figure 4.5 – Peak 4-PIOL concentration-response curves for recombinant α4β2δ receptors.

Examples of whole-cell currents elicited by GABA (1000 μM) or 4-PIOL (μM: 10, 100 or 1000) applied to α4β2δ-expressing HEK293 cells. The black and red horizontal bars indicate the duration of GABA and 4-PIOL applications, respectively.

4.2.2. 4-PIOL acts as a functional antagonist at recombinant α1β3γ2 receptors

Since synaptic receptors are activated by transiently high concentrations of GABA (in the low mM range; Maconochie *et al*., 1994; Jones and Westbrook, 1995), using HEK293 cells, the effects of 4-PIOL were evaluated on the peak GABA currents of recombinant α1β2γ2 receptors.

Our theoretical model, based on the kinetic profile of α1β3γ2 receptors (*Fig*. 4.2), predicts that 4-PIOL will display a dominant antagonist profile, in accord with previous reports (Kristiansen *et al*., 1991; Mortensen *et al*., 2002). Therefore, we evaluated the antagonist profile of 4-PIOL at recombinant α1β3γ2S receptors. Peak GABA concentration-response curves were constructed for α1β3γS receptors, in the absence, and presence, of 10, 100 and 1000 μM 4-PIOL (*Fig.* 4.6). 4-PIOL was pre-applied prior to GABA and 4-PIOL co-application (*Fig.* 4.6 A), to identify and include any 4-PIOL agonist activity in the analysis. More importantly, this ensured that 4-PIOL occupied the orthosteric binding site prior to GABA application. If 4-PIOL has a slower association rate than GABA, an inaccurately high current to GABA would be observed without a pre-application. Note that the peak response to each concentration of GABA was measured in relation to the holding current prior to 4-PIOL pre-application, and each data set was normalized to the maximum

response achieved by a saturating concentration of GABA, in the absence of 4-PIOL.

As observed for recombinant α1β3γ2L receptors (*Fig.* 4.3), pre-application of 4-PIOL to α1β3γ2S-expressing cells revealed a small agonist response, particularly when 100 µM or 1 mM 4-PIOL was applied (*Fig.* 4.6 A). This agonist activity manifested itself on the concentration-response curves, as an elevated minimum response (*Fig.* 4.6 B). To account for this elevated minimum, each data set was fitted using a modified Hill equation (*Equation* 2.2), which not only produced estimates of GABA potency (GABA EC_{50}) and n_H, but also the minimum response values reflecting the macroscopic efficacy of 4-PIOL. While 10 µM 4-PIOL did not significantly elevate the curve minimum (*Fig.* 4.6 B), 100 and 1000 µM 4-PIOL produced agonist currents that were 5.5 ± 3.2% and 6.8 ± 1.3% of the maximum GABA response (*Table* 4.2).

All three concentrations of 4-PIOL tested, (10, 100 and 1000 µM) induced a rightward shift in the GABA concentration-response curve (*Fig.* 4.6 B). The GABA EC_{50} value for α1β3γ2S receptors was increased from 4.5 ± 1.9 µM in the absence of 4-PIOL, to 9.4 ± 3.4 µM, 15.4 ± 5.4 µM and 126.7 ± 55.6 µM in the presence of 10, 100 or 1000 µM 4-PIOL respectively (*Table* 4.2).

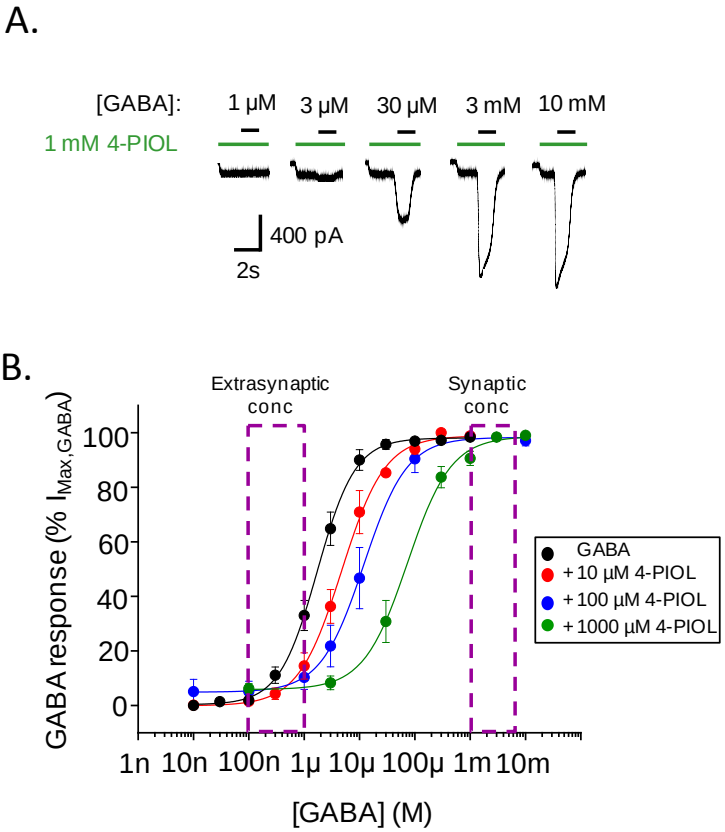

Figure 4.6 – 4-PIOL acts as an antagonist at α1β3γ2S receptors.

A. Examples of whole-cell currents produced by recombinant α1β3γ2S receptors expressed in HEK293 cells. The horizontal bars indicate the duration of GABA (black) and 1 mM 4-PIOL (green) application. Note the inward current generated by 1 mM 4-PIOL during the pre-application step. **B.** Mean peak GABA concentration-response curves constructed in the absence (black), or presence of 10 µM (red), 100 µM (blue) or 1000 µM (green) 4-PIOL (n = 4 – 13; mean ± SEM). The purple boxes (dashed lines) represent concentrations of GABA proposed to exist at extrasynaptic (100 nM -1 µM) and synaptic sites (>1mM).

Table 4.2 – Whole-cell current parameters for GABA in the absence and presence of 4-PIOL, at α1β3γ2S receptors.

	Curve Minimum ($\%\ I_{Max,GABA}$)	GABA EC_{50} (μM)	n_H
GABA	0.4 ± 0.9	4.5 ± 1.9	1.6 ± 0.1
+ 10 μM 4 PIOL	-0.3 ± 0.5	9.4 ± 3.4*	1.3 ± 0.2
+ 100 μM 4 PIOL	5.5 ± 3.2	15.4 ± 5.4*	1.2 ± 0.1
+ 1000 μM 4 PIOL	6.8 ± 1.3	126.7 ± 55.6***	1.1 ± 0.1

For α1β3γ2S receptors, the normalised peak GABA concentration-response curves, in the absence or presence of 4-PIOL, were fitted using a modified Hill equation, in which the curve minimum value was a variable (*Equation* 2.2). Tabulated are the GABA potencies (EC_{50}), Hill slopes (n_H) and curve minima, with the latter being expressed as a percentage of the peak current elicited by 1 mM GABA ($I_{Max,GABA}$). All parameters are expressed as mean ± SEM. Statistical analysis was performed relative to the control GABA concentration-response data. *P < 0.05 and ***P < 0.001.

Our theoretical model predicted that 10 and 100 μM 4-PIOL would produce only a modest (< 5 %) inhibition of extrasynaptic responses to ambient concentrations of GABA (100 nM - 1 μM), while a higher concentration of 4-PIOL (1 mM) would be required to more significantly inhibit α1β3γ2 receptors (by ~ 20 %, assuming an extracellular GABA concentration of 1 μM; see *Fig.* 4.2). However, according to our experimental data (*Fig.* 4.6 B), 4-PIOL was more potent at displacing the GABA concentration-response curve than predicted. Just a low concentration of 10 μM 4-PIOL was sufficient to halve the normalised response to 1 μM GABA from 33.0 ± 5.5 % (in the absence of 4-PIOL) to 14.5 ± 4.8 % (*Fig.* 4.6 B). More crucially for this synaptic receptor subtype, neither 10, nor 100, μM 4-PIOL produced any significant inhibition of peak responses to higher, synaptic concentrations of GABA (> 1 mM; *Fig.* 4.6 B), indicating that these concentrations might be capable of inhibiting responses to extrasynaptic concentrations of GABA, without depressing synaptic GABA currents. However, since 100 μM 4-PIOL (but not 10 μM 4-PIOL) produced a small (5.5 ± 3.2 %), but significantly greater enhancement of whole-cell currents at lower ambient GABA concentrations (i.e. when GABA levels were lower than ~ 100 nM; *Fig.* 4.6 B), these data indicate that 100 μM 4-PIOL may,

undesirably, enhance tonic currents in neurons, if a significant population of α1βγ2 receptors exist extrasynaptically.

Given the minimal efficacy displayed by 10 μM 4-PIOL at α1βγ2S receptors, and its potential to not inhibit synaptic currents in neurons, only the effects of 10 μM 4-PIOL were explored on steady-state GABA responses for extrasynaptic-type recombinant α4β2δ, α6β2δ and α5β3γ2L receptors.

4.2.3. 4-PIOL reduces GABA potency at recombinant α4β2δ receptors

In contrast to the transiently high GABA concentrations experienced by synaptic $GABA_A$ receptors, extrasynaptic receptors are continuously exposed to low ambient concentrations of GABA, ranging from nanomolar to low micromolar (Farrant and Nusser, 2005; Glykys and Mody, 2007). Crucially recent evidence suggests that even these low concentrations of GABA can induce significant levels of desensitisation in δ-containing receptors (Feng *et al*., 2009; Mortensen *et al*., 2010; Bright *et al*., 2011; Houston *et al*., 2012; McGee *et al*., 2013), which influences their modulation by agents such as the 'super-agonist', THIP (Houston *et al*., 2012), and the open channel blocker, penicillin (Feng *et al*., 2009). Therefore, when studying the effects of 4-PIOL on extrasynaptic-type α5β3γ2, α4β2δ and α6β2δ receptors, we specifically studied the effects of 4-PIOL on the steady-state GABA currents of these receptor isoforms. In addition, the effects of 4-PIOL were also studied on the steady-state GABA currents of recombinant α1β3γ2L receptors, for reasons that will be discussed in *Section* 4.2.6.

To generate steady-state GABA concentration-response curves for α4β2δ-, α6β2δ-, α5β3γ2L- and α1β3γ2L-expressing cells, whole-cell currents were recorded in response to prolonged (> 30 s) applications of increasing concentrations of GABA (0.01 nM – 1000 μM; e.g. *Fig.* 4.7 A), either in the absence, or presence of pre- and co-applied 10 μM 4-PIOL. Steady-state current measurements were made relative to the holding current prior to 4-PIOL

pre-application, to include any 4-PIOL agonist activity in the analysis. For each cell, the steady-state GABA current elicited by each concentration of GABA (with or without 4-PIOL) was normalised to the steady-state current produced by 1 mM GABA alone.

The steady-state GABA concentration-response curve for α4β2δ receptors (*Fig.* 4.7 B) was shifted significantly leftwards when compared to its respective peak current concentration-response curve (*Fig.* 4.7 *B*). Consequently, the GABA EC_{50} for steady-state currents was 4.5 - fold lower than that for peak responses (GABA EC_{50}: 0.2 ± 0.02 μM and 0.7 ± 0.1 μM respectively; p = 0.0004; *Table* 4.3 and *Table* 4.4). The increased steady-state GABA potencies meant that relative to the maximal steady-state response, much higher responses were achieved with lower concentrations of GABA. For instance, at α4β2δ receptors, 1 μM GABA produced a near maximal steady-state response (95.2 ± 3.4 %; *Fig.* 4.7 B), whereas this same concentration activated receptors to 61.4 ± 4.9 % of the maximum GABA peak response (*Fig.* 4.7 B). Notably, the steady-state GABA concentration-response curve for α4β2δ receptors (*Fig.* 4.7 B) appeared to be steeper than the peak GABA concentration-response curve. However, statistical analysis of the Hill slopes obtained for peak and steady-state GABA concentration-response curves (2.6 ± 0.3 and 1.3 ± 0.1 respectively), revealed this was not significant (p = 0.06).

Pre- and co-application of 4-PIOL induced a rightward shift of the steady-state α4β2δ GABA concentration-response curve (*Fig.* 4.7 B). Accordingly, the GABA EC_{50} for steady-state currents was significantly increased from 0.2 ± 0.02 μM to 0.3 ± 0.1 μM (*Table* 4.3; p = 0.03). More crucially, at GABA concentrations thought to underlie tonic inhibition, 4-PIOL could inhibit steady-state GABA responses by up to ~ 30 %, if for instance, the extracellular GABA concentration is 300 nM (*Fig.* 4.7 B).

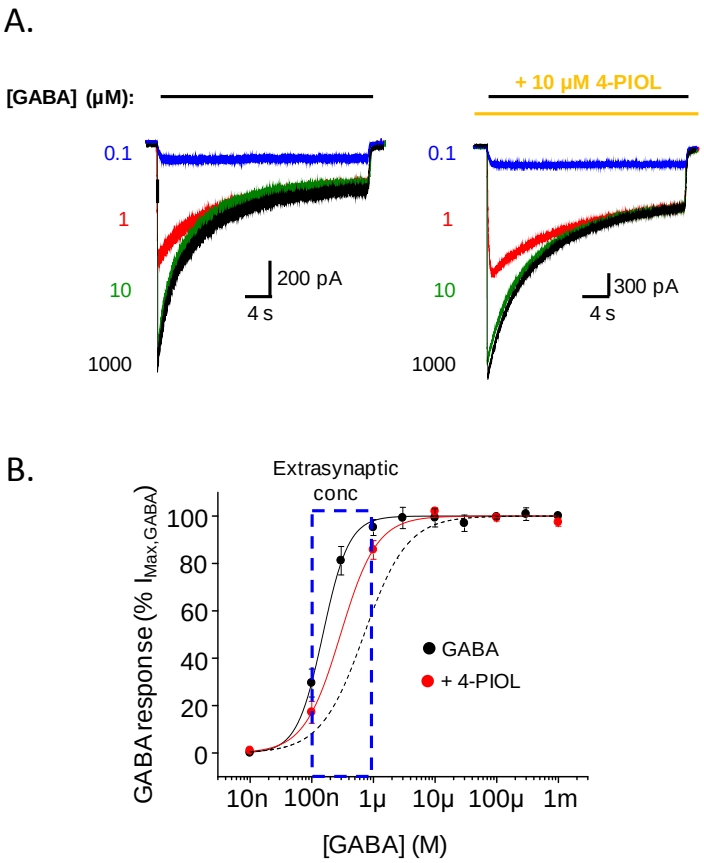

Figure 4.7 – Steady-state GABA concentration-response data for recombinant α4β2δ receptors.

A. Examples of whole-cell currents elicited by prolonged GABA applications applied to recombinant α4β2δ receptors expressed in HEK293 cells in the absence (left panel), or presence (right panel), of 10 μM 4-PIOL. The black and yellow horizontal bars indicate the duration of GABA (μM: 0.1 - blue; 1 - red; 10 - green; 1000 - black) and 4-PIOL application respectively. **B.** Mean steady-state GABA concentration-response curves in the absence (black continuous curve), or presence (red continuous curve) of 10 μM 4-PIOL (n = 4 – 8; mean ± SEM). Steady-state currents elicited by GABA (with or without 4-PIOL) were normalised to steady-state responses produced by 1000 μM GABA alone. The blue box (dashed lines) indicates GABA concentrations thought to underlie tonic inhibition (100 nM -1 μM). The Hill fit for the mean peak α4β2δ GABA concentration-response curve is also shown (black dashed curve).

4.2.4. 4-PIOL reduces steady-state GABA potency of recombinant α6β2δ receptors

As for α4β2δ receptors, steady-state GABA concentration-response curves were generated for α6β2δ receptors. Whole-cell currents were recorded in response to prolonged applications of increasing concentrations of GABA (0.01 – 1000 µM; *Fig.* 4.8 A), either in the absence, or presence of pre-applied 4-PIOL (10 µM). In the absence of 4-PIOL, the mean steady-state GABA concentration-response curve (*Fig.* 4.8 B) was again shifted significantly leftwards when compared to its respective peak GABA concentration-response curve (*Fig.* 4.8 B). Accordingly, steady-state currents mediated by α6β2δ receptors demonstrated a significantly higher sensitivity for GABA (EC_{50}: 0.1 ± 0.01 µM; *Table* 4.3) when compared to peak responses (GABA EC_{50}: 0.3 ± 0.03 µM; *Table* 4.4; p = 0.002). Intriguingly, at GABA concentrations thought to underlie tonic inhibition (100 nM – 1 µM), the steady-state current for α6β2δ receptors was found to be close to saturating (*Fig.* 4.8 B), indicating that steady-state currents of native α6β2δ receptors might also be close to saturating, if ambient GABA concentrations exceed 100 nM.

Although 4-PIOL appeared to induce a rightward shift in the α6β2δ steady-state GABA concentration-response curve (*Fig.* 4.8 B), a comparison of their respective GABA EC_{50}s revealed that this shift was not statistically significant (p = 0.19; *Table* 4.3).

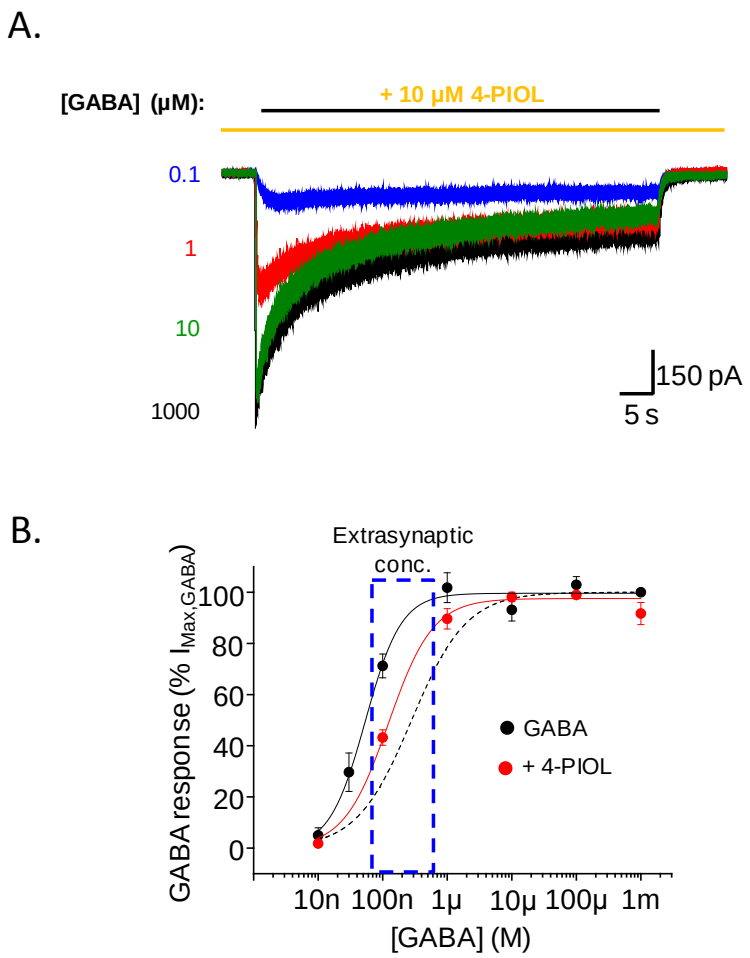

Figure 4.8 – Steady-state GABA concentration-response data for recombinant α6β2δ receptors.

A. Examples of whole-cell currents elicited by prolonged GABA applications applied to recombinant α6β2δ receptors expressed in HEK293 cells, in the presence of 10 μM 4-PIOL. The black and yellow horizontal bars indicate the duration of GABA (μM: 0.1 - blue; 1 - red; 10 - green; 1000 - black) and 4-PIOL applications respectively. **B.** Mean steady-state GABA concentration-response curves in the absence (black continuous curve), or presence (red continuous line) of 10 μM 4-PIOL (n = 4; mean ± SEM). Steady-state currents elicited by GABA (with or without 4-PIOL) were normalised to steady-state responses produced by 1000 μM GABA alone. The blue box (dashed lines) indicates GABA concentrations thought to underlie tonic inhibition (100 nM -1 μM). The Hill fit for the mean peak α6β2δ GABA concentration-response curve is also shown (black dashed curve).

4.2.5. 4-PIOL (10 μM) has no effect on GABA potency at recombinant α5β3γ2L receptors

Given the proposed synaptic and extrasynaptic locations of α5βγ2 receptors in hippocampal neurons (Fritschy *et al*., 1998; Brünig *et al*., 2002; Crestani *et al*., 2002; Caraiscos *et al*., 2004; Serwanski *et al*., 2006), we assessed the effect of 4-PIOL on both peak and steady-state currents of recombinant α5β3γ2L receptors.

Whole-cell currents were recorded for α5β3γ2L receptors, in response to prolonged applications of increasing concentrations of GABA (0.1 nM – 1000 μM; *Fig.* 4.9 A), either in the absence, or presence of pre-applied 4-PIOL (10 μM). In the absence of 4-PIOL, the mean steady-state GABA concentration-response curve was shifted significantly leftwards relative to the peak GABA concentration-response curve (*Fig*. 4.9 B). Consequently the GABA EC_{50} for steady-state responses was significantly lower (~ 6 - fold) than that obtained for peak responses (EC_{50}s: 2.0 ± 0.4 and 11.9 ± 3.6 μM respectively; p = 0.02; *Table* 4.3 and *Table* 4.4).

Pre-application of 10 μM 4-PIOL elicited an inward current (*Fig.* 4.8 A), consistent with the previously described agonist activity of 4-PIOL at this receptor subtype (*Fig.* 4.4). To include the agonist activity of 4-PIOL in the concentration-response analysis, both peak and steady-state current measurements were made relative to the holding current prior to 4-PIOL pre-application. Moreover, the normalised concentration-response curves were fitted using a modified Hill equation (*Equation* 2.2), to account for the elevated curve minimum (*Fig.* 4.9 B).

Curiously, pre-application (and co-application) of 10 μM 4-PIOL induced no significant displacement of either the peak, or steady-state, GABA concentration-response curves (*Fig.* 4.9 B). Accordingly, the GABA sensitivities of peak, and steady-state responses in the presence of 4-PIOL (GABA EC_{50}: 6.2 ± 1.1 μM and 1.3 ± 0.3 μM, respectively) were similar to their respective GABA sensitivities measured with GABA alone (11.9 ± 3.6 μM and 2.0 ± 0.4 μM

respectively; p = 0.19 and p = 0.21). In fact, pre-application of 4-PIOL elevated the curve minimum in the steady-state GABA concentration-response curve (*Fig.* 4.9 B), indicating that at low GABA concentrations (e.g. 100 nM GABA), 4-PIOL may enhance tonic currents in native systems, where α5 subunit-containing receptors are present.

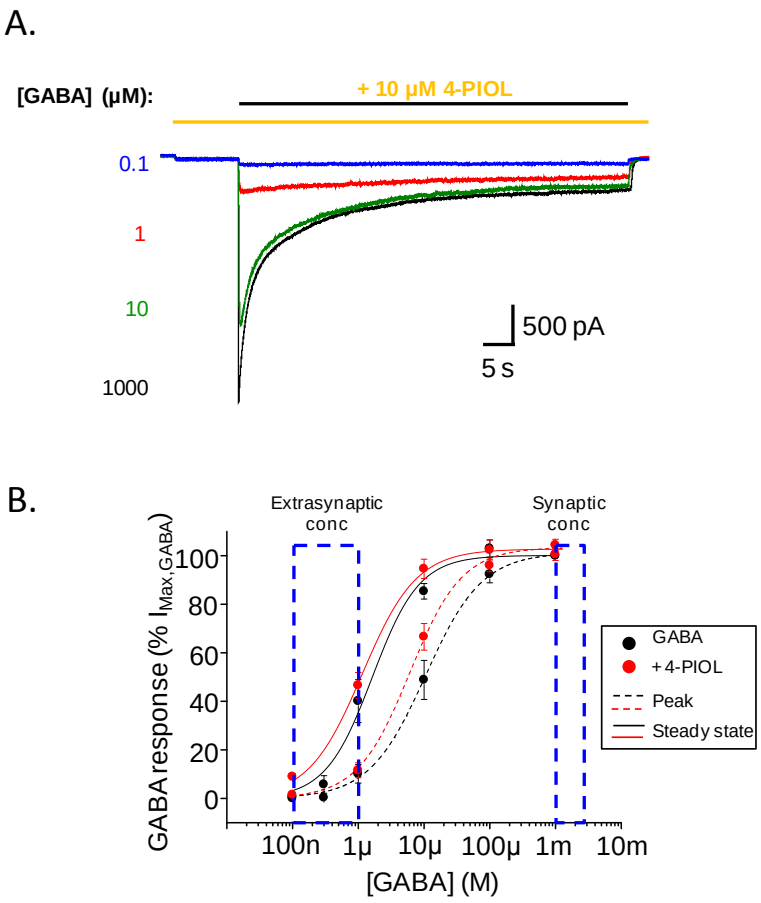

Figure 4.9 - Peak and steady-state GABA responses of recombinant α5β3γ2L receptors.

A. Examples of whole-cell currents elicited by prolonged GABA applications applied to recombinant α5β3γ2L receptors expressed in HEK293 cells, in the presence of 10 μM 4-PIOL. The black and yellow horizontal bars indicate the duration of GABA (μM: 0.1 - blue; 1 - red; 10 - green; 1000 - black) and 4-PIOL applications respectively. **B.** Mean Peak (dashed curves) and steady-state (continuous curves) GABA concentration-response curves in the absence (black), or presence (red) of 10 μM 4-PIOL (n = 4 – 8; mean ± SEM). Peak and steady-state GABA responses were respectively normalized to peak and steady-state responses produced by a saturating concentration of GABA in the absence of 4-PIOL. The blue boxes (dashed lines) indicate GABA concentrations thought to underlie tonic (100 nM -1 μM) and phasic inhibition (> 1 mM).

4.2.6. 4-PIOL can bidirectionally regulate extrasynaptic-type recombinant α1β3γ2L receptors

Although α1βγ2 receptors are important mediators of phasic inhibition in several brain regions (Nusser *et al*., 1996; Somogyi *et al*., 1996; Okada *et al*., 2000; Crestani *et al*., 2002; Prenosil *et al*., 2006), their presence at extrasynaptic sites has also been suggested (Nusser *et al*., 1998; Mangan *et al*., 2005; Thomas *et al*., 2005; Kasugai *et al*., 2010). While it is unlikely that α1βγ2 receptors will significantly contribute to tonic inhibition, due to their low GABA sensitivity (Brown *et al*., 2002; Mortensen *et al*., 2010), their presence at extrasynaptic sites might make them amenable to 4-PIOL modulation in neuronal systems. Therefore, steady-state concentration-response curves were also generated for α1β3γ2L receptors. As for the other extrasynaptic receptor subtypes studied, the whole-cell currents elicited by prolonged applications of GABA were allowed to attain steady-state, either in the absence, or presence, of pre- and co-applied 4-PIOL (10 μM; *Fig.* 4.10 A). The mean steady-state concentration-response curve (*Fig.* 4.10 B) to GABA alone was shifted significantly leftwards when compared to its respective peak concentration-response curve (*Fig.* 3.1). Accordingly, the GABA EC_{50} value determined for steady-state responses was significantly lower (~ 4 - fold) than that obtained for peak responses (1.9 ± 0.5 μM and 8.7 ± 2.3 μM respectively; p = 0.03; *Table* 4.3 and *Table* 4.4).

In these experiments, pre-application of 10 μM 4-PIOL induced no significant shift in the holding current (*Fig.* 4.10 A). This was unexpected, since we previously demonstrated that this low concentration of 4-PIOL can elicit small agonist responses at α1β3γ2L receptors (*Fig.* 4.3 A), even if it does only correspond to ~ 0.1 % of the current induced by a saturating concentration of GABA (*Fig.* 4.3 C). One explanation for this discrepancy might relate to the different ways that 4-PIOL was applied to cells in each experiment. In Figure 4.3, 4-PIOL was rapidly applied to cells, whereas, in Figure 4.10, 4-PIOL was pre-applied more slowly. Given that the 10 μM 4-PIOL current is already very small 4-PIOL current, this slower application may make it unresolvable from the baseline holding current.

A lack of discernible 4-PIOL efficacy meant that the steady-state GABA concentration-response curve for α1β3γ2L receptors exhibited no elevated curve minimum (*Fig.* 4.10 B). However, as for the peak GABA responses (*Fig.* 4.6 B), 4-PIOL induced a rightward shift in the steady-state GABA concentration-response curve (*Fig.* 4.10 B), causing the GABA EC_{50} value to increase significantly, from 1.9 ± 0.5 µM to 5.6 ± 0.6 µM (*Table* 4.3; p = 0.0012). Crucially, at GABA concentrations thought to mediate tonic inhibition, although 4-PIOL did not significantly affect the steady-state response to 100 nM GABA, when the GABA concentration was raised to 1 µM, 4-PIOL significantly reduced the steady-state GABA current by ~ 30 % (*Fig.* 4.10 B; p = 0.005).

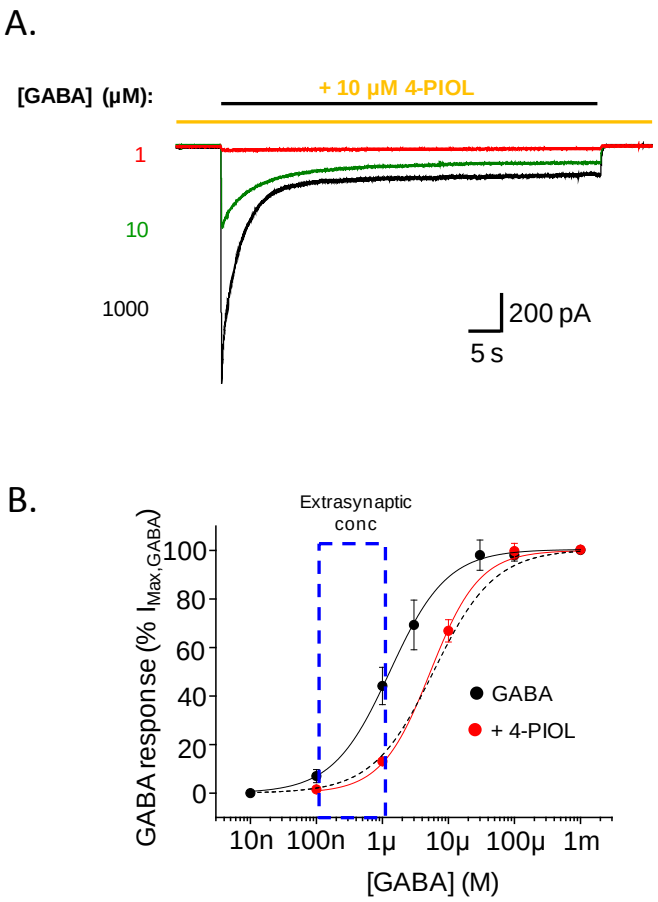

Figure 4.10 – Steady-state GABA responses of recombinant α1β3γ2L receptors.

A. Examples of whole-cell currents elicited by prolonged GABA applications applied to recombinant α1β3γ2L receptors expressed in HEK293 cells, in the presence of 10 μM 4-PIOL. The black and yellow horizontal bars indicate the duration of GABA (μM: 1 - red; 10 - green; 1000 - black) and 4-PIOL applications respectively. **B.** Mean steady-state GABA concentration-response curves in the absence (black continuous line), or presence (red continuous curve) of 10 μM 4-PIOL (n = 4; mean ± SEM). Steady-state GABA currents were normalized to the steady-state response achieved by 1 mM GABA alone. The blue box (dashed lines) indicates GABA concentrations thought to underlie tonic inhibition (100 nM -1 μM). The Hill fit for the peak α1β3γ2L GABA concentration-response curve is also shown (black dashed curve).

Table 4.3 – Steady-state GABA concentration-response curve parameters in the absence, or presence, of 10 μM 4-PIOL

	GABA only (Steady-state)		+ 10 μM 4-PIOL (Steady-state)	
Subunit combination	**GABA EC_{50} (μM)**	**n_H**	**GABA EC_{50} (μM)**	**n_H**
α1β3γ2L	1.9 ± 0.5	1.2 ± 0.1	5.6 ± 0.6**	1.2 ± 0.1
α5β3γ2L	2.0 ± 0.4	1.3 ± 0.2	1.3 ± 0.3	1.1 ± 0.03
α4β2δ	0.2 ± 0.02	2.6 ± 0.3	0.3 ± 0.1*	1.6 ± 0.1
α6β2δ	0.1 ± 0.01	1.4 ± 0.2	0.1 ± 0.01	1.1 ± 0.1

For α1β3γ2L, α4β2δ and α6β2δ receptors, the normalised steady-state GABA concentration-response curves, in the absence or presence of 4-PIOL were fitted using the Hill equation (*Equation* 2.1). For α5β3γ2L receptors, the normalised data were fitted using a modified Hill equation (*Equation* 2.2). The GABA EC_{50}s and n_H obtained from these fits (mean ± SEM) are shown. For each subunit combination, statistical analysis was performed relative to the control GABA concentration-response data. *P < 0.05 and **P < 0.01.

Table 4.4 – Peak GABA concentration-response curve parameters in the absence, or presence, of 10 μM 4-PIOL

	GABA only (Peak)		+ 10 μM 4-PIOL (Peak)	
Subunit combination	**GABA EC_{50} (μM)**	**n_H**	**GABA EC_{50} (μM)**	**n_H**
α1β3γ2S	4.5 ± 1.9	1.6 ± 0.1	9.4 ± 3.4*	1.3 ± 0.2
α1β3γ2L	8.7 ± 2.3	1.3 ± 0.1	21.1 ± 3.5*	1.3 ± 0.1
α5β3γ2L	11.9 ± 3.6	1.1 ± 0.1	6.2 ± 1.1	1.2 ± 0.1
α4β2δ	0.7 ± 0.1	1.3 ± 0.1	2.2 ± 0.4 **	1.0 ± 0.1
α4β3δ	1.9 ± 0.5	1.1 ± 0.1	3.9 ± 0.7 **	0.9 ± 0.03
α6β2δ	0.3 ± 0.03	1.1 ± 0.04	0.7 ± 0.03 ***	1.0 ± 0.1

For α1β3γ2(S or L), α4β2δ and α6β2δ receptors, the normalised peak GABA concentration-response curves, in the absence or presence of 4-PIOL were fitted using the Hill equation (*Equation* 2.1). For α5β3γ2L receptors, the normalised data were fitted using a modified Hill equation (*Equation* 2.2). GABA EC_{50}s and n_H obtained from these fits (mean ± SEM) are shown. For each subunit combination, statistical analysis was performed relative to the control GABA concentration-response data. *P < 0.05, **P < 0.01 and ***P < 0.001.

4.2.7. 4-PIOL regulation of extrasynaptic-type $GABA_A$ receptors depends on the ambient GABA concentration

In the nervous system, extrasynaptically-located $GABA_A$ receptors will be continuously activated by low, ambient concentrations of GABA. To evaluate the functional effects of 4-PIOL on pre-activated recombinant receptors, GABA (0.1, 0.3 and 1 µM) was pre-applied to α4β2δ-, α6β2δ-, α5β3γ2L- or α1β3γ2L-expressing HEK293 cells for 1 - 2 min, until a steady-state response was achieved, and subsequently, GABA was co-applied with 10 µM 4-PIOL (*Fig.* 4.11).

Strikingly, for α4β2δ receptors, co-application of 4-PIOL significantly inhibited the steady-state GABA current at all three GABA concentrations tested (*Fig.* 4.11 A). Co-application of 4-PIOL reduced the steady-state currents for 0.1, 0.3 and 1 µM GABA, by 70.6 ± 2.7 %, 56.1 ± 4.5 % and 31.5 ± 1.3 %, respectively (*Fig.* 4.12; p = 0.03, 0.04 and 0.02, respectively). Thus, 4-PIOL potently inhibits extrasynaptic-type responses of recombinant α4β2δ receptors. Notably, the level of inhibition achieved by 4-PIOL appears to decrease with increasing GABA concentrations, possibly because GABA has a high apparent affinity (*Fig.* 4.7 B) at this αβδ receptor isoform. Thus, at high GABA concentrations, 10 µM 4-PIOL may be less effective at competing with GABA for its binding site.

By contrast only a modest inhibition of steady-state currents was produced by 4-PIOL at recombinant α6β2δ receptors (*Fig.* 4.11 B). While the steady-state currents elicited by 0.1, 0.3 and 1 µM GABA were reduced by 26.5 ± 3.9 %, 20.9 ± 3.0 and 9.6 ± 4.0 % respectively by 4-PIOL co-application (*Fig.* 4.12), the shifts in the holding current induced by 4-PIOL were not statistically significant (p = 0.25, 0.23 and 0.32 respectively). Thus the extent of inhibition achieved by 10 µM 4-PIOL appears to be significantly less than that observed for α4β2δ receptors. Given that desensitised α6β2δ receptors exhibit the highest GABA potency (relative to the other subtypes studied; *Table* 4.3; One-way ANOVA – p = 0.002), this concentration of 4-PIOL may be insufficient to efficiently compete with GABA for the orthosteric binding site.

In accord with the concentration-response curve data for α5β3γ2L receptors, 4-PIOL exhibited minimal agonist, and antagonist effects at recombinant α5β3γ2L receptors (*Fig.* 4.11 C). 4-PIOL seemingly enhanced the steady-state current elicted by 0.1 μM GABA (*Fig.* 4.11 C) by 23.0 ± 1.5 % (*Fig.* 4.12), consistent with its previously described weak partial agonist profile at α5β3γ2L receptors (*Fig.* 4.4 and *Fig.* 4.9 A). Furthermore, in accord with the relative lack of antagonist activity observed previously (*Fig.* 4.9 B), 4-PIOL produced at most a very small inhibition of steady-state GABA currents elicited by 1 μM GABA (*Fig.* 4.12; 6.8 ± 0.9 %; $p = 0.01$; one tailed paired t-test).

Lastly, the effects of 4-PIOL were studied on the extrasynaptic-type responses elicited from recombinant α1β3γ2L receptors. Significantly, when co-applied, 4-PIOL enhanced the response to 0.1 μM GABA (*Fig.* 4.11 D; $p = 0.02$) by 76.9 ± 21.5 % (*Fig.* 4.12). However, when co-applied with 1 μM GABA, 4-PIOL produced only a small inhibition of the steady-state GABA current (12.9 ± 3.3 %; Fig. 4.12; $p = 0.05$).

Overall, 4-PIOL potently inhibits the tonic-type currents of recombinant α4β2δ receptors, but not recombinant α6β2δ receptors. Conversely, 4-PIOL potently enhances the extrasynaptic-type responses of α1β3γ2L and α5β3γ2L receptors when GABA concentrations are low, but produces only a modest inhibition of steady-state GABA responses when GABA concentrations are raised (to 1 μM GABA). Thus, 4-PIOL modulation of α1β3γ2L and α5β3γ2L GABA responses will be highly dependent on the ambient GABA concentration.

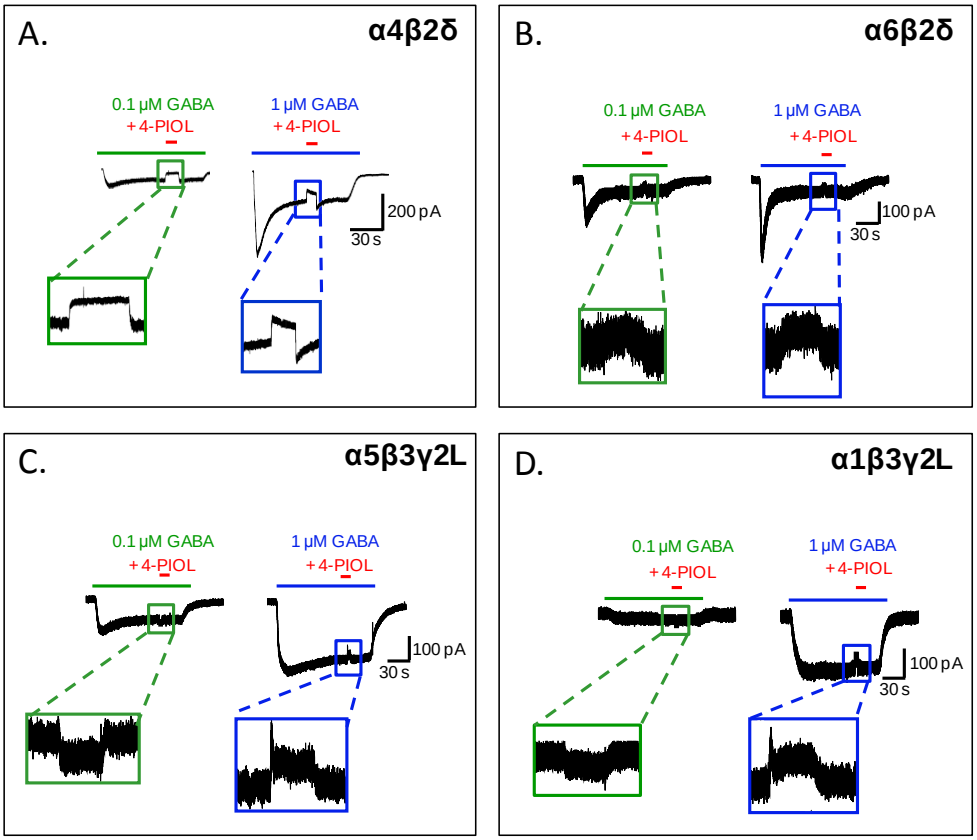

Figure 4.11 – Functional effects of 4-PIOL on steady-state GABA currents

Example traces of whole-cell currents elicited by prolonged applications (~ 3 min) of 0.1 μM (green horizontal bar) and 1 μM GABA (blue horizontal bar) at recombinant α4β2δ (**A**), α6β2δ (**B**), α5β3γ2L (**C**) and α1β3γ2L (**D**) receptors. As indicated by the red horizontal bars, 10 μM 4-PIOL was co-applied for 4 s once a steady-state GABA current was achieved.

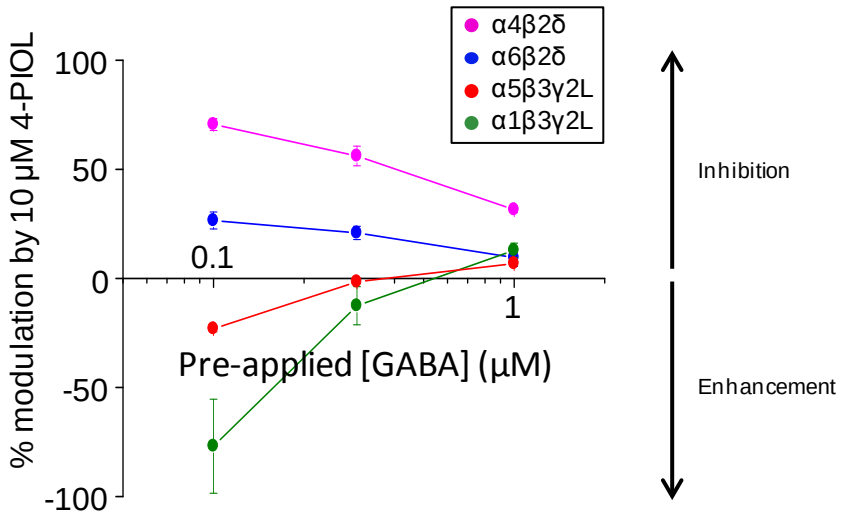

Figure 4.12 – Summary of 4-PIOL agonist and antagonist profiles at extrasynaptic-type receptors

Quantitative analysis of data depicted in *Fig*. 4.11. The data for α4β2δ (magenta), α6β2δ (blue), α5β3γ2L (red) and α1β3γ2L (green) receptors were accrued from 4 - 5 cells, and are expressed as mean ± SEM. For each concentration (0.1, 0.3 and 1 µM) of pre-applied GABA, the change in holding current produced by 4-PIOL is expressed as a percentage of the steady-state current to GABA alone. Negative values represent an enhancement of the steady-state GABA current.

4.3. Discussion

In this chapter, the actions of 4-PIOL were assessed on recombinant synaptic- and extrasynaptic-type $GABA_A$ receptors expressed in HEK293 cells, to investigate whether 4-PIOL can inhibit tonic GABA currents without affecting synaptic GABA currents. The subtypes studied were: α1βγ2, α5βγ2, α4βδ and α6βδ receptors, since these are the major subtypes thought to exist at synaptic and extrasynaptic sites in several brain regions (Laurie *et al*., 1992a; Wisden *et al*., 1992; Pirker *et al*., 2000; Caraiscos *et al*., 2004; Cope *et al*., 2005; Bright *et al*., 2007; Glykys *et al*., 2008; Hörtnagl *et al*., 2013), including hippocampal pyramidal neurons, cerebellar granule cells and thalamic relay neurons (the three cell types that will be studied in *Chapters* 5 and 6).

4.3.1. 4-PIOL acts as a weak partial agonist at α1β3γ2 and α5β3γ2 receptors

At recombinant α1β3γ2 and α5β3γ2 receptors, 4-PIOL acted as a weak partial agonist generating whole-cell currents that were ~ 2 % and 8 % of the maximum GABA current. Although 4-PIOL has previously been demonstrated to exhibit weak partial agonist behaviour at recombinant α1β2γ2 receptors expressed in *Xenopus* oocytes (Mortensen *et al*., 2002) and HEK293 cells (Mortensen *et al*., 2004), there are no previous reports demonstrating the functional effects of 4-PIOL on α5β3γ2 receptors. It is intriguing to note that 4-PIOL acts as a low efficacy partial agonist in hippocampal neurons (Kristiansen *et al*., 1991), and given that the α5 subunit is prominently expressed in the hippocampus (Sur *et al*., 1999; Pirker *et al*., 2000; Sieghart and Sperk, 2002), we would predict that the agonist effect of 4-PIOL in this cell type is probably, in part, mediated by α5-containing receptors (also see *Chapter* 5).

The biophysical mechanisms underlying the low efficacy of 4-PIOL have previously been investigated by analysing whole-cell current fluctuations elicited by 4-PIOL in olfactory bulb neurons (Kristiansen *et al*., 1991), and by single

channel analysis of α1β2γ2 receptors expressed in HEK293 cells (Mortensen *et al*., 2004). Both studies indicated that the low efficacy of 4-PIOL likely reflects its inability to produce frequent and prolonged channel openings, especially given that the single channel conductances induced by 4-PIOL and the full agonist GABA, were indistinguishable at ~ 25 – 29 pS (Kristiansen *et al*., 1995; Mortensen *et al*., 2004).

4.3.2. 4-PIOL does not activate α4β2δ and α6β2δ receptors

Intriguingly, applications of 4-PIOL (10 µM or 100 µM) produced no discernible agonist activity at recombinant α4β2δ, or α6β2δ, receptors. Although the functional effects of 4-PIOL on recombinant α6β2δ receptors have not been previously studied, our data for α4β2δ receptors concurs with a previous study showing a lack of 4-PIOL agonist activity at recombinant α4β3δ receptors expressed in *Xenopus* oocytes (Stórustovu and Ebert, 2006). However, as will be discussed in *Chapter* 6, co-application of 4-PIOL with the δ-selective positive allosteric modulator, DS2 (Wafford *et al*., 2009; Jensen *et al*., 2013), unveils a small 4-PIOL activated current (see *Fig.* 6.6 A), indicating that at least for α4β2δ receptors expressed in HEK293 cells, 4-PIOL is capable of gating this receptor under certain conditions.

The different agonist profiles of 4-PIOL at αβγ and αβδ receptors can be added to a range of pharmacological differences already known to exist between these two receptor subtypes. Perhaps the most important ligand to consider is GABA itself. While GABA acts as a full agonist at α1βγ2 receptors, its relatively lower efficacy at δ-containing receptors has resulted in its classification as a partial agonist at this receptor subtype (Bianchi and Macdonald, 2003). Conversely, whilst compounds such as THIP, muscimol and isoguvacine have been shown to exhibit ‘super-agonist’ activity at αβδ receptors (Brown *et al*., 2002; Stórustovu and Ebert, 2006; Mortensen *et al*., 2010), they act only as full, or partial, agonists at γ2-containing receptors (Möhler, 2006). Thus, our finding that 4-PIOL acts as a weak partial agonist on α1β3γ2 and α5β3γ2 receptors,

but not on α4β2δ, or α6β2δ receptors, is a different but unsurprising profile, especially considering that different α-subunits will contribute to the orthosteric binding site.

With regards to the importance of the $GABA_A$ receptor β subunit, it has recently been demonstrated that β3-containing receptors expressed in *Xenopus* oocytes exhibit a higher efficacy when activated by thio-4-PIOL, a 4-PIOL analogue, when compared with β2-containing receptors (Hoestgaard-Jensen *et al*., 2010). Although the mechanistic reason(s) for this difference remain unclear, in our hands, applications of 4-PIOL (10, or 100 μM) to β2-, or β3-containing α4βδ receptors, revealed no discernible agonist activity at either receptor isoform, expressed in HEK293 cells. Moreover, for α4β2δ and α4β3δ receptors, the rightward shifts respectively induced by 10 and 100 μM 4-PIOL were comparable for both receptor isoforms (see *Appendix* 1), indicating that the identity of the β subunit has little effect on 4-PIOL function, in the HEK293 cell expression system.

4.3.3. 4-PIOL antagonises GABA responses for αβγ and αβδ receptors

As predicted by our theoretical model (*Fig*. 4.2), 4-PIOL induced a rightward shift in the GABA concentration-response curves of α1β3γ2 receptors. However, the potency of 4-PIOL inhibiting GABA responses was greater than anticipated, with 10 and 100 μM 4-PIOL both significantly inhibiting responses to extrasynaptic concentrations of GABA. Indeed, the more significant curve shift (~ 30 - fold) caused by 1000 μM 4-PIOL at α1β3γ2 receptors, produced a small (~ 5 %) inhibition of the 1 mM GABA response, clearly making it too high a concentration for the purpose of inhibiting tonic, but not phasic inhibition. Since our data demonstrated that 10 μM 4-PIOL inhibits responses to extrasynaptic concentrations of GABA, without affecting phasic currents, only this concentration of 4-PIOL was assessed at recombinant, α4β2δ, α6β2δ, α5β3γ2 and α1β3γ2 receptors.

All the recombinant receptors we studied demonstrated considerable levels of desensitisation, including α4βδ and α6βδ receptors, prompting us to study the effects of 4-PIOL on their steady-state currents. This is particularly important when considering extrasynaptic $GABA_A$ receptors, since in native neurons, they may be continuously exposed to low, but potentially desensitising concentrations of GABA (Feng *et al*., 2009; Mortensen *et al*., 2010; Bright *et al*., 2011; Houston *et al*., 2012; McGee *et al*., 2013). For each receptor isoform, two forms of analysis were performed. First, steady-state GABA concentration-response curves were generated to assess the potency of GABA in the absence and presence of pre-applied 4-PIOL (10 μM). Pre-application of 4-PIOL induced a rightward shift in the steady-state GABA concentration-response curve of α1β3γ2, α4β2δ and α6β2δ receptors, but not α5β3γ2 receptors. Moreover, 10 μM 4-PIOL consistently produced a 10 – 30 % inhibition of steady-state responses to typical 'extrasynaptic concentrations' of GABA (100 nM – 1 μM) for each receptor isoform studied, except for α5β3γ2 receptors. In fact, for α5β3γ2 receptors, 4-PIOL produced a small, but significant enhancement of GABA steady-state currents to low (100 nM) concentrations of GABA (*Fig.* 4.9 B). Thus, where α5 subunit-containing receptors are present (e.g. on hippocampal pyramidal neurons; Caraiscos *et al*., 2004), 4-PIOL may actually enhance α5-mediated tonic currents in native systems.

The effects of 10 μM 4-PIOL were additionally assessed on recombinant α4β2δ, α6β2δ, α5β3γ2 and α1β3γ2 receptors pre-exposed to low concentrations of GABA (100 nM – 1 μM), to more precisely emulate the situation experienced by native neuronal extrasynaptic receptors. While 4-PIOL potently inhibited the steady-state GABA currents of α4β2δ receptors (by ~ 40 – 80 %), no significant inhibition was observed for α6β2δ receptors, presumably due to the higher GABA apparent affinity displayed by the latter receptor subtype. For α1β3γ2 and α5β3γ2 receptors, 10 μM 4-PIOL displayed a dominant agonist profile when the GABA concentration was low (0.1 μM GABA), and produced at most, a very small inhibition when the pre-applied GABA concentration was raised to 1 μM. These data are summarised in *Fig*. 4.13.

Overall, our data indicate that 10 µM 4-PIOL should potently inhibit α4β2δ-mediated tonic currents, without significantly affecting α1β3γ2-mediated phasic currents. Moreover, 10 µM 4-PIOL is not expected to affect α6β2δ-mediated tonic currents (e.g. in the cerebellum), and any potential inhibition of extrasynaptic γ2-containing receptors will depend on the ambient GABA concentration in neuronal preparations, and may be minimal. Finally, where α5 subunit-containing $GABA_A$ receptors predominate, 10 µM 4-PIOL is expected to produce only a small inhibition in the GABA response.

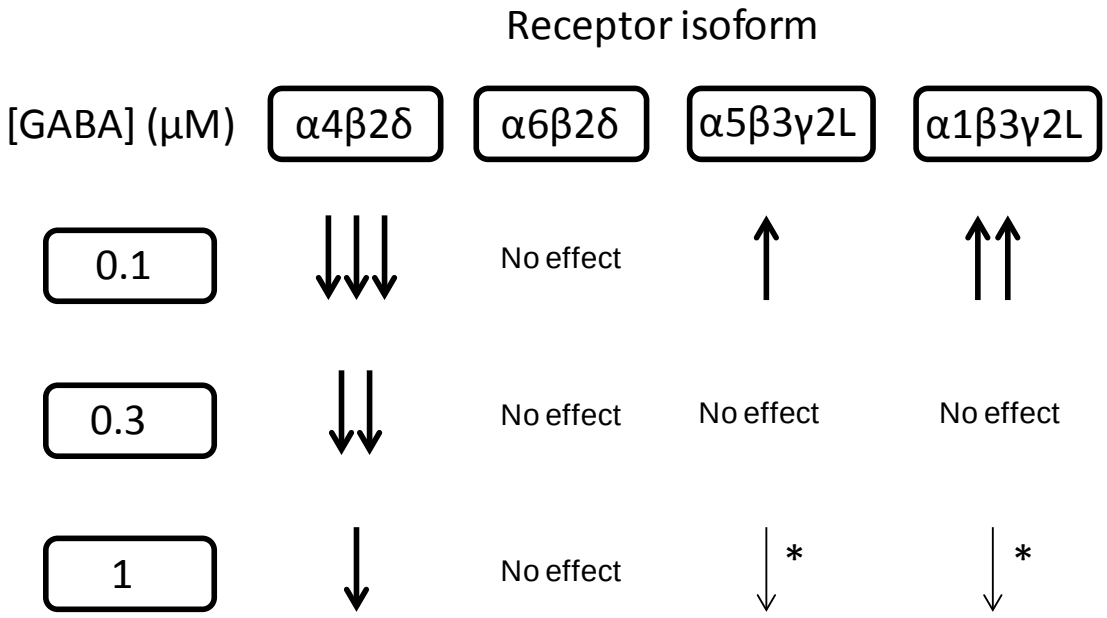

Figure 4.13 – Summary: 10 µM 4-PIOL regulation of extrasynaptic-type receptors

For each receptor isoform, the upwards and downwards arrows, respectively, represent a 10 µM 4-PIOL mediated enhancement and reduction of the (pre-applied) steady-state GABA (0.1, 0.3, or 1 µM) current. The number and width of the arrows represents the strength of effect. *Note that only a very modest inhibition was produced by 10 µM 4-PIOL at recombinant α1β3γ2L and α5β3γ2L receptors, when the pre-applied GABA concentration was 1 µM.

4.4. Conclusion

1. 4-PIOL acts as weak partial agonist at recombinant α1β3γ2 and α5β3γ2 receptors, but not α4β2δ and α6β2δ receptors.

2. For α1β3γ2 receptors, 10 μM, 4-PIOL does not inhibit peak responses to synaptic concentrations of GABA (> 1 mM).

3. At recombinant α4β2δ receptors, 10 μM 4-PIOL inhibits steady-state currents elicited by low ambient concentrations of GABA (0.1 – 1 μM).

4. 4-PIOL (10 μM) does not significantly enhance, or inhibit, the steady-state GABA currents of α6β2δ receptors.

5. At recombinant α1β3γ2 and α5β3γ2 receptors, 4-PIOL (10 μM) exhibits a dominant agonist profile at low ambient GABA concentrations, although a small inhibition can be achieved by raising the ambient GABA concentration to 1 μM.

Chapter 5: Functional effects of 4-PIOL on hippocampal neurons and cerebellar granule cells

5.1. Introduction

In this chapter, the functional effects of 4-PIOL were assessed on the tonic, and phasic currents of CGCs and hippocampal neurons in culture, two neuronal populations which exhibit tonic currents mediated by different $GABA_A$ receptor isoforms.

5.1.1. GABAergic neurotransmission onto CGCs

Traditionally, the cerebellum is viewed as the major processing centre for motor coordination and learning, although it has also been implicated in cognitive processing (Rochefort *et al*., 2013). The cellular architecture and circuitry of the cerebellum is well defined, and comprises a small number of neuronal subtypes (Purkinje, Golgi, stellate, basket and CGCs; *Fig*. 5.1). Sensory information is relayed into the cerebellum via mossy fibres, and is transmitted via CGCs, to Purkinje cells, which provide the final output from the cerebellar cortex (*Fig*. 5.1). CGCs are the smallest (somata diameter: 5 - 8 μm), and most abundant neuronal cell type in the human brain (Wisden *et al*., 1996), and represent the only glutamatergic neurons within the cerebellum. While CGCs provide excitatory inputs on to Golgi cells (and indeed other neuronal subtypes in the cerebellum; *Fig*. 5.1) via parallel fibres, Golgi cells reciprocally provide GABAergic inputs onto the distal dendrites of CGCs (*Fig*. 5.1), giving rise to both $GABA_A$ receptor mediated sIPSCs, and tonic currents in CGCs (Kaneda *et al*., 1995; Brickley *et al*., 1996; Wall and Usowicz, 1997).

Studies indicate that mature CGCs *in vivo*, most likely express $GABA_A$ receptors with the subunit combinations: α1βγ2, α6βγ2, α6βδ, and α1α6βγ2 (Wisden *et al*., 1992, 1996; Jones *et al*., 1997; Sieghart and Sperk, 2002); see *Section* 1.2.1). Here, we have studied the effects of 4-PIOL in CGCs maintained in culture. Before using cultures, one must also consider whether the $GABA_A$ receptors expressed in culture, reflect those expressed *in vivo*. Immunostaining studies suggest that cultured CGCs exhibit a similar developmental, and subcellular expression pattern for α1, α6, β2, β3, γ2 and δ subunits (Thompson and Stephenson, 1994; Caruncho *et al*., 1995; Gao and Fritschy, 1995) when compared to *in vivo* preparations (Laurie *et al*., 1992a; Wisden *et al*., 1992; Nusser *et al*., 1998; Hörtnagl *et al*., 2013). Moreover, CGCs in culture have previously been demonstrated to exhibit tonic currents (Leao *et al*., 2000).

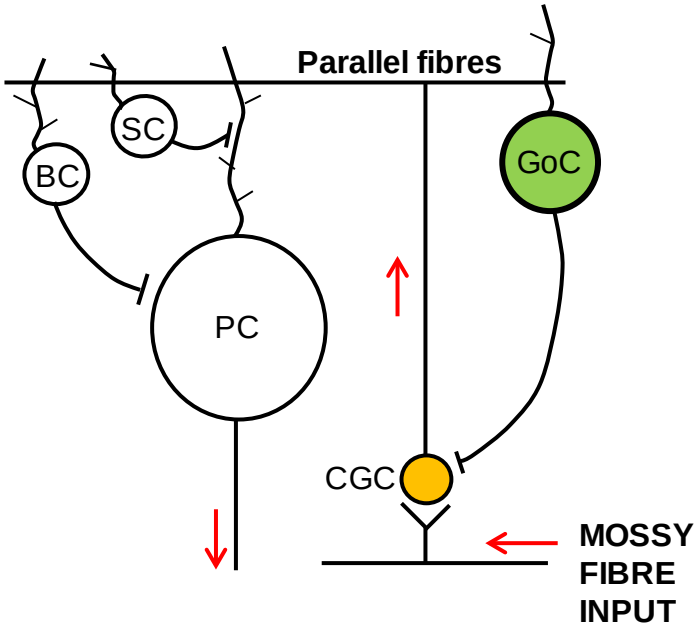

Figure 5.1 – Neurons and circuits of the cerebellum

Mossy fibres enter the cerebellum and synapse onto cerebellar granule cells (CGCs). CGCs give rise to specialised axons, termed parallel fibres, which provide glutamatergic inputs onto Purkinje cells (PC), basket cells (BC), stellate cells (SC) and Golgi cells (GoC). GoCs reciprocally provide GABAergic inputs onto CGCs, while BCs and SCs provide inhibitory inputs onto PCs. PCs are GABAergic cells and provide the final output from the cerebellum. The red arrows indicate the flow of information through the cerebellum.

5.1.2. GABAergic neurotransmission in hippocampal neurons

The hippocampus contributes to several psychological processes, including cognition, emotion, spatial memory formation and learning (Fanselow and Dong, 2010). Accordingly, hippocampal dysfunction is associated with many neurological disorders, including anxiety, depression, epilepsy and cognitive impairments (de Lanerolle *et al*., 2003; Bannerman *et al*., 2004; MacQueen and Frodl, 2011; Rudolph and Möhler, 2014). The hippocampus is a well defined structure, comprising of two interlocking parts, formed by the CA region, composed of the CA1, CA2 and CA3 sub-regions, and the dentate gyrus (*Fig*. 5.2). Signals enter the hippocampus from the entorhinal cortex, and pass unidirectionally through the hippocampus via a 'trisynaptic loop', consisting of dentate gyrus granule cells, CA1 pyramidal neurons, and CA3 pyramidal neurons (Moser, 2011; *Fig*. 5.2). In addition to these principal neurons, the hippocampus contains a huge diversity of GABAergic interneurons, which control the spatial and temporal firing patterns of principal cells (Klausberger *et al*., 2002, 2003; Kullmann and Lamsa, 2011).

Several neuronal subtypes in the hippocampus are reported to express tonic currents, including CA1 and CA3 pyramidal neurons (Bai *et al*., 2001; Caraiscos *et al*., 2004; Glykys *et al*., 2008), some CA1 inhibitory interneurons (Semyanov, 2003; Mann and Mody, 2010) and dentate gyrus granule cells (DGGCs; Nusser and Mody, 2002). Fast inhibitory neurotransmission in the hippocampus is likely mediated primarily by α1βγ2 and α2βγ2 receptors (Prenosil *et al*., 2006), with a potential contribution from α5βγ2 receptors to 'slow' IPSCs (Pearce, 1993; Banks *et al*., 1998; Prenosil *et al*., 2006; Zarnowska *et al*., 2009). By contrast, tonic currents in CA1 and CA3 pyramidal cells are predominantly mediated by α5βγ2 and α4βδ receptors (Caraiscos *et al*., 2004; Glykys *et al*., 2008), although αβ (Mortensen and Smart, 2006) and α1βδ receptors (Glykys *et al*., 2007) may also contribute in pyramidal cells and interneurons, respectively.

The effects of 4-PIOL were studied on hippocampal neurons maintained in culture. Cultured hippocampal neurons express a similar array of $GABA_A$ receptor subunits as those expressed *in vivo,* including α1, α4, α5, γ2 and δ

subunits (Killisch *et al*., 1991; Sieghart and Sperk, 2002; Mangan *et al*., 2005). Moreover, tonic currents have also been detected in cultured hippocampal neurons (Bai *et al*., 2001; Caraiscos *et al*., 2004; Mortensen and Smart, 2006), which are predominantly thought to be mediated by α5βγ2 receptors (Bai *et al*., 2001; Caraiscos *et al*., 2004).

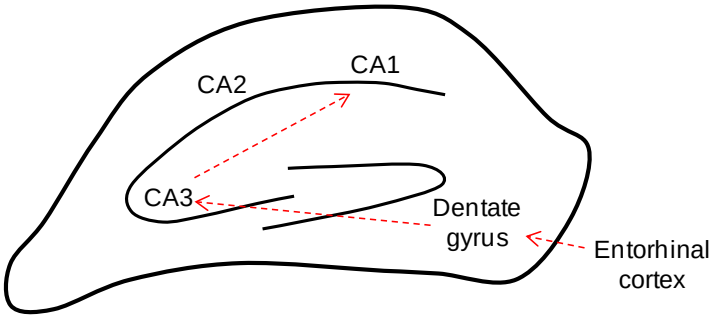

Figure 5.2 – Schematic of the hippocampal formation

The hippocampus consists of two main subdivisions: the *Cornu ammonis* (CA) region and the dentate gyrus. The CA region can be further subdivided into the CA1, CA2 and CA3 sub-regions, which contain the cell bodies of the pyramidal cells, while the dentate gyrus contains the cell bodies of granule cells. Both granule cells and pyramidal neurons are extensively innervated by inhibitory GABAergic interneurons. The red dashed arrows represent the classical trisynaptic loop, which transmits signals from the entorhinal cortex to CA1 pyramidal neurons, via dentate gyrus granule cells and CA3 pyramidal neurons. Note that this is a simplified schematic and many other reciprocal connections between the hippocampal sub-regions also exist.

5.2. Results

Whole-cell currents were recorded from cultured CGCs and hippocampal neurons, in the presence of D-APV and CNQX, to isolate GABAergic currents. All experiments started with a period of stable baseline recording, and bicuculline (BIC; 20 µM) was applied at the end of each experiment to a) verify that all synaptic events were GABAergic, and b) to reveal any $GABA_A$-mediated tonic current. The properties of sIPSCs were determined as detailed in *Section* 2.6.4, providing mean estimates for sIPSC frequency, amplitude, rise time and weighted decay (τ_w). Changes in tonic current were determined as described in *Section* 2.6.5, by measuring the change in holding current induced by each drug condition. RMS baseline noise analysis was not performed on recordings from CGCs or hippocampal neurons, since control epochs were frequently contaminated by a high frequency of synaptic events (see *Table* 5.1 and *Table* 5.2).

5.2.1. Effect of 4-PIOL on endogenous tonic and phasic currents of CGCs

CGCs are characteristically small cells which display small whole-cell capacitances and high input resistances (Kaneda *et al*., 1995). Accordingly, CGCs in culture were identified by their soma size, and displayed a mean whole-cell capacitance of 9.9 ± 2.1 pF, and a mean input resistance of 15.2 ± 7.9 GΩ. Under control conditions (i.e. in the presence of CNQX and D-APV), a high frequency of sIPSCs were recorded from CGCs (7.2 ± 1.01 Hz; *Table* 5.1), with an average amplitude, rise time and τ_w of 409 ± 113 pA, 1.1 ± 0.1 ms and 17.7 ± 1.6 ms respectively (n = 8; *Table* 5.1). Application of BIC abolished all sIPSCs (*Fig.* 5.3 A), confirming their GABAergic origin. Moreover, BIC induced an outward current (*Fig.* 5.3 A), indicating the presence of an endogenous tonic current, with a mean magnitude of 22.8 ± 8.5 pA.

To verify the functional expression of δ-containing receptors, whole-cell currents were recorded from cultured CGCs, in response to brief applications of a δ-selective concentration of the $GABA_A$ receptor agonist, THIP (1 μM; Brown *et al*., 2002; Cope *et al*., 2005; Stórustovu and Ebert, 2006; Herd *et al*., 2009). THIP enhanced the tonic currents of CGCs (*Fig*. 5.3 B) by an average of 67.5 ± 21.7 pA, thus confirming that δ-containing receptors were present in these cells.

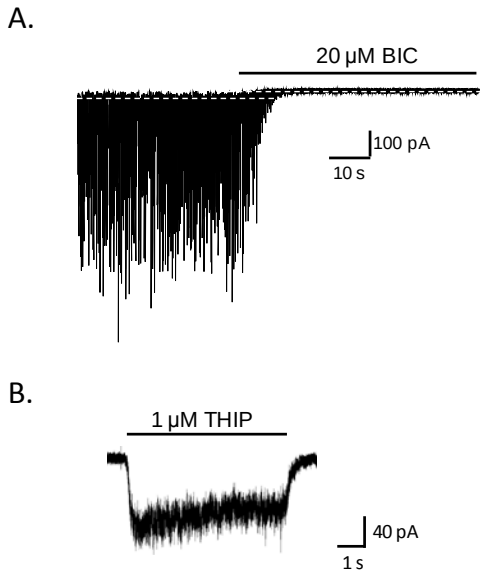

Figure 5.3 – CGCs in culture exhibit tonic currents.

Representative current traces from cultured CGCs in the presence of CNQX (10 μM) and D-APV (20 μM). Bicuculline (20 μM BIC; **A**), or THIP (1 μM; **B**), were applied for the duration indicated by the black horizontal bars. All recordings were performed at room temperature, from CGCs maintained in culture for 7 – 17 days *in vitro* (DIV). The holding potential was -60 mV.

The effects of 4-PIOL (10 µM) were next investigated on the endogenous tonic and phasic currents of CGCs. Following a period of control recording, 4-PIOL was bath applied to cells (*Fig.* 5.4 A) revealing a small tendency to enhance tonic current (9.8 ± 4.0 pA), although this increase was not found to be statistically significant (*P* = 0.058). Similarly, 4-PIOL exerted no significant effect on sIPSC amplitude (% control: 93.2 ± 14.9; *P* = 0.66; *Fig.* 5.4 B), or rise time (% control: 107 ± 4.1; *P* = 0.24; *Fig*. 5.4 C). Moreover, although the frequency of sIPSCs appeared to be reduced in 4-PIOL (% control: 64.0 ± 14.2; *Fig*. 5.4 D), this reduction was also not quite significant (*P* = 0.057; one-tailed paired t-test). In addition, although 4-PIOL may appeared to have prolonged the τ_w of sIPSCs (% control: 112 ± 1.1; *P* = 0.0024), this effect was not reversed by washout of 4-PIOL (*P* = 0.87; *Fig*. 5.4 E), indicating that factors independent of 4-PIOL application may underlie sIPSC prolongation, such as a washout of intracellular components.

Overall, these data indicated that 10 µM 4-PIOL does not significantly alter the endogenous tonic, or phasic, currents of cultured CGCs.

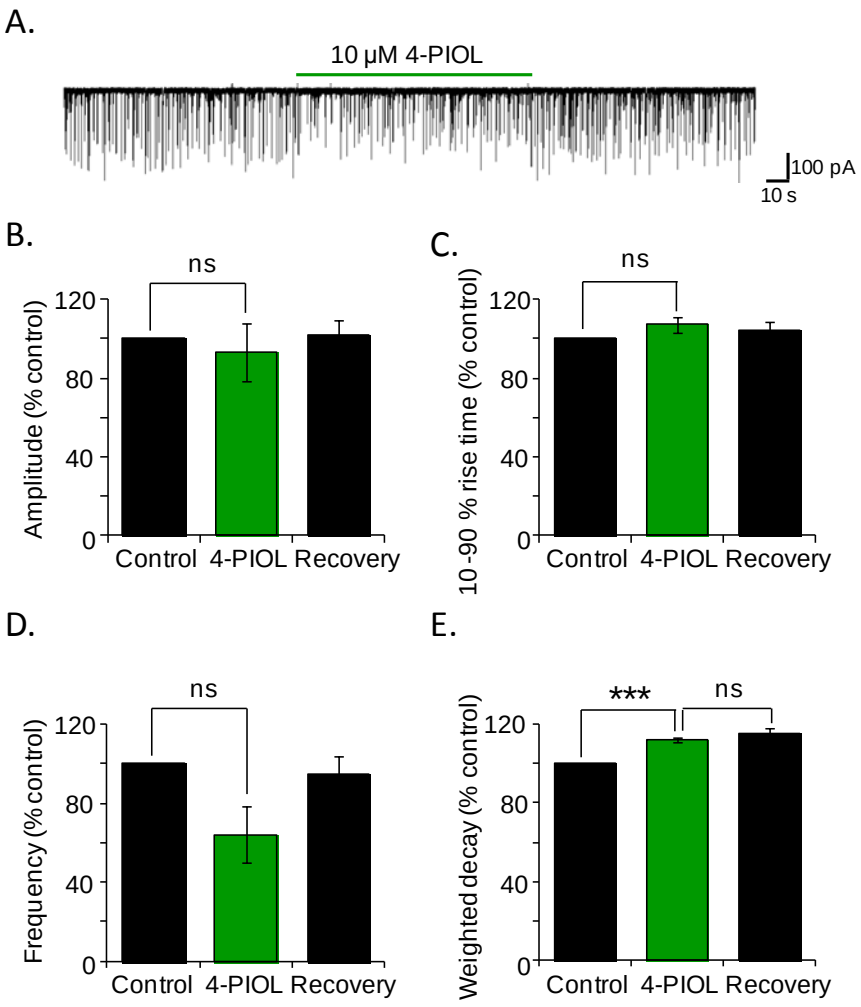

Figure 5.4 – 4-PIOL (10 µM) does not modulate tonic, or phasic, currents in CGCs

A. A representative current trace showing the effect of 10 µM 4-PIOL on sIPSCs and tonic $GABA_A$ receptor mediated currents in cultured CGCs. 4-PIOL was bath applied, for the duration indicated by the horizontal green bar. All recordings were performed at room temperature, in the presence of CNQX (10 µM) and D-APV (20 µM). The holding potential was -60 mV. Bar graphs showing the normalised data for sIPSC amplitude (**B**), 10-90 % rise time (**C**), frequency (**D**) and weighted decay (**E**), in control aCSF (black), or aCSF containing 10 µM 4-PIOL (green). Data represent mean ± SEM (n = 8) from CGCs maintained in culture for 7 – 17 DIV. Paired t-tests were used to compare sIPSC parameters in control or 10 µM 4-PIOL solution, and P>0.05 was considered as not statistically significant (ns). ***P < 0.001.

5.2.2. Effect of 4-PIOL on elevated CGC tonic currents

Although CGCs in culture exhibited endogenous tonic currents, the GABA concentrations and origin of GABA mediating this tonic current remain undefined. Therefore, to standardise and control the unknown variable of the extracellular GABA concentration, low concentrations of GABA (0.3 µM and 1 µM; *Fig. 5.5* A and *Fig*. 5.5 B respectively) were pre-applied to CGCs, until steady-state currents were achieved, and subsequently, 4-PIOL was co-applied. Similar to its effects on endogenous CGC tonic currents, co-application of 4-PIOL produced no significant shift in the holding current when the pre-applied GABA concentration was raised to 0.3 µM (*Fig. 5.5* A) or 1 µM GABA (*Fig*. 5.5 B). Taken together, these data indicate that 10 µM 4-PIOL acts neither as an agonist, nor an antagonist, on CGC tonic currents, at GABA concentrations thought to mediate tonic currents.

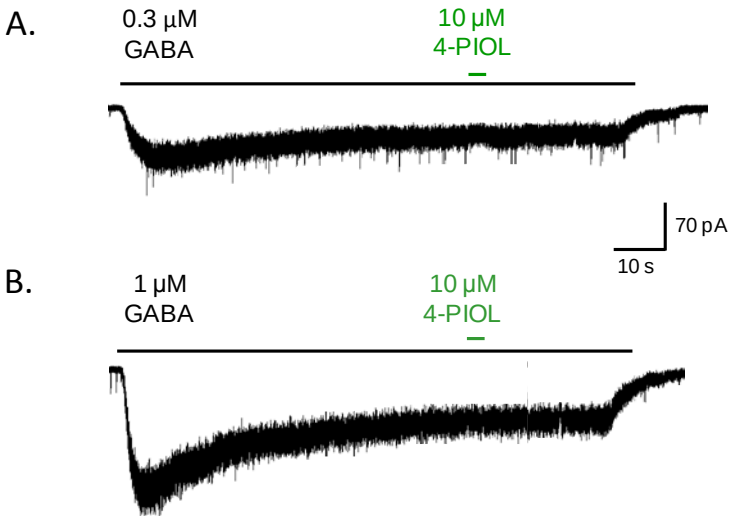

Figure 5.5 – 4-PIOL (10 µM) does not modulate elevated GABA tonic currents in CGCs

Representative traces of whole-cell currents elicited by prolonged applications of 0.3 (**A**) or 1 µM (**B**) GABA (black horizontal bars). As indicated by the green horizontal bars, 10 µM 4-PIOL, was co-applied for 4 s once a steady-state GABA current was achieved. Note that 10 µM 4-PIOL produced no significant change in the steady-state GABA currents. The holding potential was -60 mV.

5.2.3. 4-PIOL modulation of hippocampal tonic and phasic currents

The effects of 4-PIOL were additionally assessed on whole-cell currents recorded from hippocampal neurons. Under control conditions, cultured hippocampal neurons displayed a high frequency of sIPSCs (6.9 ± 1.7 Hz; *Table* 5.2), with an average amplitude, rise time and τ_w of 2058 ± 672 pA, 2.0 ± 0.3 ms and 31.4 ± 3.0 ms respectively (*Table* 5.2). All sIPSCs were abolished by bath application of 20 μM BIC (*Fig*. 5.6), thus confirming their GABAergic origin. Moreover, BIC produced an outward current, revealing an endogenous tonic current with a mean magnitude of 42.8 ± 6.3 pA (*Fig*. 5.6).

To assess the effects of 4-PIOL on endogenous tonic and phasic currents of hippocampal neurons, 10 μM 4-PIOL was bath applied to cells following a period of control recording (*Fig.* 5.7 A). 4-PIOL significantly enhanced the $GABA_A$ receptor mediated tonic currents, by 72.0 ± 14.2 pA (*P* = 0.0025), consistent with the previously observed weak partial agonist profile of 4-PIOL on hippocampal neurons (Kristiansen *et al*., 1995).

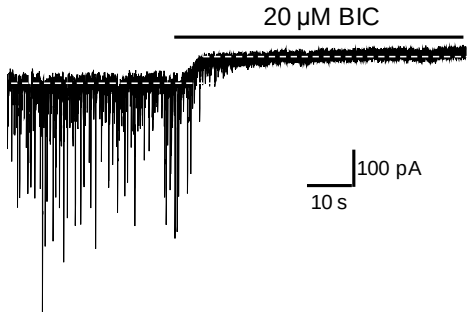

Figure 5.6 – Cultured Hippocampal neurons display a $GABA_A$ receptor mediated tonic current.

An example (from n = 8 cells) whole-cell current trace recorded from a cultured hippocampal neuron, in the presence of CNQX (10 μM) and D-APV (20 μM). Bicuculline (20 μM BIC) was bath applied for the duration indicated by the black horizontal bar. All hippocampal recordings were performed at room temperature and the holding potential was -60 mV. Recordings were made from hippocampal neurons maintained in culture for 11 – 21 DIV.

Unexpectedly, 10 µM 4-PIOL also significantly inhibited both the frequency (% control: 49.8 ± 9.5 %*; Fig*. 5.7 B; *P* = 0.002) and amplitude of sIPSCs (% control: 58.6 ± 16.8 %; *Fig*. 5.7 C; *P* = 0.047 – Wilcoxon matched pairs test). However, 4-PIOL did not significantly affect the rise time (% control: 110 ± 12.1; *Fig*. 5.7 D; *P* = 0.50) or τ_w (% control: 100 ± 3.4; *Fig*. 5.7 E; *P* = 0.75) of sIPSCs. By generating a frequency histogram for sIPSC amplitudes (*Fig*. 5.7 F), under control conditions, and in 4-PIOL (*Fig*. 5.7 F), three sIPSC amplitude populations were detected, with mean amplitudes of 39.6 ± 1.0, 647.4 ± 26.4 and 1989.7 ± 45.1 pA respectively (*Fig*. 5.7 F; control). Most notably, the highest amplitude population was shifted to a lower mean amplitude (1438.7 ± 19.0) in 4-PIOL (*Fig*. 5.7 F; see arrows), and there was a higher frequency of the smallest amplitude events. The middle amplitude population appeared to be unchanged in 4-PIOL.

5.2.4. 4-PIOL bidirectionally modulates elevated tonic currents of hippocampal neurons

Given that hippocampal neurons express α5βγ receptors (Pirker *et al*., 2000; Bai *et al*., 2001; Caraiscos *et al*., 2004; Hörtnagl *et al*., 2013), and our recombinant expression studies indicate that 4-PIOL can enhance, or moderately inhibit, the steady-state GABA currents of recombinant α5β3γ2 receptors, depending on the ambient GABA concentration (see *Chapter* 4; *Fig.* 4.11 – *Fig*. 4.13), the effect of altering the ambient GABA concentration on 4-PIOL behaviour was investigated. Low concentrations of GABA (0.3 µM and 1 µM; *Fig. 5.8* A and *Fig*. 5.8 B respectively) were pre-applied to hippocampal neurons, until steady-state currents were achieved, and subsequently, 4-PIOL was co-applied. Co-application of 10 µM 4-PIOL with 0.3 µM GABA significantly enhanced the tonic current by 62.8 ± 9.9 pA (*P* = 0.03 – Wilcoxon matched pairs test), similar to the enhancement observed under control conditions (72.0 ± 14.2 pA; *P* = 0.90). However, when the pre-applied GABA concentration was raised to 1 µM GABA, 10 µM 4-PIOL significantly reduced the steady-state 1 µM GABA current, by 52.5 ± 7.1 pA (*P* = 0.0004 – paired t-test). This

corresponded to a 73.6 ± 28.1 % enhancement of the steady-state 0.3 μM GABA current, and a smaller 12.4 ± 2.0 % inhibition of the steady-state 1 μM GABA current (*Fig*. 5.8 C).

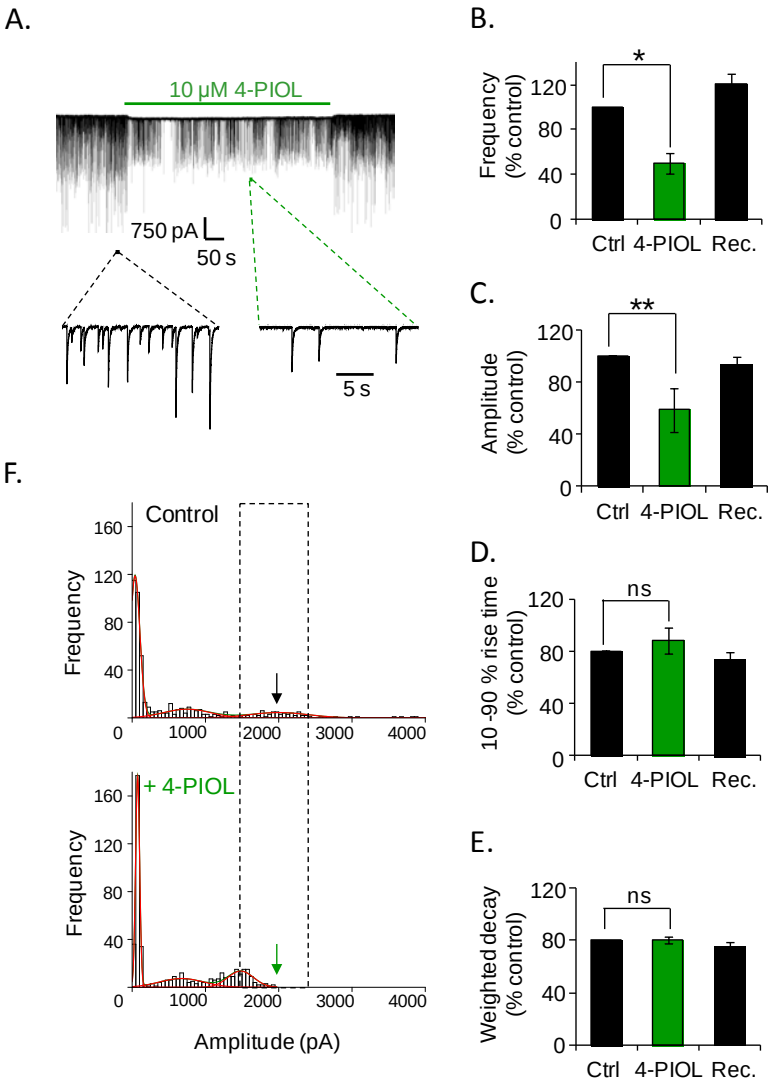

Figure 5.7 – 4-PIOL (10 µM) alters GABAergic currents in hippocampal neurons.

A. A representative current trace showing the effect of 10 µM 4-PIOL on sIPSCs and tonic $GABA_A$ receptor mediated currents on cultured hippocampal neurons. 4-PIOL was bath applied, for the duration indicated by the horizontal green bar. All recordings were performed at room temperature, in the presence of CNQX (10 µM) and D-APV (20 µM), and cells were held at -60 mV. Expanded recordings are shown below. Note that 4-PIOL induced an inward current. Bar graphs show the normalised data for sIPSC frequency (**B**), amplitude (**C**), 10-90 % rise time (**D**), and weighted decay (**E**), in control aCSF (ctrl; black), or aCSF containing 10 µM 4-PIOL (green). Data represent mean ± SEM (n = 8) from hippocampal neurons maintained in culture for 11 – 21 DIV. Paired t-tests were used to compare sIPSC parameters in control or 10 µM 4-PIOL conditions. $P > 0.05$ was considered as not statistically significant (ns). *$P < 0.05$ and **$P < 0.01$. **F.** Frequency histograms were generated for sIPSC amplitudes, for the cell presented in panel **A**, and fitted with the Gaussian distribution function (red curves) as described in Section 2.6.4.

Table 5.1 – sIPSC parameters for cultured CGCs

	Control	+ 10 µM 4-PIOL	Recovery
Frequency (Hz)	7.2 ± 1.0	4.5 ± 1.3	7.0 ± 1.4
Amplitude (pA)	409 ± 113	374 ± 123	398 ± 104
10-90 % rise time (ms)	1.1 ± 0.1	1.2 ± 0.1	1.2 ± 0.04
Weighted tau (ms)	17.7 ± 1.6	19.8 ± 1.7	20.2 ± 1.6

Each sIPSC parameter (mean ± SEM) was calculated, as detailed in *Section* 2.6.4. Note that the mean sIPSC amplitude for each cell, in each condition, was calculated using the largest 100 amplitude events.

Table 5.2 – sIPSC parameters for cultured hippocampal neurons

	Control	+ 10 µM 4-PIOL	Recovery
Frequency (Hz)	6.9 ± 1.7	4.0 ± 1.6 *	8.0 ± 2.0
Amplitude (pA)	2058 ± 672	872 ± 290 **	1855 ± 701
10-90 % rise time (ms)	2.0 ± 0.3	2.1 ± 0.3	1.8 ± 0.3
Weighted tau (ms)	31.4 ± 3.0	31.7 ± 3.7	29.9 ± 3.1

Each sIPSC parameter (mean ± SEM) was calculated as detailed in *Section* 2.6.4. Note that the mean sIPSC amplitude for each cell, in each condition, was calculated using the largest 100 amplitude events. *P < 0.05 and **P < 0.01.

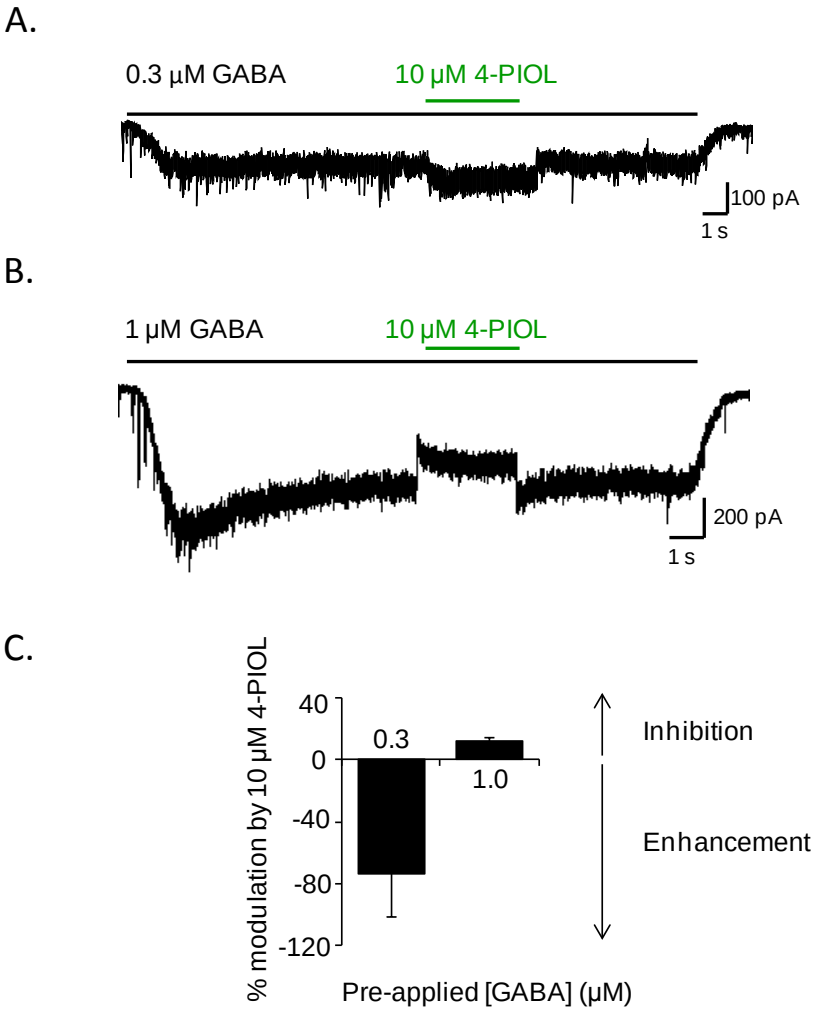

Figure 5.8 – 4-PIOL bidirectionally modulates elevated tonic currents in cultured hippocampal neurons.

Representative traces of whole-cell currents elicited by prolonged applications of 0.3 (**A**) or 1 µM (**B**) GABA (black horizontal bars). As indicated by the green horizontal bars, 10 µM 4-PIOL was co-applied, once a steady-state GABA current was achieved. The holding potential was -60 mV. **C.** A Bar graph showing the percentage modulation induced by 10 µM 4-PIOL. Note that negative and positive values respectively represent an enhancement, or inhibition, of the steady-state GABA current.

5.3. Discussion

In this chapter, the effects of 4-PIOL were assessed on tonic and phasic currents of cultured CGCs and hippocampal neurons, whose tonic currents are thought to be mediated by different $GABA_A$ receptor isoforms.

5.3.1. 4-PIOL (10 μM) has no affect on tonic or phasic currents of CGCs

As predicted from our recombinant expression studies, sIPSCs recorded from CGCs were unaffected by 10 μM 4-PIOL. Moreover, tonic currents were also unaffected by 10 μM 4-PIOL, even when ambient was GABA altered. These data concur with our recombinant expression studies, where 10 μM 4-PIOL did not significantly inhibit the 'synaptic-type' responses of α1β3γ2S receptors (*Fig*. 4.6), or the 'extrasynaptic-type' responses of α6β2δ receptors (*Fig*. 4.10 B), the two main $GABA_A$ receptor isoforms likely to be expressed in CGCs (Laurie *et al*., 1992a; Thompson and Stephenson, 1994; Gao and Fritschy, 1995; Nusser *et al*., 1998).

Only two studies have previously explored the agonist and antagonist profile of 4-PIOL on CGCs. Though not measuring GABA currents and relying on an indirect binding assay, Rabe *et al*. (2000) demonstrated that a high concentration of 4-PIOL (300 μM) did not significantly alter the binding of [^{35}S]TBPS (an open channel blocker) to CGC membranes, concluding a lack of 4-PIOL agonist efficacy in this cell type. However, by using a more direct electrophysiological approach, Hansen *et al*. (2001) found that 4-PIOL acted as a weak partial agonist with a low potency (~ 300 μM). Thus, the low 4-PIOL agonist efficacy and potency might explain why no agonist profile was detected using the [^{35}S]TBPS binding assay (Rabe *et al*., 2000), and also why 10 μM 4-PIOL produced no enhancement of CGC tonic currents in this study.

5.3.2. 4-PIOL significantly inhibits phasic currents in hippocampal neurons

By comparison with CGCs, in cultured hippocampal neurons, 10 μM 4-PIOL significantly reduced the amplitude and frequency of sIPSCs, which was coupled with an enhancement of tonic currents. The inhibition of sIPSC amplitude was particularly surprising, since 10 μM 4-PIOL did not significantly inhibit the 'synaptic-type' responses of recombinant α1β3γ2L receptors (*Fig*. 4.3), or synaptic events in CGCs. The reduction in sIPSC amplitude might arise from 4-PIOL directly inhibiting a subset of synaptic $GABA_A$ receptors in hippocampal neurons, which are not expressed in CGCs. For instance, it is intriguing to note that the α2 subunit is prominently expressed in the hippocampus, but shows only low levels of expression in CGCs (Laurie *et al*., 1992a; Sperk *et al*., 1997; Pirker *et al*., 2000; Hörtnagl *et al*., 2013). Moreover, although α1β3γ2 receptors significantly contribute to sIPSCs in CA1 pyramidal neurons (Prenosil *et al*., 2006), a significant, emerging role for α2βγ2 receptors has also been demonstrated (Prenosil *et al*., 2006). Therefore, it might be interesting to assess the effects of 4-PIOL on the peak GABA responses of recombinant α2βγ2L receptors expressed in HEK293 cells.

The reduction in IPSC frequency most likely indicates that 4-PIOL also acts on presynaptic $GABA_A$ receptors. The simplest explanation is that 4-PIOL activates presynaptic $GABA_A$ receptors (Kullmann *et al*., 2005), which hyperpolarise presynaptic axon terminals or pre-terminal regions, and leads to a reduction in neuronal excitability and consequently, reduced GABA release. However, this is unlikely since Cl^- appears to be largely depolarising in axonal and synaptic compartments (Zhang and Jackson, 1993; Ruiz *et al*., 2010). Indeed axonal depolarisation has been demonstrated to either increase, or decrease, neurotransmitter release (Zhang and Jackson, 1993; Turecek and Trussell, 2002; Axmacher and Draguhn, 2004; Ruiz *et al*., 2010) depending on the synapse studied and presumably on the concentration of intracellular Cl^- (Ruiz *et al*., 2003). At inhibitory synapses in the hippocampus, it was previously demonstrated that $GABA_A$ receptor agonists reduce the frequency of IPSCs recorded from CA3 pyramidal neurons (Axmacher and Draguhn, 2004), in accord with our findings, assuming that 4-PIOL is activating presynaptic $GABA_A$

receptors. Although the precise mechanism(s) leading to reduced neurotransmitter release remain uncertain, possible explanations might include a depolarisation-induced inactivation of Na^+ (or Ca^{2+}) channels, and/or a shunting of excitatory potentials.

It is important to note that although we found a prominent presynaptic effect of 4-PIOL *in vitro*, it is unclear whether this presynaptic effect will be retained *in vivo*, especially since hippocampal neurons in culture have less well defined synaptic connections. Therefore, it would be interesting to assess whether the effects of 4-PIOL on phasic conductances differs in acute brain slices, where many more of the original synaptic inputs are conserved.

5.3.3. 4-PIOL bidirectionally modulates the tonic currents of hippocampal neurons

When the GABA concentration was low, 4-PIOL generated an inward current, which is consistent with the previously described weak partial agonist profile of 4-PIOL on cultured hippocampal neurons (Kristiansen *et al*., 1995). However, when the ambient GABA concentration was raised to 1 μM GABA, 4-PIOL switched its action to that of an antagonist, albeit producing only a modest (~ 12 %) inhibition of the steady-state 1 μM GABA current. These data emulate our findings for recombinant α1β3γ2L and α5β3γ2L receptors (*Fig*. 4.13), where 4-PIOL exhibited a dominant agonist profile at low ambient GABA concentrations, but produced a modest inhibition when the ambient GABA concentration was raised to 1 μM.

Although hippocampal neurons likely express an array of $GABA_A$ receptor isoforms, including α5βγ2L, α4βδ and αβ receptors (Mangan *et al*., 2005; Mortensen and Smart, 2006; Glykys *et al*., 2008), we would predict that the agonist profile of 4-PIOL in hippocampal neurons is predominantly mediated by γ2-containing receptors since the 4-PIOL current in hippocampal neurons was previously demonstrated to be positively modulated by the benzodiazepine

agonist, midazolam (Kristiansen *et al*., 1995). Moreover, our recombinant expression studies suggest that 4-PIOL shows no significant agonist efficacy at δ-containing receptors (*Section* 4.2.1). Given that α5β3γ2L receptors are proposed to be the major mediators of tonic conductances in hippocampal pyramidal neurons (Bai *et al*., 2001; Caraiscos *et al*., 2004; Glykys *et al*., 2008), 4-PIOL may be activating this receptor isoform, especially since a small agonist response was observed with 10 μM 4-PIOL on recombinant α5β3γ2L receptors (see *Chapter* 4). However, other γ2-receptor isoforms may also be involved, since tonic currents in CA1 pyramidal neurons have been demonstrated to be potentiated by the non-benzodiazepine agonist, zolpidem, indicating the additional presence of extrasynaptic α(1, 2 or 3)βγ2 receptors (Liang *et al*., 2004).

Overall, 10 μM 4-PIOL does not significantly affect phasic, or tonic, currents of cultured CGCs. By contrast, 10 μM 4-PIOL respectively enhances and inhibits the tonic and phasic currents of cultured hippocampal neurons, although a small inhibition of tonic currents can be achieved by raising ambient GABA to 1 μM.

5.4. Conclusion

1. The sIPSC properties of cultured CGCs are unaltered by 10 μM 4-PIOL.

2. 4-PIOL (10 μM) exhibits no discernible agonist, or antagonist, profile on CGC tonic currents.

3. 4-PIOL (10 μM) significantly reduces the frequency and amplitude of sIPSCs in hippocampal cultures.

4. In hippocampal neurons, 4-PIOL (10 μM) exhibits a dominant agonist profile at low ambient GABA concentrations, although a small inhibition can be achieved by raising the ambient GABA concentration to 1 μM GABA.

Chapter 6: Pharmacological characterisation of 4-PIOL in Thalamic relay neurons

6.1. Introduction

Our previous recombinant expression studies (see *Chapter* 4) indicated that by considering all the extrasynaptic $GABA_A$ receptor subtypes that were studied, α4βδ, α6βδ, α5βγ2L and α1βγ2L, only the GABA responses from extrasynaptic-type α4βδ receptors were substantially inhibited by 10 μM 4-PIOL. The extent of the inhibition was ~ 30 – 70 % when the ambient GABA concentration ranged from 0.1 – 1 μM GABA (see *Figs*. 4.11 – 4.13).

To further examine whether 10 μM 4-PIOL could selectively inhibit α4βδ-mediated tonic currents in neurons, the functional effects of 4-PIOL were assessed on tonic and phasic currents of dLGN relay neurons. Relay neurons of the dLGN are reported to exhibit tonic currents that are mediated by extrasynaptic $GABA_A$ receptors composed of α4βδ subunits (Belelli *et al*., 2005; Cope *et al*., 2005; Bright *et al*., 2007; Nani *et al*., 2013; Ye *et al*., 2013).

The dLGN receives sensory inputs from retinal ganglion cells, and acts as a processing centre for visual information. Signals are transmitted from the dLGN to the primary visual cortex and the RTN via TC relay neurons. These reciprocally provide excitatory and inhibitory inputs back onto the dLGN relay neurons (see *Fig*. 6.1). In rodents, the dLGN is the only thalamic nucleus in which relay neurons are additionally modulated by local GABAergic interneurons (Ohara *et al*., 1983). Thalamocortical networks are involved in the generation of normal behaviours such as sleep and arousal (Steriade *et al*., 1993; McCormick and Bal, 1997), and abnormal activity in these circuits contributes towards the generation of absence seizures (see *Section* 1.3.3).

In addition to tonic currents in dLGN relay neurons that are largely mediated by α4βδ receptors, phasic currents are predominantly mediated by α1βγ2 receptors. However, α2βγ2 receptors are also reported to mediate dLGN phasic currents during the first postnatal month of development (Soltesz *et al*., 1990; Okada *et al*., 2000; Peden *et al*., 2008). Here, the effects of 4-PIOL were assessed on phasic and tonic currents of dLGN relay neurons in coronal brain slices taken from young (postnatal day 14) rats.

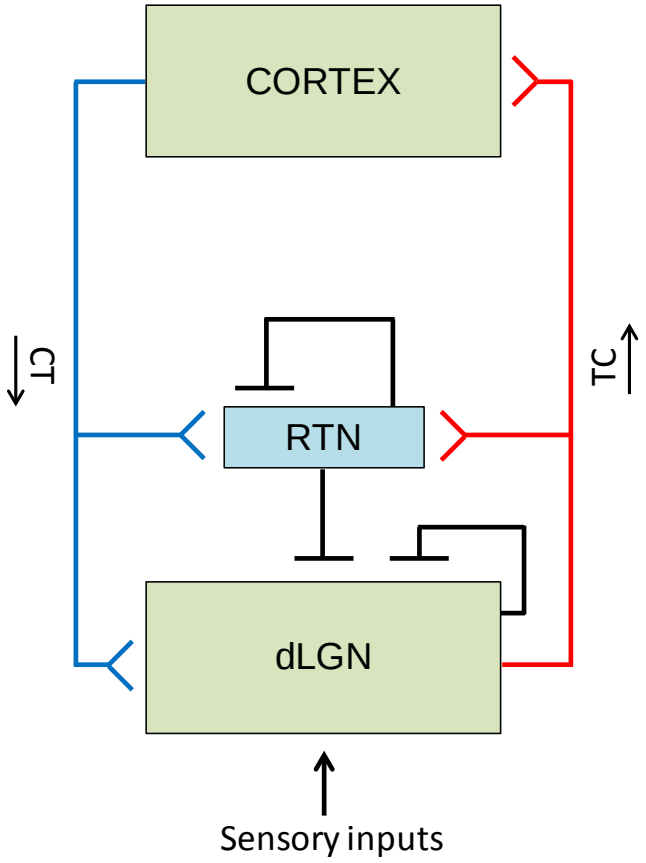

Figure 6.1 – Schematic of thalamocortical circuitry

Thalamocortical (TC) relay neurons of the dorsal lateral geniculate nucleus (dLGN) receive sensory inputs from retinal ganglion cells, and send excitatory projections to the thalamic reticular nucleus (RTN), and the primary visual cortex (red). TC relay neurons reciprocally receive excitatory inputs from corticothalamic (CT) relay neurons, and inhibitory inputs from local and RTN interneurons (black).

6.2. Results

Acute brain slices were prepared as described in *Section* 2.6.2, and maintained in control aCSF prior to experimentation. Whole-cell currents were recorded from a single dLGN relay neuron per brain slice at room temperature. All recordings were performed in the presence of kynurenic acid (2 mM) to isolate GABAergic currents, and BIC (20 μM) was bath applied at the end of each experiment, to confirm the GABAergic origin of all synaptic events, and unveil any $GABA_A$ receptor mediated tonic current. The frequency, amplitude and rise time of sIPSCs were determined as described in *Section* 2.6.4. To quantify changes in the tonic currents, drug-induced changes in holding current and RMS baseline noise were measured, as detailed in *Section* 2.6.5. To account for cell-to-cell variability in size, changes in holding current will be expressed as current density (pA/pF), which was calculated by normalising drug-induced changes in holding current (pA) to whole-cell capacitance (pF).

6.2.1. Characterising tonic and phasic currents in dLGN neurons

The dLGN was identified in coronal brain slices by its position relative to the hippocampus, and the ventral lateral geniculate nucleus (vLGN; *Fig*. 6.2 A). In rodents, the visual thalamus (dLGN) contains both thalamic relay neurons, and GABAergic interneurons (Ohara *et al*., 1983). Previous studies indicate that dLGN interneurons display far higher input resistances (> 500 MΩ), a smaller soma and distinct (bipolar) morphologies compared to thalamic relay neurons (Sherman and Koch, 1986; Williams *et al*., 1996; Zhu *et al*., 1999; Bright *et al*., 2007; Krahe *et al*., 2011). Moreover, while dLGN relay neurons have been demonstrated to exhibit $GABA_A$ receptor mediated tonic currents (Cope *et al*., 2005; Bright *et al*., 2007; Ye *et al*., 2013), this tonic conductance is absent in dLGN interneurons (Bright *et al*., 2007), which is a useful diagnostic identifier of this cell type.

To further distinguish between interneurons and relay neurons, the input resistance and whole-cell capacitance was determined for all dLGN neurons. However, in control aCSF, dLGN neurons displayed a wide range of input resistances and membrane capacitances, which showed no significant correlation (*Fig*. 6.2 B; *P* = 0.998). Thus, it was difficult to assign individual neurons as interneurons, or relay neurons, based purely on these parameters. As an alternative, the morphologies of some cells was investigated, by filling cells with the fluorescent dye, Lucifer yellow, via the recording electrode, and imaging the filled cells (*Section* 2.7). A representative image of a filled cell is shown in *Fig*. 6.2 C, demonstrating that that the dendrites of these cells were radially distributed (*Fig*. 6.2 C), which is consistent with the morphology of dLGN relay neurons (Williams *et al*., 1996; Bright *et al*., 2007; Krahe *et al*., 2011).

Thus, we had to rely on the presence, or absence, of a tonic current to identify thalamic relay cells. For all cells, the presence of a tonic current was probed using the $GABA_A$ receptor antagonist, BIC. BIC application induced an outward current (*Fig*. 6.2 D), relative to the holding current recorded in control aCSF (i.e. with no exogenously-added GABA). This shift had a mean magnitude of 23.8 ± 2.08 pA (e.g. *Fig*. 6.2 D), which when normalised to whole-cell capacitance, corresponded to a tonic $GABA_A$ receptor current of 0.13 ± 0.01 pA/pF. Concurrently, BIC also reduced the RMS baseline noise, by 9.6 ± 1.5 pA, consistent with the closing of tonically-active $GABA_A$ receptors. A high frequency of IPSCs (11.5 ± 1.6 Hz) was detected from dLGN relay neurons, with a mean amplitude and rise time of 56.4 ± 4.3 pA and 2.5 ± 0.2 ms respectively. All sIPSCs were also abolished by BIC application, confirming GABAergic origin (*Fig*. 6.2 D). The mean values determined for each sIPSC parameter, and BIC-sensitive tonic currents, are listed in *Table* 6.1 and 6.2 respectively.

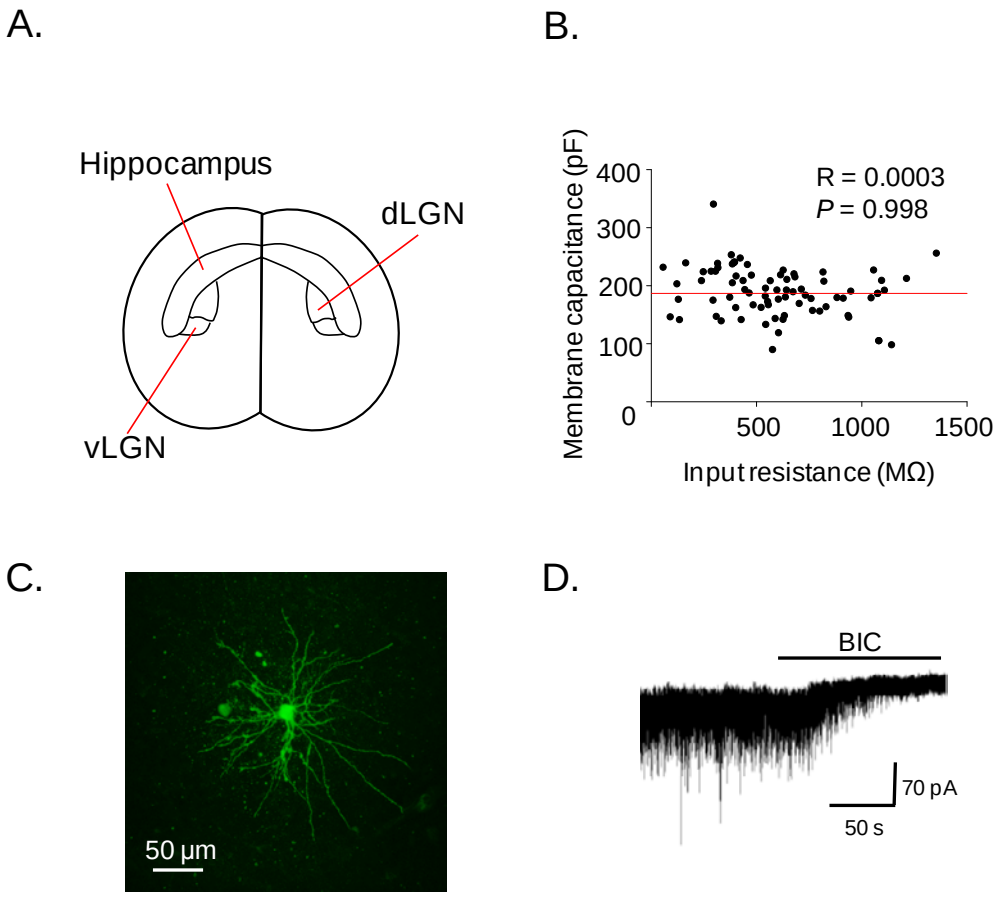

Figure 6.2 – Characterisation of dLGN relay neurons

A. Schematic diagram of a coronal brain slice, showing the location of the dorsal lateral geniculate nucleus (dLGN), the ventral lateral geniculate nucleus (vLGN) and the hippocampus. **B.** Scatter plot of the input resistance against membrane capacitance recorded for all cells from the dLGN bathed in control aCSF (n = 85). Linear regression analysis was performed on these data (red line), and R and *P* represent Pearson's correlation coefficient and *P*-values respectively. Input resistance and membrane capacitance were measured from transient current changes induced by 10 mV hyperpolarising steps. **C.** Representative confocal image of a dLGN relay neuron filled with Lucifer yellow via the recording electrode. Image represents a Z-projection of 45 (x 2 µm) stacks. **D.** Representative whole-cell current trace from a dLGN relay neuron. Bath application of BIC (20 µM) reveals a $GABA_A$ receptor mediated tonic current, and blocks all sIPSCs. All recordings were performed at room temperature in the presence of kynurenic acid (2 mM), and the holding potential was -60 mV.

6.2.2. 4-PIOL modulation of dLGN tonic and phasic currents

According to our recombinant expression studies (*Chapter* 4), 10 µM 4-PIOL showed no discernible agonist activity at recombinant α4βδ receptors, but was predicted to reduce α4βδ-mediated tonic currents, assuming that the ambient GABA concentration in slices is 0.1 – 1 µM GABA (*Figs*. 4.11 – 4.13). Moreover, 10 µM 4-PIOL did not inhibit the 'synaptic-type' responses of recombinant α1βγ2L receptors. Thus, we might expect 4-PIOL to exert similar effects on dLGN phasic and tonic currents, which are respectively thought to be mediated by α1βγ2L and α4βδ receptors respectively (Cope *et al*., 2005; Bright *et al*., 2007; Ye *et al*., 2013).

Therefore, it was unexpected that bath application of 10 µM 4-PIOL to dLGN slices significantly enhanced tonic currents by 57.4 ± 3.3 pA (*Fig*. 6.3 A), which corresponded to a current density of 0.34 ± 0.03 pA/pF. 4-PIOL also increased the RMS baseline noise by 13.2 ± 1.6 pA; *Table* 6.3). To verify that this 4-PIOL-induced increase in tonic current was mediated by $GABA_A$ receptors, we assessed its sensitivity to BIC. For each cell, a control response to 10 µM 4-PIOL was first recorded and washed out, prior to a second 4-PIOL application co-applied with BIC (*Fig*. 6.3 A). The 4-PIOL current was abolished in the presence of BIC (% control 4-PIOL response: 2.2 ± 0.5; *Fig*. 6.3 B), as was the 4-PIOL-induced change in RMS baseline noise (*Fig*. 6.3 C), indicating that 4-PIOL was indeed activating $GABA_A$ receptors.

Notably, 4-PIOL also reduced both the frequency (% control: 13.3 ± 2.2 %; *Fig*. 6.4 A and B; $P = 0.001$) and amplitude of sIPSCs (% control: 71.8 ± 2.7 %; *Fig*. 6.4 A and C; $P = 0.01$) relative to those measured in control aCSF. Although 4-PIOL appeared to reduce the 10 – 90 % rise time of sIPSCs (*Fig*. 6.4 D; $P = 0.0002$), this effect was not reversed by washout of 4-PIOL (*Fig*. 6.4 D; $P = 0.09$), indicating that factors independent of 4-PIOL application may underlie the slower activation profile of sIPSCs. Due to the low frequency of sIPSCs, and increased RMS baseline noise in 4-PIOL (13.2 ± 1.6 pA; *Table* 6.2), no detailed analysis of sIPSC decay times was performed. Taken together, these data indicate that 4-PIOL enhanced dLGN tonic currents, possibly by a direct agonist

action at extrasynaptic $GABA_A$ receptors, and simultaneously inhibited the frequency and amplitude of sIPSCs (discussed further in *Section* 6.3.1).

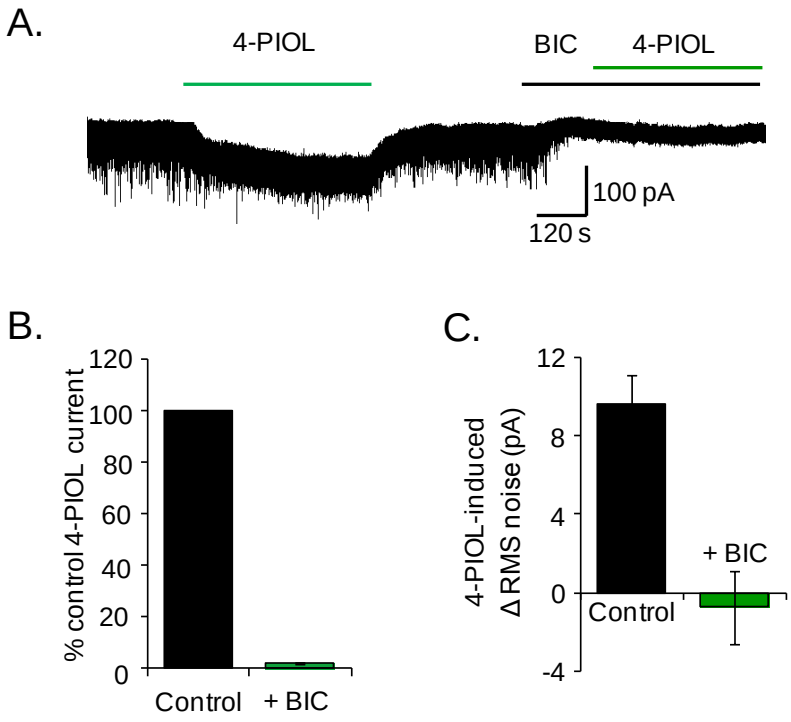

Figure 6.3 – 4-PIOL enhances GABAergic tonic currents in dLGN relay neurons

A. Representative membrane current trace recorded from a dLGN relay neuron in response to bath applied 4-PIOL (10 µM) in the absence, or presence, of BIC (20 µM). 4-PIOL and BIC were respectively applied for the durations indicated by the green and black horizontal bars. **B.** Bar chart of 4-PIOL response in BIC (green), expressed as a percentage of the control 4-PIOL response (black) recorded from the same dLGN relay neuron. **C.** Bar chart of the change in RMS baseline noise induced by 4-PIOL, in the absence (black) and presence (green) of BIC.

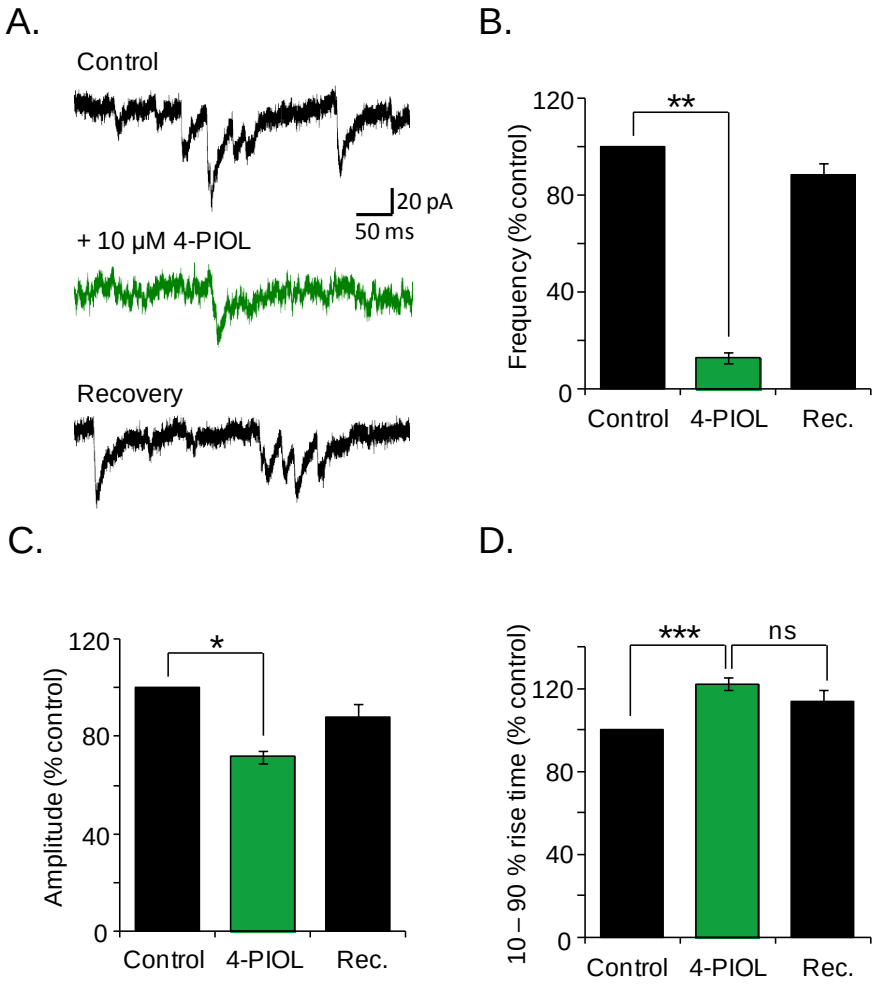

Figure 6.4 – sIPSC parameters for dLGN relay neurons

A. Representative sIPSCs recorded from dLGN relay neurons, in control aCSF (black), or during 4-PIOL (10 µM) treatment. All recordings were performed at room temperature, in the presence of kynurenic acid (2 mM). Bar graphs showing the normalised data for sIPSC frequency (**B**), amplitude (**C**) and 10-90 % rise time (**D**) in control aCSF (black), or aCSF containing 4-PIOL (green). For each cell, sIPSC parameters were calculated as described in *Section* 2.6.4, and these data represent the mean (± SEM) data from 6 cells. Paired t-tests were used to compare sIPSC parameters and data were classified as not statistically significant (ns) if $P > 0.05$. *$P < 0.05$, **$P < 0.01$ and ***$P < 0.001$. Note that the non-normalised sIPSC parameters are listed in *Table* 6.1.

Table 6.1 – sIPSC parameters for dLGN relay neurons

	Control	+ 10 μM 4-PIOL	Recovery
Frequency (Hz)	11.5 ± 1.6	1.5 ± 0.3**	10.2 ± 1.6
Amplitude (pA)	56.4 ± 4.3	40.2 ± 2.7*	49.0 ± 2.6
10-90 % rise time (ms)	2.5 ± 0.2	3.1 ± 0.2	2.9 ± 0.3

Each sIPSC parameter (mean ± SEM; n = 6) was calculated as detailed in *Section* 2.6.4. Note that the mean sIPSC amplitude for each cell, in each condition, was calculated using the largest 100 amplitude events. Statistical analyses were performed relative to control, with *P < 0.05 and **P < 0.01.

6.2.3. DS2 modulation of the 4-PIOL current

To investigate whether the 4-PIOL current in dLGN relay neurons was mediated by δ–containing receptors, we investigated whether the 4-PIOL current could be modulated by the δ-selective positive allosteric modulator, DS2 (Wafford *et al*., 2009; Jensen *et al*., 2013). A concentration of 10 μM DS2 was chosen, since this concentration was reported previously to potentiate δ-mediated GABA currents in recombinant expression systems and thalamic relay neurons (Wafford *et al*., 2009; Jensen *et al*., 2013; Ye *et al*., 2013). For each cell, a control response to 10 μM 4-PIOL was first recorded (and washed out), followed by a second response to 10 μM 4-PIOL in the presence of pre-applied 10 μM DS2 (*Fig*. 6.5 A). As expected, DS2 significantly enhanced dLGN tonic currents (*Fig*. 6.5 A), giving rise to a BIC-sensitive tonic current that was significantly greater than that measured in control aCSF (1.0 ± 0.3 pA/pF; *Fig*. 6.5 B; P = 0.002). Intriguingly, DS2 also potentiated the 4-PIOL current (% control 4-PIOL response: 236.3 ± 28.9; *Fig*. 6.5 C; $P < 0.0001$), indicating that the 4-PIOL current in dLGN relay neurons might also be mediated by δ-containing receptors.

Since the modulatory actions of DS2 have only been characterised on GABA-mediated currents (Wafford *et al*., 2009; Jensen *et al*., 2013), and not currents evoked by other $GABA_A$ receptor agonists, we investigated the DS2 modulation of the 4-PIOL current using recombinant α1β3γ2L and α4β2δ receptors. These two receptor isoforms were chosen because they represent the major synaptic and extrasynaptic $GABA_A$ receptor subtypes thought to be expressed in dLGN relay neurons (Soltesz *et al*., 1990; Okada *et al*., 2000; Pirker *et al*., 2000; Cope *et al*., 2005; Bright *et al*., 2007; Hörtnagl *et al*., 2013; Nani *et al*., 2013).

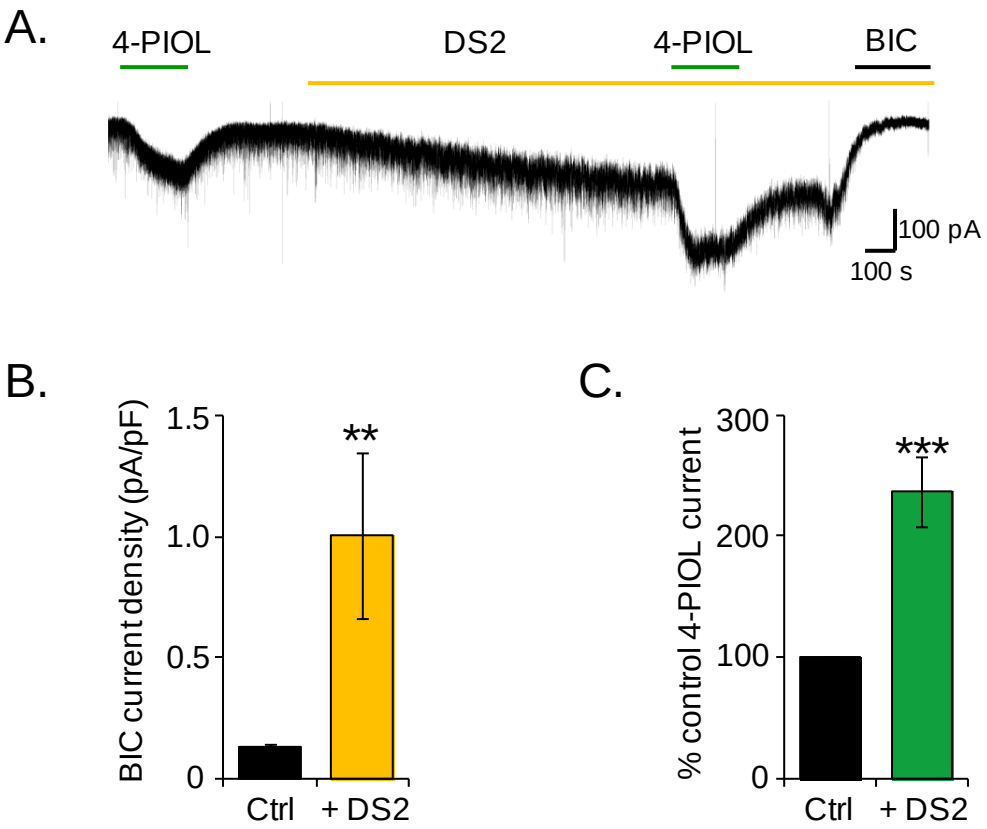

Figure 6.5 – DS2 modulation of dLGN tonic and 4-PIOL currents

A. Representative membrane current trace recorded from a dLGN relay neuron, in response to bath applied 4-PIOL (10 µM) in the absence, or presence, of DS2 (10 µM). Bicuculline (BIC; 20 µM) was applied at the end of each experiment. 4-PIOL, DS2 and BIC were respectively applied for the duration indicated by the green, yellow and black horizontal bars. **B.** Bar graph of BIC current density under control conditions (ctrl; black), or in the presence of DS2 (yellow). For each cell, the current change (pA) induced by BIC was normalised to the whole-cell capacitance (pF), and data represents the mean (± SEM) BIC current density (pA/pF) from 30 (control), or 5 (+ DS2) cells. **C.** Bar graph of the 4-PIOL response in DS2 (green), expressed as a percentage of the control 4-PIOL response (black) recorded from the same dLGN relay neuron (n = 5). An unpaired (**B**), or a paired t-test (**C**) was used to assess for statistical significance. **P < 0.01 and ***P < 0.001.

Whole-cell currents were recorded from HEK293 cells expressing recombinant α4β2δ (*Fig*. 6.6 A), or α1β3γ2L (*Fig*. 6.6 B) receptors, in response to brief applications of 10 μM 4-PIOL, in the absence, or presence, of pre-applied 10 μM DS2. Under control conditions, 10 μM 4-PIOL elicited no discernible agonist response at α4β2δ receptors (*Fig*. 6.6 A), but produced a small inward current at α1β3γ2L receptors (*Fig*. 6.6 B), in accord with our previous findings (see *Chapter* 4). Strikingly however, 4-PIOL co-application with DS2, unveiled an agonist current at α4β2δ receptors, which was 8.9 ± 3.8 % (*Fig*. 6.6 A; *P* = 0.047) of the response achieved by 1 mM GABA applied to the same cell. Unexpectedly, DS2 also potentiated the 4-PIOL current mediated at α1β3γ2L receptors (% control 4-PIOL current: 153.8 ± 24.7 %; *Fig*. 6.6 B; *P* = 0.017), albeit to a lesser extent than that observed for α4β2δ receptors. These findings make it difficult to interpret the DS2-mediated potentiation of the 4-PIOL current in dLGN relay neurons, since DS2 may be unveiling a δ-mediated component to the 4-PIOL current, which may not be present under control conditions.

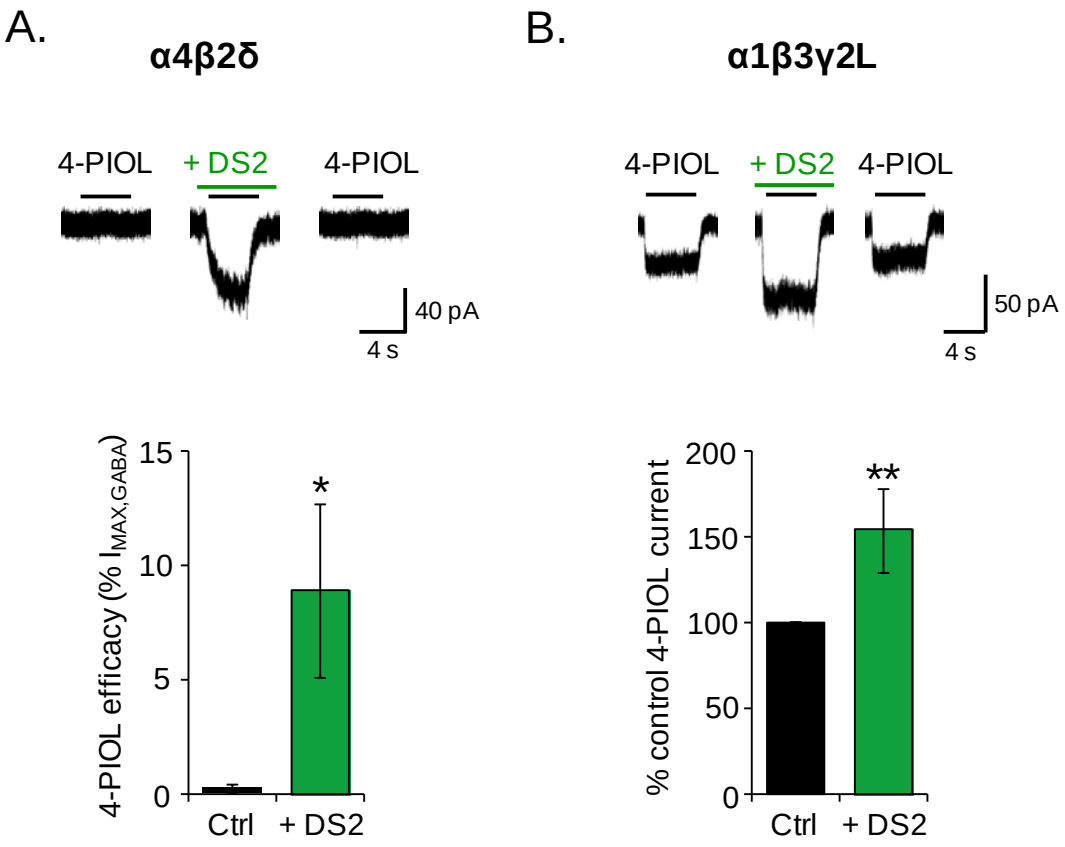

Figure 6.6 – DS2 modulation of recombinant α4β2δ and α1β3γ2L 4-PIOL responses

Example 10 μM 4-PIOL current traces (top panels) for recombinant α4β2δ (**A**) and α1β3γ2L (**B**) expressed in HEK293 cells, in the absence (black), or presence of DS2 (green; 10 μM). Bar graphs represent the mean (± SEM) normalised 4-PIOL response under control (ctrl; black) and DS2 (green) treated conditions. For α4β2δ-expressing cells, 4-PIOL current responses were normalised to the current response evoked by a saturating concentration of GABA (1 mM), which was applied to the same cell (n = 5). For α1β3γ2L receptors, the 4-PIOL response recorded in the presence of DS2 is expressed as a percentage of the control 4-PIOL response recorded from the same HEK293 cell (n = 6). Paired t-tests were used to assess statistical significance. *P < 0.05 and **P < 0.01.

6.2.4. THIP modulation of the 4-PIOL current

To further investigate whether the 4-PIOL current in dLGN relay neurons was mediated by δ–containing receptors, we assessed the ability of 4-PIOL to compete with a δ-selective concentration of the $GABA_A$ receptor agonist, THIP (1 μM: Brown *et al*., 2002; Stórustovu and Ebert, 2006; Mortensen *et al*., 2010). If THIP and 4-PIOL are competing for the same orthosteric binding site, we might expect that the pre-application of THIP would reduce the 4-PIOL current, or vice versa. To investigate this possibility, 1 μM THIP was pre-applied to recombinant α4β2δ receptors expressed in HEK293 cells, until a steady-state current was achieved, and subsequently 10 μM 4-PIOL was co-applied with THIP (*Fig*. 6.7 A). Strikingly, 4-PIOL co-application reduced the steady-state THIP current, by 56.8 ± 5.7 %, suggesting that 4-PIOL can potently compete with THIP for the orthosteric binding site. It is unlikely that 4-PIOL is producing this effect via an allosteric binding site, since the structure of 4-PIOL suggests that it would fit the orthosteric binding site. Moreover, 4-PIOL induced a parallel rightward shift in the GABA concentration-response curve for recombinant α4βδ receptors, indicating that they both compete for the same (orthosteric) binding site (see *Appendix* 1).

If 4-PIOL is acting on δ-containing receptors in dLGN relay neurons, we might also expect 4-PIOL (10 μM) to reduce the steady-state THIP (1 μM) current in dLGN relay neurons. To first confirm the presence of a δ-mediated THIP current, whole-cell currents were recorded from dLGN relay neurons, in response to 1 μM THIP (*Fig*. 6.7 B). As expected, THIP significantly enhanced the dLGN tonic current by 0.53 ± 0.06 pA/pF, confirming the functional expression of δ-containing receptors in dLGN relay neurons. Curiously, co-application of 4-PIOL with THIP generated an inward current with a mean current that was similar to the control 4-PIOL current (0.35 ± 0.06 pA/pF and 0.34 ± 0.03 pA/pF respectively; *Fig*. 6.7 C; *Table* 6.3; $P = 0.67$). These data indicate that THIP and 4-PIOL may not be competing for the same δ-containing receptor(s), in dLGN relay neurons.

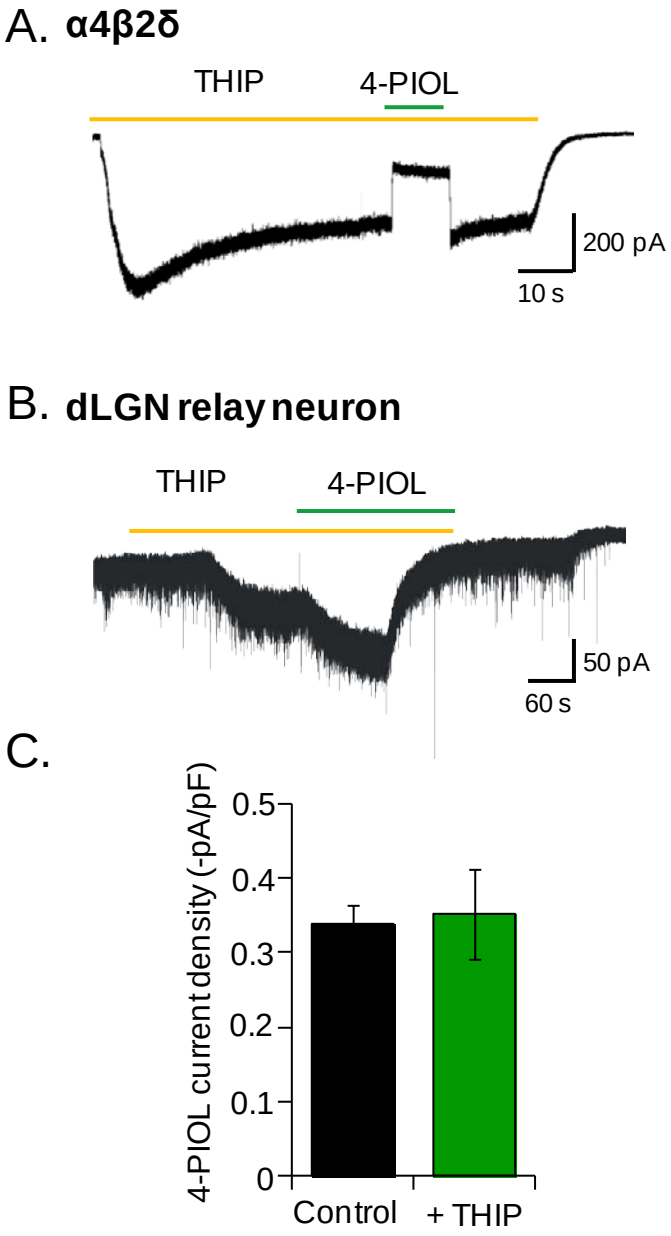

Figure 6.7 –THIP modulation of 4-PIOL currents

Representative membrane current trace recorded from an α4β2δ-expressing HEK293 cell (**A**) or a dLGN relay neuron (**B**) in response to THIP (1 µM) and 4-PIOL (10 µM). The yellow and green horizontal bars, respectively, indicate the duration of THIP and 4-PIOL application. **C.** Bar graph of 4-PIOL current recorded from dLGN relay neurons in the absence (black), or presence, of THIP. For each cell (n = 4), 4-PIOL-induced current changes were normalised to whole-cell capacitance (pF). Data represent mean ± SEM.

If THIP and 4-PIOL are acting on different $GABA_A$ receptors, no significant correlation would be expected between the THIP and 4-PIOL responses of different dLGN relay neurons. To explore this possibility, 10 μM 4-PIOL and 1 μM THIP were individually applied to each dLGN relay neuron (*Fig*. 6.8 A), and a scatter plot was generated to compare the THIP and 4-PIOL currents for each cell (*Fig*. 6.8 B). Indeed, linear regression analysis revealed that there was no significant correlation between these two currents (Pearson's correlation coefficient, R = -0.31; *P* = 0.28), indicating that 4-PIOL was activating a distinct receptor population from the δ-containing receptors activated by THIP.

Given that tonic currents in dLGN relay neurons are largely mediated by δ-containing receptors (Cope *et al*., 2005; Bright *et al*., 2007; Nani *et al*., 2013; Ye *et al*., 2013), we also investigated whether there was any correlation between the THIP and BIC currents for individual dLGN relay neurons. A new scatter plot comparing these currents revealed a positive correlation (*Fig*. 6.8 C; R = 0.61; *P* = 0.02), indicating that cells with a larger THIP induced current (and hence a higher expression of δ-containing receptors), also display a larger $GABA_A$ receptor mediated tonic current. These data indicate that a higher expression of δ-containing receptors may underlie the larger tonic currents, although other factors, such as the ambient GABA concentration, will also be important.

Since 4-PIOL and THIP are likely to be acting on different $GABA_A$ receptors in dLGN relay neurons, it was intriguing to explore whether receptors mediating the 4-PIOL current, also contribute to dLGN tonic currents. Therefore, another scatter plot was generated to compare the 4-PIOL and BIC currents recorded from individual dLGN relay neurons (*Fig*. 6.8 D). No significant correlation was observed between 4-PIOL and BIC currents (*Fig*. 6.8 D; R = 0.32; *P* = 0.17), indicating that the receptors that mediate the 4-PIOL current, are unlikely to contribute significantly to $GABA_A$ receptor mediated tonic currents in dLGN relay neurons, under our experimental conditions.

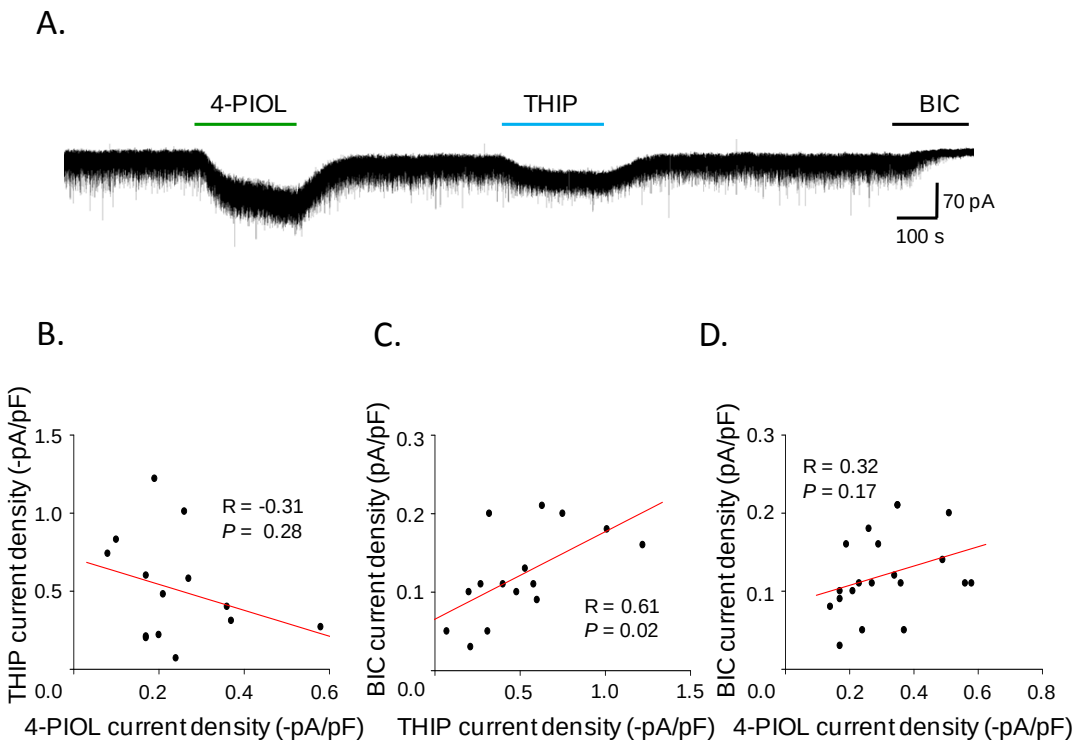

Figure 6.8 – Correlational analysis of dLGN THIP, BIC and 4-PIOL currents

A. Representative membrane current trace recorded from a dLGN relay neuron in response to individual applications of THIP (1 µM) and 4-PIOL (10 µM). The green and blue horizontal bars indicate the duration of 4-PIOL and THIP application respectively. Scatter plots of 4-PIOL current density versus the THIP current density (**B**), THIP current density versus BIC current density (**C**), and 4-PIOL current density versus BIC current density (**D**). Linear regression analysis was performed on these data (red lines), and R and *P* represent Pearson's correlation coefficient and *P*-values, respectively.

6.2.5. Diazepam modulation of the 4-PIOL current

Since 4-PIOL activated recombinant γ2-containing receptors, but not recombinant δ-containing receptors, the possibility that 4-PIOL was activating a population of γ2-containing receptors in dLGN relay neurons was explored.

The presence of γ2-containing receptors was probed using the benzodiazepine agonist, diazepam (Pritchett *et al*., 1989). For each dLGN relay neuron, a control response to 10 μM 4-PIOL was first recorded (and subsequently washed out), followed by a second response to 10 μM 4-PIOL in the presence of pre-applied 500 nM diazepam (*Fig*. 6.9 A). Unexpectedly, pre-application of 500 nM diazepam significantly increased the dLGN tonic current, giving rise to a BIC-sensitive tonic current (0.24 ± 0.04 pA/pF) that was significantly greater than that measured in control aCSF (0.13 ± 0.01 pA/pF; *Table* 6.2; *Fig*. 6.9 B; *P* = 0.003). These data will be discussed in more detail in *Section* 6.3.4. Diazepam also increased the amplitude of the IPSCs suggesting that GABA release at these inhibitory synapses was not saturating.

Co-application of 4-PIOL with diazepam revealed a significantly larger inward current than the control 4-PIOL current (% control 4-PIOL response: 160.3 ± 14.3 %; *Fig*. 6.9 C; P = 0.003), indicating that the 4-PIOL current is likely to be mediated by γ2-containing receptors in dLGN relay neurons. As a control, whole-cell currents were also recorded from dLGN relay neurons, exposed to two sequential applications of 4-PIOL (10 μM) in the absence of diazepam (*Fig*. 6.9 A). No potentiation of the second 4-PIOL response was observed in the absence of diazepam (% control 4-PIOL response: 99.1 ± 7.6; *P* = 0.97).

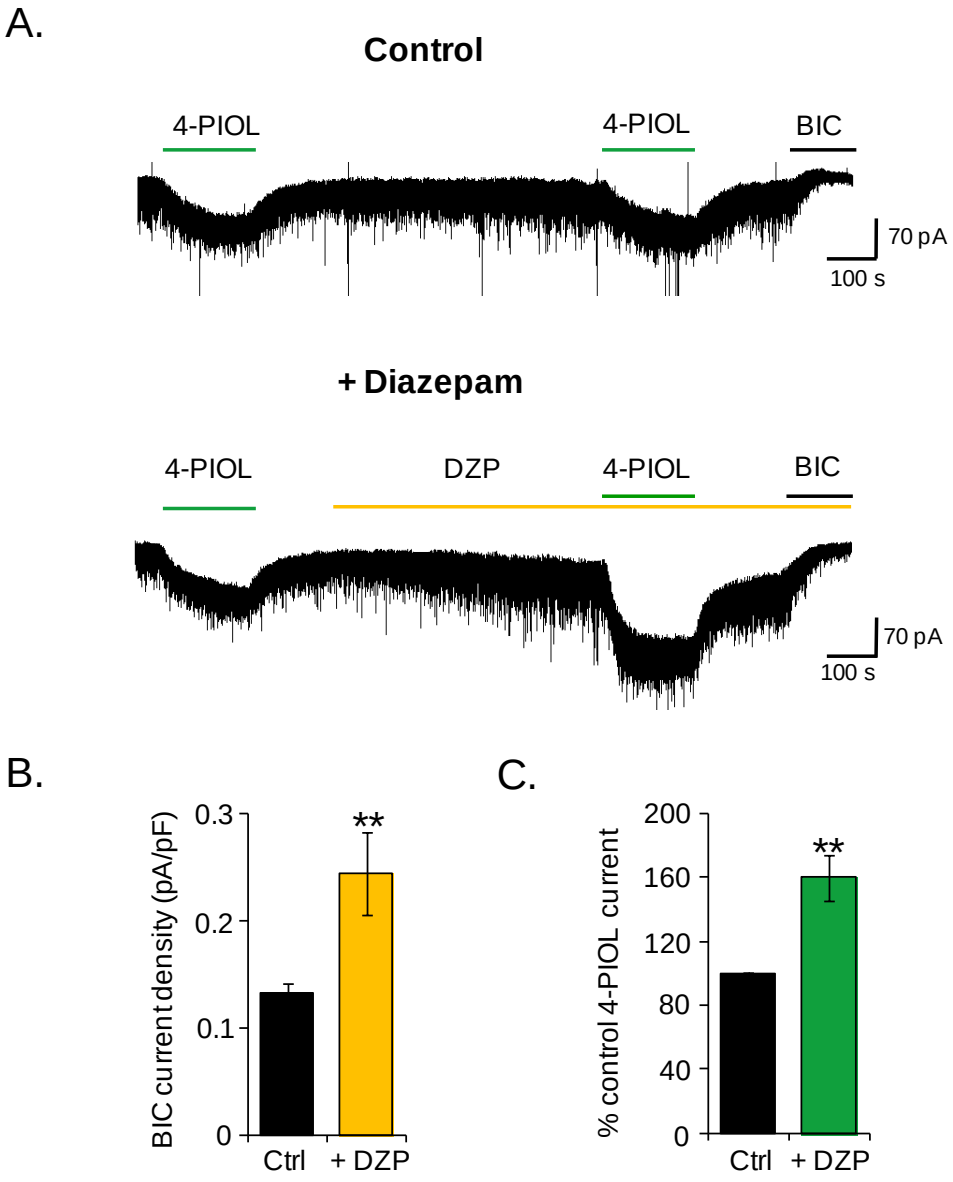

Figure 6.9 – Diazepam modulation of dLGN tonic and 4-PIOL currents

A. Representative membrane current trace recorded from a dLGN relay neuron in response to bath applied 4-PIOL (10 µM) in the absence, or presence, of diazepam (500 nM). Bicuculline (BIC; 20 µM) was applied at the end of each experiment. 4-PIOL, diazepam and BIC were respectively applied for the durations indicated by the green, yellow and black horizontal bars. **B.** Bar graph of BIC current density under control conditions (ctrl; black), or in the presence of diazepam (yellow). For each cell, the current change (pA) induced by BIC was normalised to whole-cell capacitance (pF), and data represents the mean (± SEM) BIC current density (pA/pF) from 30 (control), or 5 (+ DZP), cells. **C.** Bar graph of the 4-PIOL response in diazepam (green), expressed as a percentage of the control 4-PIOL response (black) recorded from the same dLGN relay neuron. An unpaired (**B**), or a paired t-test (**C**) was used to assess for statistical significance. **P < 0.01.

Although diazepam is established to only potentiate the agonist responses of γ2-containing $GABA_A$ receptors (Pritchett *et al*., 1989), this was verified using a recombinant HEK293 expression system. Whole-cell currents were recorded from α4β2δ- (*Fig*. 6.10 A) or α1β3γ2L- (*Fig*. 6.10 B) expressing cells in response to brief applications of 4-PIOL (10 μM), either in the absence, or presence, of pre-applied diazepam (500 nM). As expected, 4-PIOL (10 μM) elicited no discernible agonist response at α4β2δ receptors, either in the absence, or presence, of diazepam (*Fig*. 6.10 A). A saturating concentration of GABA (1 mM) was also applied to each α4β2δ-expressing cell, to confirm the functional expression of α4β2δ receptors (*Fig*. 6.10 A). By contrast, at α1β3γ2L receptors (*Fig*. 6.10 B), diazepam significantly potentiated the 4-PIOL response (% control response: 246.6 ± 50.1; *Fig*. 6.10 C).

Thus, although δ-containing receptors are expressed in dLGN relay neurons, the 4-PIOL current appears to be largely mediated by γ2-containing receptors, with little, or no, contribution from δ-containing receptors.

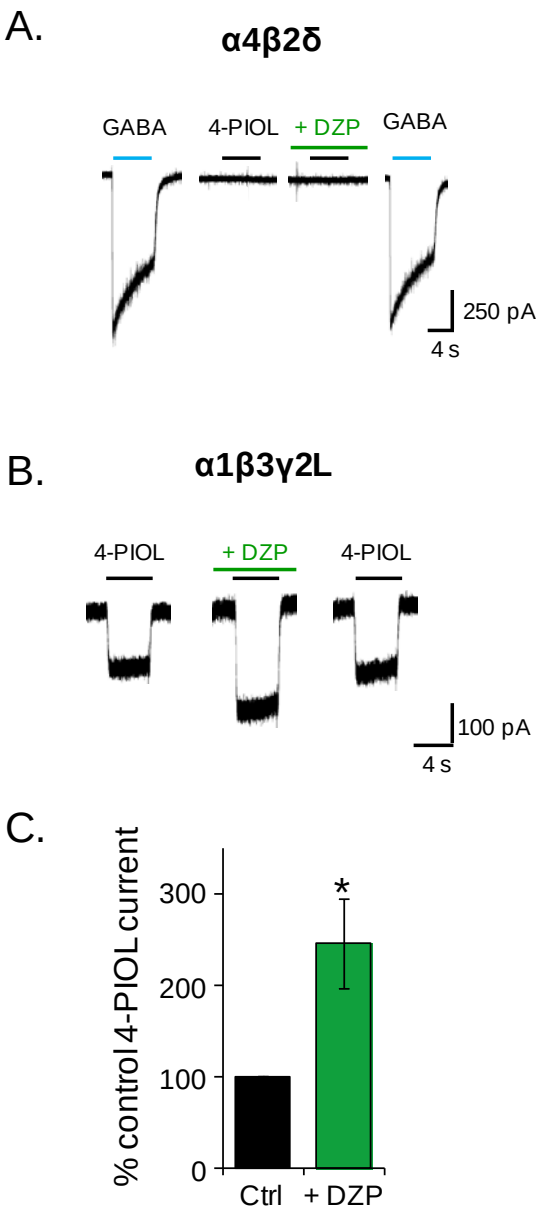

Figure 6.10 – Diazepam modulation of 4-PIOL currents at recombinant α4β2δ and α1β3γ2L receptors

A. Example whole-cell membrane current traces for recombinant α4β2δ receptors expressed in HEK293 cells, in response to GABA (1000 μM), or 4-PIOL (10 μM), in the absence, or presence, of diazepam (DZP; 500 nM). The durations of GABA, 4-PIOL and diazepam applications are respectively indicated by the blue, black and green horizontal bars. **B.** Example whole-cell membrane current traces for recombinant α1β3γ2L in the response to 4-PIOL (10 μM) in the absence, or presence, of diazepam (500 nM). **C.** Bar graph of the 4-PIOL response in diazepam (green), expressed as a percentage of the control 4-PIOL response (black) recorded from the same α1β3γ2L-expressing HEK293 cell. Data represent mean ± SEM (n = 5; *P < 0.05).

6.2.6. 4-PIOL modulation of dLGN tonic currents is dependent on ambient GABA concentrations

For recombinant α1β3γ2L receptors, 10 μM 4-PIOL enhanced the steady-state GABA current when the GABA concentration was low (~ 0.1 μM GABA), but produced a small inhibition of steady-state GABA current when the ambient GABA level was raised to 1 μM GABA (*Fig*. 4.11 – *Fig*. 4.13). In dLGN relay neurons, the robust 4-PIOL enhancement of baseline tonic currents (mainly via γ2-containing receptors) indicates that ambient GABA levels in the slice may be low. To determine whether 4-PIOL could switch from acting as an agonist (at low ambient GABA levels), to acting as an antagonist (at higher ambient GABA levels) in dLGN relay neurons, GABA levels were raised in slices, by inhibiting GABA uptake. Since GABA uptake in the thalamus is largely mediated by the GABA transporters, GAT1 and GAT3 (De Biasi *et al*., 1998), slices were pre-incubated (for at least 30 min) in aCSF supplemented with the GAT1 inhibitor, NNC-711 (10 μM; Borden *et al*., 1994) and the GAT2/3 inhibitor, SNAP-5114 (20 μM; Borden, 1996). These were both present throughout all subsequent electrophysiological recordings. Following a period of control recording (in the presence of the GAT inhibitors), 10 μM 4-PIOL was applied to dLGN relay neurons in treated slices, and subsequently washed out. BIC was applied to GAT-inhibited slices at the end of each experiment to measure the tonic current (*Fig*. 6.11 A). Notably, the BIC current was significantly larger in GAT blockers than in control aCSF (0.7 ± 0.1 pA/pF and 0.13 ± 0.01 pA/pF respectively; *Fig*. 6.11 B; $P < 0.0001$), consistent with elevated ambient GABA levels in treated slices persistently activating extrasynaptic $GABA_A$ receptors. Curiously, cells from treated slices showed a lack of sIPSCs (*Fig*. 6.11 A). Although the mechanistic reason(s) for the lack of IPSCs remains unclear, the elevated GABA levels may have desensitised postsynaptic $GABA_A$ receptors, or reduced presynaptic release of GABA, via an activation of presynaptic $GABA_A$ and/or $GABA_B$ receptors.

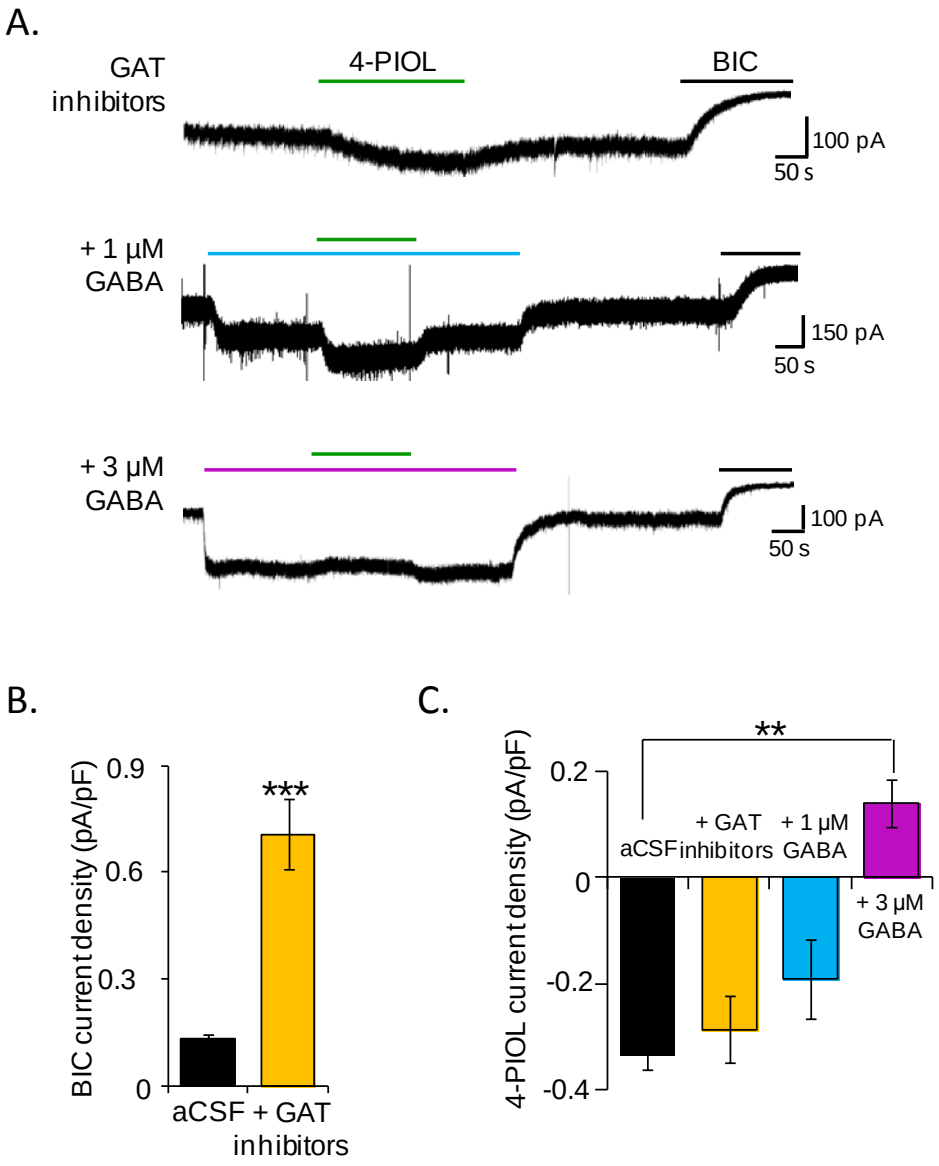

Figure 6.11 – Increasing ambient GABA unveils the antagonist profile of 4-PIOL

A. Representative whole-cell membrane current traces recorded from a dLGN relay neurons, in response to bath applied 4-PIOL (10 µM) in the presence of GAT inhibitors (10 µM NNC-711 and 20 µM SNAP-5114). Slices were incubated in aCSF supplemented with GAT inhibitors for at least 30 min prior to electrophysiological recordings. All recordings were performed at room temperature. **B.** Bar graph of BIC current in control aCSF (black; n = 30), or in the presence of GAT inhibitors (yellow; n = 25). For each cell, the current change (pA) induced by BIC was normalised to its whole-cell capacitance (pF), and data represents the mean ± SEM. **C.** Bar graph of the mean 4-PIOL current density measured in aCSF (black; n = 42), GAT inhibitors (yellow; n = 8), or GAT inhibitors supplemented with 1 µM (blue; n = 11), or 3 µM, GABA (magenta; n = 4). **P < 0.01 and ***P < 0.001.

Co-application of 4-PIOL with GAT inhibitors enhanced the tonic current by 0.29 ± 0.06 pA/pF (*Fig*. 6.11 A; *Fig*. 6.11 C). This 4-PIOL-induced current was similar to that observed in control aCSF (0.34 ± 0.03 pA/pF; *Fig*. 6.11 C; P = 0.47). This indicated that ambient GABA levels in the slice may still be too low to alter the response profile for 4-PIOL. To further increase ambient GABA levels, 1 μM and 3 μM GABA were individually applied to GAT-inhibited slices, followed by co-application with 10 μM 4-PIOL (*Fig*. 6.11 A). Both 1 μM and 3 μM GABA enhanced the baseline tonic current (*Fig*. 6.11 A) by 0.8 ± 0.1 and 1.6 ± 0.2 pA/pF respectively. Co-application of 10 μM 4-PIOL with 1 μM GABA also elicited an inward current (*Fig*. 6.11 A), although the resultant 4-PIOL current was significantly smaller than that observed in control aCSF (0.19 ± 0.07 pA/pF; *Fig*. 6.11 C). By contrast, co-application of 10 μM 4-PIOL with 3 μM GABA produced an outward current (*Fig*. 6.11 A), with a mean current density of 8.4 ± 4.1 pA/pF.

Thus, as observed for recombinant α1β3γ2L receptors, 4-PIOL exhibited a dominant agonist profile at low GABA concentrations (< 1 μM), but produced a small inhibition of dLGN tonic currents when the ambient GABA concentration is increased.

Table 6.2 – Modulation of BIC-sensitive tonic currents in dLGN relay neurons

Pre-applied drug	BIC current density (pA/pF)	Δ RMS noise (pA)
Control aCSF	0.13 ± 0.01 (30)	-9.6 ± 1.5 (41)
DS2 (10 µM)	1.0 ± 0.3 (5)	-23.4 ± 4.4 (5)
Diazepam (0.5 µM)	0.24 ± 0.04 (9)	-4.6 ± 0.5 (9)
GAT inhibitors	0.7 ± 0.1 (25)	-39.0 ± 7.5 (25)

Values represent the change in tonic current density (pA/pF), or RMS baseline noise (pA) induced by BIC, relative to a control recording epoch in the presence of a pre-applied drug. Where GAT inhibitors were used, slices were incubated in 20 µM SNAP-5114 + 10 µM NNC-711 for at least 30 min before patching onto a cell. Values are reported as mean ± SEM, and the number of cells for each condition, are indicated in parentheses.

Table 6.3 – 4-PIOL regulation of dLGN tonic currents

Pre-applied drug	4-PIOL current density (pA/pF)	Δ RMS noise induced by 4-PIOL (pA)
Control aCSF	-0.34 ± 0.03 (42)	13.2 ± 1.6 (42)
+ Bicuculline (20 µM)	-0.01 ± 0.002 (4)	-0.8 ± 1.8 (4)
+ THIP (1 µM)	-0.35 ± 0.06 (4)	9.2 ± 1.3 (4)
+ Diazepam (0.5 µM)	-0.51 ± 0.06 (5)	10.6 ± 2.7 (5)
+ DS2 (10 µM)	-0.90 ± 0.18 (5)	21.6 ± 8.8 (5)
+ GAT inhibitors	-0.29 ± 0.06 (8)	4.8 ± 2.3 (8)
+ GABA (1 µM)	-0.19 ± 0.07 (11)	1.6 ± 1.6 (11)
+ GABA (3 µM)	0.14 ± 0.04 (4)	-8.4 ± 4.1 (4)

Values represent the mean (± SEM) change in tonic current density (pA/pF) or RMS baseline noise (pA) induced by 4-PIOL (10 µM), relative to a control recording epoch in the presence of a pre-applied drug. For changes in holding current, negative values represent an inward current (i.e. enhancement of tonic current) and positive values indicate an outward current (reduction in tonic current). For changes in RMS baseline noise, positive values represent enhanced tonic currents and negative values signify a decrease.

6.3. Discussion

In this chapter, the effects of 10 μM 4-PIOL were investigated on the tonic and phasic currents from dLGN relay neurons, to probe whether 4-PIOL could selectively inhibit tonic currents in the thalamus. Unexpectedly, 4-PIOL enhanced dLGN tonic currents (see *Section* 6.3.3), yet reduced both the frequency and amplitude of sIPSCs (see *Section* 6.3.1). Both effects were unexpected since our recombinant expression studies (see *Chapter* 4) indicated that 4-PIOL (10 μM) should clearly inhibit α4β2δ-mediated tonic currents, without significantly affecting α1β3γ2-mediated phasic currents.

6.3.1. 4-PIOL inhibits phasic currents in dLGN relay neurons

The reduced sIPSC amplitude was surprising, since 4-PIOL (10 μM) did not inhibit 'synaptic-type' responses of recombinant α1β3γ2L receptors (*Fig*. 4.3). This reduction in sIPSC amplitude might arise from 4-PIOL directly inhibiting synaptic receptor isoforms other than α1β3γ2L receptors. For instance, in the dLGN, the α2 subunit has been suggested to contribute to sIPSCs early in postnatal development (Okada *et al*., 2000; Peden *et al*., 2008). Since our experiments were conducted on the thalamic slices from young (postnatal day 14) rats, α2-containing receptors may also have been present in our preparation, and 4-PIOL might differentially modulate this receptor isoform. It might therefore be interesting to assess the actions of 4-PIOL on recombinant α2-containing receptors.

The effect on IPSC frequency by 4-PIOL indicates that 4-PIOL may act on presynaptic $GABA_A$ receptors to reduce GABA release (potential mechanisms are discussed in *Section* 5.3.2). However, this reduction in IPSC frequency might also reflect a reduced ability to detect lower amplitude IPSCs in 4-PIOL, since this compound increased the RMS baseline noise of dLGN relay neurons

(by ~ 13 pA). Thus it is difficult to distinguish between a presynaptic effect and a postsynaptic effect from these data.

6.3.2. DS2 (10 μM) modulates both α4β2δ and α1β3γ2L receptors

In dLGN relay neurons, the 4-PIOL current was potentiated by the δ-selective, positive allosteric modulator, DS2 (Wafford *et al*., 2009; Jensen *et al*., 2013). However, DS2 also unveiled a previously undetected 4-PIOL current at recombinant α4β2δ receptors, and unexpectedly, also potentiated the 4-PIOL current at recombinant α1β3γ2L receptors. Therefore, although α4β2δ receptors might contribute to the 4-PIOL response in dLGN relay neurons, DS2 might also be unveiling a δ-mediated component to the 4-PIOL current, which may not have been present under control conditions, or it may also be potentiating the 4-PIOL current at γ2-containing receptors (discussed further in *Section* 6.3.3). The DS2 modulation of α1β3γ2L receptors was particularly surprising, given its reported δ-selective profile (Wafford *et al*., 2009; Jensen *et al*., 2013). However, it is interesting to note that DS2 did produce a small modulation of α1β3γ2L-GABA currents in a previous study, and a small residual DS2 current was still apparent in thalamic relay neurons from δ knockout mice (Jensen *et al*., 2013). Thus DS2 can also modulate γ2-containing receptors, albeit to a lesser extent than δ-containing receptors.

6.3.3. 4-PIOL enhances dLGN tonic currents via γ2-containing receptors

In dLGN relay neurons, 4-PIOL appeared not to compete for the same orthosteric binding sites as 1 μM THIP, which selectively activates δ-containing receptors (Brown *et al*., 2002; Stórustovu and Ebert, 2006; Mortensen *et al*., 2010). Moreover, no correlation was observed between the THIP and 4-PIOL induced currents of different dLGN relay neurons, indicating that 4-PIOL was unlikely to be acting on the same δ-containing receptors as THIP. Indeed, the 4-

PIOL current in dLGN relay neurons was potentiated by the benzodiazepine agonist, diazepam, suggesting that the 4-PIOL current was unlikely to be mediated by δ-containing receptors, but instead, was predominantly mediated by synaptic and/or extrasynaptic γ2-containing receptors. Since α1 and α4 subunits are the most prevalent α isoforms expressed in the dLGN (Soltesz *et al*., 1990; Wisden *et al*., 1992; Pirker *et al*., 2000; Hörtnagl *et al*., 2013) and α4βγ2 should be insensitive to modulation by diazepam (Pritchett *et al*., 1989), it is more likely that 4-PIOL was acting at α1βγ2 receptors. However, other αβγ2 receptor isoforms may conceivably contribute, and the use of more subtype selective benzodiazepines would be required to probe their presence in dLGN relay neurons.

Given that δ-containing receptors are proposed to be the main mediators of tonic currents in dLGN relay neurons, the significant presence of γ2-containing receptors was unexpected. However, a previous study indicated that only ~ 13 % of $GABA_A$ receptors expressed in the thalamus contain δ subunits, whereas ~ 50 % of thalamic $GABA_A$ receptors contain the γ2 subunit (Sur *et al*., 1999). However, it is important to note that these data represent the pooled data from several thalamic nuclei, and include both cell surface, and intracellular receptor populations. Indeed, *in situ* hybridisation and immunocytochemical studies have only detected very low levels of γ2 subunit expression in the dLGN of adult rodents (Wisden *et al*., 1992; Pirker *et al*., 2000; Hörtnagl *et al*., 2013). However, expression of the γ2 subunit appears to be developmentally regulated, since γ2 mRNA levels decline during development (Laurie *et al*., 1992b). Thus, the significant population of γ2-containing receptors detected in our study, might arise from our use of relatively young (P14) rats.

6.3.4. Ambient GABA levels in thalamic slices are low (< 1 μM GABA)

According to our recombinant expression studies, the dominant agonist profile of 4-PIOL at γ2-containing receptors prevails at low ambient GABA concentrations, an indicator that ambient GABA levels in the slice were also low. In accord with this, dLGN tonic currents were significantly enhanced by 1 μM GABA when GABA uptake was blocked. Thus, under our experimental conditions, the ambient GABA concentration in the slice is predicted to be significantly lower than 1 μM GABA. Microdialysis studies indicate that ambient GABA concentrations *in vivo* range from 30 nM to 2.9 μM (Glaeser and Hare, 1975; Lerma *et al*., 1986; de Groote and Linthorst, 2007; Wlodarczyk *et al*., 2013), while the use of 'sniffer patches' has indicated that ambient GABA levels in hippocampal slices is ~ 100 nM (Wlodarczyk *et al*., 2013). Moreover, GABA levels are efficiently critically regulated by GABA transporters, which reach a steady-state when extracellular GABA levels are 0.1 – 0.4 μM (Attwell *et al*., 1993; Richerson and Wu, 2003; Wu *et al*., 2007).

Given the significant presence of γ2-containing receptors on dLGN relay neurons in our study, it was intriguing to explore the possibility that these receptors may also contribute to dLGN tonic currents. Although diazepam significantly enhanced dLGN tonic currents, it is difficult to rule out the possibility that diazepam also increased the affinity of γ2-containing receptors for GABA, thus recruiting a population of extrasynaptic $GABA_A$ receptors that may not have been active under control conditions. Moreover, since diazepam also prolonged sIPSC decay times (e.g. Nusser *et al*., 1997; Perrais and Ropert, 1999; Mozrzymas *et al*., 2007), the diazepam-induced enhancement of tonic currents may also arise from a summation of sIPSCs, which could not be accurately defined due to the relatively high frequency of sIPSCs observed in this study. It might therefore be interesting to evaluate the effects of diazepam on thalamic relay neurons treated with TTX, since this may significantly reduce the baseline frequency of IPSCs.

Indeed, a lack of correlation between the 4-PIOL and the BIC induced change in tonic currents under control conditions, indicates that the γ2-containing receptors that mediate the 4-PIOL response are unlikely to significantly contribute to the dLGN tonic currents. Given the low ambient GABA levels detected in our slice preparations, and the low GABA sensitivity of γ2-containing receptors (Brown *et al*., 2002; Mortensen *et al*., 2010, 2011), this finding is somewhat unsurprising. However, this does not discount the possibility that γ2-containing receptors may contribute to dLGN tonic currents when GABA levels are significantly increased, for instance, during pathophysiological disease states (see General Discussion).

6.3.5. 4-PIOL (10 μM) can bidirectionally modulate dLGN tonic currents

The dominant agonist profile of 4-PIOL at low ambient GABA concentrations (< 1 μM), and its weak antagonist profile at higher ambient GABA concentrations (~ 3 μM), is similar to the profile observed for recombinant γ2-containing receptors (see *Fig*. 4.11 – *Fig*. 4.13). However, there appears to be a slight discrepancy regarding the GABA concentration at which 4-PIOL switches its profile. In thalamic relay neurons, a higher concentration of GABA (3 μM) had to be pre-applied to thalamic relay neurons to unveil an antagonist profile for 4-PIOL, whereas for recombinant α1β3γ2L receptors (*Fig*. 4.11 – *Fig*. 4.13), 1 μM GABA was sufficient to unveil this profile. One explanation for this slight discrepancy, might be that the concentration of GABA pre-applied to slices may not reflect the precise GABA concentration experienced by cells in slices, possibly due to limitations in drug penetrability, or an incomplete block of GABA uptake systems in the slice.

Overall, our findings indicate that although δ-containing receptors are functionally expressed in dLGN relay neurons, the effects of 4-PIOL on dLGN tonic currents are dominated by the significant presence of γ2-containing receptors. Moreover, 4-PIOL also significantly reduces dLGN phasic currents.

6.4. Conclusion

In dLGN relay neurons:

1. 4-PIOL (10 μM) enhances $GABA_A$ receptor mediated tonic currents, mainly by activating γ2-containing receptors.

2. 4-PIOL (10 μM) reduces the frequency and amplitude of sIPSCs in dLGN relay neurons.

3. At low ambient GABA concentrations (< 1 μM), 10 μM 4-PIOL exhibits a dominant agonist profile, but switches to an inhibitor of dLGN tonic currents when the ambient GABA concentration is increased (to ~ 3 μM).

Chapter 7: General Discussion

For some time, enhanced tonic currents, arising from elevated ambient GABA levels in the brain, have been implicated in the pathology of several neurological disorders, including absence seizures, cognitive impairments in DS and AD, and motor deficits following stroke (see *Section* 1.3). Moreover, emerging evidence has indicated that antagonists and/or inverse agonists that selectively inhibit extrasynaptic α5- and/or δ-containing $GABA_A$ receptors may prove therapeutically useful as treatments for such conditions. This formed the focus of this thesis, which was to explore how to reduce the level of tonic inhibition without affecting synaptic inhibition. From a theoretical perspective, we decided not to use an overt GABA antagonist, but to explore the subtle antagonist properties of GABA partial agonists. In particular, we studied whether 4-PIOL, a weak partial agonist with a reported functional antagonist profile, might be effective, and therefore useful as a selective inhibitor of $GABA_A$ receptor mediated tonic currents.

7.1. Summary of key findings

7.1.1. Stoichiometry of recombinant α4β3δ receptors

Tonic GABA current relies heavily on extrasynaptic $GABA_A$ receptors and often this requires the presence of the δ subunit. Since the subunit stoichiometry of δ-containing receptors has remained elusive, and may affect the pharmacological profile of 4-PIOL on $GABA_A$ receptors, we first examined the subunit stoichiometry of recombinant α4β3δ receptors using a functional electrophysiological approach (Patel *et al*., 2014). Recombinant α4β3δ receptors displayed a preferred subunit stoichiometry of 2α: 2β: 1δ, which was not altered by varying the cDNA transfection ratio by 10 - fold. These findings agree with the previously reported subunit stoichiometry of recombinant α4β3δ

receptors, although other groups have reported more variable subunit stoichiometries for unconstrained and constrained αβδ receptors (Barrera *et al*., 2008; Baur *et al*., 2009; Kaur *et al*., 2009; Wagoner and Czajkowski, 2010). However, as discussed in *Chapter* 4 (*Section* 4.4), some of the variability might be explained by differences in expression systems, and/or the use of different α or β isoforms (Baur *et al*., 2009; Kaur *et al*., 2009; Wagoner and Czajkowski, 2010). Given this variability, it will be important to establish the precise subunit arrangement(s) of native δ-containing receptors $GABA_A$, especially since this will critically define the functional and pharmacological properties of native extrasynaptic $GABA_A$ receptors.

7.1.2. Effects of 4-PIOL on recombinant $GABA_A$ receptors

Promisingly, a low concentration of 4-PIOL (10 μM) inhibited the 'extrasynaptic-type' GABA responses of recombinant α4β2δ receptors, without significantly inhibiting the 'synaptic-type' GABA responses of recombinant α1β3γ2 receptors, as predicted by our theory. By contrast, 4-PIOL (10 μM) did not affect the 'extrasynaptic-type' responses of recombinant α6β2δ receptors, but could enhance or inhibit the 'extrasynaptic-type' responses of recombinant α1β3γ2 and α5β3γ2 receptors, depending on the ambient GABA concentration (Sieghart and Sperk, 2002; Farrant and Nusser, 2005; Kasugai *et al*., 2010). Therefore, this data predicted that 4-PIOL (10 μM) should not alter α1β3γ2-mediated phasic currents in neurons, but might significantly inhibit α4β2δ-mediated tonic currents. Moreover, 4-PIOL was predicted not to alter α6β2δ tonic currents, but might be capable of either enhancing the activity of extrasynaptic α1β3γ2 or α5β3γ2 receptors, depending on the ambient GABA concentration.

7.1.3. 4-PIOL regulation of tonic and phasic currents varies between brain areas

Given that tonic and phasic currents in CGCs are largely thought to be mediated by α6βδ and α1βγ2 receptors respectively (Sieghart and Sperk, 2002; Farrant and Nusser, 2005), it was perhaps unsurprising that 4-PIOL (10 μM) exerted no effect on either tonic or phasic currents in this cell type.

In hippocampal neurons, 4-PIOL (10 μM) bidirectionally modulated tonic currents, depending on the ambient GABA concentration, which might also be predicted from the recombinant expression studies, since they are largely thought to express α5βγ2-mediated tonic currents, but have also been demonstrated to express an extrasynaptic population of α(1-3)βγ2 receptors (Kasugai *et al*., 2010). Unexpectedly however, 4-PIOL also reduced the frequency and amplitude of phasic currents in cultured hippocampal neurons (discussed below). Also unexpectedly, 4-PIOL (10 μM) enhanced α4β2δ-mediated tonic currents in dLGN neurons, and simultaneously reduced the frequency and amplitude of sIPSCs. By using subtype-selective pharmacological tools, it was demonstrated that this 4-PIOL-mediated enhancement of tonic currents was likely to be mediated by γ2-containing receptors (discussed further in *Section* 7.2.1), and could be bidirectionally modulated by altering the ambient GABA concentration.

The mechanism(s) that underlie the 4-PIOL mediated reduction in sIPSC frequency and amplitude in hippocampal and TC relay neurons (but not CGCs) is unknown. Possible explanations to account for reduction in frequency include a presynaptic effect on GABA release, possibly by membrane depolarisation or hyperpolarisation, or a shunting of action potentials. However, the effect on frequency may be complicated by the 4-PIOL-induced increase in RMS baseline noise, which might mask small amplitude events. However, it is possible that 4-PIOL might be directly inhibiting synaptic receptor isoforms which were not studied in our recombinant expression studies. For instance, α2βγ2 receptors have also been shown to contribute to phasic currents in hippocampal, and young dLGN relay neurons (Okada *et al*., 2000; Prenosil *et al*., 2006; Peden *et al*., 2008), and so it would be interesting to assess the

effects of 4-PIOL on this receptor isoform using a heterologous expression system.

7.2. The therapeutic potential of 4-PIOL

7.2.1. Functional importance of extrasynaptic γ2-containing $GABA_A$ receptors?

Receptors containing the γ2 subunit are typically thought to accumulate at synaptic sites. However, immunohistochemical and functional studies indicate that a significant number of α1 – α3 subunit, which typically associate with γ2 subunits, may also exist at extrasynaptic sites in several cell types, including the three studied here (Soltesz *et al*., 1990; Nusser *et al*., 1998; Mangan *et al*., 2005; Thomas *et al*., 2005; Kasugai *et al*., 2010). Our study indicates that the functional effects of 4-PIOL on tonic currents, at least in dLGN relay neurons and hippocampal neurons, are largely dominated by its actions on γ2-containing receptors, although we cannot exclude a contribution by δ-containing receptors.

In dLGN relay neurons, the presence of a THIP-sensitive tonic current confirmed the functional expression of δ-containing receptors. However, the functional profile of 4-PIOL most closely resembled its actions at recombinant γ2-containing receptors, indicating that although δ-$GABA_A$ receptors were expressed, the number of γ2-containing receptors may significantly outnumber δ-containing receptors on the cell surface of dLGN relay neurons. Although our data indicate that this population of γ2-containing receptors are unlikely to significantly contribute to basal tonic currents, under our experimental conditions, it is intriguing to speculate that they may contribute to tonic currents *in vivo*, depending on the ambient GABA concentration, especially if it is raised. Moreover, it would be interesting to determine the relative expression levels of extrasynaptic δ and γ2-containing receptors, since this will critically determine the functional effects of compounds such as 4-PIOL, which can modulate both receptor isoforms. These expression levels may vary between different cell

types, which might explain why 4-PIOL enhanced tonic currents in hippocampal and dLGN relay neurons, but not CGCs. Although all three neuronal populations are likely to express extrasynaptic αβγ receptors (Soltesz *et al*., 1990; Nusser *et al*., 1998; Thomas *et al*., 2005; Kasugai *et al*., 2010), CGCs might express fewer γ2-containing receptors, relative to δ-containing receptors, possibly explaining why the effects of 4-PIOL on CGC tonic currents most similarly resembled its actions at recombinant α6βδ receptors.

7.2.2. Ambient GABA levels are low in neuronal preparations

In all three neuronal preparations, the ambient GABA concentration was significantly lower than 1 μM, since exogenous applications of 1 μM GABA significantly enhanced tonic currents. However, it is important to note our experimental conditions differ from the *in vivo* situation, which may significantly affect ambient GABA levels. For instance, our recordings were performed at room temperature. Physiological temperatures have not only been shown to increase the GABA sensitivity of $GABA_A$ receptors (Jenkins *et al*., 1999; Perrais and Ropert, 1999; Millingen *et al*., 2011), but may also affect ambient GABA levels, by increasing the frequency of sIPSCs and by increasing the efficiency of GABA reuptake (Otis and Mody, 1992; Perrais and Ropert, 1999; Mitchell and Silver, 2003). Moreover, during recordings, our culture/slice preparations were continuously perfused with aCSF, which might lead to a reduction in ambient GABA by wash-out effects.

The previous consensus is that δ-containing receptors desensitize more slowly than their γ2-containing counterparts (Farrant and Nusser, 2005), although more recent evidence indicates that they may in fact show quite appreciable desensitisation, even to low concentrations of GABA (Feng *et al*., 2009; Mortensen *et al*., 2010; Bright *et al*., 2011; Houston *et al*., 2012; McGee *et al*., 2013). Consistent with the latter findings, both δ- and γ2-containing receptors displayed significant levels of desensitisation in our recombinant expression studies. Since both receptor isoforms may exist at extrasynaptic sites, it is

interesting to note that at the low ambient GABA levels thought to mediate tonic currents (0.1 – 1 μM), recombinant α4/6βδ receptors in fact showed higher levels of desensitisation than α1βγ2 receptors (see *Fig*. 4.11). Thus, while this strong desensitisation profile might limit further activation of high affinity δ-containing receptors, for instance during synaptic spillover (Bright *et al*., 2011; Ye *et al*., 2013), less desensitised extrasynaptic/perisynaptic γ2-containing receptors may instead be able to respond.

The functional profile of 4-PIOL (at both δ- and γ2-containing receptors) was strongly influenced by the ambient GABA concentration, which is perhaps unsurprising, given that both 4-PIOL and GABA act via the same orthosteric binding site. This was predicted by our theoretical model. The ability of 4-PIOL to modulate steady-state GABA currents was considerably diminished by raising ambient GABA levels (see *Fig*. 4.12), a finding that likely reflects a reduced ability of 4-PIOL to compete with GABA for this binding site. Similar observations have been made for the orthosteric agonist, THIP, whose enhancement of δ-mediated tonic currents in CGCs was attenuated at higher ambient GABA concentrations (Houston *et al*., 2012). Thus, when evaluating the potential effects of compounds on tonic currents, an important consideration to make is how they modulate tonic currents at different ambient GABA concentrations.

7.2.3. Therapeutic potential of 4-PIOL

This project was aimed at selectively reducing tonic currents in conditions associated with elevated ambient GABA levels (e.g. absence seizures, cognitive impairments and functional recovery from stroke; Brickley and Mody, 2012; Egawa and Fukuda, 2013; Rudolph and Möhler, 2014; see *Section* 1.3). Our findings indicate that the ability of 4-PIOL to enhance, or reduce, tonic currents (at least in hippocampal and TC relay neurons), will critically depend on a number of factors, including which $GABA_A$ receptor isoforms are expressed, their relative expression levels on the neuronal cell surface, and the

ambient GABA level. For instance, 4-PIOL might produce a minimal (or no) inhibition of tonic currents at GABA concentration > 1 μM, but may actually enhance tonic currents if ambient GABA levels are < 1 μM. Thus 4-PIOL might exacerbate these conditions at ambient GABA concentrations < 1 μM, assuming that a large population of γ2-containing receptors exists at extrasynaptic sites. Unfortunately, there is no information as yet regarding the extent to which GABA levels are elevated in such conditions. Given its enhancement of tonic currents at low ambient GABA concentrations, 4-PIOL might instead be useful for neurological conditions which are associated with reduced tonic $GABA_A$ receptor mediated transmission, such as Fragile X syndrome, sleep and psychiatric disorders (Brickley and Mody, 2012; Whissell *et al*., 2014). However, it will first be important to understand why 4-PIOL inhibited phasic currents in hippocampal and TC relay neurons. Thus, although 4-PIOL is unlikely to be useful therapeutically, other low efficacy/potency partial agonist may prove therapeutically useful, but their functional effects will need to be assessed carefully, against a panel of critical factors, such as those noted above.

References

Abramian, A.M., Comenencia-Ortiz, E., Vithlani, M., Tretter, E.V., Sieghart, W., Davies, P.A., et al. (2010). Protein kinase C phosphorylation regulates membrane insertion of $GABA_A$ receptor subtypes that mediate tonic inhibition. J. Biol. Chem. *285*: 41795–41805.

Althoff, T., Hibbs, R.E., Banerjee, S., and Gouaux, E. (2014). X-ray structures of GluCl in apo states reveal a gating mechanism of Cys-loop receptors. Nature *512*: 333–337.

Angelotti, T.P., and Macdonald, R.L. (1993). Assembly of $GABA_A$ receptor subunits: α1β1 and α1β1γ2S subunits produce unique ion channels with dissimilar single-channel properties. J. Neurosci. *13*: 1429–1440.

Ben-Ari, Y., Khalilov, I., Kahle, K.T., and Cherubini, E. (2012). The GABA excitatory/inhibitory shift in brain maturation and neurological disorders. Neurosci. *18*: 467–486.

Ashby, M.C., Ibaraki, K., and Henley, J.M. (2004). It's green outside: tracking cell surface proteins with pH-sensitive GFP. Trends Neurosci. *27*: 257–261.

Atack, J.R. (2010). Preclinical and clinical pharmacology of the $GABA_A$ receptor α5 subtype-selective inverse agonist α5IA. Pharmacol. Ther. *125*: 11–26.

Atack, J.R., Bayley, P.J., Seabrook, G.R., Wafford, K.A., McKernan, R.M., and Dawson, G.R. (2006). L-655,708 enhances cognition in rats but is not proconvulsant at a dose selective for α5-containing $GABA_A$ receptors. Neuropharmacology *51*: 1023–1029.

Attwell, D., Barbour, B., and Szatkowski, M. (1993). Nonvesicular release of neurotransmitter. Neuron *11*: 401–407.

Axmacher, N., and Draguhn, A. (2004). Inhibition of GABA release by presynaptic ionotropic GABA receptors in hippocampal CA3. Neuroreport *15*: 329–334.

Backus, K.H., Arigoni, M., Drescher, U., Scheurer, L., Malherbe, P., Möhler, H., et al. (1993). Stoichiometry of a recombinant $GABA_A$ receptor deduced from mutation-induced rectification. Neuroreport *5*: 285–288.

Bai, D., Zhu, G., Pennefather, P., Jackson, M.F., MacDonald, J.F., and Orser, B.A. (2001). Distinct functional and pharmacological properties of tonic and quantal inhibitory postsynaptic currents mediated by γ-aminobutyric $acid_A$ receptors in hippocampal neurons. Mol. Pharmacol. *59*: 814–824.

Ballard, T.M., Knoflach, F., Prinssen, E., Borroni, E., Vivian, J.A., Basile, J., et al. (2009). RO4938581, a novel cognitive enhancer acting at $GABA_A$ α5 subunit-containing receptors. Psychopharmacology *202*: 207–223.

Banke, T.G., and McBain, C.J. (2006). GABAergic input onto CA3 hippocampal interneurons remains shunting throughout development. J. Neurosci. *26*: 11720–11725.

Banks, M.I., Li, T.B., and Pearce, R.A. (1998). The synaptic basis of $GABA_A$,slow. J. Neurosci. *18*: 1305–1317.

Bannerman, D.M., Rawlins, J.N.P., McHugh, S.B., Deacon, R.M.J., Yee, B.K., Bast, T., et al. (2004). Regional dissociations within the hippocampus--memory and anxiety. Neurosci. Biobehav. Rev. *28*: 273–283.

Barrera, N.P., Betts, J., You, H., Henderson, R.M., Martin, I.L., Dunn, S.M.J., et al. (2008). Atomic force microscopy reveals the stoichiometry and subunit arrangement of the α4β3δ $GABA_A$ receptor. Mol. Pharmacol. *73*: 960–967.

Baumann, S.W., Baur, R., and Sigel, E. (2001). Subunit Arrangement of γ-Aminobutyric Acid Type A Receptors. J. Biol. Chem. *276*: 36275–36280.

Baur, R., Kaur, K.H., and Sigel, E. (2009). Structure of α6β3δ $GABA_A$ receptors and their lack of ethanol sensitivity. J. Neurochem. *111*: 1172–1181.

Baur, R., Minier, F., and Sigel, E. (2006). A $GABA_A$ receptor of defined subunit composition and positioning: concatenation of five subunits. FEBS Lett. *580*: 1616–1620.

Baur, R., and Sigel, E. (2005). Benzodiazepines Affect Channel Opening of $GABA_A$ Receptors Induced by Either Agonist Binding Site. Mol. Pharmacol. *67*: 1005–1008.

Bedford, F.K., Kittler, J.T., Muller, E., Thomas, P., Uren, J.M., Merlo, D., et al. (2001). $GABA_A$ receptor cell surface number and subunit stability are regulated by the ubiquitin-like protein Plic-1. Nat. Neurosci. *4*: 908–916.

Belelli, D., Casula, A., Ling, A., and Lambert, J.J. (2002). The influence of subunit composition on the interaction of neurosteroids with $GABA_A$ receptors. Neuropharmacology *43*: 651–661.

Belelli, D., and Herd, M.B. (2003). The contraceptive agent Provera enhances $GABA_A$ receptor-mediated inhibitory neurotransmission in the rat hippocampus: evidence for endogenous neurosteroids? J. Neurosci. *23*: 10013–10020.

Belelli, D., and Lambert, J.J. (2005). Neurosteroids: endogenous regulators of the $GABA_A$ receptor. Nat. Rev. Neurosci. *6*: 565–575.

Belelli, D., Peden, D.R., Rosahl, T.W., Wafford, K.A., and Lambert, J.J. (2005). Extrasynaptic $GABA_A$ receptors of thalamocortical neurons: a molecular target for hypnotics. J. Neurosci. *25*: 11513–11520.

Benson, J.A., Löw, K., Keist, R., Möhler, H., and Rudolph, U. (1998). Pharmacology of recombinant γ-aminobutyric acid A receptors rendered diazepam-insensitive by point-mutated α-subunits. FEBS Lett. *431*: 400–404.

Bessaïh, T., Bourgeais, L., Badiu, C.I., Carter, D.A., Toth, T.I., Ruano, D., et al. (2006). Nucleus-specific abnormalities of GABAergic synaptic transmission in a genetic model of absence seizures. J. Neurophysiol. *96*: 3074–3081.

Bettler, B., Kaupmann, K., Mosbacher, J., and Gassmann, M. (2004). Molecular structure and physiological functions of $GABA_B$ receptors. Physiol. Rev. *84*: 835–867.

Bianchi, M.T., and Macdonald, R.L. (2001). Mutation of the 9' leucine in the $GABA_A$ receptor γ2L subunit produces an apparent decrease in desensitization by stabilizing open states without altering desensitized states. Neuropharmacology *41*: 737–744.

Bianchi, M.T., and Macdonald, R.L. (2003). Neurosteroids shift partial agonist activation of $GABA_A$ receptor channels from low- to high-efficacy gating patterns. J. Neurosci. *23*: 10934–10943.

Biasi, S. De, Vitellaro-Zuccarello, L., and Brecha, N.C. (1998). Immunoreactivity for the GABA transporter-1 and GABA transporter-3 is restricted to astrocytes in the rat thalamus. A light and electron-microscopic immunolocalization. Neuroscience *83*: 815–828.

Bieda, M.C., Su, H., and Maciver, M.B. (2009). Anesthetics discriminate between tonic and phasic γ-aminobutyric acid receptors on hippocampal CA1 neurons. Anesth. Analg. *108*: 484–490.

Bliss, T.V., and Collingridge, G.L. (1993). A synaptic model of memory: long-term potentiation in the hippocampus. Nature *361*: 31–39.

Bocquet, N., Nury, H., Baaden, M., Poupon, C. Le, Changeux, J.-P., Delarue, M., et al. (2009). X-ray structure of a pentameric ligand-gated ion channel in an apparently open conformation. Nature *457*: 111–114.

Bogdanov, Y., Michels, G., Armstrong-Gold, C., Haydon, P.G., Lindstrom, J., Pangalos, M., et al. (2006). Synaptic $GABA_A$ receptors are directly recruited from their extrasynaptic counterparts. EMBO J. *25*: 4381–4389.

Bollan, K., King, D., Robertson, L.A., Brown, K., Taylor, P.M., Moss, S.J., et al. (2003). $GABA_A$ receptor composition is determined by distinct assembly signals within α and β subunits. J. Biol. Chem. *278*: 4747–4755.

Borden, L.A. (1996). GABA transporter heterogeneity: pharmacology and cellular localization. Neurochem. *29*: 335–356.

Borden, L.A., Murali Dhar, T.G., Smith, K.E., Weinshank, R.L., Branchek, T.A., and Gluchowski, C. (1994). Tiagabine, SK&F 89976-A, CI-966, and NNC-711 are selective for the cloned GABA transporter GAT-1. Eur. J. Pharmacol. *269*: 219–224.

Borghese, C.M., and Harris, R.A. (2007). Studies of ethanol actions on recombinant δ-containing γ-aminobutyric acid type A receptors yield contradictory results. Alcohol *41*: 155–162.

Borghese, C.M., Stórustovu, S. í, Ebert, B., Herd, M.B., Belelli, D., Lambert, J.J., et al. (2006). The δ subunit of γ-aminobutyric acid type A receptors does not confer sensitivity to low concentrations of ethanol. J. Pharmacol. Exp. Ther. *316*: 1360–1368.

Bormann, J., Hamill, O.P., and Sakmann, B. (1987). Mechanism of anion permeation through channels gated by glycine and γ-aminobutyric acid in mouse cultured spinal neurones. J. Physiol. *385*: 243–286.

Bowery, N.G., Bettler, B., Froestl, W., Gallagher, J.P., Marshall, F., Raiteri, M., et al. (2002). International Union of Pharmacology. XXXIII. Mammalian γ-Aminobutyric $Acid_B$ Receptors: Structure and Function. Pharmacol. Rev. *54*: 247–264.

Braudeau, J., Delatour, B., Duchon, A., Pereira, P.L., Dauphinot, L., Chaumont, F. de, et al. (2011). Specific targeting of the $GABA_A$ receptor α5 subtype by a selective inverse agonist restores cognitive deficits in Down syndrome mice. J. Psychopharmacol. *25*: 1030–1042.

Brickley, S.G., Cull-Candy, S.G., and Farrant, M. (1996). Development of a tonic form of synaptic inhibition in rat cerebellar granule cells resulting from persistent activation of $GABA_A$ receptors. J. Physiol. *497:* 753–759.

Brickley, S.G., and Mody, I. (2012). Extrasynaptic $GABA_A$ receptors: their function in the CNS and implications for disease. Neuron *73*: 23–34.

Brickley, S.G., Revilla, V., Cull-Candy, S.G., Wisden, W., and Farrant, M. (2001). Adaptive regulation of neuronal excitability by a voltage-independent potassium conductance. Nature *409*: 88–92.

Bright, D.P., Aller, M.I., and Brickley, S.G. (2007). Synaptic Release Generates a Tonic $GABA_A$ Receptor-Mediated Conductance That Modulates Burst Precision in Thalamic Relay Neurons. J. Neurosci. *27*: 2560–2569.

Bright, D.P., Renzi, M., Bartram, J., McGee, T.P., MacKenzie, G., Hosie, A.M., et al. (2011). Profound Desensitization by Ambient GABA Limits Activation of γ-Containing $GABA_A$ Receptors during Spillover. J. Neurosci. *31*: 753–763.

Bright, D.P., and Smart, T.G. (2013). Protein kinase C regulates tonic $GABA_A$ receptor-mediated inhibition in the hippocampus and thalamus. Eur. J. Neurosci. *38*: 3408–3423.

Brown, N., Kerby, J., Bonnert, T.P., Whiting, P.J., and Wafford, K.A. (2002). Pharmacological characterization of a novel cell line expressing human α4β3δ $GABA_A$ receptors. Br. J. Pharmacol. *136*: 965–974.

Brünig, I., Scotti, E., Sidler, C., and Fritschy, J.-M. (2002). Intact sorting, targeting, and clustering of γ-aminobutyric acid A receptor subtypes in hippocampal neurons *in vitro*. J. Comp. Neurol. *443*: 43–55.

Byberg, J.R., Labouta, I.M., Falch, E., Hjeds, H., Krogsgaard-Larsen, P., Curtis, D.R., et al. (1987). Synthesis and biological activity of a $GABA_A$ agonist which has no effect on benzodiazepine binding and of structurally related glycine antagonists. Drug Des. Deliv. *1*: 261–274.

Caddick, S.J., Wang, C., Fletcher, C.F., Jenkins, N.A., Copeland, N.G., and Hosford, D.A. (1999). Excitatory but not inhibitory synaptic transmission is reduced in lethargic (Cacnb4(lh)) and tottering (Cacna1atg) mouse thalami. J. Neurophysiol. *81*: 2066–2074.

Caraiscos, V.B., Elliott, E.M., You-Ten, K.E., Cheng, V.Y., Belelli, D., Newell, J.G., et al. (2004). Tonic inhibition in mouse hippocampal CA1 pyramidal neurons is mediated by α5 subunit-containing γ-aminobutyric acid type A receptors. PNAS *101*: 3662–3667.

Caruncho, H.J., Puia, G., Möhler, H., and Costa, E. (1995). The density and distribution of six $GABA_A$ receptor subunits in primary cultures of rat cerebellar granule cells. Neuroscience *67*: 583–593.

Cestari, I.N., Min, K.T., Kulli, J.C., and Yang, J. (2000). Identification of an amino acid defining the distinct properties of murine β1 and β3 subunit-containing $GABA_A$ receptors. J. Neurochem. *74*: 827–838.

Chandra, D., Jia, F., Liang, J., Peng, Z., Suryanarayanan, A., Werner, D.F., et al. (2006). $GABA_A$ receptor α4 subunits mediate extrasynaptic inhibition in thalamus and dentate gyrus and the action of gaboxadol. PNAS. *103*: 15230–15235.

Chang, Y., Wang, R., Barot, S., and Weiss, D.S. (1996). Stoichiometry of a Recombinant $GABA_A$ Receptor. J Neurosci. *16*: 5415–5424.

Chang, Y., and Weiss, D.S. (1999). Allosteric activation mechanism of the α1β2γ2 γ-aminobutyric acid type A receptor revealed by mutation of the conserved M2 leucine. Biophys. J. *77*: 2542–2551.

Chebib, M., and Johnston, G.A. (1999). The 'ABC' of GABA receptors: a brief review. Clin. Exp. Pharmacol. Physiol. *26*: 937–940.

Cheng, V.Y., Martin, L.J., Elliott, E.M., Kim, J.H., Mount, H.T.J., Taverna, F.A., et al. (2006). α5 $GABA_A$ receptors mediate the amnestic but not sedative-hypnotic effects of the general anesthetic etomidate. J. Neurosci. *26*: 3713–3720.

Clarkson, A.N. (2012). Perisynaptic GABA Receptors The Overzealous Protector. Adv. Pharmacol. Sci. *2012*: 708428.

Clarkson, A.N., Huang, B.S., Macisaac, S.E., Mody, I., and Carmichael, S.T. (2010). Reducing excessive GABA-mediated tonic inhibition promotes functional recovery after stroke. Nature *468*: 305–309.

Colas, D., Chuluun, B., Warrier, D., Blank, M., Wetmore, D.Z., Buckmaster, P., et al. (2013). Short-term treatment with the $GABA_A$ receptor antagonist pentylenetetrazole produces a

sustained pro-cognitive benefit in a mouse model of Down's syndrome. Br. J. Pharmacol. *169*: 963–973.

Collinson, N., Kuenzi, F.M., Jarolimek, W., Maubach, K.A., Cothliff, R., Sur, C., et al. (2002). Enhanced learning and memory and altered GABAergic synaptic transmission in mice lacking the α5 subunit of the $GABA_A$ receptor. J. Neurosci. *22*: 5572–5580.

Connolly, C.N., Krishek, B.J., McDonald, B.J., Smart, T.G., and Moss, S.J. (1996). Assembly and cell surface expression of heteromeric and homomeric γ-aminobutyric acid type A receptors. J. Biol. Chem. *271*: 89–96.

Cope, D.W., Giovanni, G. Di, Fyson, S.J., Orban, G., Errington, A.C., Lorincz, M.L., et al. (2009). Enhanced tonic $GABA_A$ inhibition in typical absence epilepsy. Nat Med *15*: 1392–1398.

Cope, D.W., Hughes, S.W., and Crunelli, V. (2005). $GABA_A$ receptor-mediated tonic inhibition in thalamic neurons. J. Neurosci. *25*: 11553–11563.

Corpéchot, C., Collins, B.E., Carey, M.P., Tsouros, A., Robel, P., and Fry, J.P. (1997). Brain neurosteroids during the mouse oestrous cycle. Brain Res. *766*: 276–280.

Corringer, P.-J., Poitevin, F., Prevost, M.S., Sauguet, L., Delarue, M., and Changeux, J.-P. (2012). Structure and pharmacology of pentameric receptor channels: from bacteria to brain. Structure *20*: 941–956.

Crestani, F., Keist, R., Fritschy, J.-M., Benke, D., Vogt, K., Prut, L., et al. (2002). Trace fear conditioning involves hippocampal α5 $GABA_A$ receptors. PNAS *99*: 8980–8985.

Crunelli, V., and Leresche, N. (2002). Childhood absence epilepsy: Genes, channels, neurons and networks. Nat Rev Neurosci *3*: 371–382.

Dalby, N.O. (2003). Inhibition of γ-aminobutyric acid uptake: anatomy, physiology and effects against epileptic seizures. Eur. J. Pharmacol. *479*: 127–137.

Danober, L., Deransart, C., Depaulis, A., Vergnes, M., and Marescaux, C. (1998). Pathophysiological mechanisms of genetic absence epilepsy in the rat. Prog. Neurobiol. *55*: 27–57.

Davies, P.A., Kirkness, E.F., and Hales, T.G. (1997). Modulation by general anaesthetics of rat $GABA_A$ receptors comprised of α1β3 and β3 subunits expressed in human embryonic kidney 293 cells. Br. J. Pharmacol. *120*: 899–909.

Davisson, M.T., Schmidt, C., and Akeson, E.C. (1990). Segmental trisomy of murine chromosome 16: a new model system for studying Down syndrome. Prog. Clin. Biol. Res. *360*: 263–280.

Dawson, G.R., Maubach, K.A., Collinson, N., Cobain, M., Everitt, B.J., MacLeod, A.M., et al. (2006). An inverse agonist selective for α5 subunit-containing $GABA_A$ receptors enhances cognition. J. Pharmacol. Exp. Ther. *316*: 1335–1345.

Diaz, M.R., Wadleigh, A., Hughes, B.A., Woodward, J.J., and Valenzuela, C.F. (2011). Bestrophin1 Channels are Insensitive to Ethanol and Do not Mediate Tonic GABAergic Currents in Cerebellar Granule Cells. Front. Neurosci. *5*: 148.

Draguhn, A., Verdorn, T.A., Ewert, M., Seeburg, P.H., and Sakmann, B. (1990). Functional and molecular distinction between recombinant rat $GABA_A$ receptor subtypes by Zn^{2+}. Neuron *5*: 781–788.

Drasbek, K.R., and Jensen, K. (2006). THIP, a hypnotic and antinociceptive drug, enhances an extrasynaptic $GABA_A$ receptor-mediated conductance in mouse neocortex. Cereb. Cortex *16*: 1134–1141.

Ebert, B., Storustovu, S., Mortensen, M., and Frølund, B. (2002). Characterization of $GABA_A$ receptor ligands in the rat cortical wedge preparation: evidence for action at extrasynaptic receptors? Br. J. Pharmacol. *137*: 1–8.

Ebert, B., Wafford, K.A., Whiting, P.J., Krogsgaard-Larsen, P., and Kemp, J.A. (1994). Molecular pharmacology of γ-aminobutyric acid type A receptor agonists and partial agonists in oocytes injected with different α, β and γ receptor subunit combinations. Mol. Pharmacol. *46*: 957–963.

Egawa, K., and Fukuda, A. (2013). Pathophysiological power of improper tonic $GABA_A$ conductances in mature and immature models. Front. Neural Circuits *7*: 170.

Errington, A.C., Cope, D.W., and Crunelli, V. (2011). Augmentation of Tonic $GABA_A$ Inhibition in Absence Epilepsy: Therapeutic Value of Inverse Agonists at Extrasynaptic $GABA_A$ Receptors. Adv. Pharmacol. Sci. *2011*: 1–12.

Essrich, C., Lorez, M., Benson, J.A., Fritschy, J.M., and Lüscher, B. (1998). Postsynaptic clustering of major $GABA_A$ receptor subtypes requires the γ2 subunit and gephyrin. Nat. Neurosci. *1*: 563–571.

Falch, E., Larsson, O.M., Schousboe, A., and Krogsgaard-Larsen, P. (1990). GABA-A agonists and GABA uptake inhibitors: Structure-activity relationships. Drug Dev. Res. *21*: 169–188.

Fanselow, M.S., and Dong, H.-W. (2010). Are the dorsal and ventral hippocampus functionally distinct structures? Neuron *65*: 7–19.

Fariello, R.G., and Golden, G.T. (1987). The THIP-induced model of bilateral synchronous spike and wave in rodents. Neuropharmacology *26*: 161–165.

Farrant, M., and Nusser, Z. (2005). Variations on an inhibitory theme: phasic and tonic activation of $GABA_A$ receptors. Nat Rev Neurosci *6*: 215–229.

Faulhaber, J., Steiger, A., and Lancel, M. (1997). The $GABA_A$ agonist THIP produces slow wave sleep and reduces spindling activity in NREM sleep in humans. Psychopharmacology *130*: 285–291.

Feng, H.-J., Botzolakis, E.J., and Macdonald, R.L. (2009). Context-dependent modulation of αβγ and αβδ $GABA_A$ receptors by penicillin: Implications for phasic and tonic inhibition. Neuropharmacology *56*: 161–173.

Fernandez, F., Morishita, W., Zuniga, E., Nguyen, J., Blank, M., Malenka, R.C., et al. (2007). Pharmacotherapy for cognitive impairment in a mouse model of Down syndrome. Nat. Neurosci. *10*: 411–413.

Filatov, G.N., and White, M.M. (1995). The role of conserved leucines in the M2 domain of the acetylcholine receptor in channel gating. Mol. Pharmacol. *48*: 379–384.

Fritschy, J.M., Benke, D., Mertens, S., Oertel, W.H., Bachi, T., and Möhler, H. (1992). Five subtypes of type A γ-aminobutyric acid receptors identified in neurons by double and triple immunofluorescence staining with subunit-specific antibodies. PNAS *89*: 6726–6730.

Fritschy, J.M., Johnson, D.K., Möhler, H., and Rudolph, U. (1998). Independent assembly and subcellular targeting of $GABA_A$-receptor subtypes demonstrated in mouse hippocampal and olfactory neurons *in vivo*. Neurosci. Lett. *249*: 99–102.

Frolund, B., Kristiansen, U., Brehm, L., Hansen, A.B., Krogsgaard-Larsen, P., and Falch, E. (1995). Partial $GABA_A$ Receptor Agonists. Synthesis and *in Vitro* Pharmacology of a Series of Nonannulated Analogs of 4,5,6,7-Tetrahydroisoxazolo[4,5-c]pyridin-3-ol. J. Med. Chem. *38*: 3287–3296.

Gao, B., and Fritschy, J.M. (1995). Cerebellar granule cells *in vitro* recapitulate the *in vivo* pattern of $GABA_A$-receptor subunit expression. Brain Res. Dev. Brain Res. *88*: 1–16.

Gielen, M.C., Lumb, M.J., and Smart, T.G. (2012). Benzodiazepines modulate $GABA_A$ receptors by regulating the preactivation step after GABA binding. J. Neurosci. *32*: 5707–5715.

Glaeser, B.S., and Hare, T.A. (1975). Measurement of GABA in human cerebrospinal fluid. Biochem. Med. *12*: 274–282.

Glykys, J., Mann, E.O., and Mody, I. (2008). Which $GABA_A$ receptor subunits are necessary for tonic inhibition in the hippocampus? J. Neurosci. *28*: 1421–1426.

Glykys, J., and Mody, I. (2007). The main source of ambient GABA responsible for tonic inhibition in the mouse hippocampus. J. Physiol. *582*: 1163–1178.

Glykys, J., Peng, Z., Chandra, D., Homanics, G.E., Houser, C.R., and Mody, I. (2007). A new naturally occurring $GABA_A$ receptor subunit partnership with high sensitivity to ethanol. Nat. Neurosci. *10*: 40–48.

Groote, L. de, and Linthorst, A.C.E. (2007). Exposure to novelty and forced swimming evoke stressor-dependent changes in extracellular GABA in the rat hippocampus. Neuroscience *148*: 794–805.

Hamann, M., Rossi, D.J., and Attwell, D. (2002). Tonic and spillover inhibition of granule cells control information flow through cerebellar cortex. Neuron *33*: 625–633.

Hansen, S.L., Ebert, B., Fjalland, B., and Kristiansen, U. (2001). Effects of $GABA_A$ receptor partial agonists in primary cultures of cerebellar granule neurons and cerebral cortical neurons reflect different receptor subunit compositions. Br. J. Pharmacol. *133*: 539–549.

Harney, S.C., Frenguelli, B.G., and Lambert, J.J. (2003). Phosphorylation influences neurosteroid modulation of synaptic $GABA_A$ receptors in rat CA1 and dentate gyrus neurones. Neuropharmacology *45*: 873–883.

Hassaine, G., Deluz, C., Grasso, L., Wyss, R., Tol, M.B., Hovius, R., et al. (2014). X-ray structure of the mouse serotonin 5-HT_3 receptor. Nature *512*: 276–281.

Héja, L., Nyitrai, G., Kékesi, O., Dobolyi, A., Szabó, P., Fiáth, R., et al. (2012). Astrocytes convert network excitation to tonic inhibition of neurons. BMC Biol. *10*: 26.

Herd, M.B., Belelli, D., and Lambert, J.J. (2007). Neurosteroid modulation of synaptic and extrasynaptic $GABA_A$ receptors. Pharmacol. Ther. *116*: 20–34.

Herd, M.B., Foister, N., Chandra, D., Peden, D.R., Homanics, G.E., Brown, V.J., et al. (2009). Inhibition of thalamic excitability by 4,5,6,7-tetrahydroisoxazolo[4,5-c]pyridine-3-ol: a selective role for δ-$GABA_A$ receptors. Eur. J. Neurosci. *29*: 1177–1187.

Hibbs, R.E., and Gouaux, E. (2011). Principles of activation and permeation in an anion-selective Cys-loop receptor. Nature *474*: 54–60.

Hilf, R.J.C., and Dutzler, R. (2008). X-ray structure of a prokaryotic pentameric ligand-gated ion channel. Nature *452*: 375–379.

Hoestgaard-Jensen, K., Dalby, N.O., Wolinsky, T.D., Murphey, C., Jones, K.A., Rottländer, M., et al. (2010). Pharmacological characterization of a novel positive modulator at α4β3δ-containing extrasynaptic $GABA_A$ receptors. Neuropharmacology *58*: 702–711.

Hörtnagl, H., Tasan, R.O., Wieselthaler, A., Kirchmair, E., Sieghart, W., and Sperk, G. (2013). Patterns of mRNA and protein expression for 12 $GABA_A$ receptor subunits in the mouse brain. Neuroscience *236*: 345–372.

Hosford, D.A., and Wang, Y. (1997). Utility of the lethargic (lh/lh) mouse model of absence seizures in predicting the effects of lamotrigine, vigabatrin, tiagabine, gabapentin, and topiramate against human absence seizures. Epilepsia *38*: 408–414.

Hosie, A.M., Clarke, L., Silva, H. da, and Smart, T.G. (2009). Conserved site for neurosteroid modulation of $GABA_A$ receptors. Neuropharmacology *56*: 149–154.

Hosie, A.M., Dunne, E.L., Harvey, R.J., and Smart, T.G. (2003). Zinc-mediated inhibition of $GABA_A$ receptors: discrete binding sites underlie subtype specificity. Nat. Neurosci. *6*: 362–369.

Hosie, A.M., Wilkins, M.E., Silva, H.M.A. da, and Smart, T.G. (2006). Endogenous neurosteroids regulate $GABA_A$ receptors through two discrete transmembrane sites. Nature *444*: 486–489.

Houston, C.M., He, Q., and Smart, T.G. (2009). CaMKII phosphorylation of the $GABA_A$ receptor: receptor subtype- and synapse-specific modulation. J. Physiol. *587*: 2115–2125.

Houston, C.M., McGee, T.P., Mackenzie, G., Troyano-Cuturi, K., Rodriguez, P.M., Kutsarova, E., et al. (2012). Are extrasynaptic $GABA_A$ receptors important targets for sedative/hypnotic drugs? J. Neurosci. *32*: 3887–3897.

Houston, C.M., and Smart, T.G. (2006). CaMK-II modulation of $GABA_A$ receptors expressed in HEK293, NG108-15 and rat cerebellar granule neurons. Eur. J. Neurosci. *24*: 2504–2514.

Huntsman, M.M., Porcello, D.M., Homanics, G.E., DeLorey, T.M., and Huguenard, J.R. (1999). Reciprocal inhibitory connections and network synchrony in the mammalian thalamus. Science *283*: 541–543.

Jenkins, A., Franks, N.P., and Lieb, W.R. (1999). Effects of temperature and volatile anesthetics on $GABA_A$ receptors. Anesthesiology *90*: 484–491.

Jensen, M.L., Wafford, K.A., Brown, A.R., Belelli, D., Lambert, J.J., and Mirza, N.R. (2013). A study of subunit selectivity, mechanism and site of action of the δ selective compound 2 (DS2) at human recombinant and rodent native $GABA_A$ receptors. Br. J. Pharmacol. *168*: 1118–1132.

Jia, F., Pignataro, L., Schofield, C.M., Yue, M., Harrison, N.L., and Goldstein, P.A. (2005). An extrasynaptic $GABA_A$ receptor mediates tonic inhibition in thalamic VB neurons. J. Neurophysiol. *94*: 4491–4501.

Jones, A., Korpi, E.R., McKernan, R.M., Pelz, R., Nusser, Z., Mäkelä, R., et al. (1997). Ligand-gated ion channel subunit partnerships: $GABA_A$ receptor α6 subunit gene inactivation inhibits δ subunit expression. J. Neurosci. *17*: 1350–1362.

Jones, M.V., and Westbrook, G.L. (1995). Desensitized states prolong $GABA_A$ channel responses to brief agonist pulses. Neuron *15*: 181–191.

Jo, S., Yarishkin, O., Hwang, Y.J., Chun, Y.E., Park, M., Woo, D.H., et al. (2014). GABA from reactive astrocytes impairs memory in mouse models of Alzheimer's disease. Nat. Med. *20*: 886–896.

Jovanovic, J.N., Thomas, P., Kittler, J.T., Smart, T.G., and Moss, S.J. (2004). Brain-derived neurotrophic factor modulates fast synaptic inhibition by regulating $GABA_A$ receptor phosphorylation, activity, and cell-surface stability. J. Neurosci. *24*: 522–530.

Kaneda, M., Farrant, M., and Cull-Candy, S.G. (1995). Whole-cell and single-channel currents activated by GABA and glycine in granule cells of the rat cerebellum. J. Physiol. *485:* 419–435.

Kanematsu, T., Yasunaga, A., Mizoguchi, Y., Kuratani, A., Kittler, J.T., Jovanovic, J.N., et al. (2006). Modulation of $GABA_A$ receptor phosphorylation and membrane trafficking by phospholipase C-related inactive protein/protein phosphatase 1 and 2A signaling complex

underlying brain-derived neurotrophic factor-dependent regulation of GABAergic inhibition. J. Biol. Chem. *281*: 22180–22189.

Karim, N., Wellendorph, P., Absalom, N., Johnston, G.A.R., Hanrahan, J.R., and Chebib, M. (2013). Potency of GABA at human recombinant $GABA_A$ receptors expressed in Xenopus oocytes: a mini review. Amino Acids *44*: 1139–1149.

Kasugai, Y., Swinny, J.D., Roberts, J.D.B., Dalezios, Y., Fukazawa, Y., Sieghart, W., et al. (2010). Quantitative localisation of synaptic and extrasynaptic $GABA_A$ receptor subunits on hippocampal pyramidal cells by freeze-fracture replica immunolabelling. Eur. J. Neurosci. *32*: 1868–1888.

Kaur, K.H., Baur, R., and Sigel, E. (2009). Unanticipated structural and functional properties of δ-subunit-containing $GABA_A$ receptors. J. Biol. Chem. *284*: 7889–7896.

Kékesi, K.A., Dobolyi, A., Salfay, O., Nyitrai, G., and Juhász, G. (1997). Slow wave sleep is accompanied by release of certain amino acids in the thalamus of cats. Neuroreport *8*: 1183–1186.

Keros, S., and Hablitz, J.J. (2005). Subtype-specific GABA transporter antagonists synergistically modulate phasic and tonic $GABA_A$ conductances in rat neocortex. J. Neurophysiol. *94*: 2073–2085.

Kersanté, F., Rowley, S.C.S., Pavlov, I., Gutièrrez-Mecinas, M., Semyanov, A., Reul, J.M.H.M., et al. (2013). A functional role for both -aminobutyric acid (GABA) transporter-1 and GABA transporter-3 in the modulation of extracellular GABA and GABAergic tonic conductances in the rat hippocampus. J. Physiol. *591*: 2429–2441.

Khan, Z.U., Gutierrez, A., and Blas, A.L. De (1994). The subunit composition of a $GABA_A$/benzodiazepine receptor from rat cerebellum. J. Neurochem. *63*: 371–374.

Killisch, I., Dotti, C.G., Laurie, D.J., Lüddens, H., and Seeburg, P.H. (1991). Expression patterns of $GABA_A$ receptor subtypes in developing hippocampal neurons. Neuron *7*: 927–936.

Kittler, J.T., Chen, G., Honing, S., Bogdanov, Y., McAinsh, K., Arancibia-Carcamo, I.L., et al. (2005). Phospho-dependent binding of the clathrin AP2 adaptor complex to $GABA_A$ receptors regulates the efficacy of inhibitory synaptic transmission. PNAS *102*: 14871–14876.

Kittler, J.T., Delmas, P., Jovanovic, J.N., Brown, D.A., Smart, T.G., and Moss, S.J. (2000). Constitutive endocytosis of $GABA_A$ receptors by an association with the adaptin AP2 complex modulates inhibitory synaptic currents in hippocampal neurons. J. Neurosci. *20*: 7972–7977.

Kittler, J.T., Rostaing, P., Schiavo, G., Fritschy, J.M., Olsen, R., Triller, A., et al. (2001). The subcellular distribution of GABARAP and its ability to interact with NSF suggest a role for this protein in the intracellular transport of $GABA_A$ receptors. Mol. Cell. Neurosci. *18*: 13–25.

Kittler, J.T., Thomas, P., Tretter, V., Bogdanov, Y.D., Haucke, V., Smart, T.G., et al. (2004). Huntingtin-associated protein 1 regulates inhibitory synaptic transmission by modulating γ-aminobutyric acid type A receptor membrane trafficking. PNAS *101*: 12736–12741.

Klausberger, T., Magill, P.J., Márton, L.F., Roberts, J.D.B., Cobden, P.M., Buzsáki, G., et al. (2003). Brain-state- and cell-type-specific firing of hippocampal interneurons *in vivo*. Nature *421*: 844–848.

Klausberger, T., Roberts, J.D.B., and Somogyi, P. (2002). Cell type- and input-specific differences in the number and subtypes of synaptic $GABA_A$ receptors in the hippocampus. J. Neurosci. *22*: 2513–2521.

Klausberger, T., Sarto, I., Ehya, N., Fuchs, K., Furtmüller, R., Mayer, B., et al. (2001). Alternate Use of Distinct Intersubunit Contacts Controls $GABA_A$ Receptor Assembly and Stoichiometry. J. Neurosci. *21*: 9124–9133.

Kleschevnikov, A.M., Belichenko, P.V., Villar, A.J., Epstein, C.J., Malenka, R.C., and Mobley, W.C. (2004). Hippocampal long-term potentiation suppressed by increased inhibition in the Ts65Dn mouse, a genetic model of Down syndrome. J. Neurosci. *24*: 8153–8160.

Kneussel, M., Brandstätter, J.H., Laube, B., Stahl, S., Müller, U., and Betz, H. (1999). Loss of postsynaptic $GABA_A$ receptor clustering in gephyrin-deficient mice. J. Neurosci. *19*: 9289–9297.

Kneussel, M., Haverkamp, S., Fuhrmann, J.C., Wang, H., Wässle, H., Olsen, R.W., et al. (2000). The γ-aminobutyric acid type A receptor ($GABA_AR$)-associated protein GABARAP interacts with gephyrin but is not involved in receptor anchoring at the synapse. PNAS *97*: 8594–8599.

Kofuji, P., Wang, J.B., Moss, S.J., Huganir, R.L., and Burt, D.R. (1991). Generation of two forms of the γ-aminobutyric acid A receptor γ2-subunit in mice by alternative splicing. J. Neurochem. *56*: 713–715.

Krahe, T.E., El-Danaf, R.N., Dilger, E.K., Henderson, S.C., and Guido, W. (2011). Morphologically Distinct Classes of Relay Cells Exhibit Regional Preferences in the Dorsal Lateral Geniculate Nucleus of the Mouse. J. Neurosci. *31*: 17437–17448.

Krishek, B.J., Moss, S.J., and Smart, T.G. (1996). Homomeric β1 γ-aminobutyric acid A receptor-ion channels: evaluation of pharmacological and physiological properties. Mol. Pharmacol. *49*: 494–504.

Krishek, B.J., Moss, S.J., and Smart, T.G. (1998). Interaction of H^+ and Zn^{2+} on recombinant and native rat neuronal $GABA_A$ receptors. J. Physiol. *507*: 639–652.

Kristiansen, U., Barker, J.L., and Serafini, R. (1995). The low efficacy γ-aminobutyric acid type A agonist 5-(4-piperidyl)isoxazol-3-ol opens brief Cl^- channels in embryonic rat olfactory bulb neurons. Mol. Pharmacol. *48*: 268–279.

Kristiansen, U., Lambert, J.D., Falch, E., and Krogsgaard-Larsen, P. (1991). Electrophysiological studies of the $GABA_A$ receptor ligand, 4-PIOL, on cultured hippocampal neurones. Br. J. Pharmacol. *104*: 85–90.

Krogsgaard-Larsen, P., Frølund, B., and Liljefors, T. (2002). Specific $GABA_A$ agonists and partial agonists. Chem. Rec. *2*: 419–430.

Kullmann, D.M., and Lamsa, K.P. (2011). Interneurons go plastic. Neuropharmacology *60*: 711.

Kullmann, D.M., Ruiz, A., Rusakov, D.M., Scott, R., Semyanov, A., and Walker, M.C. (2005). Presynaptic, extrasynaptic and axonal $GABA_A$ receptors in the CNS: where and why? Prog. Biophys. Mol. Biol. *87*: 33–46.

Labarca, C., Nowak, M.W., Zhang, H., Tang, L., Deshpande, P., and Lester, H.A. (1995). Channel gating governed symmetrically by conserved leucine residues in the M2 domain of nicotinic receptors. Nature *376*: 514–516.

Lambert, J.J., Belelli, D., Peden, D.R., Vardy, A.W., and Peters, J.A. (2003). Neurosteroid modulation of $GABA_A$ receptors. Prog. Neurobiol. *71*: 67–80.

Lanerolle, N.C. de, Kim, J.H., Williamson, A., Spencer, S.S., Zaveri, H.P., Eid, T., et al. (2003). A retrospective analysis of hippocampal pathology in human temporal lobe epilepsy: evidence for distinctive patient subcategories. Epilepsia *44*: 677–687.

Laurie, D.J., Seeburg, P.H., and Wisden, W. (1992a). The distribution of 13 $GABA_A$ receptor subunit mRNAs in the rat brain. II. Olfactory bulb and cerebellum. J. Neurosci. *12*: 1063–1076.

Laurie, D.J., Wisden, W., and Seeburg, P.H. (1992b). The distribution of 13 $GABA_A$ receptor subunit mRNAs in the rat brain. III. Embryonic and postnatal development. J. Neurosci. *12*: 4151–4172.

Leao, R.M., Mellor, J.R., and Randall, A.D. (2000). Tonic benzodiazepine-sensitive GABAergic inhibition in cultured rodent cerebellar granule cells. Neuropharmacology *39*: 990–1003.

Lee, S., Yoon, B.-E., Berglund, K., Oh, S.-J., Park, H., Shin, H.-S., et al. (2010). Channel-mediated tonic GABA release from glia. Science *330*: 790–796.

Lee, V., and Maguire, J. (2014). The impact of tonic $GABA_A$ receptor-mediated inhibition on neuronal excitability varies across brain region and cell type. Front. Neural Circuits *8*: 3.

Leil, T.A., Chen, Z.-W., Chang, C.-S.S., and Olsen, R.W. (2004). $GABA_A$ receptor-associated protein traffics $GABA_A$ receptors to the plasma membrane in neurons. J. Neurosci. *24*: 11429–11438.

Lerma, J., Herranz, A.S., Herreras, O., Abraira, V., and Martín del Río, R. (1986). *In vivo* determination of extracellular concentration of amino acids in the rat hippocampus. A method based on brain dialysis and computerized analysis. Brain Res. *384*: 145–155.

Lévi, S., Logan, S.M., Tovar, K.R., and Craig, A.M. (2004). Gephyrin is critical for glycine receptor clustering but not for the formation of functional GABAergic synapses in hippocampal neurons. J. Neurosci. *24*: 207–217.

Liang, J., Cagetti, E., Olsen, R.W., and Spigelman, I. (2004). Altered pharmacology of synaptic and extrasynaptic $GABA_A$ receptors on CA1 hippocampal neurons is consistent with subunit changes in a model of alcohol withdrawal and dependence. J. Pharmacol. Exp. Ther. *310*: 1234–1245.

Loebrich, S., Bähring, R., Katsuno, T., Tsukita, S., and Kneussel, M. (2006). Activated radixin is essential for $GABA_A$ receptor α5 subunit anchoring at the actin cytoskeleton. EMBO J. *25*: 987–999.

Lott, I.T., and Dierssen, M. (2010). Cognitive deficits and associated neurological complications in individuals with Down's syndrome. Lancet Neurol. *9*: 623–633.

Lüscher, B., Fuchs, T., and Kilpatrick, C.L. (2011). $GABA_A$ receptor trafficking-mediated plasticity of inhibitory synapses. Neuron *70*: 385–409.

Lüscher, B., and Keller, C.A. (2004). Regulation of $GABA_A$ receptor trafficking, channel activity, and functional plasticity of inhibitory synapses. Pharmacol. Ther. *102*: 195–221.

Macdonald, R.L., Kang, J.-Q., and Gallagher, M.J. (2010). Mutations in $GABA_A$ receptor subunits associated with genetic epilepsies. J. Physiol. *588*: 1861 –1869.

Maconochie, D.J., Zempel, J.M., and Steinbach, J.H. (1994). How quickly can $GABA_A$ receptors open? Neuron *12*: 61–71.

MacQueen, G., and Frodl, T. (2011). The hippocampus in major depression: evidence for the convergence of the bench and bedside in psychiatric research? Mol. Psychiatry *16*: 252–264.

Malenka, R.C., and Bear, M.F. (2004). LTP and LTD: an embarrassment of riches. Neuron *44*: 5–21.

Mangan, P.S., Sun, C., Carpenter, M., Goodkin, H.P., Sieghart, W., and Kapur, J. (2005). Cultured Hippocampal Pyramidal Neurons Express Two Kinds of $GABA_A$ Receptors. Mol. Pharmacol. *67*: 775–788.

Mann, E.O., and Mody, I. (2010). Control of hippocampal γ oscillation frequency by tonic inhibition and excitation of interneurons. Nat. Neurosci. *13*: 205–212.

Marescaux, C., Vergnes, M., and Depaulis, A. (1992). Genetic absence epilepsy in rats from Strasbourg--a review. J. Neural Transm. Suppl. *35*: 37–69.

Martínez-Cué, C., Martínez, P., Rueda, N., Vidal, R., García, S., Vidal, V., et al. (2013). Reducing $GABA_A$ α5 receptor-mediated inhibition rescues functional and neuromorphological deficits in a mouse model of down syndrome. J. Neurosci. *33*: 3953–3966.

Martin, L.J., Oh, G.H.T., and Orser, B.A. (2009). Etomidate targets α5 γ-aminobutyric acid subtype A receptors to regulate synaptic plasticity and memory blockade. Anesthesiology *111*: 1025–1035.

Mathie, A., Sutton, G.L., Clarke, C.E., and Veale, E.L. (2006). Zinc and copper: pharmacological probes and endogenous modulators of neuronal excitability. Pharmacol. Ther. *111*: 567–583.

Mattson, M.P. (2004). Pathways towards and away from Alzheimer's disease. Nature *430*: 631–639.

McCartney, M.R., Deeb, T.Z., Henderson, T.N., and Hales, T.G. (2007). Tonically active $GABA_A$ receptors in hippocampal pyramidal neurons exhibit constitutive GABA-independent gating. Mol. Pharmacol. *71*: 539–548.

McCormick, D.A., and Bal, T. (1997). Sleep and arousal: thalamocortical mechanisms. Annu. Rev. Neurosci. *20*: 185–215.

McGee, T.P., Houston, C.M., and Brickley, S.G. (2013). Copper block of extrasynaptic $GABA_A$ receptors in the mature cerebellum and striatum. J. Neurosci. *33*: 13431–13435.

McKernan, R.M., and Whiting, P.J. (1996). Which $GABA_A$-receptor subtypes really occur in the brain? Trends Neurosci. *19*: 139–143.

Michelson, H.B., and Wong, R.K. (1991). Excitatory synaptic responses mediated by $GABA_A$ receptors in the hippocampus. Science *253*: 1420–1423.

Miller, P.S., and Aricescu, A.R. (2014). Crystal structure of a human $GABA_A$ receptor. Nature *512*: 270–275.

Miller, P.S., and Smart, T.G. (2010). Binding, activation and modulation of Cys-loop receptors. Trends Pharmacol. Sci. *31*: 161–174.

Millingen, M., Bridle, H., Jesorka, A., Lincoln, P., and Orwar, O. (2011). Ligand-Specific Temperature-Dependent Shifts in EC_{50} Values for the $GABA_A$ Receptor. Anal Chem *80*: 340–343.

Minelli, A., Brecha, N.C., Karschin, C., DeBiasi, S., and Conti, F. (1995). GAT-1, a high-affinity GABA plasma membrane transporter, is localized to neurons and astroglia in the cerebral cortex. J. Neurosci. *15*: 7734–7746.

Minelli, A., DeBiasi, S., Brecha, N.C., Zuccarello, L.V., and Conti, F. (1996). GAT-3, a high-affinity GABA plasma membrane transporter, is localized to astrocytic processes, and it is not confined to the vicinity of GABAergic synapses in the cerebral cortex. J. Neurosci. *16*: 6255–6264.

Mitchell, S.J., and Silver, R.A. (2003). Shunting inhibition modulates neuronal gain during synaptic excitation. Neuron *38*: 433–445.

Mizokami, A., Kanematsu, T., Ishibashi, H., Yamaguchi, T., Tanida, I., Takenaka, K., et al. (2007). Phospholipase C-related inactive protein is involved in trafficking of γ2 subunit-containing $GABA_A$ receptors to the cell surface. J. Neurosci. *27*: 1692–1701.

Möhler, H. (2006). $GABA_A$ receptor diversity and pharmacology. Cell Tissue Res. *326*: 505–516.

Mortensen, M., Ebert, B., Wafford, K., and Smart, T.G. (2010). Distinct activities of GABA agonists at synaptic- and extrasynaptic-type $GABA_A$ receptors. J. Physiol. *588*: 1251–1268.

Mortensen, M., Frølund, B., JÃ¸rgensen, A.T., Liljefors, T., Krogsgaard-Larsen, P., and Ebert, B. (2002). Activity of novel 4-PIOL analogues at human α1β2γ2S $GABA_A$ receptors - correlation with hydrophobicity. Eur. J. Pharmacol. *451*: 125–132.

Mortensen, M., Kristiansen, U., Ebert, B., Frølund, B., Krogsgaard-Larsen, P., and Smart, T.G. (2004). Activation of single heteromeric $GABA_A$ receptor ion channels by full and partial agonists. J. Physiol. *557*: 389–413.

Mortensen, M., Patel, B., and Smart, T.G. (2011). GABA Potency at $GABA_A$ Receptors Found in Synaptic and Extrasynaptic Zones. Front. Cell. Neurosci. *6*: 1.

Mortensen, M., and Smart, T.G. (2006). Extrasynaptic αβ subunit $GABA_A$ receptors on rat hippocampal pyramidal neurons. J. Physiol. *577*: 841–856.

Mortensen, M., and Smart, T.G. (2007). Single-channel recording of ligand-gated ion channels. Nat Protoc. *2*: 2826–2841.

Moser, E.I. (2011). The multi-laned hippocampus. Nat. Neurosci. *14*: 407–408.

Moss, S.J., Smart, T.G., Porter, N.M., Nayeem, N., Devine, J., Stephenson, F.A., et al. (1990). Cloned GABA receptors are maintained in a stable cell line: allosteric and channel properties. Eur. J. Pharmacol. *189*: 77–88.

Mozrzymas, J.W., Wójtowicz, T., Piast, M., Lebida, K., Wyrembek, P., and Mercik, K. (2007). GABA transient sets the susceptibility of mIPSCs to modulation by benzodiazepine receptor agonists in rat hippocampal neurons. J. Physiol. *585*: 29–46.

Nagaya, N., and Macdonald, R.L. (2001). Two γ2L subunit domains confer low Zn^{2+} sensitivity to ternary $GABA_A$ receptors. J. Physiol. *532*: 17–30.

Nani, F., Bright, D.P., Revilla-Sanchez, R., Tretter, V., Moss, S.J., and Smart, T.G. (2013). Tyrosine phosphorylation of $GABA_A$ receptor γ2-subunit regulates tonic and phasic inhibition in the thalamus. J. Neurosci. *33*: 12718–12727.

Navarro, J.F., Burón, E., and Martín-López, M. (2002). Anxiogenic-like activity of L-655,708, a selective ligand for the benzodiazepine site of $GABA_A$ receptors which contain the α5 subunit, in the elevated plus-maze test. Prog. Neuropsychopharmacol. Biol. Psychiatry *26*: 1389–1392.

Nusser, Z., Cull-Candy, S., and Farrant, M. (1997). Differences in synaptic $GABA_A$ receptor number underlie variation in GABA mini amplitude. Neuron *19*: 697–709.

Nusser, Z., and Mody, I. (2002). Selective modulation of tonic and phasic inhibitions in dentate gyrus granule cells. J. Neurophysiol. *87*: 2624–2628.

Nusser, Z., Sieghart, W., Benke, D., Fritschy, J.M., and Somogyi, P. (1996). Differential synaptic localization of two major γ-aminobutyric acid type A receptor α subunits on hippocampal pyramidal cells. PNAS *93*: 11939–11944.

Nusser, Z., Sieghart, W., and Somogyi, P. (1998). Segregation of different $GABA_A$ receptors to synaptic and extrasynaptic membranes of cerebellar granule cells. J. Neurosci. *18*: 1693–1703.

Nutt, D.J., Besson, M., Wilson, S.J., Dawson, G.R., and Lingford-Hughes, A.R. (2007). Blockade of alcohol's amnestic activity in humans by an α5 subtype benzodiazepine receptor inverse agonist. Neuropharmacology *53*: 810–820.

Ohara, P.T., Lieberman, A.R., Hunt, S.P., and Wu, J.Y. (1983). Neural elements containing glutamic acid decarboxylase (GAD) in the dorsal lateral geniculate nucleus of the rat; immunohistochemical studies by light and electron microscopy. Neuroscience *8*: 189–211.

Okada, M., Onodera, K., Renterghem, C. Van, Sieghart, W., and Takahashi, T. (2000). Functional correlation of $GABA_A$ receptor α subunits expression with the properties of IPSCs in the developing thalamus. J. Neurosci. *20*: 2202–2208.

Olsen, R.W., and Sieghart, W. (2008). International Union of Pharmacology. LXX. Subtypes of γ-aminobutyric acid(A) receptors: classification on the basis of subunit composition, pharmacology, and function. Update. Pharmacol. Rev. *60*: 243–260.

Otis, T.S., and Mody, I. (1992). Modulation of decay kinetics and frequency of $GABA_A$ receptor-mediated spontaneous inhibitory postsynaptic currents in hippocampal neurons. Neuroscience *49*: 13–32.

Overstreet, L.S., and Westbrook, G.L. (2003). Synapse density regulates independence at unitary inhibitory synapses. J. Neurosci. *23*: 2618–2626.

Park, J.B., Skalska, S., Son, S., and Stern, J.E. (2007). Dual $GABA_A$ receptor-mediated inhibition in rat presympathetic paraventricular nucleus neurons. J. Physiol. *582*: 539–551.

Patel, B., Mortensen, M., and Smart, T.G. (2014). Stoichiometry of δ subunit containing $GABA_A$ receptors. Br. J. Pharmacol. *171*: 985–994.

Paul, S.M., and Purdy, R.H. (1992). Neuroactive steroids. FASEB J. *6*: 2311–2322.

Pearce, R.A. (1993). Physiological evidence for two distinct $GABA_A$ responses in rat hippocampus. Neuron *10*: 189–200.

Peden, D.R., Petitjean, C.M., Herd, M.B., Durakoglugil, M.S., Rosahl, T.W., Wafford, K., et al. (2008). Developmental maturation of synaptic and extrasynaptic $GABA_A$ receptors in mouse thalamic ventrobasal neurones. J. Physiol. *586*: 965–987.

Peng, Z., Hauer, B., Mihalek, R.M., Homanics, G.E., Sieghart, W., Olsen, R.W., et al. (2002). $GABA_A$ receptor changes in δ subunit-deficient mice: altered expression of α4 and γ2 subunits in the forebrain. J. Comp. Neurol. *446*: 179–197.

Perrais, D., and Ropert, N. (1999). Effect of zolpidem on miniature IPSCs and occupancy of postsynaptic $GABA_A$ receptors in central synapses. J. Neurosci. *19*: 578–588.

Perucca, E., Gram, L., Avanzini, G., and Dulac, O. (1998). Antiepileptic drugs as a cause of worsening seizures. Epilepsia *39*: 5–17.

Pirker, S., Schwarzer, C., Wieselthaler, A., Sieghart, W., and Sperk, G. (2000). $GABA_A$ receptors: immunocytochemical distribution of 13 subunits in the adult rat brain. Neuroscience *101*: 815–850.

Pollard, S., Thompson, C.L., and Stephenson, F.A. (1995). Quantitative characterization of α6 and α1α6 subunit-containing native γ-aminobutyric acid A receptors of adult rat cerebellum demonstrates two α subunits per receptor oligomer. J. Biol. Chem. *270*: 21285–21290.

Porcello, D.M., Huntsman, M.M., Mihalek, R.M., Homanics, G.E., and Huguenard, J.R. (2003). Intact synaptic GABAergic inhibition and altered neurosteroid modulation of thalamic relay neurons in mice lacking δ subunit. J. Neurophysiol. *89*: 1378–1386.

Prenosil, G.A., Schneider Gasser, E.M., Rudolph, U., Keist, R., Fritschy, J.-M., and Vogt, K.E. (2006). Specific subtypes of $GABA_A$ receptors mediate phasic and tonic forms of inhibition in hippocampal pyramidal neurons. J. Neurophysiol. *96*: 846–857.

Pritchett, D.B., Sontheimer, H., Shivers, B.D., Ymer, S., Kettenmann, H., Schofield, P.R., et al. (1989). Importance of a novel $GABA_A$ receptor subunit for benzodiazepine pharmacology. Nature *338*: 582–585.

Rabe, H., Picard, R., Uusi-Oukari, M., Hevers, W., Lüddens, H., and Korpi, E.R. (2000). Coupling between agonist and chloride ionophore sites of the $GABA_A$ receptor: agonist/antagonist efficacy of 4-PIOL. Eur. J. Pharmacol. *409*: 233–242.

Revah, F., Bertrand, D., Galzi, J.L., Devillers-Thiéry, A., Mulle, C., Hussy, N., et al. (1991). Mutations in the channel domain alter desensitization of a neuronal nicotinic receptor. Nature *353*: 846–849.

Ribak, C.E., Tong, W.M., and Brecha, N.C. (1996). Astrocytic processes compensate for the apparent lack of GABA transporters in the axon terminals of cerebellar Purkinje cells. Anat. Embryol. *194*: 379–390.

Richardson, B.D., Ling, L.L., Uteshev, V.V., and Caspary, D.M. (2011). Extrasynaptic $GABA_A$ Receptors and Tonic Inhibition in Rat Auditory Thalamus. PLoS ONE *6*: e16508.

Richerson, G.B., and Wu, Y. (2003). Dynamic equilibrium of neurotransmitter transporters: not just for reuptake anymore. J. Neurophysiol. *90*: 1363–1374.

Rochefort, C., Lefort, J.M., and Rondi-Reig, L. (2013). The cerebellum: a new key structure in the navigation system. Front. Neural Circuits *7*: 35.

Rogers, C.J., Twyman, R.E., and Macdonald, R.L. (1994). Benzodiazepine and β-carboline regulation of single $GABA_A$ receptor channels of mouse spinal neurones in culture. J. Physiol. *475*: 69–82.

Rossi, D.J., Hamann, M., and Attwell, D. (2003). Multiple modes of GABAergic inhibition of rat cerebellar granule cells. J. Physiol. *548*: 97–110.

Rudolph, U., and Knoflach, F. (2011). Beyond classical benzodiazepines: novel therapeutic potential of $GABA_A$ receptor subtypes. Nat. Rev. Drug Discov. *10*: 685–697.

Rudolph, U., and Möhler, H. (2004). Analysis of $GABA_A$ receptor function and dissection of the pharmacology of benzodiazepines and general anesthetics through mouse genetics. Annu. Rev. Pharmacol. Toxicol. *44*: 475–498.

Rudolph, U., and Möhler, H. (2014). $GABA_A$ receptor subtypes: Therapeutic potential in Down syndrome, affective disorders, schizophrenia, and autism. Annu. Rev. Pharmacol. Toxicol. *54*: 483–507.

Ruiz, A., Campanac, E., Scott, R.S., Rusakov, D.A., and Kullmann, D.M. (2010). Presynaptic $GABA_A$ receptors enhance transmission and LTP induction at hippocampal mossy fiber synapses. Nat. Neurosci. *13*: 431–438.

Ruiz, A., Fabian-Fine, R., Scott, R., Walker, M.C., Rusakov, D.A., and Kullmann, D.M. (2003). $GABA_A$ receptors at hippocampal mossy fibers. Neuron *39*: 961–973.

Saab, B.J., Maclean, A.J.B., Kanisek, M., Zurek, A.A., Martin, L.J., Roder, J.C., et al. (2010). Short-term memory impairment after isoflurane in mice is prevented by the α5 γ-aminobutyric acid type A receptor inverse agonist L-655,708. Anesthesiology *113*: 1061–1071.

Saxena, N.C., and Macdonald, R.L. (1994). Assembly of $GABA_A$ receptor subunits: role of the δ subunit. J. Neurosci. *14*: 7077–7086.

Saxena, N.C., and Macdonald, R.L. (1996). Properties of putative cerebellar γ-aminobutyric acid A receptor isoforms. Mol. Pharmacol. *49*: 567–579.

Scimemi, A. (2014). Structure, function, and plasticity of GABA transporters. Front. Cell. Neurosci. *8*: 161.

Scimemi, A., Semyanov, A., Sperk, G., Kullmann, D.M., and Walker, M.C. (2005). Multiple and plastic receptors mediate tonic $GABA_A$ receptor currents in the hippocampus. J. Neurosci. *25*: 10016–10024.

Semyanov, A. (2003). Cell type specificity of $GABA_A$ receptor mediated signaling in the hippocampus. Curr. Drug Targets CNS Neurol. Disord. *2*: 240–247.

Serwanski, D.R., Miralles, C.P., Christie, S.B., Mehta, A.K., Li, X., and Blas, A.L. De (2006). Synaptic and nonsynaptic localization of $GABA_A$ receptors containing the α5 subunit in the rat brain. J. Comp. Neurol. *499*: 458–470.

Sherman, S.M., and Koch, C. (1986). The control of retinogeniculate transmission in the mammalian lateral geniculate nucleus. Exp. Brain Res. *63*: 1–20.

Shu, H.-J., Bracamontes, J., Taylor, A., Wu, K., Eaton, M.M., Akk, G., et al. (2012). Characteristics of concatemeric $GABA_A$ receptors containing α4/δ subunits expressed in Xenopus oocytes. Br. J. Pharmacol. *165*: 2228–2243.

Sieghart, W., Ramerstorfer, J., Sarto-Jackson, I., Varagic, Z., and Ernst, M. (2012). A novel $GABA_A$ receptor pharmacology: drugs interacting with the α(+) β(-) interface. Br. J. Pharmacol. *166*: 476–485.

Sieghart, W., and Sperk, G. (2002). Subunit composition, distribution and function of $GABA_A$ receptor subtypes. Curr. Top. Med. Chem. *2*: 795–816.

Sigel, E., Baur, R., Trube, G., Möhler, H., and Malherbe, P. (1990). The effect of subunit composition of rat brain $GABA_A$ receptors on channel function. Neuron *5*: 703–711.

Smart, T.G., Moss, S.J., Xie, X., and Huganir, R.L. (1991). $GABA_A$ receptors are differentially sensitive to zinc: dependence on subunit composition. Br. J. Pharmacol. *103*: 1837–1839.

Smart, T.G., and Paoletti, P. (2012). Synaptic neurotransmitter-gated receptors. Cold Spring Harb. Perspect. Biol. *4*:

Smith, K.R., McAinsh, K., Chen, G., Arancibia-Carcamo, I.L., Haucke, V., Yan, Z., et al. (2008). Regulation of inhibitory synaptic transmission by a conserved atypical interaction of $GABA_A$ receptor β- and γ-subunits with the clathrin AP2 adaptor. Neuropharmacology *55*: 844–850.

Soltesz, I., Roberts, J.D., Takagi, H., Richards, J.G., Möhler, H., and Somogyi, P. (1990). Synaptic and Nonsynaptic Localization of Benzodiazepine/$GABA_A$ Receptor/Cl^- Channel Complex Using Monoclonal Antibodies in the Dorsal Lateral Geniculate Nucleus of the Cat. Eur. J. Neurosci. *2*: 414–429.

Somogyi, P., Fritschy, J.M., Benke, D., Roberts, J.D., and Sieghart, W. (1996). The γ2 subunit of the $GABA_A$ receptor is concentrated in synaptic junctions containing the α1 and β2/3 subunits in hippocampus, cerebellum and globus pallidus. Neuropharmacology *35*: 1425–1444.

Song, I., Savtchenko, L., and Semyanov, A. (2011). Tonic excitation or inhibition is set by $GABA_A$ conductance in hippocampal interneurons. Nat. Commun. *2*: 376.

Song, I., Volynski, K., Brenner, T., Ushkaryov, Y., Walker, M., and Semyanov, A. (2013). Different transporter systems regulate extracellular GABA from vesicular and non-vesicular sources. Front. Cell. Neurosci. *7*: 23.

Sperk, G., Schwarzer, C., Tsunashima, K., Fuchs, K., and Sieghart, W. (1997). $GABA_A$ receptor subunits in the rat hippocampus I: Immunocytochemical distribution of 13 subunits. Neuroscience *80*: 987–1000.

Stell, B.M., Brickley, S.G., Tang, C.Y., Farrant, M., and Mody, I. (2003). Neuroactive steroids reduce neuronal excitability by selectively enhancing tonic inhibition mediated by δ subunit-containing $GABA_A$ receptors. PNAS *100*: 14439–14444.

Steriade, M., and Contreras, D. (1998). Spike-wave complexes and fast components of cortically generated seizures. I. Role of neocortex and thalamus. J. Neurophysiol. *80*: 1439–1455.

Steriade, M., McCormick, D.A., and Sejnowski, T.J. (1993). Thalamocortical oscillations in the sleeping and aroused brain. Science *262*: 679–685.

Stórustovu, S. í, and Ebert, B. (2006). Pharmacological Characterization of Agonists at δ-Containing $GABA_A$ Receptors: Functional Selectivity for Extrasynaptic Receptors Is Dependent on the Absence of γ2. J. Pharmacol. Exp. Ther. *316*: 1351–1359.

Sur, C., Farrar, S.J., Kerby, J., Whiting, P.J., Atack, J.R., and McKernan, R.M. (1999). Preferential Coassembly of α4 and δ Subunits of the γ-Aminobutyric Acid A Receptor in Rat Thalamus. Mol. Pharmacol. *56*: 110–115.

Szemes, M., Davies, R.L., Garden, C.L., and Usowicz, M.M. (2013). Weaker control of the electrical properties of cerebellar granule cells by tonically active $GABA_A$ receptors in the Ts65Dn mouse model of Down's syndrome. Mol. Brain *6*: 33.

Tan, H.O., Reid, C.A., Single, F.N., Davies, P.J., Chiu, C., Murphy, S., et al. (2007). Reduced cortical inhibition in a mouse model of familial childhood absence epilepsy. PNAS *104*: 17536–17541.

Taylor, P.M., Thomas, P., Gorrie, G.H., Connolly, C.N., Smart, T.G., and Moss, S.J. (1999). Identification of amino acid residues within $GABA_A$ receptor β subunits that mediate both homomeric and heteromeric receptor expression. J. Neurosci. *19*: 6360–6371.

Thomas, P., Mortensen, M., Hosie, A.M., and Smart, T.G. (2005). Dynamic mobility of functional $GABA_A$ receptors at inhibitory synapses. Nat. Neurosci. *8*: 889–897.

Thomas, P., and Smart, T.G. (2005). HEK293 cell line: a vehicle for the expression of recombinant proteins. J. Pharmacol. Toxicol. Methods *51*: 187–200.

Thompson, C.L., and Stephenson, F.A. (1994). $GABA_A$ receptor subtypes expressed in cerebellar granule cells: a developmental study. J. Neurochem. *62*: 2037–2044.

Timmerman, W., and Westerink, B.H. (1997). Brain microdialysis of GABA and glutamate: what does it signify? Synap. *27*: 242–261.

Towers, S.K., Gloveli, T., Traub, R.D., Driver, J.E., Engel, D., Fradley, R., et al. (2004). α5 subunit-containing $GABA_A$ receptors affect the dynamic range of mouse hippocampal kainate-induced γ frequency oscillations *in vitro*. J. Physiol. *559*: 721–728.

Tretter, V., Ehya, N., Fuchs, K., and Sieghart, W. (1997). Stoichiometry and Assembly of a Recombinant $GABA_A$ Receptor Subtype. J Neurosci *17*: 2728–2737.

Turecek, R., and Trussell, L.O. (2002). Reciprocal developmental regulation of presynaptic ionotropic receptors. PNAS *99*: 13884–13889.

Twelvetrees, A.E., Yuen, E.Y., Arancibia-Carcamo, I.L., MacAskill, A.F., Rostaing, P., Lumb, M.J., et al. (2010). Delivery of $GABA_A$Rs to synapses is mediated by HAP1-KIF5 and disrupted by mutant huntingtin. Neuron *65*: 53–65.

Tyagarajan, S.K., and Fritschy, J.-M. (2014). Gephyrin: a master regulator of neuronal function? Nat. Rev. Neurosci. *15*: 141–156.

Ueno, S., Bracamontes, J., Zorumski, C., Weiss, D.S., and Steinbach, J.H. (1997). Bicuculline and gabazine are allosteric inhibitors of channel opening of the $GABA_A$ receptor. J. Neurosci. *17*: 625–634.

Unwin, N. (2005). Refined structure of the nicotinic acetylcholine receptor at 4Å resolution. J. Mol. Biol. *346*: 967–989.

Vardya, I., Hoestgaard-Jensen, K., Nieto-Gonzalez, J.L., Dósa, Z., Boddum, K., Holm, M.M., et al. (2012). Positive modulation of δ-subunit containing $GABA_A$ receptors in mouse neurons. Neuropharmacology *63*: 469–479.

Verdoorn, T.A., Draguhn, A., Ymer, S., Seeburg, P.H., and Sakmann, B. (1990). Functional properties of recombinant rat $GABA_A$ receptors depend upon subunit composition. Neuron *4*: 919–928.

Vitellaro-Zuccarello, L., Calvaresi, N., and Biasi, S. De (2003). Expression of GABA transporters, GAT-1 and GAT-3, in the cerebral cortex and thalamus of the rat during postnatal development. Cell Tissue Res. *313*: 245–257.

Vithlani, M., Terunuma, M., and Moss, S.J. (2011). The dynamic modulation of $GABA_A$ receptor trafficking and its role in regulating the plasticity of inhibitory synapses. Physiol. Rev. *91*: 1009–1022.

Wafford, K.A., Niel, M.B. van, Ma, Q.P., Horridge, E., Herd, M.B., Peden, D.R., et al. (2009). Novel compounds selectively enhance δ subunit containing $GABA_A$ receptors and increase tonic currents in thalamus. Neuropharmacology *56*: 182–189.

Wagoner, K.R., and Czajkowski, C. (2010). Stoichiometry of expressed α4β2δ γ-aminobutyric acid type A receptors depends on the ratio of subunit cDNA transfected. J. Biol. Chem. *285*: 14187–14194.

Wall, M.J., and Usowicz, M.M. (1997). Development of action potential-dependent and independent spontaneous $GABA_A$ receptor-mediated currents in granule cells of postnatal rat cerebellum. Eur. J. Neurosci. *9*: 533–548.

Wallner, M., Hanchar, H.J., and Olsen, R.W. (2003). Ethanol enhances α4β3δ and α6β3δ γ-aminobutyric acid type A receptors at low concentrations known to affect humans. PNAS *100*: 15218–15223.

Wang, H., Bedford, F.K., Brandon, N.J., Moss, S.J., and Olsen, R.W. (1999). $GABA_A$-receptor-associated protein links $GABA_A$ receptors and the cytoskeleton. Nature *397*: 69–72.

Whissell, P.D., Lecker, I., Wang, D.-S., Yu, J., and Orser, B.A. (2014). Altered expression of δ $GABA_A$ receptors in health and disease. Neuropharmacology.

Whiting, P., McKernan, R.M., and Iversen, L.L. (1990). Another mechanism for creating diversity in γ-aminobutyrate type A receptors: RNA splicing directs expression of two forms of γ2 phosphorylation site. PNAS *87*: 9966–9970.

Wieland, H.A., Lüddens, H., and Seeburg, P.H. (1992). A single histidine in $GABA_A$ receptors is essential for benzodiazepine agonist binding. J. Biol. Chem. *267*: 1426–1429.

Williams, S.R., Turner, J.P., Anderson, C.M., and Crunelli, V. (1996). Electrophysiological and morphological properties of interneurones in the rat dorsal lateral geniculate nucleus *in vitro*. J. Physiol. *490*: 129–147.

Winsky-Sommerer, R., Vyazovskiy, V.V., Homanics, G.E., and Tobler, I. (2007). The EEG effects of THIP (Gaboxadol) on sleep and waking are mediated by the $GABA_A$ δ-subunit-containing receptors. Eur. J. Neurosci. *25*: 1893–1899.

Wisden, W., Korpi, E.R., and Bahn, S. (1996). The cerebellum: a model system for studying $GABA_A$ receptor diversity. Neuropharmacology *35*: 1139–1160.

Wisden, W., Laurie, D.J., Monyer, H., and Seeburg, P.H. (1992). The distribution of 13 $GABA_A$ receptor subunit mRNAs in the rat brain. I. Telencephalon, diencephalon, mesencephalon. J. Neurosci. *12*: 1040–1062.

Wlodarczyk, A.I., Sylantyev, S., Herd, M.B., Kersanté, F., Lambert, J.J., Rusakov, D.A., et al. (2013). GABA-independent $GABA_A$ receptor openings maintain tonic currents. J. Neurosci. *33*: 3905–3914.

Wohlfarth, K.M., Bianchi, M.T., and Macdonald, R.L. (2002). Enhanced neurosteroid potentiation of ternary $GABA_A$ receptors containing the δ subunit. J. Neurosci. *22*: 1541–1549.

Wooltorton, J.R., Moss, S.J., and Smart, T.G. (1997). Pharmacological and physiological characterization of murine homomeric β3 $GABA_A$ receptors. Eur. J. Neurosci. *9*: 2225–2235.

Wu, Y., Wang, W., Díez-Sampedro, A., and Richerson, G.B. (2007). Nonvesicular inhibitory neurotransmission via reversal of the GABA transporter GAT-1. Neuron *56*: 851–865.

Wu, Z., Guo, Z., Gearing, M., and Chen, G. (2014). Tonic inhibition in dentate gyrus impairs long-term potentiation and memory in an Alzhiemer's disease model. Nat. Commun. *5*: 4159.

Yakel, J.L., Lagrutta, A., Adelman, J.P., and North, R.A. (1993). Single amino acid substitution affects desensitization of the 5-hydroxytryptamine type 3 receptor expressed in Xenopus oocytes. PNAS *90*: 5030–5033.

Yamada, J., Furukawa, T., Ueno, S., Yamamoto, S., and Fukuda, A. (2007). Molecular basis for the $GABA_A$ receptor-mediated tonic inhibition in rat somatosensory cortex. Cereb. Cortex *17*: 1782–1787.

Yan, X.X., Cariaga, W.A., and Ribak, C.E. (1997). Immunoreactivity for GABA plasma membrane transporter, GAT-1, in the developing rat cerebral cortex: transient presence in the somata of neocortical and hippocampal neurons. Brain Res. Dev. Brain Res. *99*: 1–19.

Yee, B.K., Hauser, J., Dolgov, V.V., Keist, R., Möhler, H., Rudolph, U., et al. (2004). GABA receptors containing the α5 subunit mediate the trace effect in aversive and appetitive conditioning and extinction of conditioned fear. Eur. J. Neurosci. *20*: 1928–1936.

Yeung, J.Y.T., Canning, K.J., Zhu, G., Pennefather, P., MacDonald, J.F., and Orser, B.A. (2003). Tonically activated $GABA_A$ receptors in hippocampal neurons are high-affinity, low-conductance sensors for extracellular GABA. Mol. Pharmacol. *63*: 2–8.

Ye, Z., McGee, T.P., Houston, C.M., and Brickley, S.G. (2013). The contribution of δ subunit-containing $GABA_A$ receptors to phasic and tonic conductance changes in cerebellum, thalamus and neocortex. Front. Neural Circuits *7*: 203.

Yoshiike, Y., Kimura, T., Yamashita, S., Furudate, H., Mizoroki, T., Murayama, M., et al. (2008). $GABA_A$ receptor-mediated acceleration of aging-associated memory decline in APP/PS1 mice and its pharmacological treatment by picrotoxin. PloS One *3*: e3029.

You, H., and Dunn, S.M.J. (2007). Identification of a domain in the δ subunit (S238-V264) of the α4β3δ $GABA_A$ receptor that confers high agonist sensitivity. J. Neurochem. *103*: 1092–1101.

Zarnowska, E.D., Keist, R., Rudolph, U., and Pearce, R.A. (2009). $GABA_A$ receptor α5 subunits contribute to $GABA_A$,slow synaptic inhibition in mouse hippocampus. J. Neurophysiol. *101*: 1179–1191.

Zeyden, M. van der, Oldenziel, W.H., Rea, K., Cremers, T.I., and Westerink, B.H. (2008). Microdialysis of GABA and glutamate: analysis, interpretation and comparison with microsensors. Pharmacol. Biochem. Behav. *90*: 135–147.

Zhang, S.J., and Jackson, M.B. (1993). GABA-activated chloride channels in secretory nerve endings. Science *259*: 531–534.

Zhu, J.J., Uhlrich, D.J., and Lytton, W.W. (1999). Burst firing in identified rat geniculate interneurons. Neuroscience *91*: 1445–1460.

Zurek, A.A., Bridgwater, E.M., and Orser, B.A. (2012). Inhibition of α5 γ-Aminobutyric acid type A receptors restores recognition memory after general anesthesia. Anesth. Analg. *114*: 845–855.

Appendices

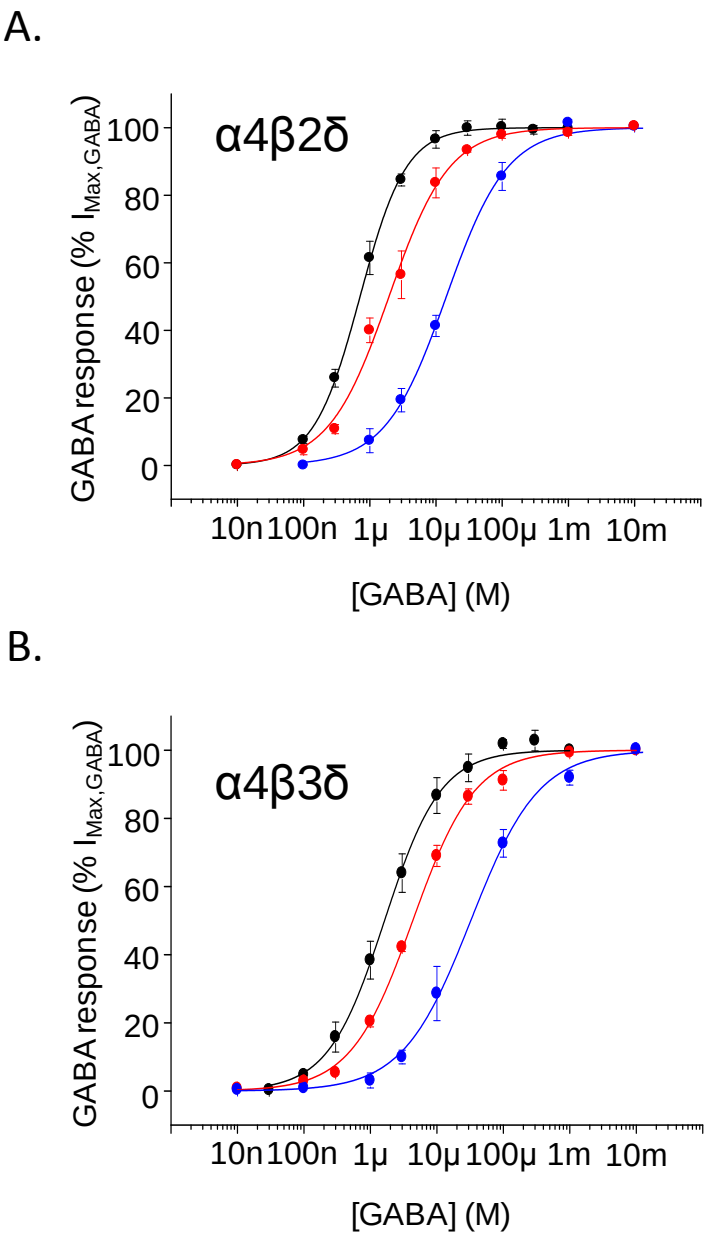

Appendix 1: Peak GABA concentration-response curves for α4β2δ and α4β3δ receptors

For HEK293 cells expressing α4β2δ (**A**) and α4β3δ (**B**) receptors, average peak GABA concentration-response curves were constructed in the absence (black), or presence of 10 µM (red) or 100 µM (blue) 4-PIOL (n = 5 – 7; mean ± SEM). Each data set was fitted using the Hill equation, using a least-squares method, and the continuous (black, red and blue) lines represent Hill fits to the mean concentration-response data.